NASA TM X-62,393 FAA-RD-74-143-II

A STOL AIRWORTHINESS INVESTIGATION USING A SIMULATION OF A DEFLECTED SLIPSTREAM TRANSPORT

Volume II – Simulation Data and Analysis

Robert L. Stapleford, Robert K. Heffley, Wayne F. Jewell, and John M. Lehman
Systems Technology, Inc.
Mountain View, Calif. 94043

Charles S. Hynes
Ames Research Center
Moffett Field, Calif. 94035

Barry C. Scott
Federal Aviation Administration
Ames Research Center
Moffett Field, Calif. 94035

October 1974

SYSTEMS TECHNOLOGY, INC.
2672 BAYSHORE FRONTAGE ROAD • MOUNTAIN VIEW, CALIFORNIA 94043 • PHONE [415] 961-4674

In reply refer to:

NASA TM X-62,393
FAA-RD-74-143-II
STI TECHNICAL REPORT 1014-3

A STOL AIRWORTHINESS INVESTIGATION USING A SIMULATION OF A DEFLECTED SLIPSTREAM TRANSPORT

Volume II – Simulation Data and Analysis

Robert L. Stapleford, Robert K. Heffley, Wayne F. Jewell, and John M. Lehman
Systems Technology, Inc.
Mountain View, Calif. 94043

Charles S. Hynes
Ames Research Center
Moffett Field, Calif. 94035

Barry C. Scott
Federal Aviation Administration
Ames Research Center
Moffett Field, Calif. 94035

October 1974

Contract NAS2-6433
Ames Research Center
National Aeronautics and Space Administration
Moffett Field, California

1. Report No. TM X-62,393 FAA-RD-74-143-II	2. Government Accession No.	3. Recipient's Catalog No.
4. Title and Subtitle A STOL AIRWORTHINESS INVESTIGATION USING A SIMULATION OF A DEFLECTED SLIPSTREAM TRANSPORT Volume II – Simulation Data and Analysis		5. Report Date 6. Performing Organization Code
7. Author(s) Robert L. Staplelord, Robert K. Heffley, Wayne F. Jewell, and John M. Lehman Charles S. Hynes, Barry C. Scott		8. Performing Organization Report No. A-5795 10. Work Unit No.
9. Performing Organization Name and Address Systems Technology, Inc. Mountain View, Calif. 94043 Ames Research Center Moffett Field, Calif. 94035	Federal Aviation Administration Ames Research Center Moffett Field, Calif. 94035	11. Contract or Grant No. NAS2-6433 13. Type of Report and Period Covered
12. Sponsoring Agency Name and Address Department of Transportation Federal Aviation Administration Ames Research Center Moffett Field, Calif. 94035	and Ames Research Center Moffett Field, Calif. 94035	14. Sponsoring Agency Code
15. Supplementary Notes		

16. Abstract

A simulator study of STOL airworthiness criteria was conducted using a model of a deflected slipstream transport. This study covered the approach, flare and landing, go-around, and takeoff phases of flight. The three volumes of this report document the results of that investigation.

Volume I (NASA TM X-62,392; FAA-RD-74-143-I) summarizes the results and discusses possible implications with regard to airworthiness criteria. The results provide a data base for future STOL airworthiness requirements and a preliminary indication of potential problem areas. Comparison of the simulation results with various proposed STOL criteria indicates significant deficiencies in many of these criteria.

Volume II (NASA TM X-62,393; FAA-RD-74-143-II) contains a detailed description of the simulation and the data obtained. These data include performance measures, pilot commentary, and pilot ratings. This volume also contains a pilot/vehicle analysis of glide slope tracking and an analysis of the flare maneuver.

Volume III (NASA TM X-62,394; FAA-RD-74-143-III) documents the aircraft model used in the simulation.

17. Key Words (Suggested by Author(s))	18. Distribution Statement
Short takeoff and landing Powered lift Airworthiness criteria	Unclassified – Unlimited STAR Category – 02

19. Security Classif. (of this report)	20. Security Classif. (of this page)	21. No. of Pages	22. Price*
Unclassified	Unclassified	242	$5.75

*For sale by the National Technical Information Service, Springfield, Virginia 22151

TABLE OF CONTENTS

Page

I. INTRODUCTION 1

II. SIMULATION DESCRIPTION 5

A. October/November 1972 Simulation Period 5

1. Simulator Apparatus 5
2. Mathematical Model 8
3. Cockpit Layout 8
4. Subject Pilots 8
5. Piloting Tasks 15
6. Data Gathering 17

B. April/May 1973 Simulation Period 23

1. Simulator Apparatus 23
2. Mathematical Model 23
3. Cockpit Layout 35
4. Subject Pilots 40
5. Piloting Tasks 40
6. Data Gathering 44

III. IIS TRACKING DATA 47

A. 1972 Results 47

1. Approach Speed 49
2. Transparency 58
3. Angle of Attack Display 58
4. Approach Angle 59

B. 1973 Results 59

1. Effects of Approach Speed, Transparency In 59
2. Effects of Approach Speed, Transparency Out 67
3. Effects of Angle of Attack Display 69

IV. FLARE AND LANDING 71

A. 1972 Tests 71

1. Test Conditions 71

Page

2. Data Analysis 71
3. Scatter Plots 71
4. Distribution Plots 80
a. Speed Effects 80
b. Transparency Effects 80
c. Glide Slope Effects 91

B. 1973 Tests 91
1. Test Conditions 91
2. Main Test Results 96
3. Comparison with 1972 Results and Flight Data . . . 106
4. Variation of Approach Attitude 106
5. Variation of Thrust Lags 110
6. Variation of Flare Technique 110

V. GO-AROUND DATA 113

A. 1972 Results 113
B. 1973 Results 122

VI. TAKEOFF DATA 124

A. Test Conditions 124
B. V_{MU} Testing 124
C. OEI Takeoffs 124
D. Abuses 127
E. Minimum Plane Penetration 133
F. Pilot Comments 136

VII. SUMMARY 137

A. ILS Tracking 137
B. Flare and Landing 138
C. Go-Around 139
D. Takeoff 139

REFERENCES 141

Page

APPENDIX A - SIMULATION MODEL CHARACTERISTICS 142

APPENDIX B - PILOT/VEHICLE ANALYSES 162

1. Glide Slope Control Without Airspeed Regulation . . . 164
2. Glide Slope Control With a Throttle-to-Attitude Crossfeed 164
3. Glide Slope Control in the Presence of Closed Loop Airspeed Control 177
4. Glide Slope Control in the Presence of Closed Loop Angle of Attack Control 193
5. Summary of Pilot/Vehicle Analyses 198

APPENDIX C - FLARE AND TOUCHDOWN ANALYSIS 205

1. Nature of the Flare Maneuver 205
2. Flare Parameter Variation 209
3. Flare Response Relative to Static Performance 213
4. Flight Test Flare/Touchdown Data 217

APPENDIX D - PILOT COMMENTS 220

LIST OF FIGURES

		Page
I-1	General Arrangement - BR 941S	2
II-1	Simulator Apparatus	6
II-2	Photograph of Cockpit Layout (October/November 1972) .	9
II-3	Instrument Panel (October/November 1972)	12
II-4	Flight Card Number 14	16
II-5	Turbulence Distribution	19
II-6	Wind Profiles, 1972	20
II-7	Approach Geometry	21
II-8	Runway/ILS Geometry	22
II-9	Digital Printout and Digital Plots (October/ November 1972) [TAKEOFF]	24
II-10	Digital Printout and Digital Plots (April/May 1973) [NORMAL APPROACH AND LANDING]	26
II-11	Digital Printout and Digital Plots (October/ November 1972) [GO-AROUND]	29
II-12	Effect of Pitch SAS	32
II-13	Effect of Turn Coordination SAS	33
II-14	SAS Block Diagrams	34
II-15	Photograph of Cockpit Layout (April/May 1973)	36
II-16	Instrument Panel (April/May 1973)	38
II-17	Pilot Evaluation	41
II-18	Modified Cooper-Harper Rating Scale	42
II-19	Runway Geometry	43
II-20	Typical Turbulence Time History	45
II-21	Wind Profiles, 1973	46
III-1	History of Glide Slope Tracking Performance	48
III-2	Effects of Approach Speed	55
III-3	Glide Slope Tracking Performance	56
III-4	Glide Slope Tracking Deviation	65
III-5	Pilot Ratings, Transparency In	66
III-6	Pilot Ratings, Transparency Out	68
IV-1	Scatter Plots	72
IV-2	Effects of Velocity	81

		Page
IV-3	Effect of Transparency	87
IV-4	Effect of Glide Slope	92
IV-5	Touchdown Scatter Plots, Calm Air	97
IV-6	Touchdown Scatter Plots with Wind and Turbulence	99
IV-7	Touchdown Distribution Plots with Wind and Turbulence	101
IV-8	Correlation of Pilot Rating to Median $\dot{h}_{TD}$	104
IV-9	Touchdown Sink Rate Potential vs Speed Margin	105
IV-10	Pilot Ratings vs Best Obtainable $\dot{h}_{TD}$	107
IV-11	Comparison of Flight and Simulation Landing Data	108
IV-12	Landing Data	109
IV-13	Flaring with Power Alone	112
V-1	Go-Around	116
V-2	Cumulative Distribution	120
V-3	1973 Go-Around Data	123
VI-1	V_{MU} Test	125
VI-2	Balanced Field Test	126
VI-3	OEI Takeoff Data	128
VI-4	Effect of Takeoff Abuses	129
VI-5	Minimum Plane Penetrated	134
A-1	Time Responses	146
A-2	Performance Curves	157
B-1	SAS Attitude Response to Step Input	163
B-2	Pilot Model for Glide Slope Control	163
B-3	Glide Slope Loop Closure, No Airspeed Regulation, Transparency In, 65 kt	165
B-4	Glide Slope Loop Closure, No Airspeed Regulation, Transparency In, 60 kt	166
B-5	Glide Slope Loop Closure, No Airspeed Regulation, Transparency In, 55 kt	167
B-6	Glide Slope Loop Closure, No Airspeed Regulation, Transparency Out, 60 kt	168
B-7	Glide Slope Loop Closure, No Airspeed Regulation, Transparency Out, 55 kt	169
B-8	Glide Slope Loop Closure, Ideal Crossfeed, Transparency In, 65 kt	171

		Page
B-9	Glide Slope Loop Closure, Ideal Crossfeed, Transparency In, 60 kt	172
B-10	Glide Slope Loop Closure, Ideal Crossfeed, Transparency In, 55 kt	173
B-11	Glide Slope Loop Closure, Ideal Crossfeed, Transparency Out, 60 kt	174
B-12	Glide Slope Loop Closure, Ideal Crossfeed, Transparency Out, 55 kt	175
B-13	Ideal Attitude Crossfeed Due to Throttle Step	176
B-14	Glide Slope Loop Closure, Simplified Crossfeed, Transparency In, 60 kt	178
B-15	Glide Slope Loop Closure, Simplified Crossfeed, Transparency In, 55 kt	179
B-16	Glide Slope Loop Closure, Simplified Crossfeed, Transparency Out, 60 kt	180
B-17	Glide Slope Loop Closure, Simplified Crossfeed, Transparency Out, 55 kt	181
B-18	Airspeed Loop Closure, Transparency In, 65 kt	183
B-19	Glide Slope Loop Closure, Transparency In, 65 kt	184
B-20	Airspeed Loop Closure, Transparency In, 60 kt	185
B-21	Glide Slope Loop Closure, Transparency In, 60 kt	186
B-22	Airspeed Loop Closure, Transparency In, 55 kt	187
B-23	Glide Slope Loop Closure, Transparency In, 55 kt	188
B-24	Airspeed Loop Closure, Transparency Out, 60 kt	189
B-25	Glide Slope Loop Closure, Transparency Out, 60 kt	190
B-26	Airspeed Loop Closure, Transparency Out, 55 kt	191
B-27	Glide Slope Loop Closure, Transparency Out, 55 kt	192
B-28	Angle of Attack Loop Closure, Transparency In, 65 kt	194
B-29	Glide Slope Loop Closure, Angle of Attack Loop Closed, Transparency In, 65 kt	195
B-30	Angle of Attack Loop Closure, Transparency In, 55 kt	196
B-31	Glide Slope Loop Closure, Angle of Attack Loop Closed, Transparency In, 55 kt	197
B-32	Generic Description of Glide Slope Control While Tracking α Tightly	199
B-33	Sample Comparison of Simplified Transfer Functions From Table B-1	201

		Page
B-34	Glide Slope Tracking Gain and Bandwidth Variations with Piloting Techniques	202
C-1	Flare Maneuver (Flight Test)	206
C-2	Flare Maneuver (Simulator)	207
C-3	Time History of Nominal Flare at 65 kt; Transparency In	210
C-4	Effect of Flare Controls	211
C-5	Effect of Transparency (Nominal Flare)	214
C-6	Flare Trajectories in $\dot{h}$ - V Plane (Optimum $\dot{h}_{TD}$ with $\Delta\theta$ Only)	215
C-7	Sink Rate Arrestment Potential	216

LIST OF TABLES

		Page
II-1	FSAA Motion Capability	7
II-2	Feel System Characteristics (October/November 1972)	10
II-3	Angle of Attack Chevrons	11
II-4	Subject Pilot Backgrounds	14
II-5	Turbulence Parameters	18
II-6	Feel System Characteristics (April/May 1973)	37
III-1	ILS Tracking Data (October/November 1972)	50
III-2	ILS Tracking Data (April/May 1973)	60
A-1	BR 941S Longitudinal Stability Derivatives Approach Configurations - 45000 lbs at .27 $\bar{c}$, 95 deg flap	143
A-2	BR 941S - Longitudinal Transfer Functions (Approach Configuration)	144
B-1	Glide Slope Transfer Function Summary	200
C-1	Tabulation of Flight Test Touchdown Conditions (FAA/NASA BR 941S Flights of July 1972)	218
D-1	Pilot Comments (October/November 1972)	221
D-2	Pilot Comments (April/May 1973)	227

LIST OF ABBREVIATIONS

AEO	All Engines Operating
A/C	Aircraft
A/S	Airspeed
BR	Breguet
CTOL	Conventional Takeoff and Landing
FAA	Federal Aviation Administration
FRL	Fuselage Reference Line
FSAA	Flight Simulator for Advanced Aircraft
fwd	Forward
G/S	Glide slope
HSI	Horizontal Situation Indicator
IFR	Instrument Flight Rules
ILS	Instrument Landing System
IVSI	Instantaneous Vertical Speed Indicator
MPP	Minimum Plane Penetrated
MPR	Maximum Practical Rotation Rate
NAL	Nominal Approach and Landing (7.5 deg glide slope)
NASA	National Aeronautics and Space Administration
OEI	One Engine Inoperative
PIO	Pilot Induced Oscillation
RPM	Revolutions Per Minute
SAL	Steep Approach and Landing (9.5 deg glide slope)
SAS	Stability Augmentation System
STOL	Short Takeoff and Landing
T	Transparency (inboard/outboard propeller differential pitch)
VFR	Visual Flight Rules

LIST OF SYMBOLS

b	Wing span (ft)
$\bar{c}$	Mean aerodynamic chord (ft)
C_{ℓ}	Rolling moment coefficient
C_L	Lift coefficient
$C_{L_{max}}$	Maximum value of lift coefficient
C_{L_α}	Lift curve slope (1/rad)
d	Glide slope deviation (ft)
h	Altitude (ft)
$\dot{h}$	Rate of climb (ft/sec)
K	Open loop gain
K_p	Open loop pilot gain
L_x	x scale length for turbulence model
M_λ	Partial derivative of pitch acceleration with respect to λ where $\lambda = u, w, \dot{w}, q,$ or δ_e
N_b^a	Transfer function numerator for 'a' response due to 'b' control
$N_{b\ d}^{a\ c}$	Coupling numerator
N_G	Gas generator RPM (% maximum)
q	Pitch rate
s	Laplace operator
S	Reference wing area (ft^2)
T_p	Pilot lead time constant
u	x component of velocity
V	Airspeed (kt)

$\bar{V}$	Mean airspeed (kt)
V_{APP}	Target approach airspeed on the glide slope (kt)
V_{EC}	Engine out speed (kt)
V_{LOF}	Lift-off speed (kt)
V_{min}	Minimum possible speed at given power setting (kt) $\frac{\partial \gamma}{\partial V} = \infty$ at V_{min}
V_{MU}	Minimum unstick speed (kt)
V_R	Target rotation speed (kt)
V_1	Critical-engine-failure speed (kt)
V_2	Takeoff safety speed (kt)
V_{35}	Speed at 35 ft height (kt)
w	z component of velocity
x_{LOF}	x distance at lift-off (ft)
x_{TD}	x distance at touchdown (ft)
x_{35}	x distance at 35 ft height (ft)
X_λ	Partial derivative of longitudinal acceleration with respect to λ -- where λ = u, w, or N_G
Y_p	Pilot transfer function
Y_x	Crossfeed
Z_λ	Partial derivative of vertical acceleration with respect to λ -- where λ = u, w, $\dot{w}$, q, δ_e, or N_G
α	Angle of attack (deg)
δ	Control deflection
Δ	Open loop transfer function denominator
Δ'	Closed loop transfer function denominator
γ	Flight path angle
σ	Standard deviation
θ	Pitch attitude (deg)

φ	Bank angle (deg)
ω	Frequency (rad/sec)
ω_b	Bandwidth (rad/sec)
ω_{180}	Frequency at which phase equals 180 deg (rad/sec)
$\measuredangle$	Angle

SUBSCRIPTS

APP	Approach
c	Commanded
CAS	Calibrated airspeed
e	Elevator
f	Flap
g	Gust
G/S	Glide slope
LOC	Localizer
N_G	Gas generator
P	Pedal
r	Rudder
ST	Longitudinal control

SPECIAL NOTATIONS

(z)	$s + z$
$[\zeta, \omega]$	$s^2 + 2\zeta\omega s + \omega^2$

SECTION I

INTRODUCTION

This volume presents the results of a simulator investigation of STOL airworthiness problems and criteria. This study is part of a long-range program to develop airworthiness standards for STOL aircraft. The program plan includes a series of simulation experiments using models of several different STOL design concepts, e.g. deflected slipstream, augmentor wing, and externally blown flap. This report covers the first simulation of that series.

The emphasis in this study has been on low-speed longitudinal flight path control since this is the area where STOL aircraft differ most from CTOL aircraft. Most of the simulation time was devoted to the approach and landing phases of flight as this was felt to be the most critical area. Considerably smaller amounts of time were spent on aborted landings (go-arounds) and takeoffs.

The specific aircraft simulated was the French Breguet 941S, a deflected slipstream STOL transport in the 50,000 lb gross weight class. A three-view drawing of the airplane is given in Fig. I-1. The aircraft has a unique feature called transparency, which is a difference in pitch between the inboard and outboard propellers. This difference is normally an automatic function of flap position. The inboard pitch is 5 deg greater for flap angles between 68 and 93 deg and is 12 deg greater for flap angles between 93 and 95 (limit) deg. Transparency considerably alters the longitudinal characteristics of the approach configuration (see Appendix A) by changing the lift distribution over the wing. The lift distribution is shifted inboard which increases the induced drag.

The simulation tests were conducted both with and without the transparency feature. This in effect provided data on two different approach configurations while only requiring one simulator model.

In July 1972, prior to the simulation exercise, the French government provided the participating pilots flight time in the actual airplane. This allowed them to develop the appropriate piloting techniques under

BR 941S

S = 901.8 FT²
b = 76.77 FT
c̄ = 12.15 FT

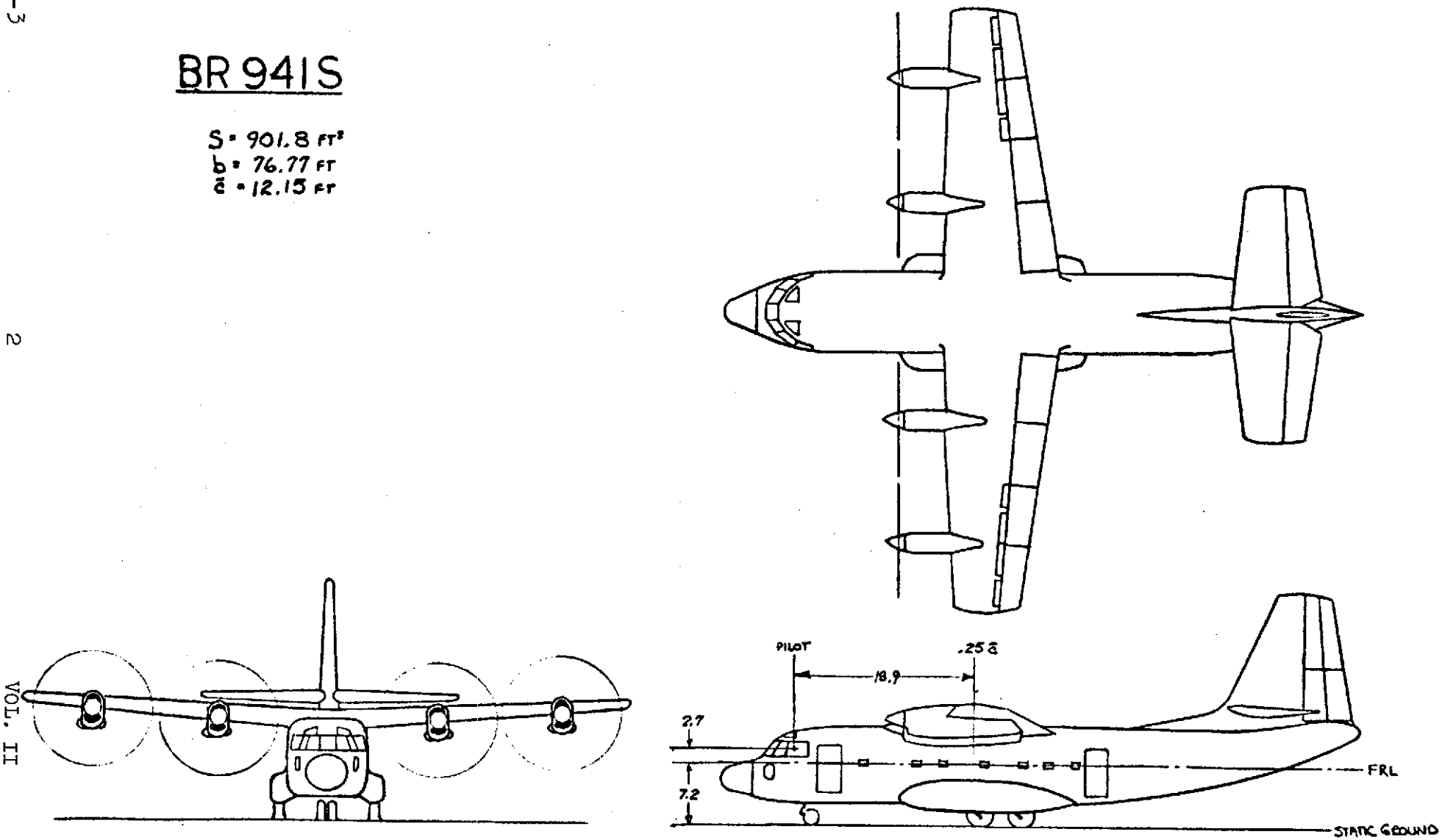

FIG. I-1

General Arrangement - BR 941S

realistic conditions. It also provided the pilots a basis for evaluating the realism of the simulation. Considerable time was spent tuning the simulator model until the pilots felt it generally matched the airplane quite well.

The first simulation experiment was conducted in October/November 1972. While a large amount of useful data was obtained during this period, the pilots felt that the workload during an IFR approach with turbulence was too high for airline operations. Furthermore, the high workload made it very difficult to accurately assess the effects of changing approach speed.

Because of these difficulties modifications were made to the simulator model and a second simulation experiment was conducted in April/May 1973. The modifications are discussed in Section II which is a description of the simulator apparatus and test procedures for both experiments. The main modification, in terms of workload reduction, was the addition of a directional SAS. This increased the dutch roll frequency and damping and greatly improved the turn coordination. The major problem in October/November 1972 was difficulty in tracking the localizer because of very poor turn coordination.

Sections III through VI present data for various flight phases as follows:

Section III - ILS Tracking
Section IV - Flare and Landing
Section V - Go-Around
Section VI - Takeoff

Each section, except VI, is organized into two parts---one for the results of the October/November 1972 simulation and the other part for the results of the April/May 1973 simulation. The results of both simulations and for all flight phases are summarized in Section VII.

Supporting material is contained in the appendices. Appendix A covers longitudinal dynamics - stability derivatives, transfer functions, and step responses.

A closed-loop pilot/vehicle analysis of glide slope tracking is presented in Appendix B. The analysis covers the effects of changes in approach speed and piloting technique. The results are useful in understanding the simulator data of Section III.

Appendix C contains an analysis of the flare maneuver and also some flight test results. The analysis includes the effects of approach speed, flare height, pitch change, and thrust input.

Pilot comments and ratings from both simulations are tabulated in Appendix D.

SECTION II

SIMULATION DESCRIPTION

This section describes the various aspects of the simulation, the specific conditions examined, and the means of collecting data. This description of the simulation is broken down into the following:

- Simulator Apparatus
- Mathematical Model
- Cockpit Layout
- Subject Pilots
- Piloting Tasks
- Data Gathering

A. OCTOBER/NOVEMBER 1972 SIMULATION PERIOD

1. Simulator Apparatus

The simulator apparatus was composed of three primary elements: the simulator cab, the visual display system, and the digital computer. Fig. II-1 shows the relationship of these in block diagram form.

The Ames Research Center Flight Simulator for Advanced Aircraft (FSAA) was used in this experiment. This is a six-degree-of-freedom moving base simulator with an especially long lateral travel. Table II-1 gives a breakdown on motion capability. The simulator is described in more detail in Ref. 1.

The visual scene apparatus consisted of the VFA-II Redifon system. This provided the pilot with a virtual image color TV display of a STOL runway and surrounding terrain for the purpose of heads-up navigation in the final stages of the approach. Detailed runway geometry will be described under Piloting Tasks.

Simulation computation was carried out entirely on an XDS Sigma 8 Digital Computer.

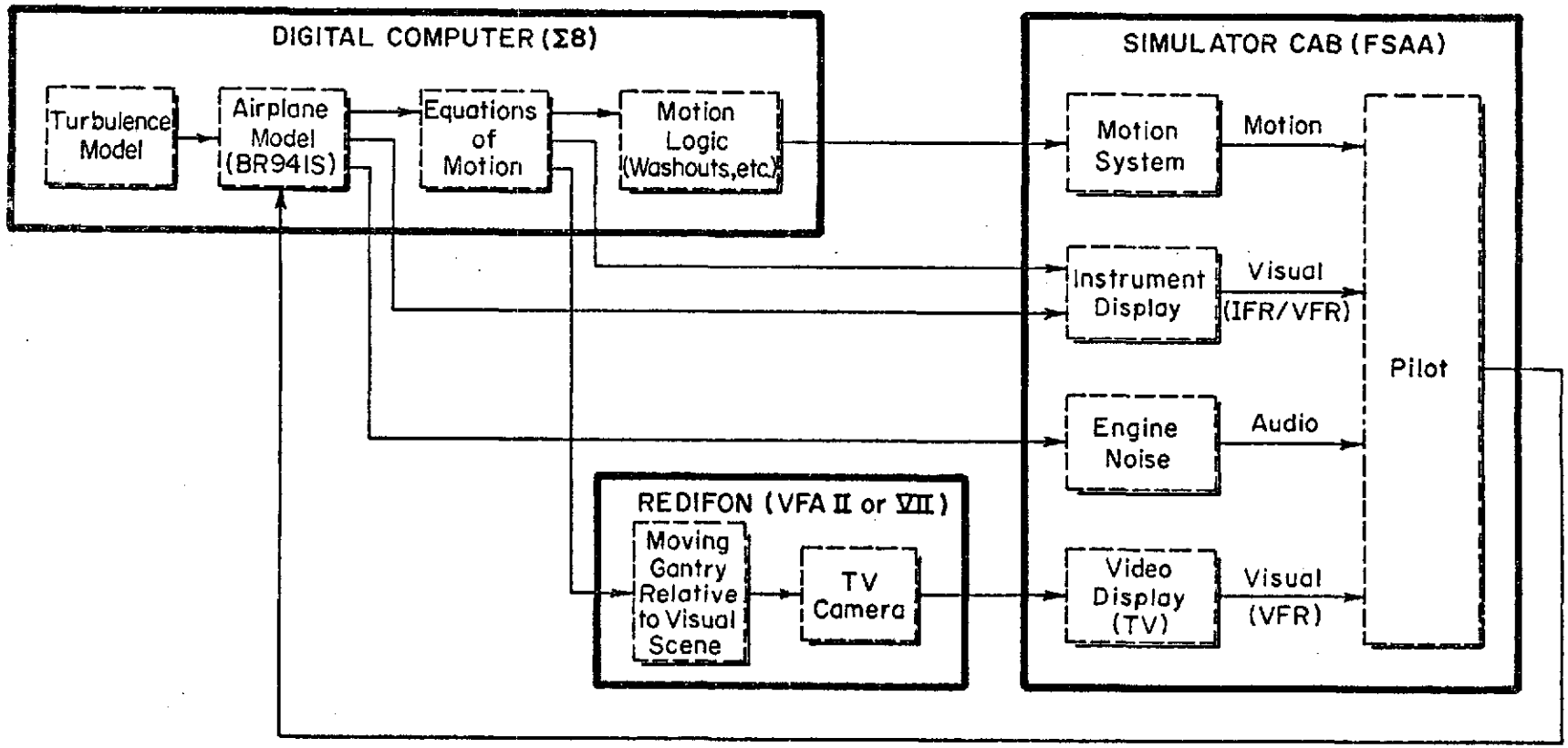

Figure II-1. Simulator Apparatus

TABLE II-1

FSAA MOTION CAPABILITY

Motion	Displacement *	Acceleration	Velocity	Frequency†
Roll	± 36°	1.6 rad/sec^2	0.5 rad/sec	3.1 Hz
Pitch	± 18°	1.6 rad/sec^2	0.5 rad/sec	1.5 Hz
Yaw	± 24°	1.6 rad/sec^2	0.5 rad/sec	1.7 Hz
Vertical	± 4 ft	10 ft/sec^2	6.9 ft/sec	2.2 Hz
Longitudinal	± 3 ft	8 ft/sec^2	5.05 ft/sec	1.8 Hz
Lateral	± 40-50 ft	10 ft/sec^2	16 ft/sec	1.0 Hz

* Usable

† At 30° phase lag

2. Mathematical Model

The math model used was based on the Breguet 941S airplane. Although the model included all configurations from full flaps to cruise, only the 45 to 95 deg flap range was used in the experiment, and this was limited to airspeeds at or below 80 kt. The model was designed to be most accurate in this low speed/high lift configuration range. Both a detailed model description and a comparison with flight test points are included in Volume III of this report.

3. Cockpit Layout

The FSAA cab accommodates side-by-side pilot and copilot seats. In this experiment the pilot occupied the normal left seat position. Primary controls closely resembled those of the BR 941S and consisted of a stick, rudder pedals, and a left-hand throttle (fighter type layout). Secondary controls included a flap handle, a propeller RPM handle, a flap/transparency switch atop the throttle, and pitch and roll trim switches. Toe-brakes were not operational during this series of tests. Fig. II-2 shows a photograph of the cockpit layout used. Detailed control characteristics of the actual BR 941S are given in Volume III. The cockpit layout of the actual BR 941S is shown in Ref. 2. Table II-2 gives the feel system characteristics used in the simulation.

Instruments consisted of those required for flying an ILS approach including all the basic flight and engine instruments. Nominal sensitivity of the glide slope indicator was $\pm$ 2 deg (1 deg/dot). Localizer sensitivity was $\pm$ 5 deg. Angle of attack chevrons were utilized, with a nominal 'on speed' value set by the computer operator. Table II-3 depicts the angle of attack chevrons in detail. Fig. II-3 shows the control and instrument layout and identifies each.

4. Subject Pilots

Formal testing was conducted with FAA and NASA pilots. Their respective backgrounds are outlined in Table II-4.

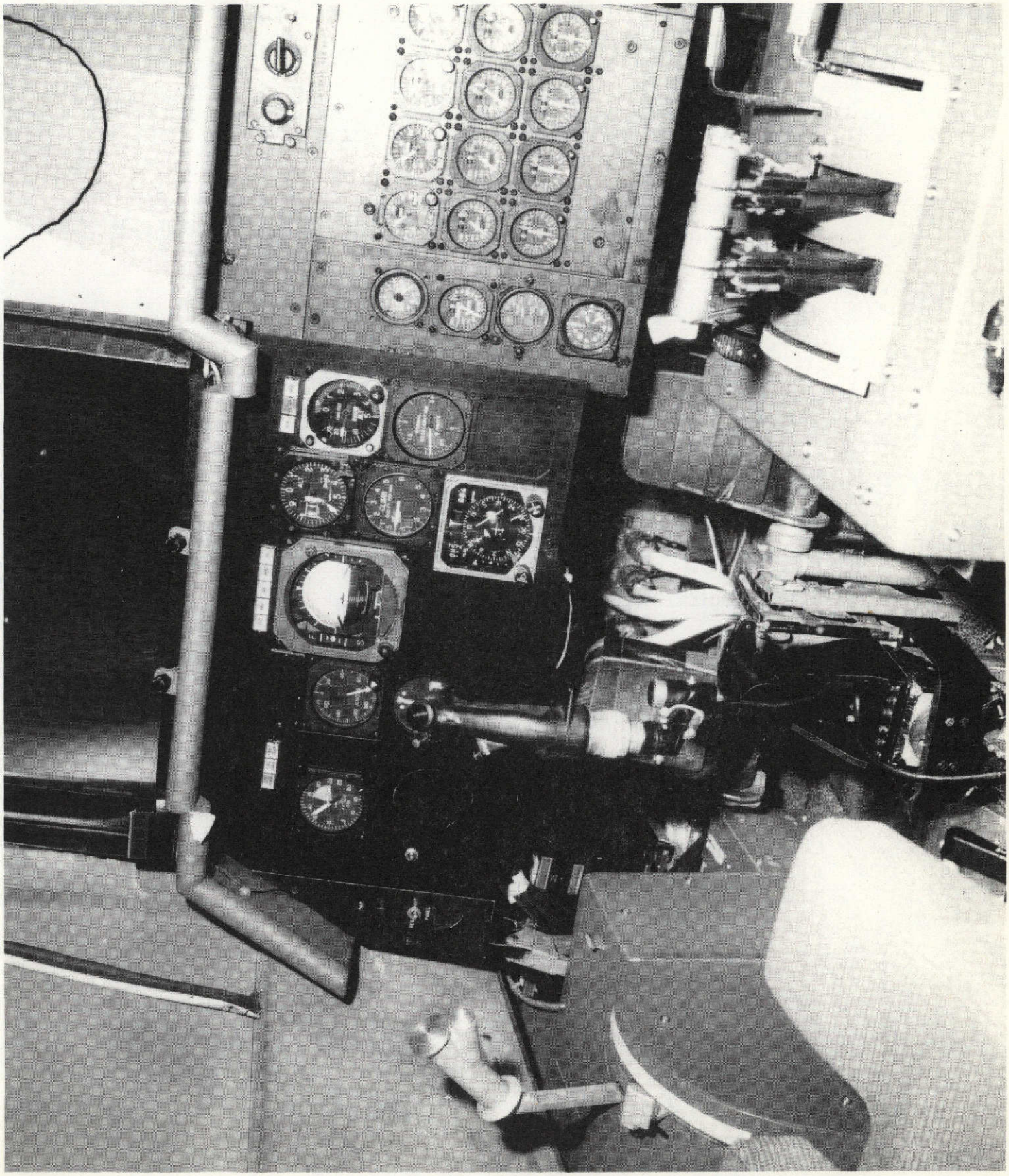

Figure II-2

Photograph of Cockpit Layout
(October/November 1972)

TABLE II-2

FEEL SYSTEM CHARACTERISTICS
(October/November 1972)

	BREAKOUT	GRADIENT	LIMITS
Longitudinal Stick	±1.7 lb	6.5 lb/in	4.18 in fwd 5.85 in aft
Lateral Stick	±1.5 lb	3.25 lb/in	±4.9 in
Rudder Pedals	10 lb	35 lb/in	±3.3 in

TABLE II-3

ANGLE OF ATTACK CHEVRONS

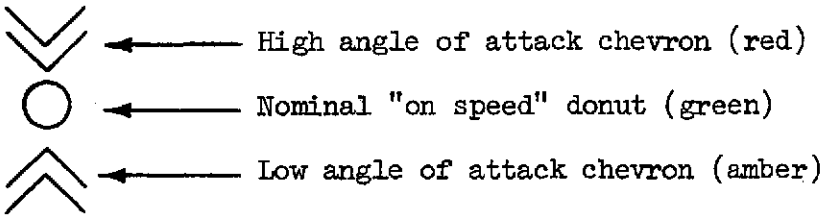

ANGLE OF ATTACK ERROR (deg)	DISPLAY
Greater than +4	Red Chevron Only
+2 to +4	Green Donut and Red Chevron
-2 to +2	Green Donut Only
-2 to -4	Green Donut and Amber Chevron
Less than -4	Amber Chevron Only

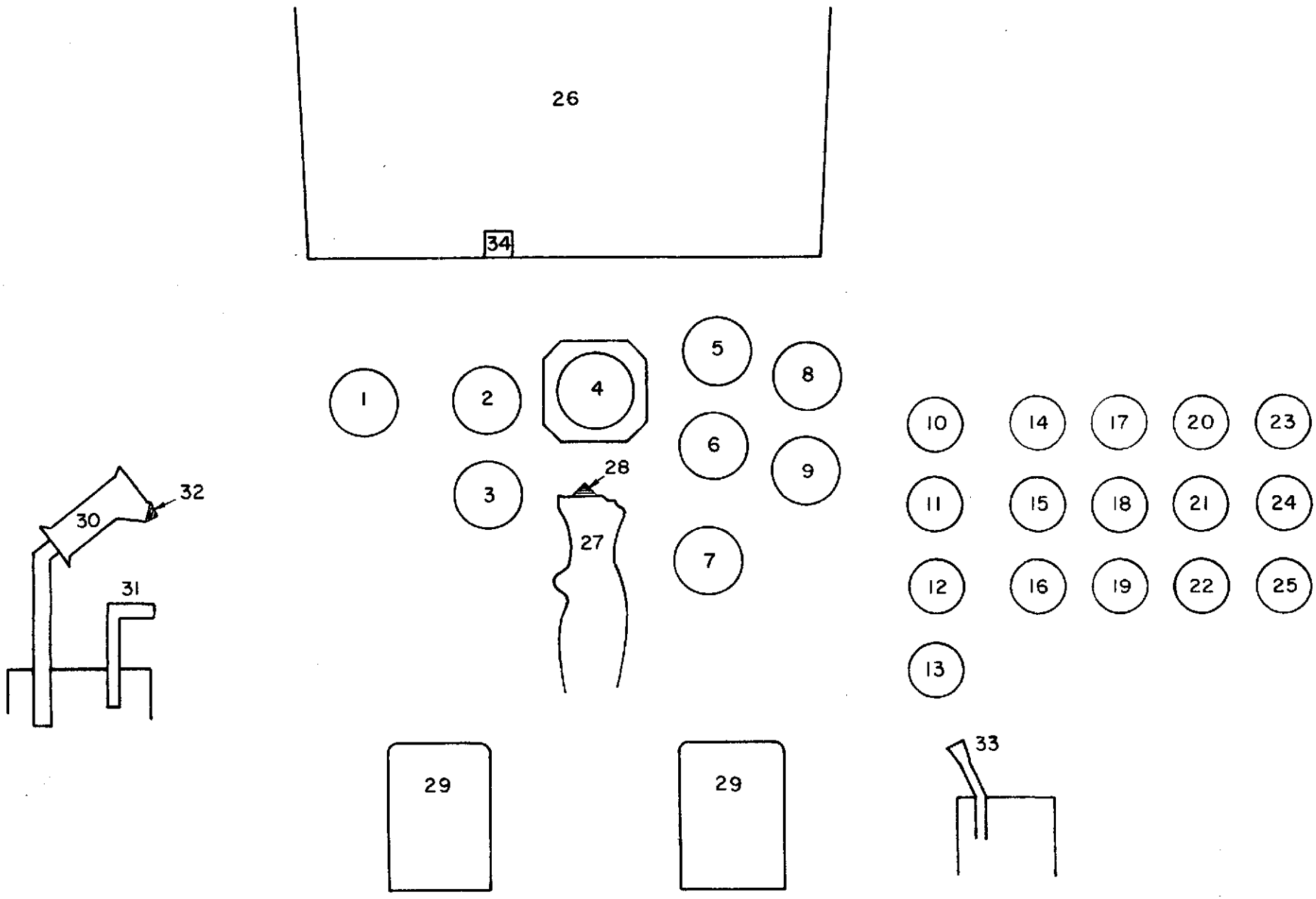

a. Layout

Figure II-3. Instrument Panel (October/November 1972)

Figure II-3

b. Key to Instrument Panel Layout

1. Angle of attack
2. Indicated airspeed
3. Turn and bank indicator
4. Artificial horizon (including glide slope and localizer display)
5. Barometric altimeter
6. IVSI
7. HSI (including localizer display)
8. Radar altimeter
9. Normal accelerometer
10. Not used
11. Cross-shaft RPM
12. Flap position
13. Clock
14. No. 1 propeller pitch
15. No. 1 engine RPM
16. Not used
17. No. 2 propeller pitch
18. No. 2 engine RPM
19. Not used
20. No. 3 propeller pitch
21. No. 3 engine RPM
22. Not used
23. No. 4 propeller pitch
24. No. 4 engine RPM
25. Not used
26. Virtual image TV display
27. Control stick
28. Pitch/roll trim button
29. Rudder pedals
30. Throttle
31. Flap handle
32. Drag switch (flap/transparency control)
33. Propeller RPM handle
34. Angle of attack chevrons

Table II-4

SUBJECT PILOT BACKGROUND

LTC. ROBERT CHUBBOY (USA) R & D SPECIALIST FAA	RICHARD GOUGH FLIGHT TEST PILOT FAA	GORDON HARDY RESEARCH PILOT NASA	ROBERT KENNEDY FLIGHT TEST PILOT FAA
• Current rotary wing and light single and twin engine fixed wing. • Extensive STOL test and operational experience (DHC-2, 4, 5, 6). • Extensive rotary wing test and operational experience in a wide range of helicopters. • Extensive research simulator experience in a wide variety of aircraft.	• Current experience in conventional airplane airworthiness certification programs (DC-10, L-1011, etc.). • Research test pilot for USAF flying wide range of conventional fixed wing aircraft. (fighter, bomber, trainer, utility, light STOL). • Limited STOL experience (YC-134, BR 941 S). • Little rotary wing experience. • Little ground based simulator experience. • R & D subject in TIFS (Concorde).	• Current flight experience largely in conventional aircraft (CV-340, CV-990, Lear Jet). • Limited experience in several STOL aircraft (DHC-5, DHC-6, AWJSRA, BR941S) as research pilot. • No helicopter experience. • Extensive light aircraft experience. • Military experience in conventional single engine fighter/attack aircraft. • Research simulator experience in a range of handling qualities experiments (space shuttle, DHC-6, AWJSRA, etc.).	• Seven years experience as FAA flight test pilot. (participated in STOL project at NAFEC using DHC-6 and Heliporter). • Experienced test pilot for Piasecki and Vertol in ducted fan aircraft and helicopters. • Considerable simulator experience. • Military experience in wide range of aircraft (fighter, bomber, transport, helicopter, etc.).

5. Piloting Tasks

The simulation effort was divided between the approach phase (about 95%) and the takeoff phase. In the approach phase the following were evaluated:

- Nominal approach and landing (-7.5 deg glide slope)
- Nominal approach with α display
- Steep approach (-9.5 deg glide slope)
- Approaches with and without transparency.

The takeoff phase consisted of evaluating various combinations of V_R and V_2 with and without turbulence.

For each of the tasks (e.g. nominal approach and landings, steep approach, etc.) the pilot was given a formal flight card containing pilot instructions. A sample card is shown in Fig. II-4.

For approach and landing the following sequence of events took place:

- Airplane was initially trimmed for straight and level flight at 80 kt and 1600 ft, 45 deg flap, about 5 miles from airport, in IFR conditions, near localizer edge, and inbound to localizer at 45 deg intercept angle.
- Pilot was given surface wind conditions (this information was intentionally not always accurate).
- Pilot intercepted localizer (approximately 084 deg) and turned on inbound leg.
- Prior to glide slope intercept, 70 deg flap was selected and airspeed trimmed at 65 kt.
- Pilot intercepted glide slope and selected full flaps (and transparency if used) to begin descent.
- If VFR at decision height, then landing was continued to touchdown and rollout.
- If IFR at decision height, the pilot applied full throttle and brought flaps to 70 deg position with thumb switch. Target airspeed was 60 kt.
- After missed approach configuration was set and the pilot had a stabilized situation, then 45 deg flap was selected and airspeed trimmed at 70 kt.
- Pilot continued missed approach climb on 90 deg heading to 1100 ft.

Figure II-4

FLIGHT CARD NUMBER 14

MANEUVER	CONFIGURATION	CONDITION
Nominal Approach and Landing:	Initial: T.O. Flaps (δ_f = 45 deg)	Initial: Speed = 80 knots; altitude = 1600 ft;
	Approach: Flap 95 deg	Level flight (γ = 0 deg)
Formal Testing	Go-around: Flap 70 deg	Approach: G/S = -7.5 deg --- 65 kt

Pilot Task

Aircraft will be initially trimmed at 1600 ft in the takeoff configuration (i.e., δ_f = 45 deg) with power for level flight along 45 deg heading. Continue heading to localizer intercept and execute constant altitude line-up. Bank angle should not exceed 25 deg. Convert to approach configuration while maintaining constant altitude. Descend along 7.5 deg glide slope after G/S intercept using 95 deg flap. After breakout pilot will complete visual approach and landing using full reverse thrust after complete firm controllable touchdown.

Pilot should avoid applying full reverse at touchdown to prevent loss of lateral control.

If breakout does not occur at the decision height (i.e., 200 ft), he will execute straight-out go-around.

Normally, 10 runs will be flown in this Formal Testing phase.

Evaluation

1. Ability to execute line-up, conversion, and glide slope capture.
2. Opinion of performance and precision of flight path control and landing maneuver.
3. Was approach speed adequate? Was there enough margin to counter wind shear?
4. Describe control technique for:
   a. Line-up
   b. Glide slope tracking
   c. Flare and touchdown

The approach and landing sequence, as outlined above, was typically flown 10 times during any one series of runs for a given approach speed and configuration. During these 10 approaches the mean wind was varied in random order. In 3 out of the 10 cases the ceiling was set low enough to force the pilot to go around. An engine was failed on 2 out of the 3 go-arounds as well as during one of the landings. Pilots were not warned prior to the go-around and/or engine out conditions.

The turbulence model used during these tests was designed to generate the spectra given by the Dryden form of the continuous random gust model given in Section 3.7.2.1 and 3.7.5 of Ref. 5. Wideband Gaussian noise sequences, generated internally in the program, were filtered to produce the required spectra. The spectra are functions of the scale lengths L_w, L_u, and L_v defined in Table II-5.

During the 1972 tests, it was discovered that the noise generators were not producing enough low frequency power to adequately reproduce the Dryden spectra. This problem was corrected prior to the 1973 tests.

During the 1972 tests, the nominal turbulence level was set such that the standard deviation of the u gusts (σ_{u_g}) was 3 ft/sec. Fig. II-5 indicates the probability of exceeding a given turbulence level on an average day as a function of σ_{u_g} ($\sigma_{u_g} \geq 3$ ft/sec 35% of the time).

The wind conditions simulated in the 1972 tests are depicted in Fig. II-6, where wind speed is shown as a function of altitude. For all cases, the runway heading was 090 deg. For all cases except 6, the wind speed was held constant for altitudes greater than 300 ft. For Case 6 the gradient (4 kt per 100 ft) was constant up to 500 ft.

The runway and ILS geometry was set largely according to Ref. 3. The overall approach geometry is shown in Fig. II-7. A larger scale view of the runway and ILS geometry is shown in Fig. II-8. The localizer offset angle was adjusted so that regardless of glide slope angle, the slant range from the decision height to the runway centerline intersection remained constant at 500 ft.

6. Data Gathering

Data gathered in the course of this experiment can be grouped as:

- Digital printout of specific performance metrics

TABLE II-5

TURBULENCE PARAMETERS

I	$h \geq 1750$ ft	$L_u = L_v = L_w = 1750$ ft
II	$100 < h < 1750$	$L_w = h$ $L_v = L_u = 145\ (h)^{1/3}$ ft
III	$h \leq 100$	$L_w = 100$ ft $L_u = L_v = 671.35$ ft

Note: For all conditions $\sigma_{u_g} = \sigma_{v_g}$ and $\sigma_{w_g} = \sigma_{u_g} \sqrt{\frac{L_w}{L_u}}$

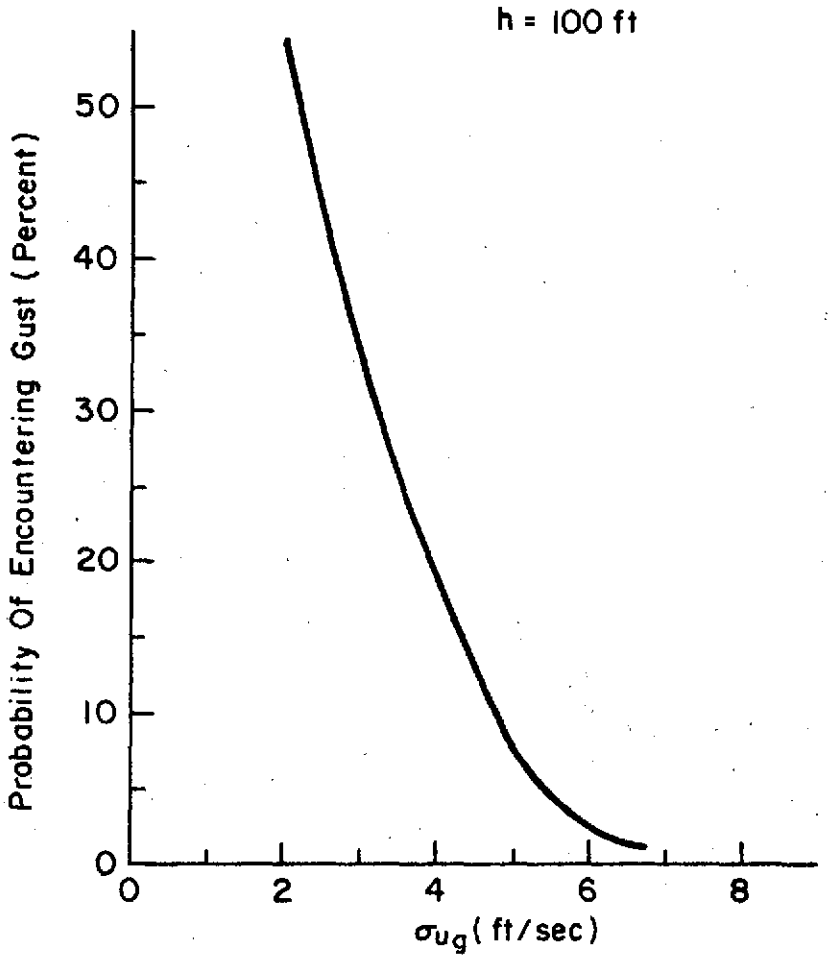

Figure II-5. Turbulence Distribution

Notes:

1. HW Indicates Headwind
2. TW Indicates Tailwind
3. Cases 1, 2 & 3 Are Go-Arounds
4. Runway Heading = 090 deg
5. σ_{u_g} = 3 ft/sec
6. x/y → Wind Heading = x deg at y kt
7. In Case 6 the wind gradient is constant up to 500 ft (10kt headwind at and above 500ft)

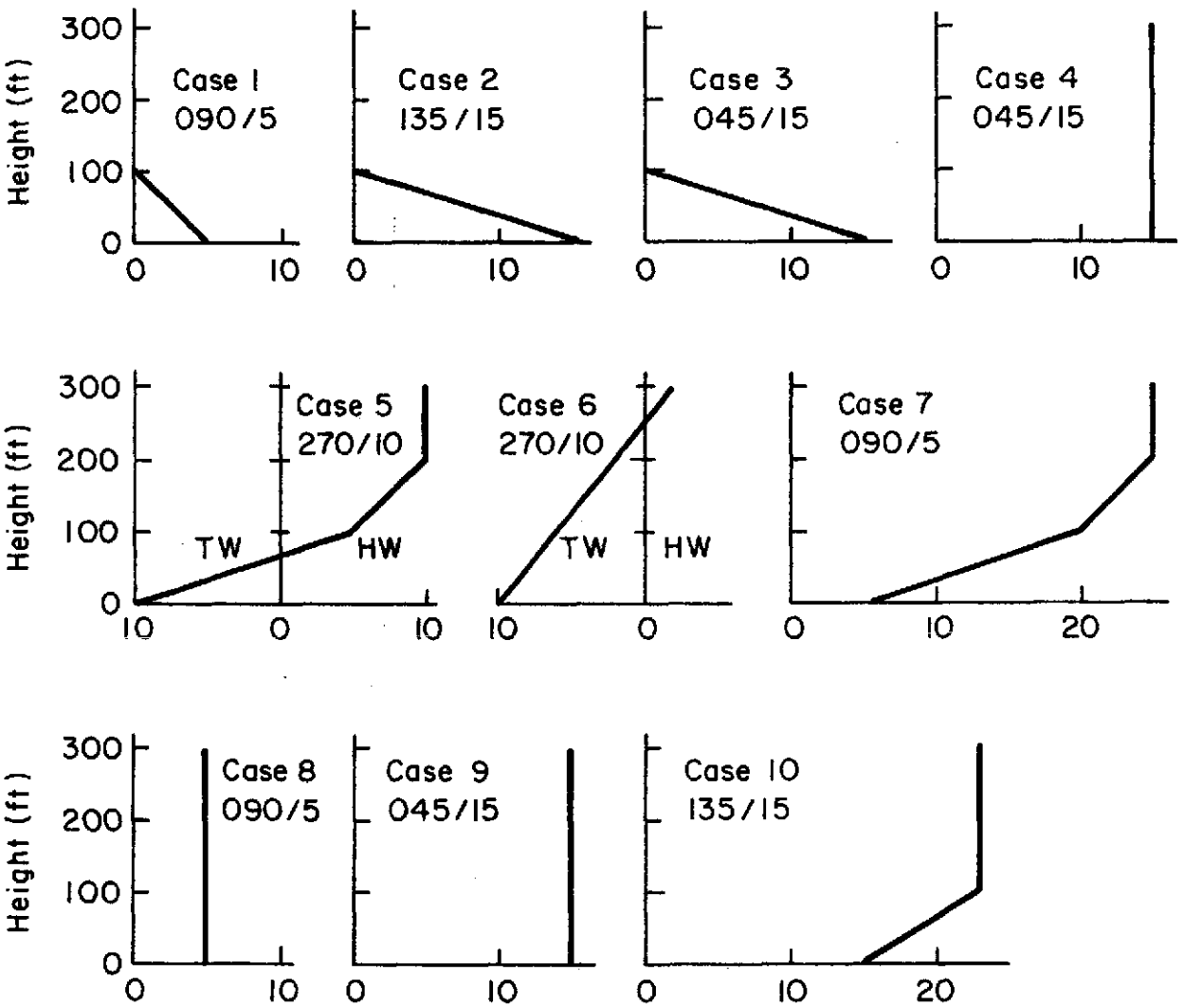

Figure II-6. Wind Profiles, 1972

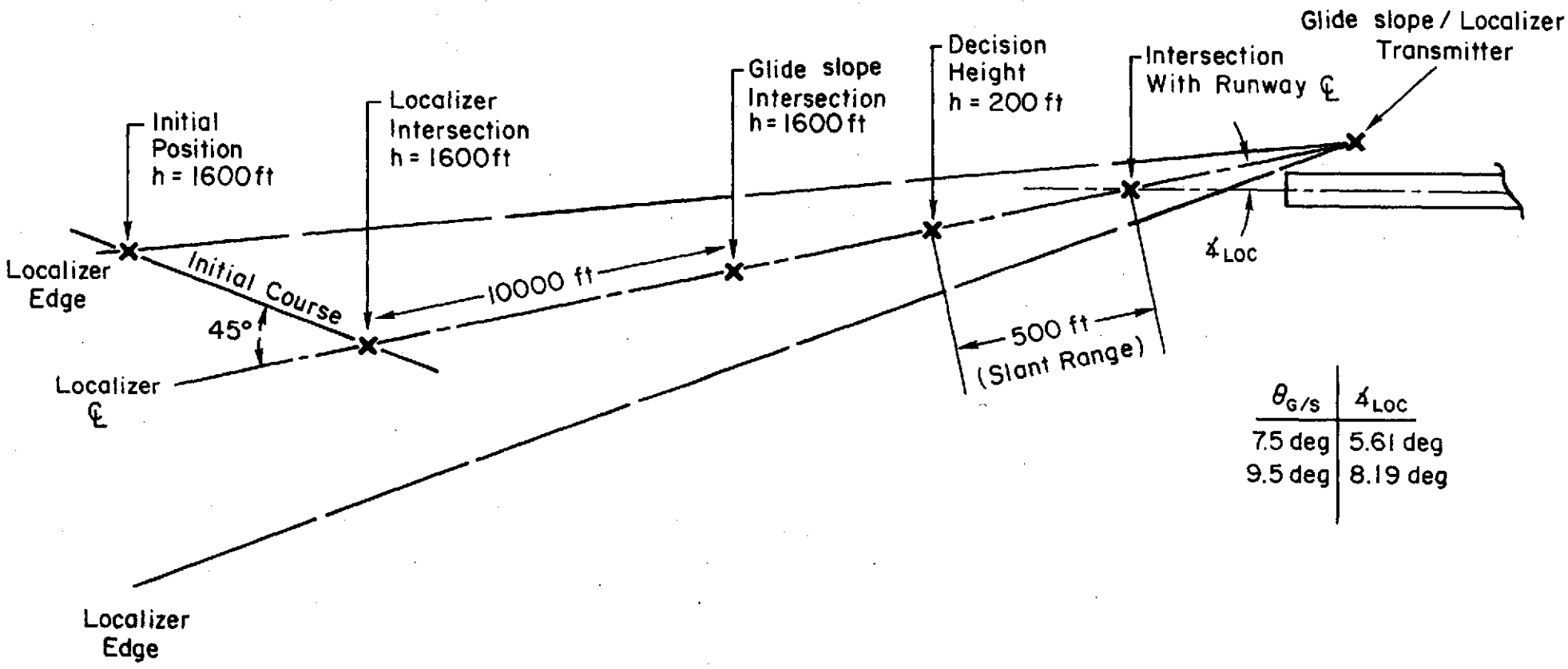

Figure II-7. Approach Geometry

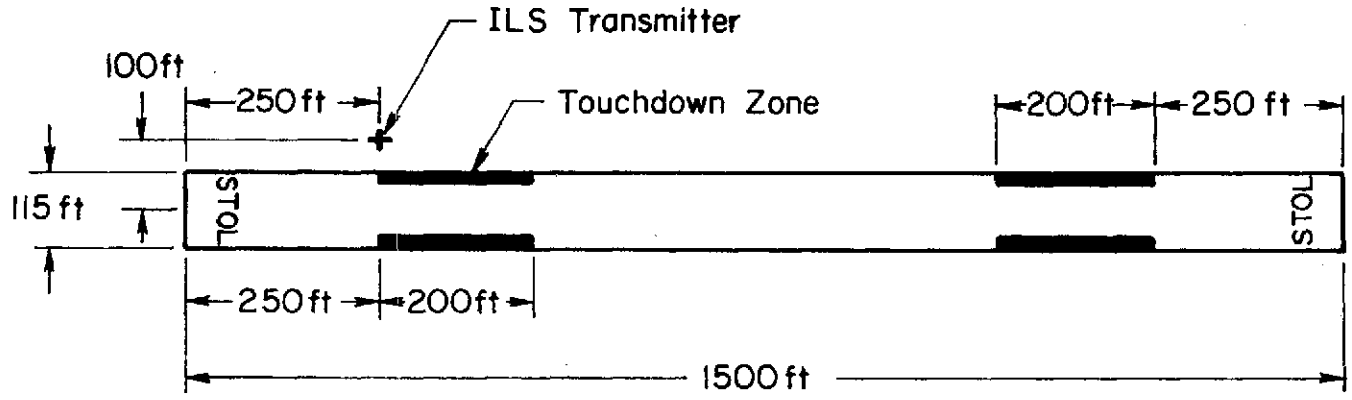

Figure II-8. Runway/ILS Geometry

- Digital plots of aircraft position and ILS
- Analog strip chart recordings of aircraft variables, control inputs, and disturbances
- Pilot comments given during formal debriefings
- Pilot comments recorded on request during the runs.

Samples of the digital printouts are given in Figs. II-9 through II-11 for takeoff, landing, and missed approach situations.

B. APRIL/MAY 1973 SIMULATION PERIOD

The simulation description for this period is the same as for the previous period with the following exceptions.

1. Simulator Apparatus

The FSAA was again used but with the VFA-VII Redifon. This involved use of a different visual scene and an improved optical system (increased depth of field).

2. Mathematical Model

The same basic BR 941S model was used. However, to reduce pilot workload certain stability and control modifications were made. The most important of these was the addition of a longitudinal and directional SAS. The longitudinal SAS consisted of an attitude command/attitude hold system. The effect of this was to quicken short period response and damp the flight path modes. Fig. II-12 shows the effect of the longitudinal SAS on a step control input.

The directional SAS was intended to help coordinate turns. It decreased the long heading delay of the bare airframe (about 4 sec) and increased the dutch roll damping. Fig. II-13 shows the effect of the SAS on a step lateral input. In order to provide sufficient de-crab control the pedal-to-rudder gearing was increased by a factor of 2 with the SAS on*. Fig. II-13 shows that the de-crab response to a rudder step was slightly improved over the unaugmented airplane. Both SAS designs are shown in block diagram form in Fig. II-14.

---

* The directional SAS was automatically turned off at ground contact.

```
                    BREGUET REAL-TIME DATA PRINTOUT

  RUN NUMBER = 13                    DATE: 09:[illegible] NOV 1[illegible]72

  WAIT = 52000.
  CG   = .27
  ITRAN= 0


  REDIFON BREAKOUT =   750.FT
  GLIDE SLOPE ANGLE =   7.50 DEG

 RMS UTURB = 3.26 F/S   RMS VTURB = 4.37 F/S   RMS WTURB =  2.26F/S

  ENGINE FAILURE OCCURED AT   31.08  SEC
      X =   .2961E 04  FT              WHEEL HEIGHT =    .2216E 03  FT    VCAL =   73.1 KTS

  XIC =      0. FT          YIC =    -10.  FT
  HIC =      3. FT        VEQIC =   5.00 KTS
  DELTA PSI =     .0 DEG        GLAPIC =  43.1 DEG

AT ROTATION:      TIME=14.22 SEC
                  X  =     632.75 FT          VCAL  =      64.81 KTS
                  AX =       7.54 FT/SEC      DELTF =      43.13 DEG

AT LIFT OFF:
                  TIME =      15.76 SEC        X    =    1861.17 FT
                  VCAL =      68.63 KTS        THET =      10.62 DEG
                  ALFA =       9.18 DEG        ANZ  =       1.06 G
                  Y    =     -14.30 FT         PSI  =      89.39 DEG
                  PHI  =       1.12 DEG        BETA =      -6.87 DEG

FROM START TO LIFTOFF:
                          MAX                 MIN
  THETD =                 6.34                 -.64   DEG/SEC
  THETA =                10.62                -1.07   DEG
  ALFA  =                 9.26                -2.97   DEG
  ANZ   =                 1.18                  .98   G

DATA AT 35 FT:

                          TIME= 19.82 SEC     X= 1550. FT     HDOT= 10.36 FT/SEC
                          VCAL= 72.90 KTS     DELTF=   43. DEG

DATA FROM LIFTOFF TO 35 FT:

                          MAX                 MIN
  HDOT  =                10.35                 2.87   FT/SEC
  VCAL  =                72.86                68.63   KTS
  THETA =                11.80                 3.57   DEG
  ALFA  =                 9.53                 3.94   DEG
  ANZ   =                 1.12                  .94   G


DATA AT 1000 FT:

                          TIME=113.82 SEC     X=12871. FT     HDOT= 15.26 FT/SEC
                          VCAL= 69.10 KTS     DELTF=   43. DEG

DATA BETWEEN 35 FT AND 1000

                          MAX                 MIN
  HDOT  =                19.63                 1.73   FT/SEC
  VCAL  =                76.55                67.90   KTS
  THETA =                16.71                 9.17   DEG
  ALFA  =                11.79                 3.53   DEG
  ANZ   =                 1.08                  .86   G

MINIMUM OBSTACLE CLEARANCE PLANE =  5.05 DEG
```

Figure II-9

Digital Printout and Digital Plots (October/November 1972)

a. Takeoff

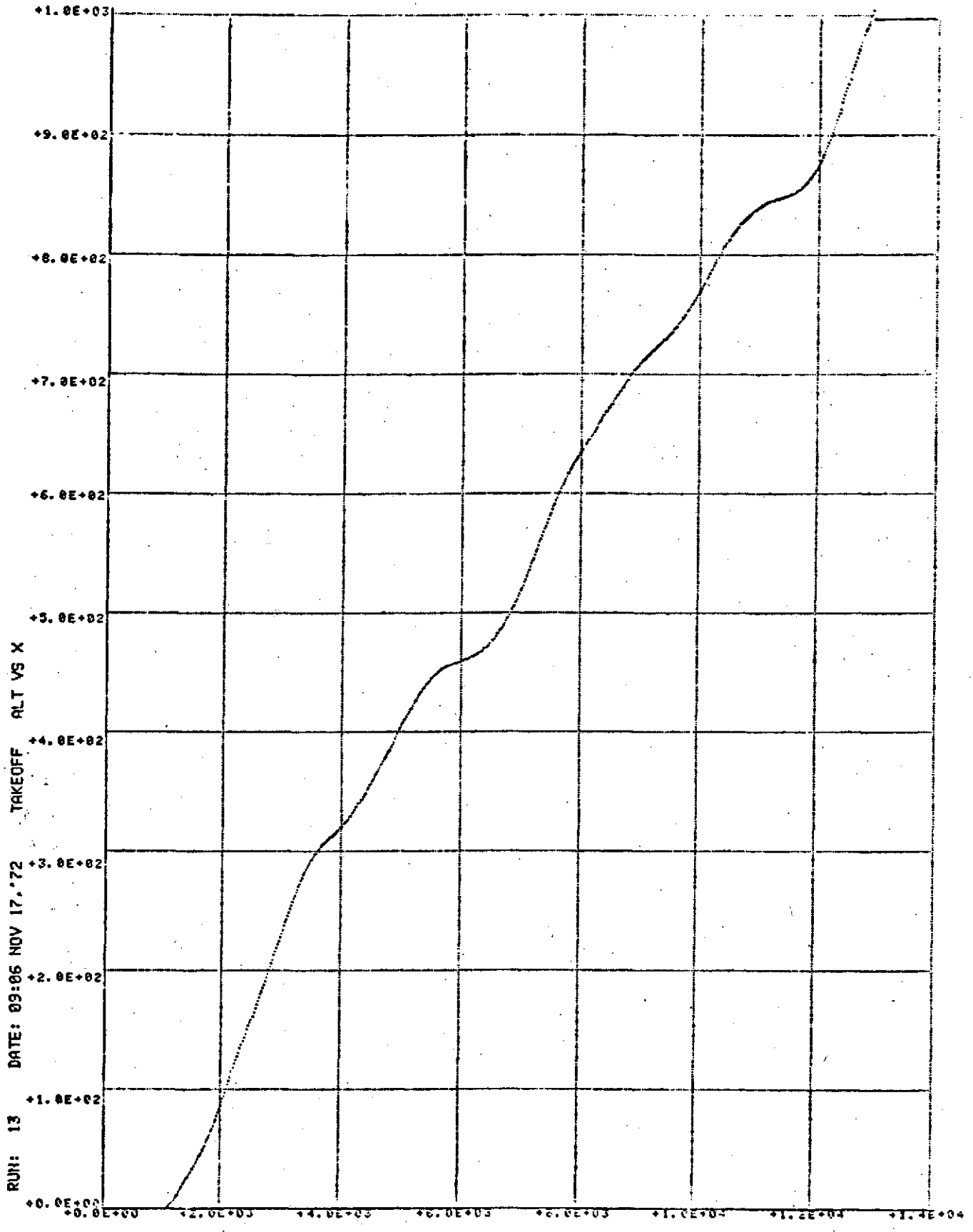

Figure II-9 Concluded

b. Altitude (ft) versus distance from Start of Runway (ft).

BREGUET REAL-TIME DATA PRINTOUT

RUN NUMBER = 12 DATE: 09:31 MAY 03,'73

UNIT = 45088. PITCH SAS = 1
CG = .27 YAW SAS = 1
ITRAN= 0

REDIFON BREAKOUT = 228.FT
GLIDE SLOPE ANGLE = 7.50 DEG

RMS UTURB = 5.87 F/S RMS VTURB = 3.75 F/S RMS WTURB = 2.96F/S

THERE WAS NO ENGINE FAILURE THIS RUN

XIC = -11945. FT YIC = 1087. FT
HIC = 1608. FT VEDIC = 65.88 KTS
DELTA PSI = 8.3 DEG FLAPIC = 95.0 DEG

FROM 1808 FT TO 388 FT

QUANTITY	MAX	HEIGHT	MIN	HEIGHT	MEAN	RMS DEV
LOCALIZER ERROR	1.82 DEG	388. FT	-.79 DEG	701. FT	-.224 DEG	.452 DEG
GLIDE SLOPE ERROR	.41 DEG	587. FT	-.76 DEG	892. FT	-.157 DEG	.407 DEG
CALIBRATED AIRSPEED	69.52 KTS	321. FT	63.05 KTS	705. FT	66.744 KTS	1.714 KTS
VERTICAL VELOCITY	-5.31 FT/S	619. FT	-15.63 FT/S	479. FT	-10.531 FT/S	2.671 FT/S
PITCH ANGLE	-4.49 DEG	622. FT	-7.54 DEG	419. FT	-5.670 DEG	.620 DEG
ANGLE OF ATTACK	2.71 DEG	393. FT	-3.24 DEG	568. FT	-.789 DEG	.868 DEG
NORMAL LOAD FACTOR	1.12 ND	393. FT	.87 ND	587. FT	.996 ND	.039 ND
BANK ANGLE	5.97 DEG	369. FT	-4.82 DEG	490. FT	.571 DEG	2.337 DEG
COLUMN DISPLACEMENT	.43 IN	362. FT	-1.54 IN	526. FT	-.418 IN	.305 IN
WHEEL DISPLACEMENT	3.79 IN	411. FT	-4.34 IN	356. FT	.006 IN	1.478 IN
THROTTLE POSITION	98.92 PCT	824. FT	88.12 PCT	458. FT	89.735 PCT	2.001 PCT
RUDDER PEDAL DISPL.	.65 IN	303. FT	-.10 IN	757. FT	.067 IN	.097 IN
DELTA PSI	9.65 DEG	626. FT	3.73 DEG	451. FT	6.828 DEG	1.590 DEG
PITCH RATE	2.56 DEG/S	407. FT	-2.79 DEG/S	524. FT	.003 DEG/S	.850 DEG/S
GS ERROR RATE	.22 DEG/S	300. FT	-.16 DEG/S	428. FT	.015 DEG/S	.050 DEG/S
LOC ERROR RATE	.42 DEG/S	315. FT	-.17 DEG/S	456. FT	.022 DEG/S	.091 DEG/S
VELOCITY RATE	24.85 KTS/S	798. FT	-22.24 KTS/S.	796. FT	.012 KTS/S	4.755 KTS/S

AT BREAKOUT:
RUN TIME =115.8SEC LOC. ERROR = -.16DEG G/S ERROR = .56DEG
ALTITUDE = 218.FEET X DISTANCE FROM THRESHOLD = -1294.FEET Y DISTANCE FROM THRESHOLD = 47.FEET

FROM BREAKOUT TO 35 FT WHEEL HEIGHT

QUANTITY	MAX	HEIGHT	MIN	HEIGHT	MEAN	RMS
CALIBRATED AIRSPEED	69.85 KTS	77. FT	62.23 KTS	35. FT	67.69 KTS	1.35 KTS
VERTICAL VELOCITY	-7.94 F/S	107. FT	-16.69 F/S	207. FT	-12.81 F/S	2.28 F/S
PITCH ANGLE	-4.84 DEG	124. FT	-7.94 DEG	80. FT	-6.32 DEG	.82 DEG
ANGLE OF ATTACK	1.37 DEG	158. FT	-3.84 DEG	89. FT	-.35 DEG	.97 DEG
NORMAL LOAD FACTOR	1.09 ND	149. FT	.88 ND	89. FT	1.01 ND	.04 ND
BANK ANGLE	13.38 DEG	152. FT	-3.71 DEG	35. FT	3.46 DEG	4.59 DEG
COLUMN DISPLACEMENT	.56 IN	36. FT	-1.33 IN	73. FT	-.55 IN	.37 IN
WHEEL DISPLACEMENT	4.07 IN	36. FT	-4.01 IN	49. FT	.12 IN	2.17 IN
THROTTLE POSITION	98.45 PCT	41. FT	87.51 PCT	66. FT	88.16 PCT	.65 PCT
RUDDER PEDAL DISPL.	1.08 IN	145. FT	-.72 IN	178. FT	.14 IN	.48 IN
DELTA PSI	9.65 DEG	100. FT	-2.27 DEG	187. FT	5.57 DEG	4.19 DEG

LANDING DATA

	MAX	MIN	
HDOT =	-9.19	-12.98	FT/SEC
ANZ =	1.19	.90	G
THETA =	.54	-6.31	DEG
ALFA =	7.59	-.98	DEG
THROT.=	95.58	89.68	PCT
PSI =	6.36	5.83	DEG
PHI =	2.74	-3.69	DEG
DCOL =	2.70	.16	IN

AT 35 FT WHEEL HEIGHT:
RUN TIME = 130.4 SEC X = -5. FEET Y = 2. FEET VCAL = 62.2 KNOTS
HDOT =-11.85 FT/SEC THROTTLE =83.98 PCT LOAD FACTOR = .92 ALFA = -.7 DEG
THETA = -6.38 DEG HEADING OFFSET= 6.4 DEG PHI= -3.7 DEG BETA= 1.8 DEG

AT TOUCHDOWN:
RUN TIME = 133.2 SEC X = 249. FEET Y = 3. FEET VCAL = 57.9 KNOTS
HDOT = -8.95 FT/SEC THROTTLE =35.50 PCT LOAD FACTOR =1.26 ALFA = 6.2 DEG
THETA = .53 DEG HEADING OFFSET= 6.3 DEG PHI= 2.2 DEG BETA= -.0 DEG

AT REVERSE THRUST

RUN TIME =148.4?SEC X DISTANCE = 901.FT Y DISTANCE = 3.2FT

AT END OF RUN

RUN TIME =145.2?SEC X DISTANCE =1144.FT Y DISTANCE = 7.2FT

NO GO-AROUND

MINIMUM OBSTACLE CLEARANCE PLANE = 89.99 DEG AT WHEEL = 869. FT

Figure II-10
Printout and Digital Plots (April/May 1973)
a. Normal Approach and Landing

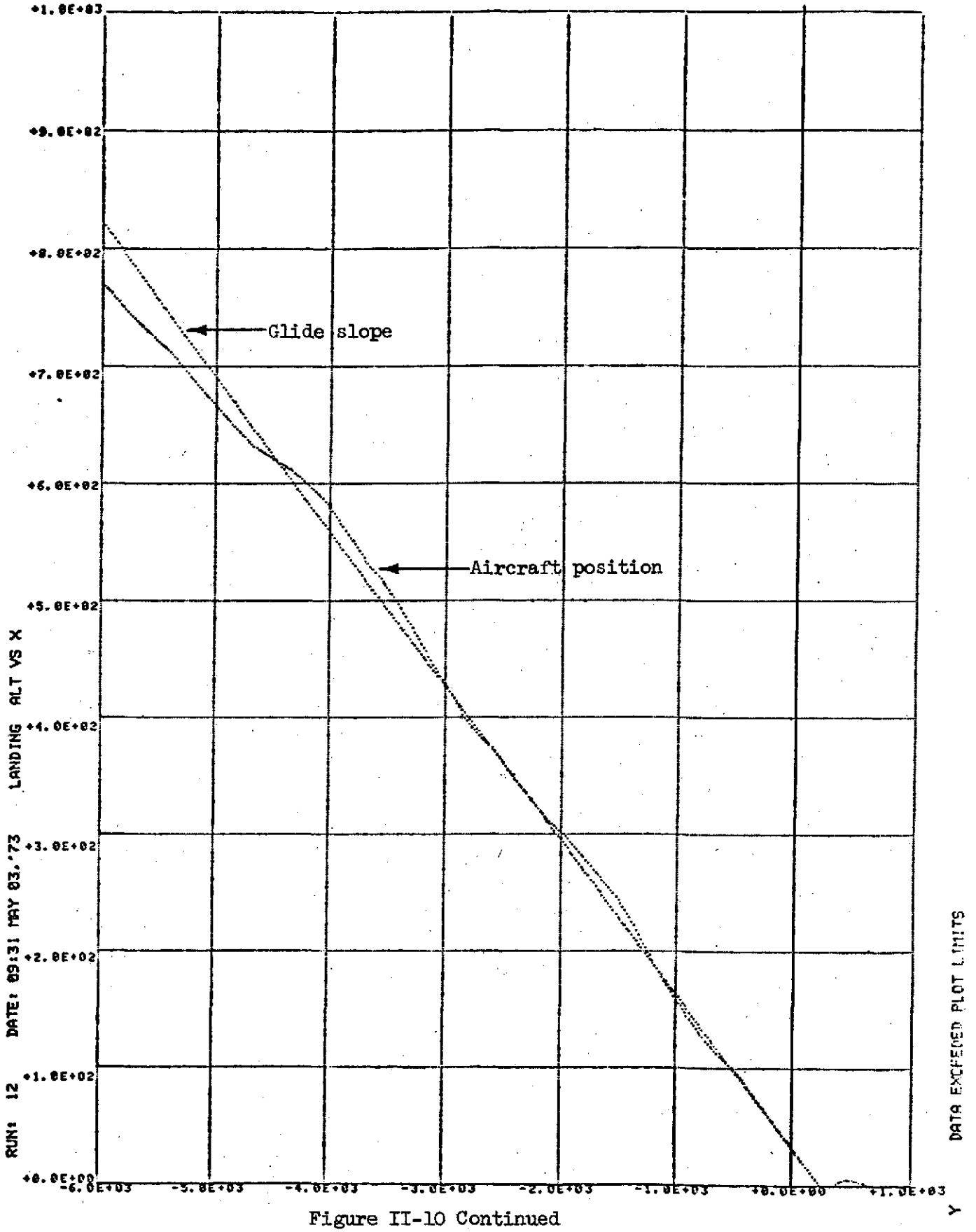

Figure II-10 Continued

b. Altitude (ft) Versus Distance From Start of Runway (ft).

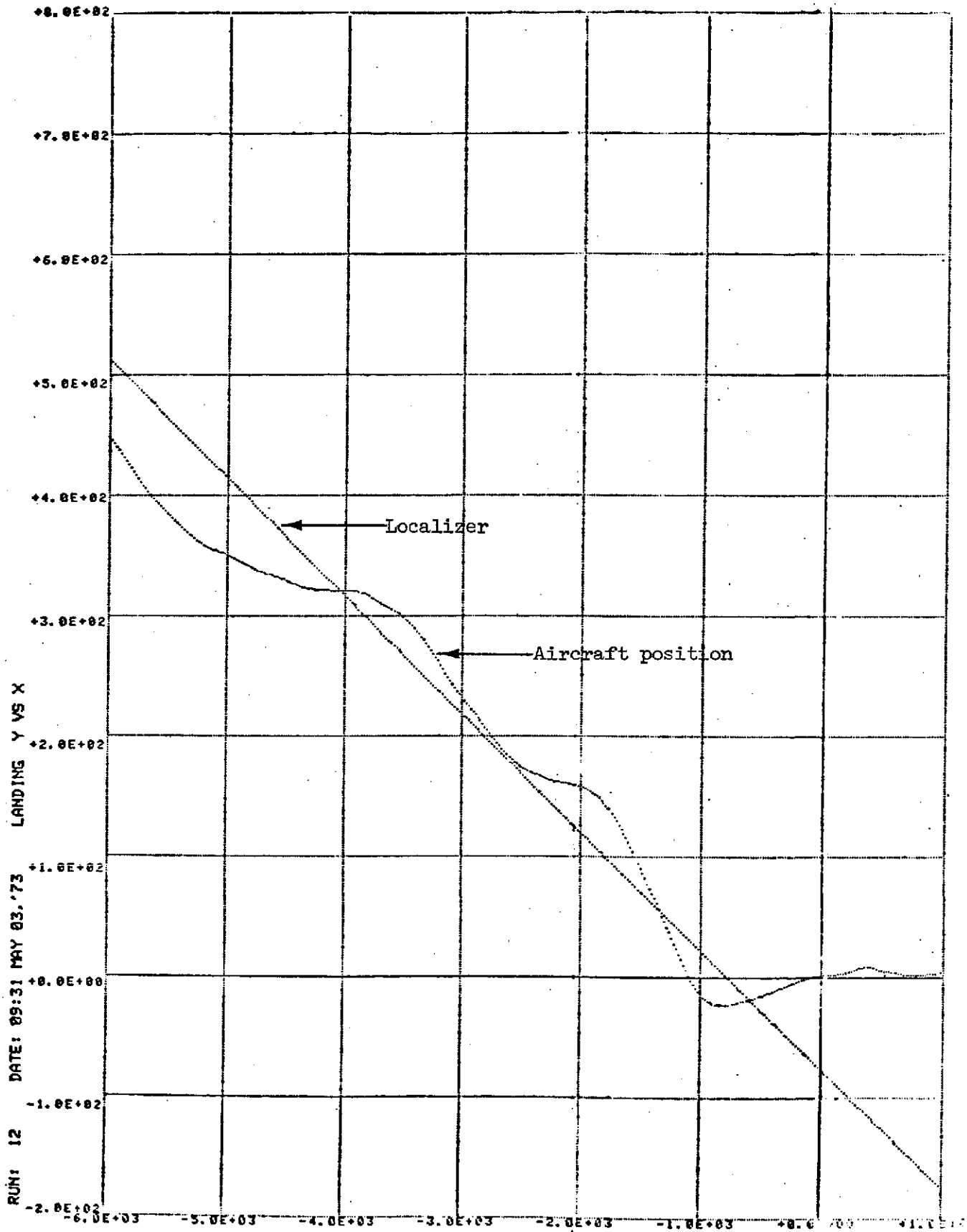

Figure II-10 Concluded

c. Lateral Position (ft) versus Distance From Start of Runway (ft).

```
                    BREGUET PEAL-TIME DATA PRINTOUT

 RUN NUMBER = 14                    DATE: 10:04 NOV 07,'72

 WAIT = 45000.
 CG   = .27
 ITRAN= 1


 REDIFON BREAKOUT =   75.FT
 GLIDE SLOPE ANGLE =  7.50 DEG

RMS UTURB = 3.88 F/S   RMS VTURB = 3.14 F/S   RMS WTURB = 2.84F/S

 ENGINE FAILURE OCCURED AT  190.85  SEC
      X = -.2542E 04  FT              WHEEL HEIGHT =    .3956E 03  FT

 XIC = -24478. FT          YIC =  -137.  FT
 HIC =  1600. FT          VEOIC =  80.00 KTS
 DELTA PSI =   39.4 DEG          FLAPIC =  43.0 DEG

                  FROM 1000 FT TO 300 FT
    QUANTITY              MAX        HEIGHT        MIN        HEIGHT       MEAN        RMS DEV
 LOCALIZER ERROR        -.15 DEG     723. FT    -1.09 DEG     518. FT    -.58 DEG     .32 DEG
 GLIDE SLOPE ERROR       .84 DEG     300. FT      .04 DEG     559. FT     .34 DED     .24 DEG
 CALIBRATED AIRSPEED   66.72 KTS     301. FT    61.32 KTS     893. FT   63.59 KTS   1.57 KTS
 VERTICAL VELOCITY     -9.03 F/S    1000. FT   -20.54 F/S     780. FT  -14.05 F/S   3.21 F/S
 PITCH ANGLE           -9.04 DEG     958. FT   -12.21 DEG     604. FT  -10.68 DEG     .78 DEG
 ANGLE OF ATTACK        -.44 DEG     354. FT    -6.20 DEG     660. FT   -3.32 DEG     .98 DEG
 NORMAL LOAD FACTOR     1.10 ND      323. FT      .85 ND      364. FT     .98 ND      .04 ND
 SIDESLIP ANGLE         3.59 DEG     315. FT    -4.08 DEG     875. FT    -.52 DEG    1.44 DEG
 COLUMN DISPLACEMENT    1.41 IN      604. FT     -.02 IN      351. FT     .83 IN      .25 IN
 WHEEL DISPLACEMENT      .52 IN      550. FT     -.98 IN      517. FT    -.02 IN      .41 IN
 THROTTLE POSITION     95.56 PCT     324. FT    91.26 PCT     377. FT   93.28 PCT    1.79 PCT
 RUDDER PEDAL DISPL.     .18 IN      865. FT     -.52 IN      552. FT    -.00 IN      .08 IN


 AT BREAKOUT:
          RUN TIME =   .0SEC    LOC. ERROR =   .00DEG                    G/S ERROR =    .00DEG
          ALTITUDE =   0.FEET   X DISTANCE FROM THRESHOLD =    0.FEET   Y DISTANCE FROM THRESHOLD =   0.FEET


      DATA NOT VALID FOR 35<H<BREAKOUT

NO LANDING DATA, DID NOT DESCEND BELOW 35 FT

 AT GO-AROUND INITITATION:    WHEEL= 207.1 FT

                          TIME=149.01 SEC    X= -876. FT    HDOT=-14.66 FT/SEC
                          VCAL= 63.25 KTS    DELTF=   83. DEG

 AT 500 FT ALTITUDE

                          TIME=247.60 SEC    X= 3952. FT    HDOT= 22.91 FT/SEC
                          VCAL= 76.72 KTS    DELTF=   43. DEG

                         MAX                MIN
   HDOT  =              23.57              -14.50   FT/SEC
   VCAL  =              82.44               62.03   KTS
   THETA =              12.22               -5.95   DEG
   ALFA  =               3.50               -3.85   DEG
   ANZ   =               1.22                 .88   G

 AT 1000 FT ALTITUDE

                          TIME=277.54 SEC    X= 7546. FT    HDOT= 22.69 FT/SEC
                          VCAL= 73.30 KTS    DELTF=   43. DEG

                         MAX                MIN
   HDOT  =              22.94               11.50   FT/SEC
   VCAL  =              77.37               70.95   KTS
   THETA =              10.78                7.73   DEG
   ALFA  =               4.21               10.63   DEG
   ANZ   =            9999.00            9999.00   G

 MINIMUM OBSTACLE CLEARANCE PLANE =  9.91 DEG
```

Figure II-11

Digital Printout and Digital Plots (October/November 1972).

a. Go-around

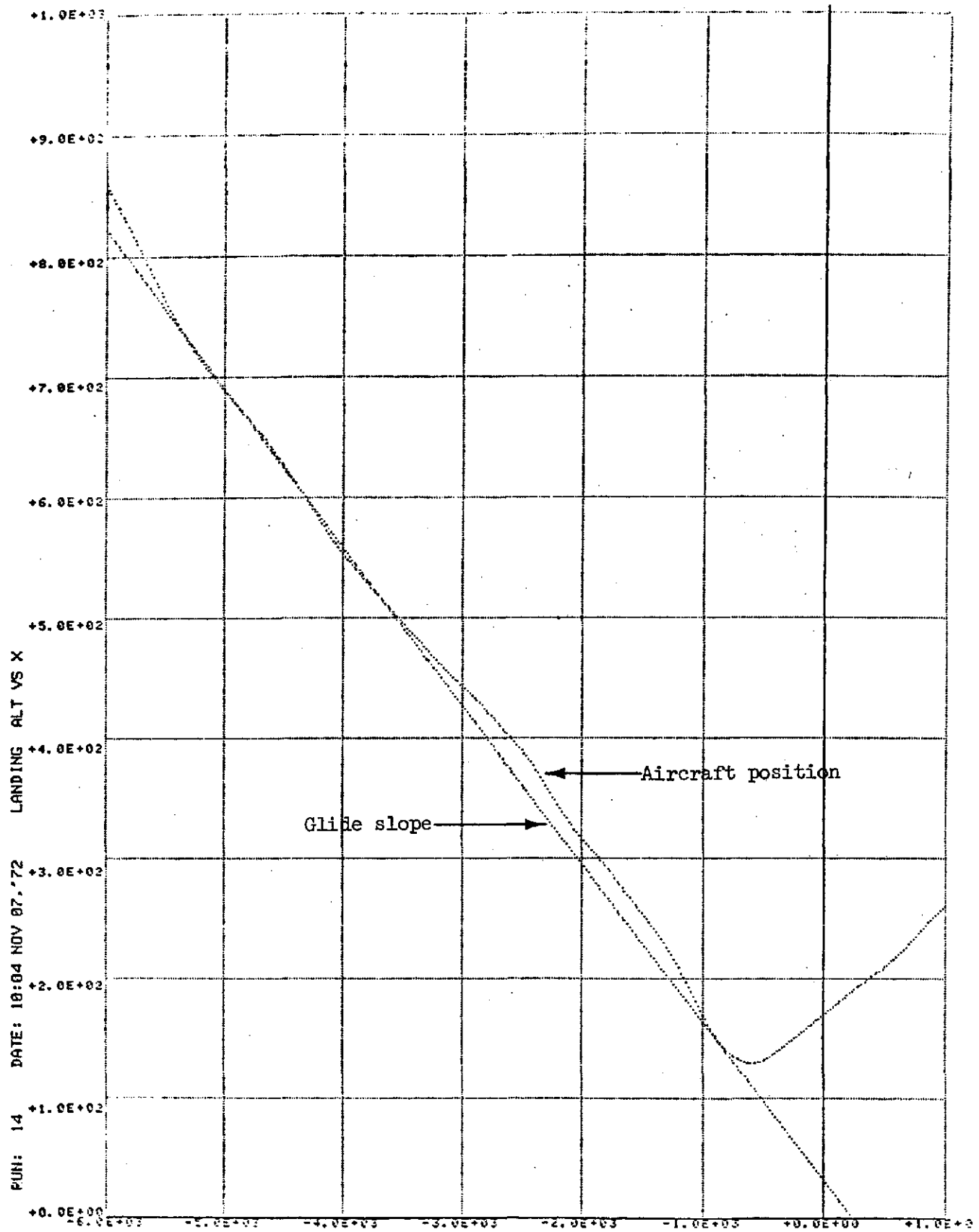

Figure II-11 Continued

b. Altitude (ft) Versus Distance From Start of Runway (ft).

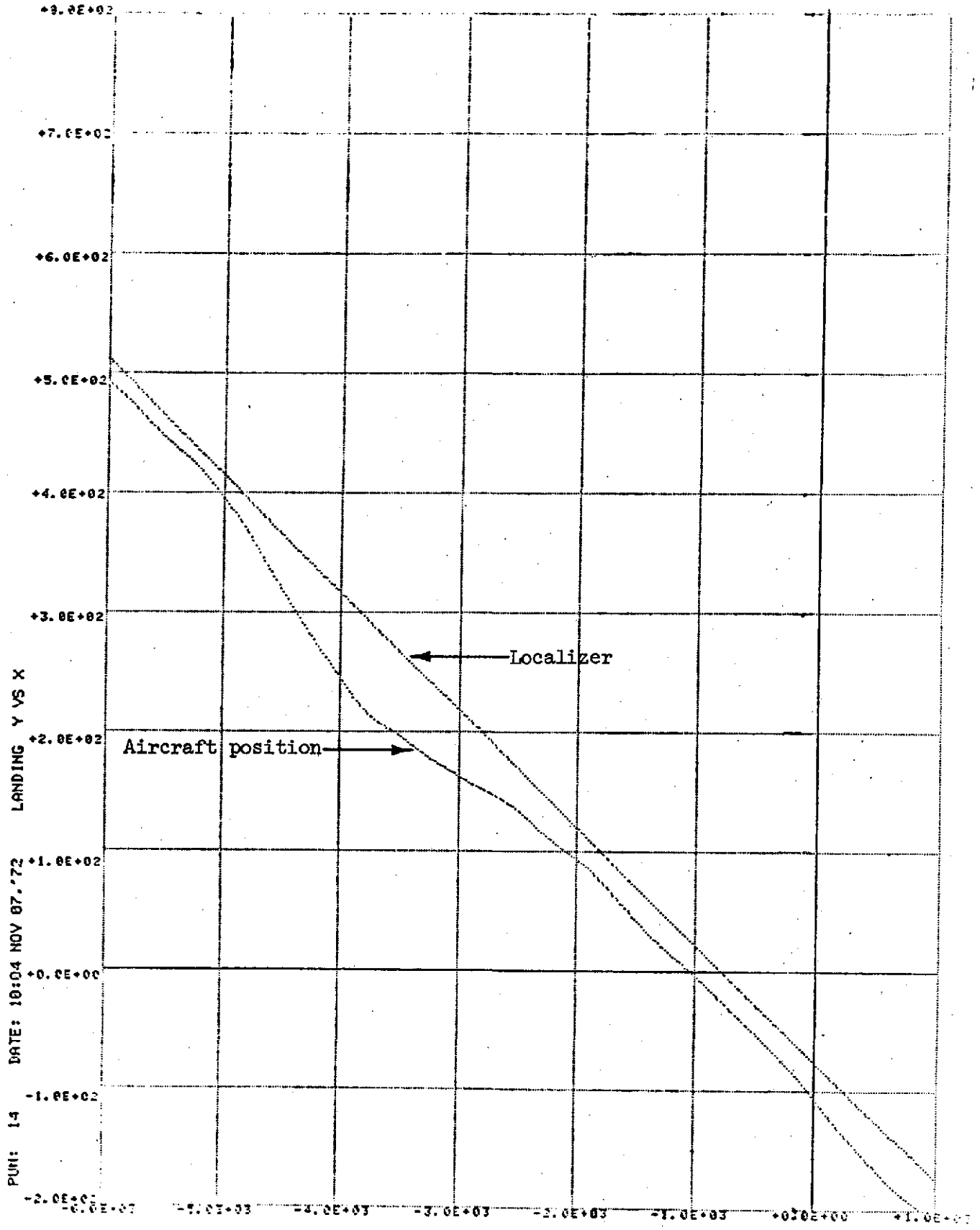

Figure II-11 Concluded

c. Lateral Position (ft) Versus Distance From Start of Runway (ft).

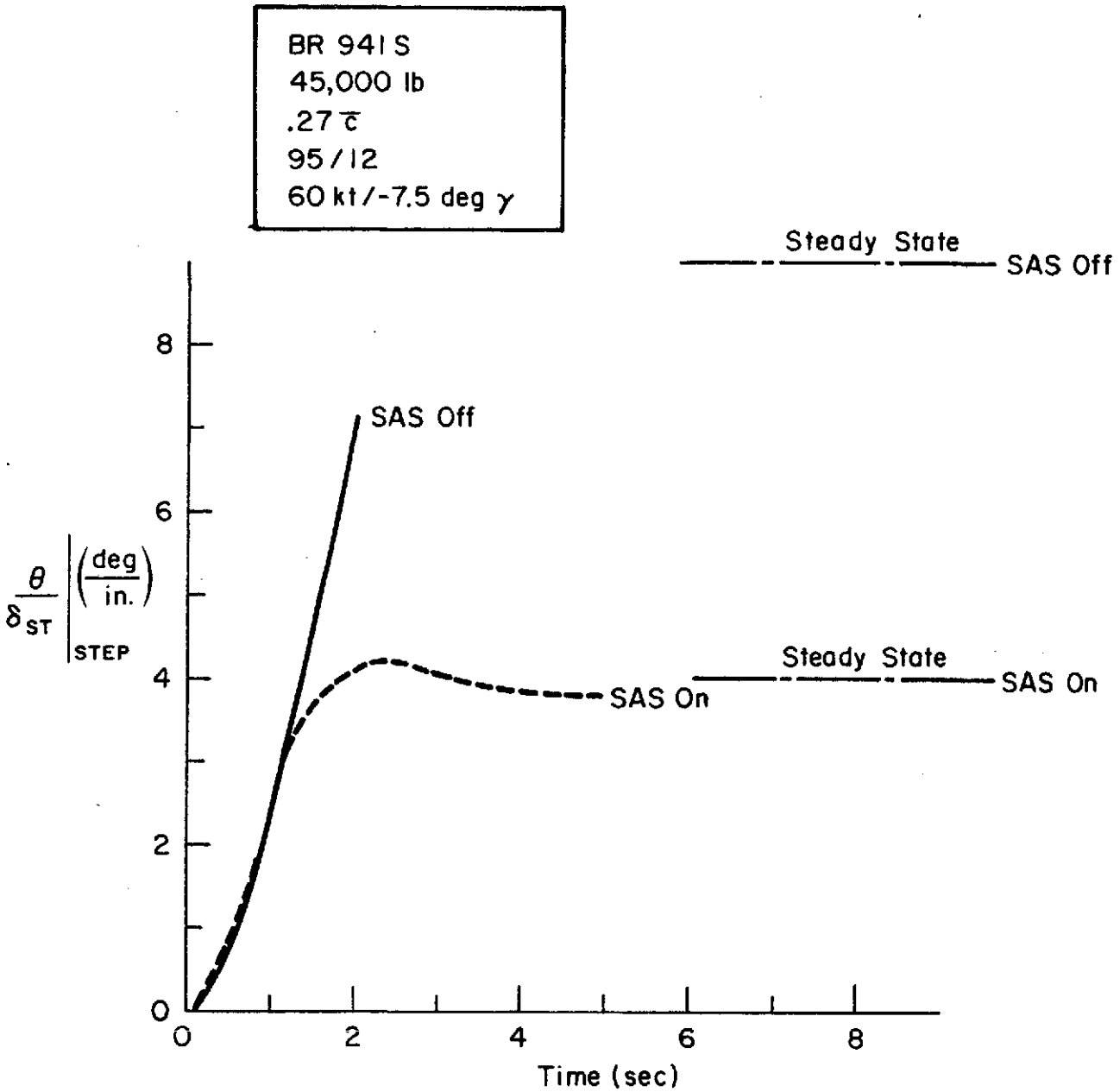

$$\text{SAS Off}: \quad \frac{\theta}{\delta_{ST}} = \frac{136.6\ [.97, .31]}{[.13, .31][.90, .86]\,(20)} \left(\frac{\text{deg}}{\text{in.}}\right)$$

$$\text{SAS On}: \quad \frac{\theta}{\delta_{ST}} = \frac{228.4\,(.20)[.97, .31]}{(.13)[.83, .38][.64, 1.8](18.6)} \left(\frac{\text{deg}}{\text{in.}}\right)$$

Figure II-12. Effect of Pitch SAS

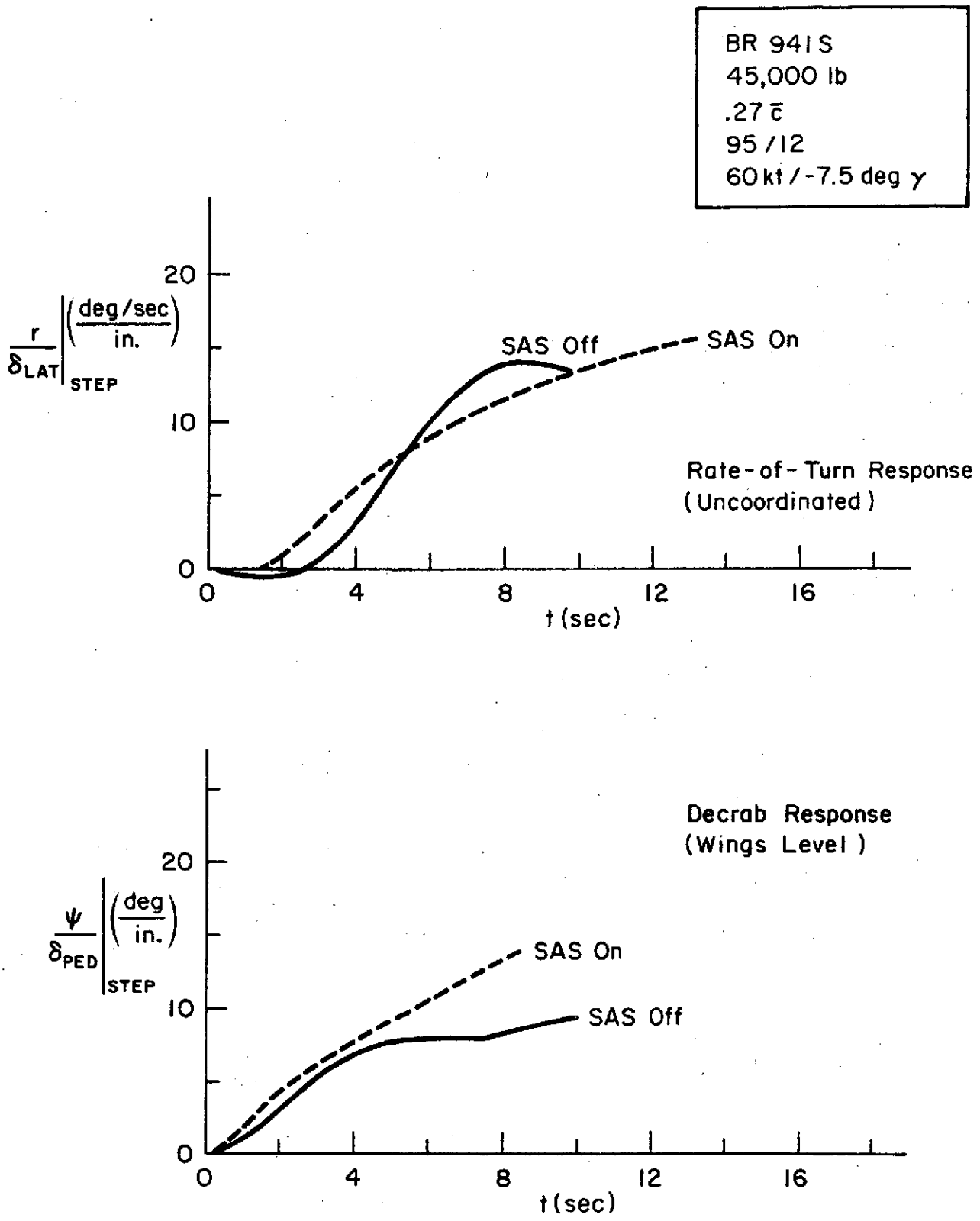

Figure II-13. Effect of Turn Coordination SAS

PITCH ATTITUDE SAS

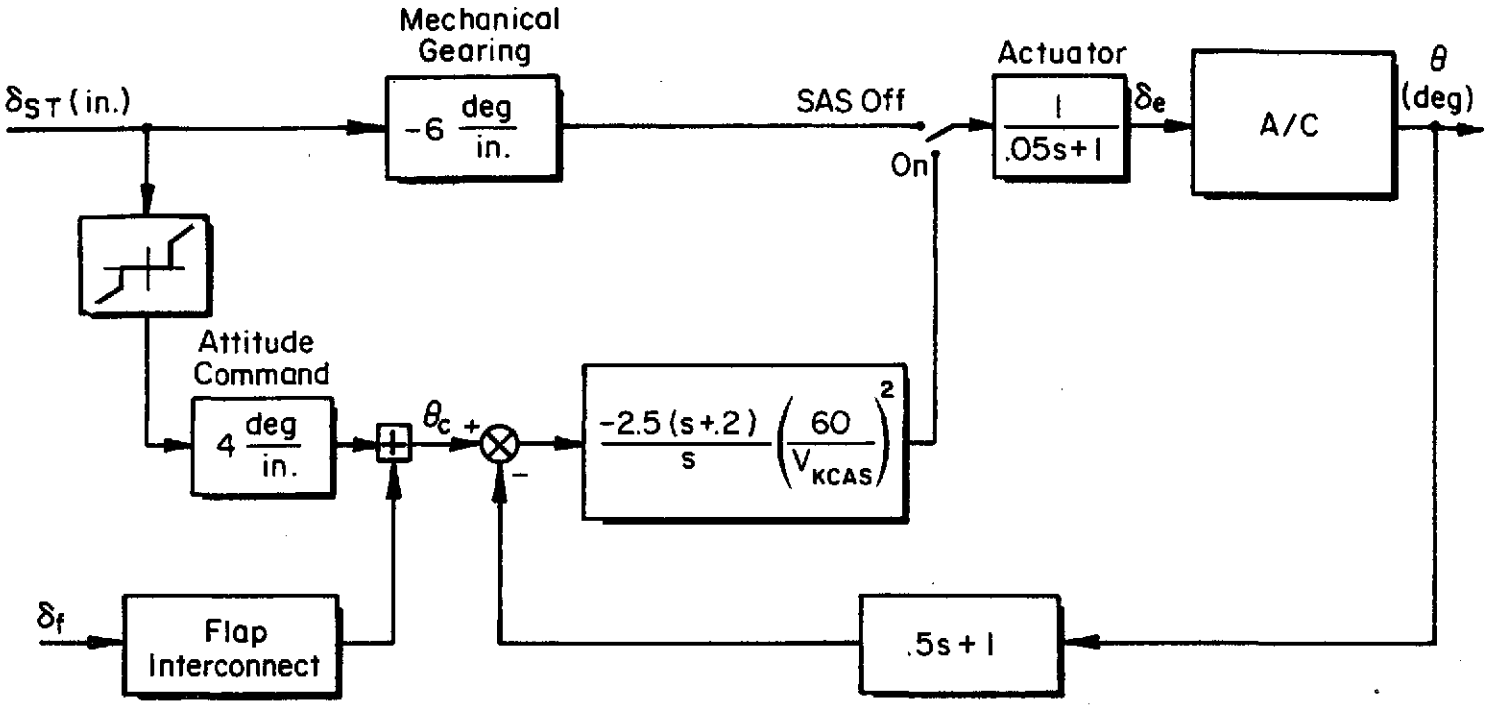

TURN COORDINATION SAS

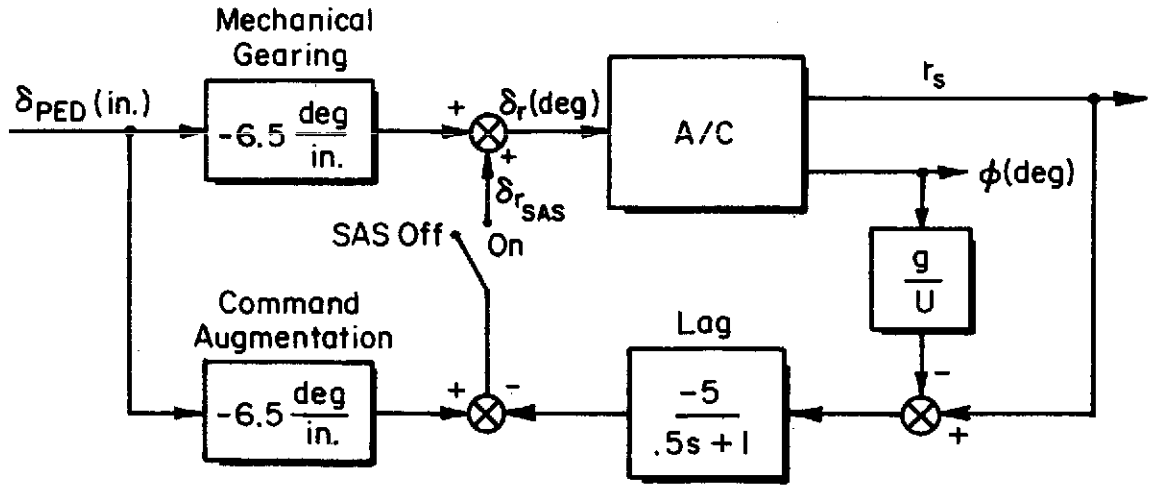

Figure II-14. SAS Block Diagrams

The lateral control with props in reverse pitch was increased from zero to $\frac{\partial C_\ell}{\partial \delta_{sp}}$ = .198/rad (independent of C_L^{Stat}) to provide a normal level of aerodynamic roll control while on the ground. This provided the pilot with a more positive degree of ground handling in the presence of crosswinds. Also, lateral gearing was linearized to cut down on control sensitivity about zero. Lateral control power was unchanged.

A wing incidence increment feature was added to the model. This was done to allow approaches with less nose down pitch attitude. Pilots felt this would aid in the overall impression of the visual scene as well as helping the flare task. The wing incidence was not used as a separate control but fixed by the computer operator. For all normal approaches the wing incidence was set for a 5 deg nose down final approach. Changes in wing incidence only changed the aircraft pitch attitude without affecting the dynamics.

3. Cockpit Layout

The cockpit layout was extensively modified for this series of tests, as shown in Fig. II-15. The fighter type stick and throttle control of the earlier experiment (and of the actual BR 941S) were replaced by a conventional transport column and wheel. The throttle control was changed to one on the center console. This was not done because of any problem with the earlier configuration but rather to be compatible with concurrent simulation of the Augmentor Wing aircraft. Table II-6 shows revised feel system characteristics.

Cockpit instruments were rearranged in an effort to reduce pilot scanning workload. In addition, the fast/slow 'bug' on the artificial horizon was mechanized to indicate either angle of attack or airspeed deviations from a nominal value set by the computer operator. In the angle of attack mode, the full scale deflection was $\pm$ 4 deg while in the airspeed mode the full scale deflection was $\pm$ 5 kt. The instrument layout is shown in Fig. II-16.

Figure II-15

Photograph of Cockpit Layout
(April/May 1973)

TABLE II-6

FEEL SYSTEM CHARACTERISTICS
(April/May 1973)

	BREAKOUT	GRADIENT	LIMITS
Longitudinal Column	± 1 lb	4.7 lb/in	4.18 in fwd 5.85 in aft
Lateral Wheel	± 1.7 lb (measured at Grip)	.153 lb/deg (measured at Grip)	± 50 deg
Rudder Pedals	8 lb	22 lb/in	± 3.0 in

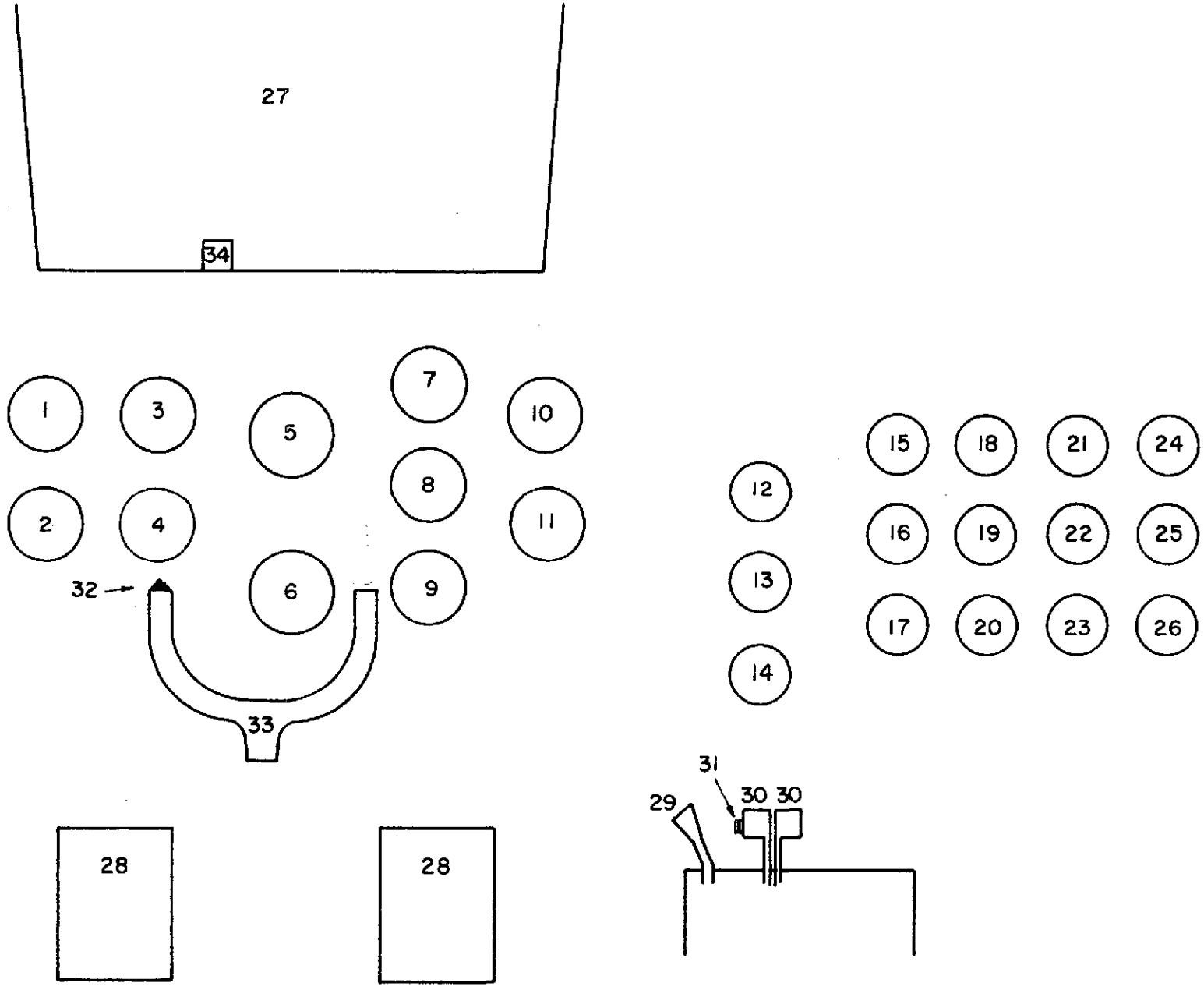

Figure II-6. Instrument Panel (April/May 1973)

a. Layout

Figure II-16 (Concluded)

b. Key to Instrument Panel Layout

1. No. 1 engine RPM
2. Turn and bank indicator
3. Indicated airspeed
4. Angle of attack
5. Artificial horizon (includes glide slope, localizer, and fast/slow indicator)
6. HSI (includes localizer data)
7. Barometric altimeter
8. IVSI
9. Magnetic compass
10. Radar altimeter
11. Normal accelerometer
12. Cross-shaft RPM
13. Flap position
14. Clock
15. No. 1 propeller pitch
16. No. 1 engine RPM
17. Not used
18. No. 2 propeller pitch
19. No. 2 engine RPM
20. Not used
21. No. 3 propeller pitch
22. No. 3 engine RPM
23. Not used
24. No. 4 propeller pitch
25. No. 4 engine RPM
26. Not used
27. Virtual image TV display
28. Rudder pedals (and brakes)
29. Flap handle
30. Throttle (includes reverse thrust lever)
31. Drag switch (flap/transparency control)
32. Pitch/roll trim switch
33. Control wheel
34. Angle of attack chevrons

4. Subject Pilots

The number of pilots participating in formal testing during this phase was reduced to two thus allowing more thorough training. The two pilots were Richard Gough (FAA) and Gordon Hardy (NASA). Both participated in the previous simulation period and therefore helped to provide continuity with the October/November 1972 effort.

5. Piloting Tasks

The main objective of the April/May 1973 simulation was to further examine the approach and landing phases of STOL operations. Special emphasis was placed on obtaining consistent piloting performance and consistent pilot ratings.

The April/May 1973 simulation period was begun with a set of NASA conducted exercises. These were primarily of a training nature and consisted of each pilot flying approaches beginning with more conventional ones (partial flaps, shallow glide slope, and higher speed) and building up to the STOL conditions typical of those flown during formal testing.

The approach task given to the pilot was identical to that of the October/November 1972 simulation. However, extensive training was provided for each new approach condition. Only after the pilot felt satisfied with his level of proficiency was formal testing begun.

Pilot evaluation during formal testing consisted of addressing the questions on the pilot evaluation sheet (Fig. II-17). Pilot ratings were assigned using the modified Cooper-Harper rating scale of Fig. II-18. The Cooper-Harper scale was revised to eliminate ambiguities in addressing the question of airworthiness as opposed to handling qualities. In this modified scale an acceptable configuration would be rated 3 1/2 or less in the calm air test conditions, and 6 1/2 or less in the adverse test conditions (turbulence and low ceiling). Failure to meet either criteria is interpreted as an unacceptable configuration.

A new runway was used in these experiments. The main differences between this one and that of the earlier tests (see Fig. II-19) were:

FIG. II-17

PILOT EVALUATION

Pilot_____ Date_____ Runs_____

Task _____ V_{APP} _____ kt

Pilot Ratings: _____ Calm air

_____ With turbulence

_____ With wind shears

ILS Tracking:

1. Evaluate task difficulty, performance, and safety margins.
2. How were the above affected by the turbulence or low visibility?
3. Describe the piloting technique used.
4. Describe any problems in tracking the ILS beam or maintaining airspeed (or α).

Flare and Landing:

5. Evaluate task difficulty, performance, and safety margins.
6. How were the above affected by the turbulence or wind shears?
7. Describe the piloting technique used.
8. Describe any problems encountered in the flare and landing.

General:

9. What were the major factors involved in each of the three ratings?
10. Add any additional comments you wish to.

FIG. II-18

Modified Cooper-Harper Rating Scale

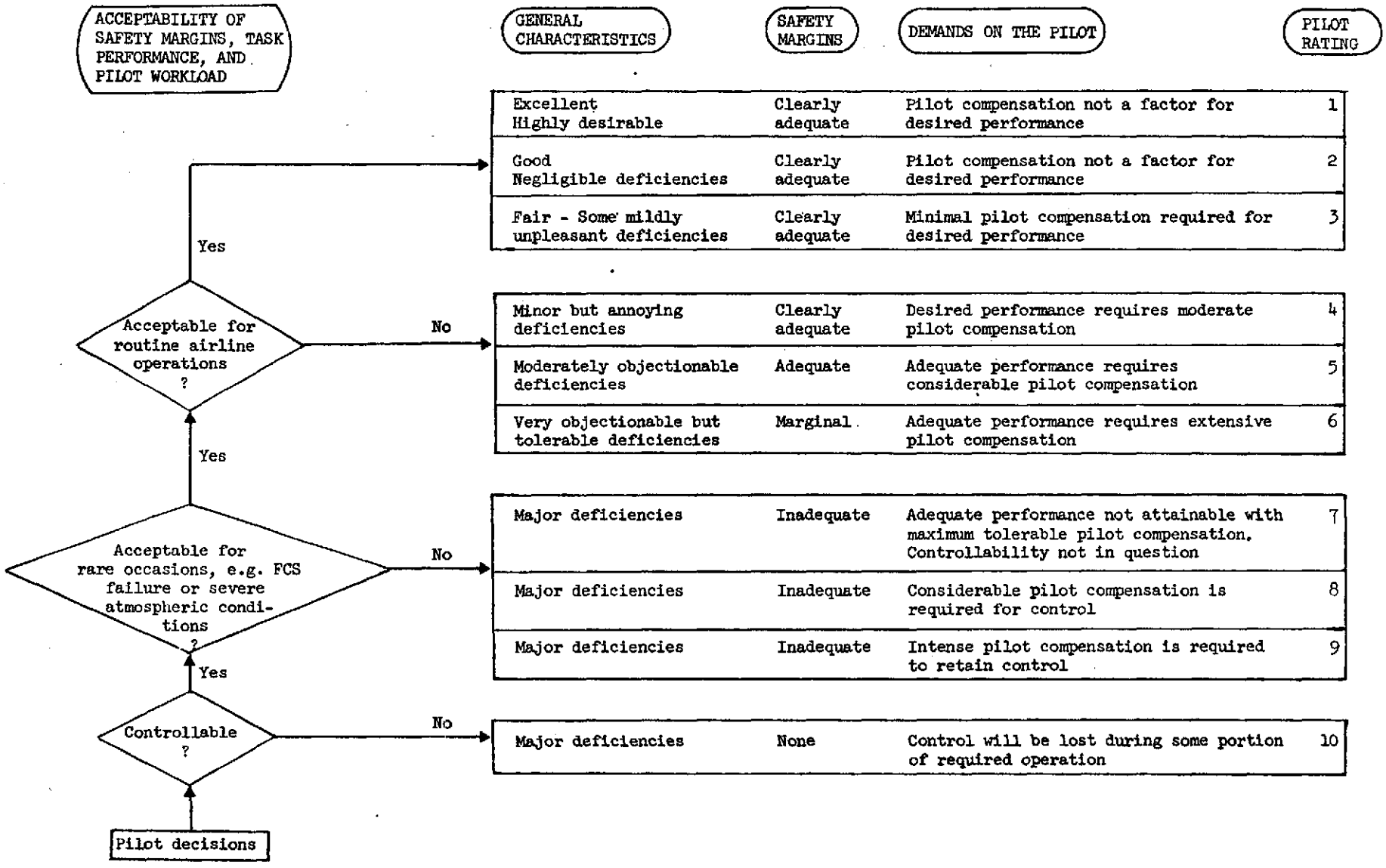

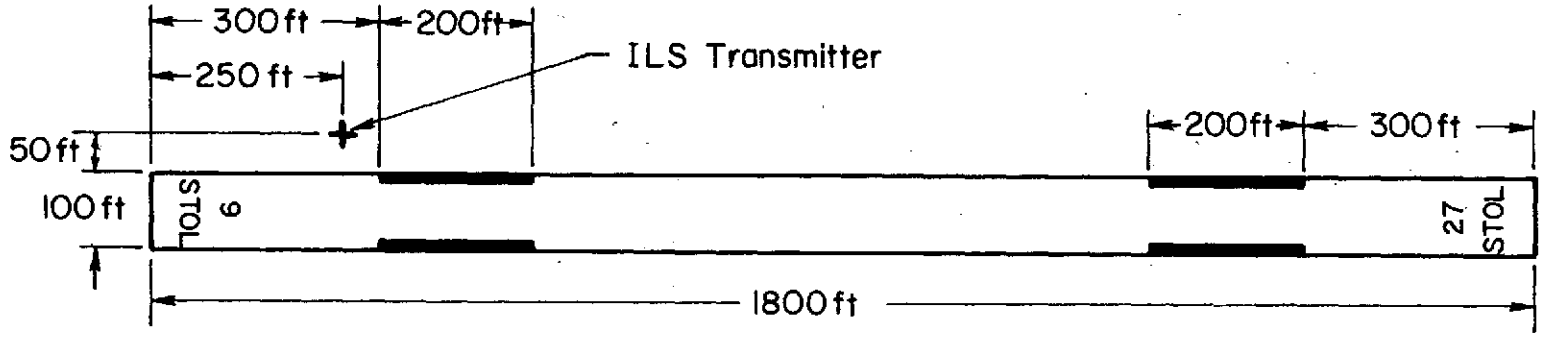

Figure II-19. Runway Geometry

- The touchdown zone was displaced 50 ft down the runway from the glide slope intercept.
- The overall runway length was extended to 1800 ft.

A VASI-like visual glide slope reference was located at the spot where, in real life, the ILS transmitter would have been located. The visual glide slope reference consisted of a horizontal bar fixed on the ground, parallel to the runway threshold, and a vertical board located in front of, and higher than, the horizontal bar. By adjusting the height of the board, different glide slopes could be set. When the board and the bar were aligned, the aircraft was on the correct glide slope. When the aircraft was approximately 2.7 deg low, the bottom edge of the board would line up with the center of the bar. It was estimated that glide slope errors of roughly 0.5 deg could readily be detected when close to the runway.

Prior to this test period the turbulence model had been revised to more adequately simulate the low frequency portion of the spectrum. Also, the nominal value of σ_{u_g} was set at 4.5 ft/sec for the 1973 tests ($\sigma_{u_g} \geq 4.5$ ft/sec 10% of the time, see Fig. II-5). With the exception of these two changes, the turbulence model was unchanged from the 1972 tests. Fig. II-20 is a typical time history of the u and w turbulence levels experienced during a descent from 1600 to 200 ft. During this descent, the nominal turbulence level was 4.5 ft/sec.

The wind conditions simulated in the 1973 tests are depicted in Fig. II-21. The wind speed at 200 ft was held constant for altitudes greater than 200 ft, and the runway heading was 090 deg.

6. Data Gathering

The same means of collecting data was used in these tests as in the previous ones. However, to facilitate data reduction, certain run data were also stored on punched cards for later automatic processing.

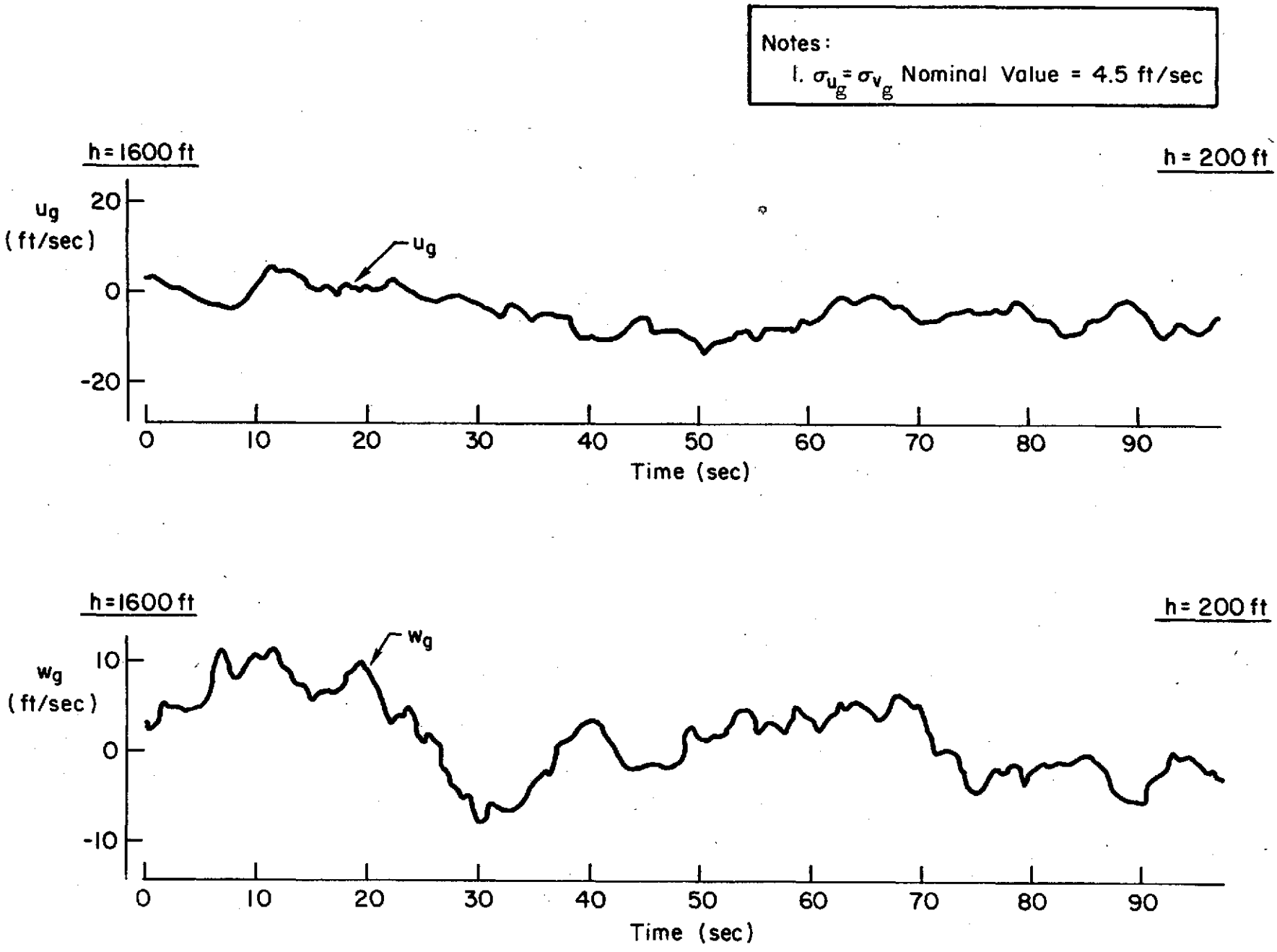

Figure II-20. Typical Turbulence Time History

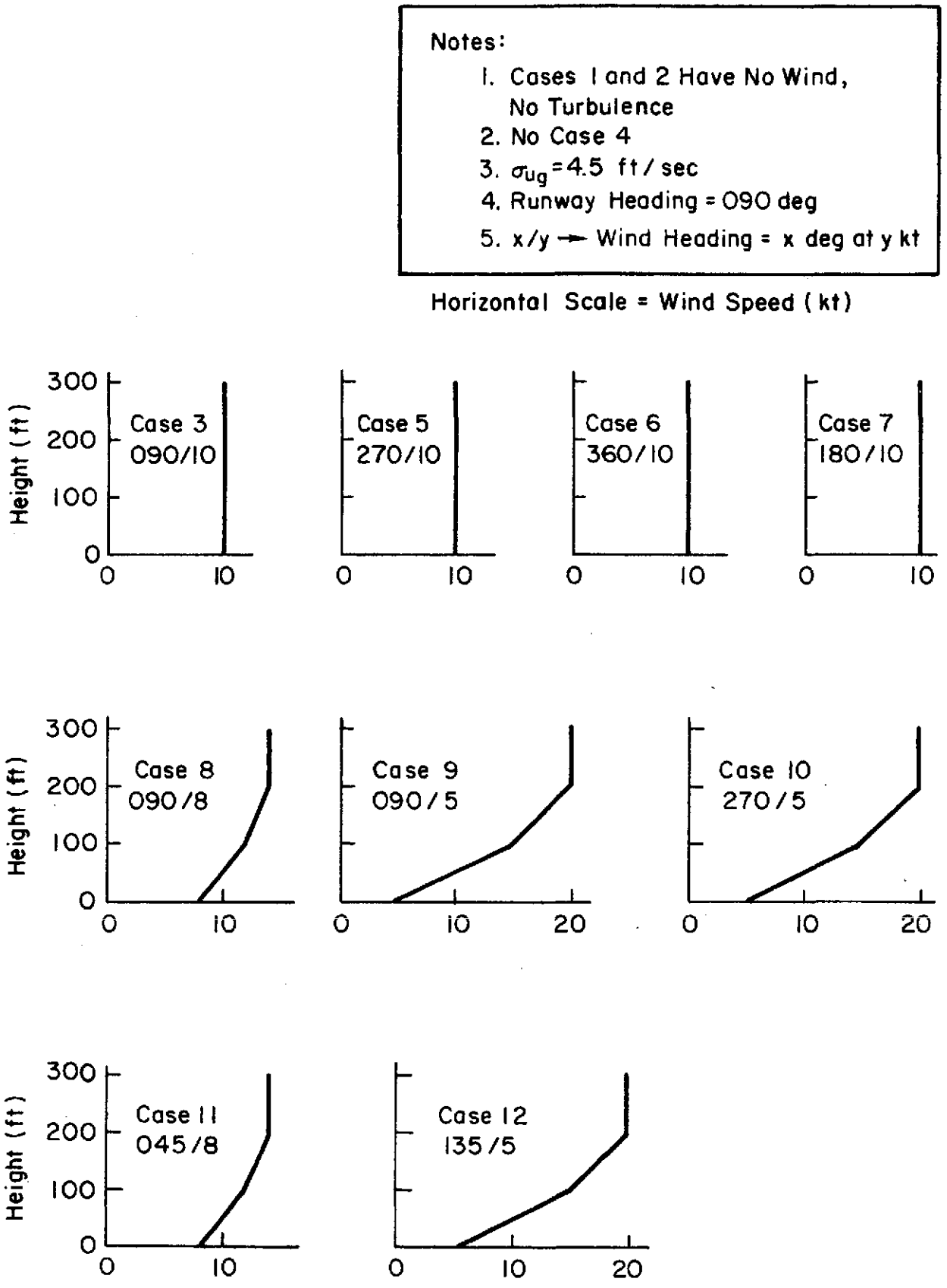

Figure II-21. Wind Profiles, 1973

SECTION III

ILS TRACKING DATA

A. 1972 RESULTS

Pilot/aircraft performance during the approach was measured by recording the means and standard deviations (σ) of several parameters from an altitude of 1000 ft to 300 ft. The parameters which will be discussed here are glide slope deviation, airspeed, pitch attitude, and thrust. The first two are direct performance measures of how well the pilot tracked the glide slope and how well he controlled his airspeed. The latter two indicate pilot control activity.

The glide slope performance for each pilot was plotted versus the number of approaches he had made, see Fig. III-1. This was done to check for long-term learning effects. In Fig. III-1 each data point represents the average* over a series of approximately 10 approaches. Each point is labelled with the approach speed in knots and, unless indicated by additional notation, is assumed to have no α display, σ_{u_g} = 3 ft/sec, T in, and γ_{APP} = -7.5 deg. Additional notation indications:

α	Angle of attack display was active
SAL	Steep approach and landing (-9.5 deg)
$\not{T}$	Transparency out
No Wind	No wind or turbulence

Examination of Fig. III-1 does not indicate any significant long-term learning effects. Furthermore, the performance is surprisingly consistent over all the test conditions except for the effects of turbulence.

The ILS tracking data have been carefully examined to determine the effects of:

- Approach speed
- Transparency in or out

---

* The average σ over several runs was computed as the square root of the average σ^2.

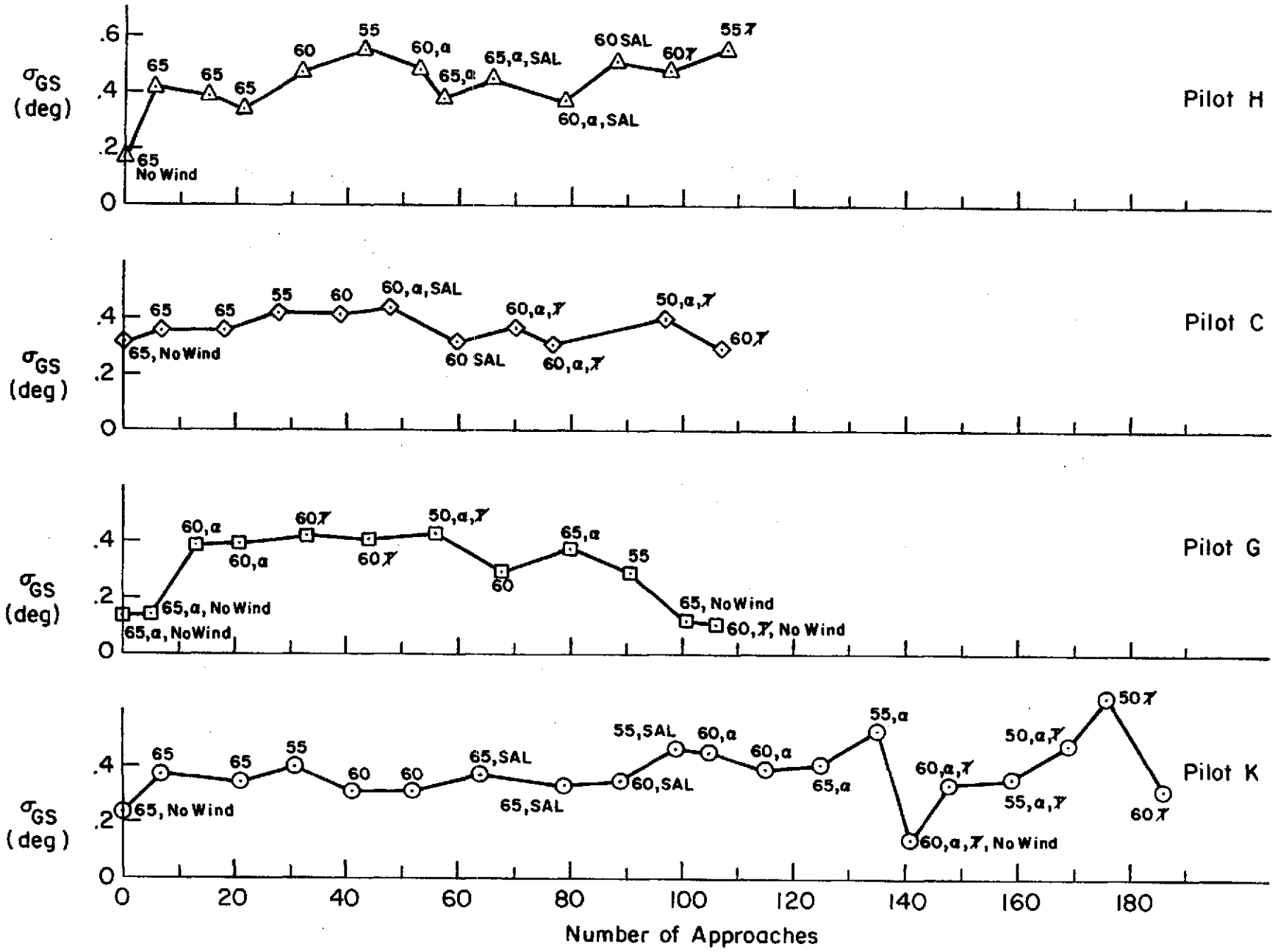

Figure III-1. History of Glide Slope Tracking Performance

- Presence or absence of α display
- Approach flight path angle (-7.5 vs -9.5)

The following paragraphs review the effects of each of these factors on performance and the pilots' subjective impressions. The general result was little or no variation in performance even for situations where the pilot comments indicated very poor characteristics and increased workload.

1. Approach Speed

Tabulations of glide slope, airspeed, pitch, and throttle* deviations and mean approach speeds are given in Table III-1 for the various test conditions. In addition, the deviations versus mean approach speeds are plotted in Fig. III-2 for the most widely tested condition - transparency in, no α display, and γ_{APP} = -7.5 deg.

In general, reducing the approach speed increases the glide slope deviations; however, the changes are relatively small and not consistent among the different pilots. In fact, reducing speed seems to increase the intersubject variability, see Fig. III-2.

A more complete set of glide slope tracking data is shown in Fig. III-3. The trends are the same as those shown in Fig. III-2 even when including the 50 kt, transparency-out case. The relatively good performance for this condition is indeed surprising. At this speed the aircraft was so far on the backside of the drag curve that an unusual piloting technique was required. Thrust was relatively ineffective in controlling flight path. The pilots found that pitch attitude was the only effective flight path control but that it was reversed, i.e. nose down to go up. Though their performance was still good the pilots considered the use of this unnatural control technique completely unacceptable. This is an extreme example of the inability to define acceptable flight conditions from pilot/aircraft performance alone.

With regard to mean airspeed, $\overline{V}$, it can be seen (Table III-1 and Fig. III-2) that the pilots generally flew slightly faster (on the order of 1-2 kt) than the target speed. This is probably a result of being

---

* Throttle variations are given in terms of gas generator percent RPM.

TABLE III-1: IIS TRACKING DATA

a. Glide Slope Deviations, $\sigma_{G/S}$ (deg)

APPROACH SPEED (kt)	TRANSPARENCY	α DISPLAY	APPROACH γ (deg)	TURBULENCE σ_{u_G} (fps)	PILOT			
					H	C	G	K
55	IN	OUT	-7.5	3.0	.55	.42	.29	.40
60	IN	OUT	-7.5	3.0	.47	.41	.29	.31
65	IN	OUT	-7.5	3.0	.38	.36	---	.36
55	IN	IN	-7.5	3.0	---	---	---	.53
60	IN	IN	-7.5	3.0	.49	---	.39	.42
65	IN	IN	-7.5	3.0	.38	---	---	.41
55	IN	OUT	-9.5	3.0	---	---	---	.47
60	IN	OUT	-9.5	3.0	.51	.32	---	.35
65	IN	OUT	-9.5	3.0	---	---	---	.36
55	IN	IN	-9.5	3.0	---	---	---	---
60	IN	IN	-9.5	3.0	.37	.44	---	---
65	IN	IN	-9.5	3.0	.45	---	.37	---
50	OUT	OUT	-7.5	3.0	---	---	---	.65
55	OUT	OUT	-7.5	3.0	.56	---	---	---
60	OUT	OUT	-7.5	3.0	.48	.30	.41	.31
50	OUT	IN	-7.5	3.0	---	.40	.43	.48
55	OUT	IN	-7.5	3.0	---	---	---	.36
60	OUT	IN	-7.5	3.0	---	.35	---	.34
65	IN	OUT	-7.5	0.0	.17	.31	.12	.23
65	IN	IN	-7.5	0.0	---	---	.14	---
60	OUT	OUT	-7.5	0.0	---	---	.11	---
60	OUT	IN	-7.5	0.0	---	---	---	.14

Note: No Pitch or Yaw SAS

TABLE III-1: Continued

b. Mean Airspeed, $\bar{V}$(kt)

APPROACH SPEED (kt)	TRANSPARENCY	α DISPLAY	APPROACH γ (deg)	TURBULENCE σ_{u_G} (fps)	PILOT			
					H	C	G	K
55	IN	OUT	-7.5	3.0	56.6	55.9	57.5	56.5
60	IN	OUT	-7.5	3.0	62.6	62.5	60.7	62.1
65	IN	OUT	-7.5	3.0	66.7	66.5	----	66.4
55	IN	IN	-7.5	3.0	----	----	----	54.6
60	IN	IN	-7.5	3.0	57.7	----	60.4	59.9
65	IN	IN	-7.5	3.0	64.2	----	----	64.9
55	IN	OUT	-9.5	3.0	----	----	----	57.5
60	IN	OUT	-9.5	3.0	63.5	62.6	----	60.9
65	IN	OUT	-9.5	3.0	----	----	----	66.1
55	IN	IN	-9.5	3.0	----	----	----	----
60	IN	IN	-9.5	3.0	59.9	60.3	----	----
65	IN	IN	-9.5	3.0	65.6	----	66.6	----
50	OUT	OUT	-7.5	3.0	----	----	----	49.7
55	OUT	OUT	-7.5	3.0	57.2	----	----	----
60	OUT	OUT	-7.5	3.0	62.9	62.3	61.7	62.6
50	OUT	IN	-7.5	3.0	----	52.3	50.9	51.8
55	OUT	IN	-7.5	3.0	----	----	----	55.7
60	OUT	IN	-7.5	3.0	----	60.5	----	61.6
65	IN	OUT	-7.5	0.0	65.7	67.1	65.5	63.8
65	IN	IN	-7.5	0.0	----	----	66.5	----
60	OUT	OUT	-7.5	0.0	----	----	62.4	----
60	OUT	IN	-7.5	0.0	----	----	----	61.8

Note: No Pitch or Yaw SAS

TABLE III-1: Continued

c. Airspeed Deviations, σ_V (kt)

APPROACH SPEED (kt)	TRANSPARENCY	α DISPLAY	APPROACH γ (deg)	TURBULENCE σ_{u_G} (fps)	PILOT			
					H	C	G	K
55	IN	OUT	-7.5	3.0	2.0	2.2	2.0	1.8
60	IN	OUT	-7.5	3.0	1.9	3.8	2.2	1.8
65	IN	OUT	-7.5	3.0	2.2	2.5	---	2.1
55	IN	IN	-7.5	3.0	---	---	---	2.3
60	IN	IN	-7.5	3.0	2.2	---	2.4	2.3
65	IN	IN	-7.5	3.0	2.1	---	---	2.3
55	IN	OUT	-9.5	3.0	---	---	---	1.8
60	IN	OUT	-9.5	3.0	2.0	2.1	---	1.8
65	IN	OUT	-9.5	3.0	---	---	---	2.0
55	IN	IN	-9.5	3.0	---	---	---	---
60	IN	IN	-9.5	3.0	1.9	1.8	---	---
65	IN	IN	-9.5	3.0	1.9	---	2.1	---
50	OUT	OUT	-7.5	3.0	---	---	---	2.0
55	OUT	OUT	-7.5	3.0	2.2	---	---	---
60	OUT	OUT	-7.5	3.0	2.2	1.9	2.1	1.8
50	OUT	IN	-7.5	3.0	---	2.3	2.5	2.2
55	OUT	IN	-7.5	3.0	---	---	---	2.0
60	OUT	IN	-7.5	3.0	---	2.4	---	1.9
65	IN	OUT	-7.5	0.0	1.4	2.0	1.5	1.5
65	IN	IN	-7.5	0.0	---	---	1.6	---
60	OUT	OUT	-7.5	0.0	---	---	1.5	---
60	OUT	IN	-7.5	0.0	---	---	---	1.2

Note: No Pitch or Yaw SAS

TABLE III-1: Continued

d. Pitch Deviations, σ_θ (deg)

APPROACH SPEED (kt)	TRANSPARENCY	α DISPLAY	APPROACH γ (deg)	TURBULENCE σ_{u_G} (fps)	PILOT			
					H	C	G	K
55	IN	OUT	-7.5	3.0	1.3	1.5	1.2	1.1
60	IN	OUT	-7.5	3.0	1.2	1.9	1.5	1.1
65	IN	OUT	-7.5	3.0	1.2	1.7	---	1.3
55	IN	IN	-7.5	3.0	---	---	---	1.5
60	IN	IN	-7.5	3.0	1.5	---	1.7	1.5
65	IN	IN	-7.5	3.0	1.3	---	---	1.3
55	IN	OUT	-9.5	3.0	---	---	---	1.3
60	IN	OUT	-9.5	3.0	1.2	1.3	---	1.1
65	IN	OUT	-9.5	3.0	---	---	---	1.1
55	IN	IN	-9.5	3.0	---	---	---	---
60	IN	IN	-9.5	3.0	1.4	1.6	---	---
65	IN	IN	-9.5	3.0	1.0	---	1.2	---
50	OUT	OUT	-7.5	3.0	---	---	---	1.5
55	OUT	OUT	-7.5	3.0	1.6	---	---	---
60	OUT	OUT	-7.5	3.0	1.4	1.3	1.5	1.2
50	OUT	IN	-7.5	3.0	---	1.3	2.1	1.3
55	OUT	IN	-7.5	3.0	---	---	---	1.1
60	OUT	IN	-7.5	3.0	---	1.7	---	1.2
65	IN	OUT	-7.5	0.0	0.7	1.5	0.7	0.7
65	IN	IN	-7.5	0.0	---	---	0.9	---
60	OUT	OUT	-7.5	0.0	---	---	0.9	---
60	OUT	IN	-7.5	0.0	---	---	---	0.5

Note: No Pitch or Yaw SAS

TABLE III-1: Concluded

e. Throttle Deviations, σ_{N_G} (% RPM)

APPROACH SPEED (kt)	TRANSPARENCY	α DISPLAY	APPROACH γ (deg)	TURBULENCE σ_{u_G} (fps)	PILOT			
					H	C	G	K
55	IN	OUT	-7.5	3.0	2.6	2.1	2.1	2.3
60	IN	OUT	-7.5	3.0	1.8	3.3	2.2	2.3
65	IN	OUT	-7.5	3.0	2.6	2.2	---	2.4
55	IN	IN	-7.5	3.0	---	---	---	2.2
60	IN	IN	-7.5	3.0	1.8	---	2.4	2.4
65	IN	IN	-7.5	3.0	1.8	---	---	2.5
55	IN	OUT	-9.5	3.0	---	---	---	2.7
60	IN	OUT	-9.5	3.0	2.1	2.4	---	2.5
65	IN	OUT	-9.5	3.0	---	---	---	2.7
55	IN	IN	-9.5	3.0	---	---	---	---
60	IN	IN	-9.5	3.0	2.7	2.3	---	---
65	IN	IN	-9.5	3.0	2.0	---	2.5	---
50	OUT	OUT	-7.5	3.0	---	---	---	1.8
55	OUT	OUT	-7.5	3.0	2.8	---	---	---
60	OUT	OUT	-7.5	3.0	3.0	2.6	2.8	2.6
50	OUT	IN	-7.5	3.0	---	2.5	1.1	2.5
55	OUT	IN	-7.5	3.0	---	---	---	2.5
60	OUT	IN	-7.5	3.0	---	3.3	---	2.7
65	IN	OUT	-7.5	0.0	2.0	2.8	1.9	2.3
65	IN	IN	-7.5	0.0	---	---	1.8	---
60	OUT	OUT	-7.5	0.0	---	---	1.6	---
60	OUT	IN	-7.5	0.0	---	---	---	1.9

Note: No Pitch or Yaw SAS

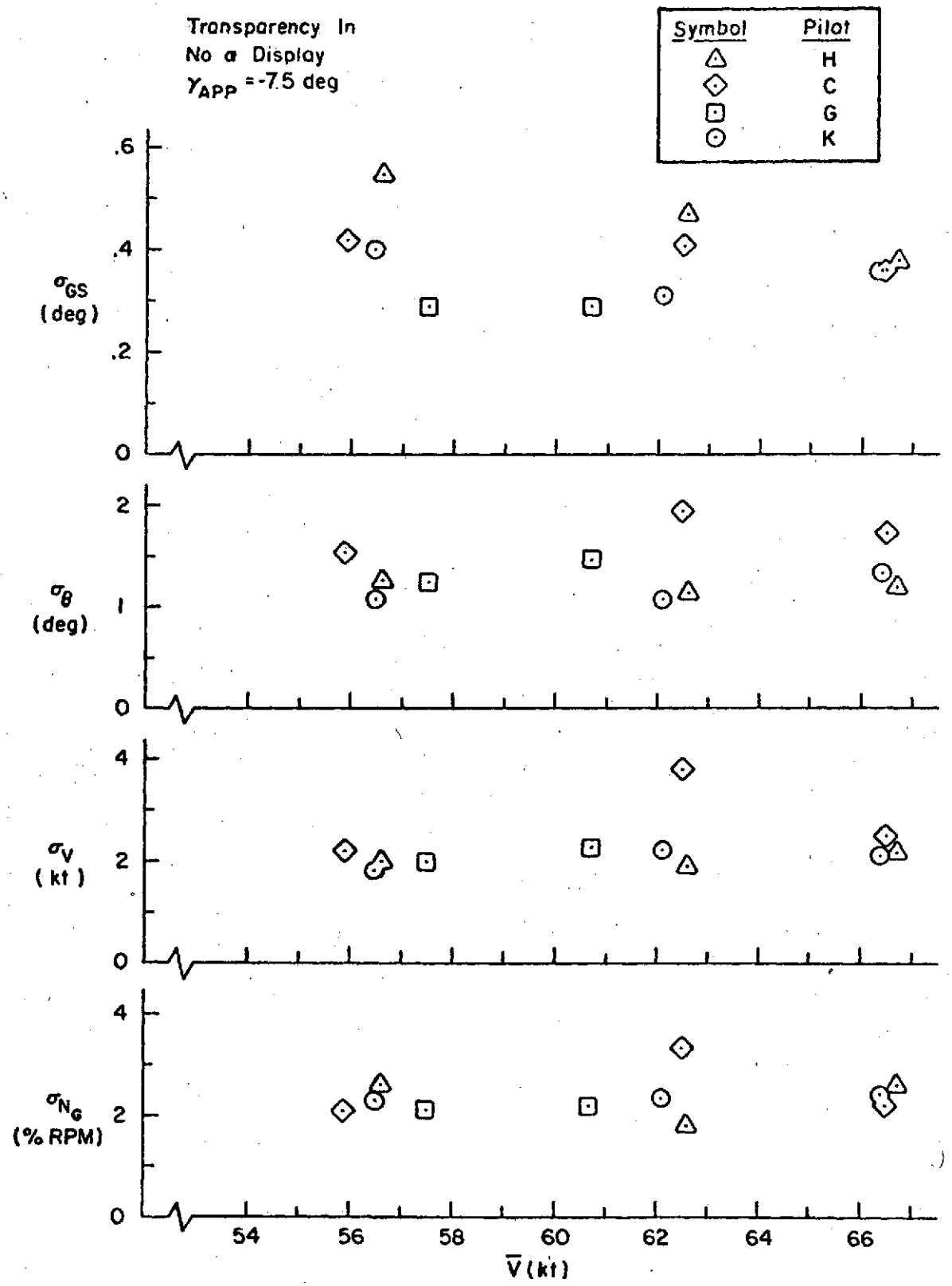

Figure III-2. Effects of Approach Speed

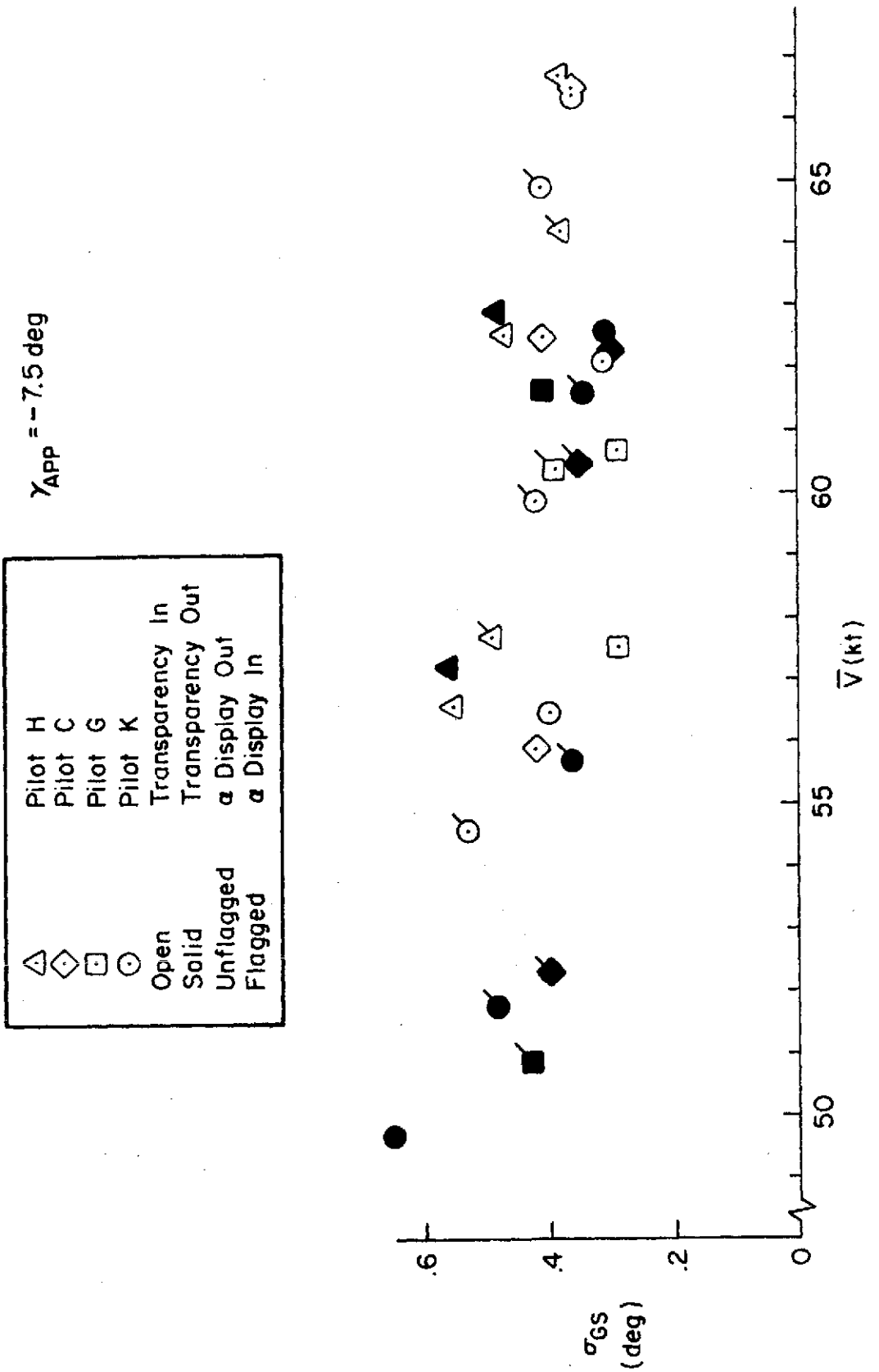

Figure III-3. Glide Slope Tracking Performance

more concerned about being slow than about being fast. Differences between the mean airspeed flown and the target speed do not seem related to the target speed.

Deviations in airspeed (σ_V), pitch attitude (σ_θ), and throttle (σ_{N_G}) are very consistent with no apparent effects due to approach speed. However, one test condition does stand out as peculiar -- 60 kt, transparency in, α display out, γ_{APP} = -7.5 deg, and Pilot C. In this case the airspeed and throttle deviations are unusually large. This same condition received a surprisingly adverse pilot reaction as will be discussed below.

Overall the effects of approach speed in ILS tracking performance are minimal. This indicates that the pilots could compensate for adverse conditions by working harder. While the effects on glide slope tracking, airspeed deviations, and control activity (as measured by σ_θ and σ_{N_G}) are small, the pilots' subjective opinions were sensitive to approach speed. A 5 kt difference frequently resulted in significant changes in task difficulty or pilot workload. While speed reductions generally resulted in a neutral or adverse pilot reaction, this was not universally true.

Some comparisons of different speeds made by pilots H and C are summarized below (γ_{APP} = -7.5 deg).

Test Conditions	Pilot	Comments
Transparency in, α display out	H	1. 60 and 65 kt cases are the same. 2. 55 kt is significantly harder than 60 or 65 kt.
	C	1. 55 kt harder than 65 kt. 2. 60 kt harder than 55 kt.
Transparency out, α display out	H	1. 60 kt harder than 55 kt.
Transparency out, α display in	C	1. 55 kt worse than 60 kt. 2. 55 kt much harder than 50 kt.

Note that in some cases (underlined in above comments) the pilots said that a 5 kt speed reduction made the ILS tracking task easier. Furthermore, this opinion was not universal among the pilots. In the transparency in case cited above, Pilot H considered 55 kt signficantly harder than 60 kt and Pilot C thought 55 kt was easier. The 60 kt case for Pilot C

is the one noted above for its unusually large airspeed and throttle deviations. No explanation for his adverse comments or unusual performance is available. In fact, the pilot/vehicle analyses of Appendix B and an examination of the aircraft characteristics indicate that speed reductions should always produce adverse effects.

2. Transparency

Table III-1 shows little effect of transparency in or out for similar approach speeds. For glide slope tracking errors this is shown quite clearly in Fig. III-3. Analytically there seems to be little reason to expect much difference as the aircraft dynamics are quite similar transparency in or out, see Appendix A. The major difference is the larger thrust margin (lower trim thrust level) transparency out.

There were few pilot comments regarding the relative merit of transparency in or out. However, Pilot C did comment that he thought transparency out was more difficult.

3. Angle of Attack Display

Table III-1 and Fig. III-3 also indicate no significant performance changes due to adding an α display. Significant pilot comments were:

- Cannot control V and α simultaneously as the two frequently gave conflicting indications, e.g. both too high
- ILS tracking was easier when controlling V rather than α
- The α display was useful as an indicator of proximity to the stall
- The α display was poorly located which made it difficult to include in the normal scan pattern.

The last comment raises some doubts as to the validity of the test results. However, it should be remembered that the pilot/vehicle analysis clearly shows that α control is detrimental to flight path control. The analysis of Appendix B shows that α can be used and airspeed ignored only at the higher approach speeds where good flight path control is possible

without airspeed regulation. Even then, the pilot must be careful not to chase α (close a tight loop). At lower approach speeds, airspeed regulation will improve the flight path control but α regulation degrades it.

4. Approach Angle

The limited amount of data for the steeper approaches ($\gamma_{APP} = -9.5$) does not indicate any significant effects. Neither do the pilot comments or a comparison of the aircraft characteristics at the two approach angles, see Appendix A. Approach angle effects, if any, were limited to the flare and landing task.

B. 1973 RESULTS

Pilot/aircraft performance was analyzed using the same metrics employed for the 1972 simulation. These are summarized in Table III-2 and the glide slope deviations are also plotted in Fig. III-4. These data show some performance improvements relative to the 1972 results. Glide slope and pitch attitude deviations are generally somewhat smaller and the mean airspeed is closer to the target approach speed. However, with the possible exception of glide slope deviations, the performance data are not useful in evaluating the effects of the experimental parameters. The main criteria for separating the acceptable and unacceptable conditions are the subjective evaluations of the pilot. The remainder of this section will therefore concentrate on reviewing the pilot comments and ratings relative to the ILS tracking task.

1. Effects of Approach Speed, Transparency In

Pilot ratings for 3 approach speeds are shown in Fig. III-5. Both pilots considered 65 kt to be a clearly acceptable approach speed. The task under calm air conditions was satisfactory for day-to-day operations. Under the adverse conditions (turbulence plus 200 ft ceiling) the task was considered acceptable for the infrequent cases when such conditions would be encountered.

TABLE III-2: ILS TRACKING DATA

a. Glide Slope Deviations, $\sigma_{G/S}$ (deg)

APPROACH SPEED (kt)	TRANSPARENCY	α DISPLAY	APPROACH γ (deg)	TURBULENCE σ_{u_G} (fps)	PILOT	
					H	G
55	IN	OUT	-7.5	4.5	---	.48
60	IN	OUT	-7.5	4.5	.32	.35
65	IN	OUT	-7.5	4.5	.36	.35
55	IN	IN	-7.5	4.5	---	.64
60	IN	IN	-7.5	4.5	---	---
65	IN	IN	-7.5	4.5	---	---
55	OUT	OUT	-7.5	4.5	---	---
60	OUT	OUT	-7.5	4.5	.19	.39
65	OUT	OUT	-7.5	4.5	.36	.43
55	OUT	IN	-7.5	4.5	---	---
60	OUT	IN	-7.5	4.5	.34	.37
65	OUT	IN	-7.5	4.5	---	---
55	IN	OUT	-7.5	0.0	---	.23
60	IN	OUT	-7.5	0.0	.05	---
65	IN	OUT	-7.5	0.0	.11	.10
55	IN	IN	-7.5	0.0	---	.18
60	IN	IN	-7.5	0.0	---	---
65	IN	IN	-7.5	0.0	---	---
55	OUT	OUT	-7.5	0.0	---	---
60	OUT	OUT	-7.5	0.0	.17	.15
65	OUT	OUT	-7.5	0.0	.07	.08
55	OUT	IN	-7.5	0.0	---	---
60	OUT	IN	-7.5	0.0	.05	.27
65	OUT	IN	-7.5	0.0	---	---

Note: Pitch and Yaw SAS On

TABLE III-2: Continued

b. Mean Airspeed, $\bar{V}$(kt)

APPROACH SPEED (kt)	TRANSPARENCY	α DISPLAY	APPROACH γ (deg)	TURBULENCE σ_{u_G} (fps)	PILOT H	PILOT G
55	IN	OUT	-7.5	4.5	----	55.0
60	IN	OUT	-7.5	4.5	59.5	60.4
65	IN	OUT	-7.5	4.5	65.3	65.6
55	IN	IN	-7.5	4.5	----	56.7
60	IN	IN	-7.5	4.5	----	----
65	IN	IN	-7.5	4.5	----	----
55	OUT	OUT	-7.5	4.5	----	----
60	OUT	OUT	-7.5	4.5	59.4	61.5
65	OUT	OUT	-7.5	4.5	64.7	66.0
55	OUT	IN	-7.5	4.5	----	----
60	OUT	IN	-7.5	4.5	58.6	60.9
65	OUT	IN	-7.5	4.5	----	----
55	IN	OUT	-7.5	0.0	----	54.2
60	IN	OUT	-7.5	0.0	59.2	----
65	IN	OUT	-7.5	0.0	64.0	62.8
55	IN	IN	-7.5	0.0	----	54.0
60	IN	IN	-7.5	0.0	----	----
65	IN	IN	-7.5	0.0	----	----
55	OUT	OUT	-7.5	0.0	----	----
60	OUT	OUT	-7.5	0.0	59.3	61.0
65	OUT	OUT	-7.5	0.0	64.0	64.4
55	OUT	IN	-7.5	0.0	----	----
60	OUT	IN	-7.5	0.0	59.2	60.1
65	OUT	IN	-7.5	0.0	----	----

Note: Pitch and Yaw SAS On

TABLE III-2: Continued

c. Airspeed Deviations, σ_V (kt)

APPROACH SPEED (kt)	TRANSPARENCY	α DISPLAY	APPROACH γ (deg)	TURBULENCE σ_{u_G} (fps)	PILOT H	PILOT G
55	IN	OUT	-7.5	4.5	----	1.90
60	IN	OUT	-7.5	4.5	1.68	2.05
65	IN	OUT	-7.5	4.5	2.07	2.31
55	IN	IN	-7.5	4.5	----	2.43
60	IN	IN	-7.5	4.5	----	----
65	IN	IN	-7.5	4.5	----	----
55	OUT	OUT	-7.5	4.5	----	----
60	OUT	OUT	-7.5	4.5	1.59	1.88
65	OUT	OUT	-7.5	4.5	1.67	1.91
55	OUT	IN	-7.5	4.5	----	----
60	OUT	IN	-7.5	4.5	1.85	1.89
65	OUT	IN	-7.5	4.5	----	----
55	IN	OUT	-7.5	0.0	----	1.25
60	IN	OUT	-7.5	0.0	.91	----
65	IN	OUT	-7.5	0.0	1.10	.94
55	IN	IN	-7.5	0.0	----	1.1
60	IN	IN	-7.5	0.0	----	----
65	IN	IN	-7.5	0.0	----	----
55	OUT	OUT	-7.5	0.0	----	----
60	OUT	OUT	-7.5	0.0	1.12	1.08
65	OUT	OUT	-7.5	0.0	.87	.88
55	OUT	IN	-7.5	0.0	----	----
60	OUT	IN	-7.5	0.0	.88	.81
65	OUT	IN	-7.5	0.0	----	----

Note: Pitch and Yaw SAS On

TABLE III-2: Continued

d. Pitch Deviations, σ_θ (deg)

APPROACH SPEED (kt)	TRANSPARENCY	α DISPLAY	APPROACH γ (deg)	TURBULENCE σ_{u_G} (fps)	PILOT	
					H	G
55	IN	OUT	-7.5	4.5	---	.71
60	IN	OUT	-7.5	4.5	.53	.55
65	IN	OUT	-7.5	4.5	.62	.71
55	IN	IN	-7.5	4.5	---	.79
60	IN	IN	-7.5	4.5	---	---
65	IN	IN	-7.5	4.5	---	---
55	OUT	OUT	-7.5	4.5	---	---
60	OUT	OUT	-7.5	4.5	.73	.72
65	OUT	OUT	-7.5	4.5	.73	.70
55	OUT	IN	-7.5	4.5	---	---
60	OUT	IN	-7.5	4.5	.64	.84
65	OUT	IN	-7.5	4.5	---	---
55	IN	OUT	-7.5	0.0	---	.45
60	IN	OUT	-7.5	0.0	.15	---
65	IN	OUT	-7.5	0.0	.29	.24
55	IN	IN	-7.5	0.0	---	.34
60	IN	IN	-7.5	0.0	---	---
65	IN	IN	-7.5	0.0	---	---
55	OUT	OUT	-7.5	0.0	---	---
60	OUT	OUT	-7.5	0.0	.49	.64
65	OUT	OUT	-7.5	0.0	.20	.24
55	OUT	IN	-7.5	0.0	---	---
60	OUT	IN	-7.5	0.0	.10	.35
65	OUT	IN	-7.5	0.0	---	---

Note: Pitch and Yaw SAS On

TABLE III-2: Concluded

e. Throttle Deviations, σ_{N_G} (% RPM)

APPROACH SPEED (kt)	TRANSPARENCY	α DISPLAY	APPROACH γ (deg)	TURBULENCE σ_{u_G} (fps)	PILOT	
					H	G
55	IN	OUT	-7.5	4.5	----	2.26
60	IN	OUT	-7.5	4.5	2.01	2.15
65	IN	OUT	-7.5	4.5	1.99	1.91
55	IN	IN	-7.5	4.5	----	2.71
60	IN	IN	-7.5	4.5	----	----
65	IN	IN	-7.5	4.5	----	----
55	OUT	OUT	-7.5	4.5	----	----
60	OUT	OUT	-7.5	4.5	2.05	3.17
65	OUT	OUT	-7.5	4.5	2.62	3.19
55	OUT	IN	-7.5	4.5	----	----
60	OUT	IN	-7.5	4.5	2.20	3.65
65	OUT	IN	-7.5	4.5	----	----
55	IN	OUT	-7.5	0.0	----	2.38
60	IN	OUT	-7.5	0.0	1.86	----
65	IN	OUT	-7.5	0.0	1.90	1.77
55	IN	IN	-7.5	0.0	----	1.91
60	IN	IN	-7.5	0.0	----	----
65	IN	IN	-7.5	0.0	----	----
55	OUT	OUT	-7.5	0.0	----	----
60	OUT	OUT	-7.5	0.0	2.01	2.35
65	OUT	OUT	-7.5	0.0	1.62	1.75
55	OUT	IN	-7.5	0.0	----	----
60	OUT	IN	-7.5	0.0	1.40	1.86
65	OUT	IN	-7.5	0.0	----	----

Note: Pitch and Yaw SAS On

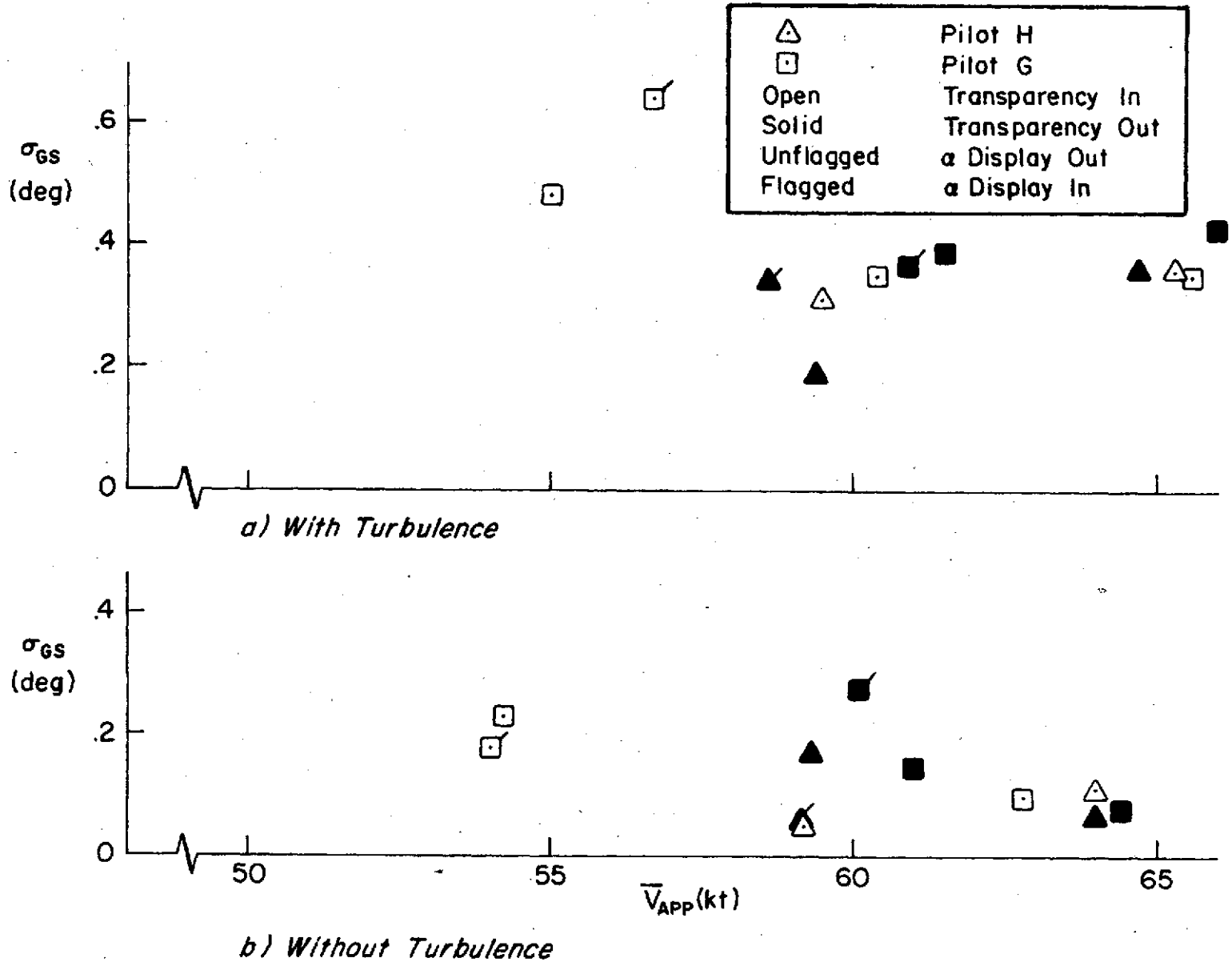

Figure III-4. Glide Slope Tracking Deviation

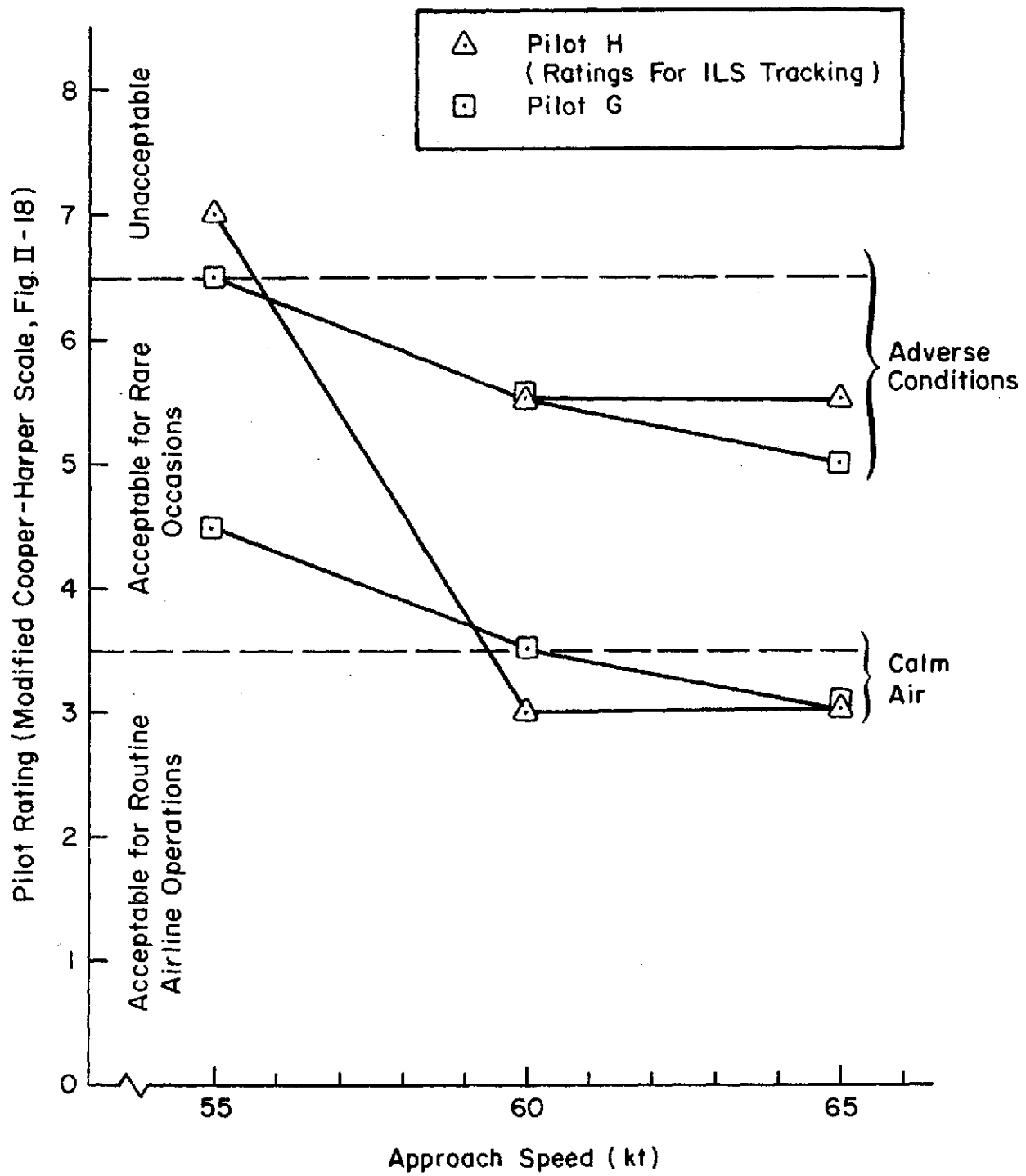

Figure III-5. Pilot Ratings, Transparency In

Pilot H considered glide slope tracking to be the same at 60 and 65 kt and said it required a high workload. He considered 55 kt to be completely unacceptable so his testing at that speed was aborted without getting performance data. The problem was, downward flight path corrections caused him to get on the "bottom side" of the γ - V curves. Bottom side refers to flight at angles of attack above that for maximum C_L. The γ - V curves (Fig. A-2) show 2 possible values of γ for a given speed and power setting. The lower value of γ is on the bottom side.

Pilot G considered 60 kt slightly worse than 65 kt, 1/2 rating point. His ratings at 55 kt are not as severe as those of Pilot H but do reflect an unacceptable situation. At 55 kt, Pilot G said the glide slope tracking was very difficult and it was very hard to stabilize airspeed---tended to get fast. His glide slope tracking performance did show some deterioration, see Fig. III-4.

The pilot complaints about difficulty in tracking the glide slope at 55 kt are confirmed by the pilot/vehicle analyses of Appendix B. The problem at slow speeds is mainly due to the low heave damping (Z_w) which in turn is due to low C_{L_α}. The pilot can compensate for the low heave damping by increasing his lead in the glide slope feedback but this increases his workload, see Appendix B.

Based on the ratings of the two pilots, the minimum target approach speed acceptable for airline operation would be very close to 60 kt. This is surprisingly close to stall; 60 kt is only 1.06 times the minimum possible speed with approach power. Apparently the pilots were willing to accept such small margins only because stall is not a catastrophic event in this airplane.

Furthermore, an increased speed margin might be required in actual airline operations to account for factors not included in the simulation. These factors include more extreme atmospheric conditions, such as a large sharp-edged gust, and additional pilot distractions or workload, such as radio communications.

2. Effects of Approach Speed, Transparency Out

The two pilots evaluated the transparency out configuration at two approach speeds, 60 and 65 kt. Their ratings are shown in Fig. III-6.

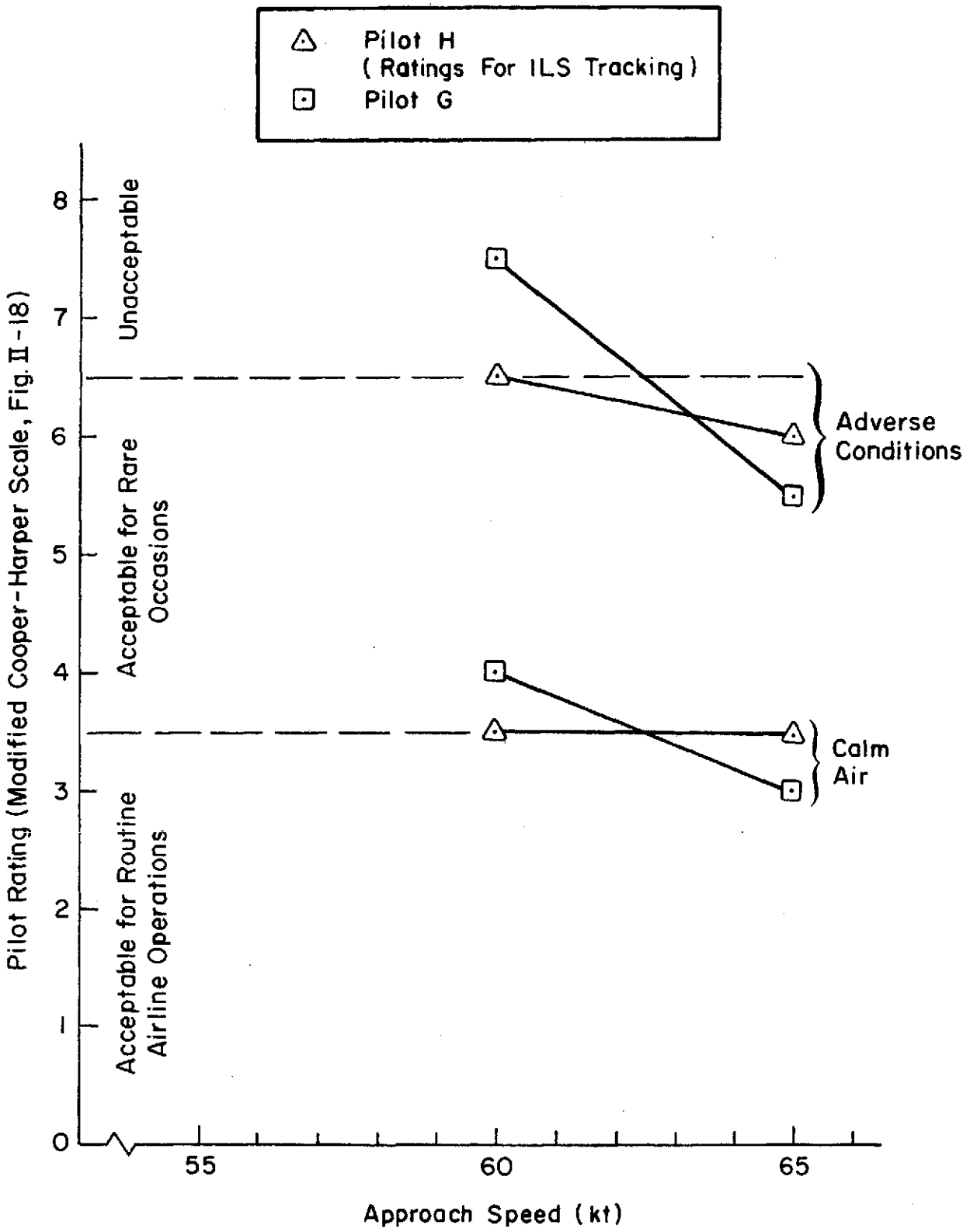

Figure III-6. Pilot Ratings, Transparency Out

At 65 kt Pilot H thought the ILS tracking was virtually the same as transparency in except for more sluggish power response. At 60 kt he mentioned many problems with glide slope tracking and the tendency to get on the bottom side of the γ - V curve. He noted that his calm air rating of 3 1/2 was subject to question and could be degraded to 6 1/2 because minor perturbations could put him on the bottom side of the γ - V curve.

At 65 kt Pilot G thought that glide slope tracking was the hardest task. Gross power changes were required and much of the time power was at flight idle. At 60 kt glide slope tracking became very hard.

From the ratings and comments of these two pilots, the minimum approach speed acceptable for airline operation would be between 60 and 65 kt although their glide slope tracking performance at 60 kt was still good, see Fig. III-4. This result is confirmed by the pilot/vehicle analyses of Appendix B. This shows a slight improvement in glide slope tracking at 60 kt with transparency in. Thus the minimum acceptable speed for glide slope tracking should be slightly higher for the transparency out configuration.

3. Effects of Angle of Attack Display

A brief experiment was conducted to determine if the presence of an α display would reduce the minimum acceptable approach speed. As shown in Fig. III-4, the α display did not improve glide slope tracking.

For the 60 kt, transparency out case, Pilot H felt the α display was helpful. It gave him more confidence in that he could avoid getting on the bottom side of the γ - V curve. In his opinion you could probably operate the aircraft slightly slower with an α display.

Pilot G ignored the α display unless he got a steady red chevron. He thought the α information might be very useful but needed to see more to be sure. His ratings with the α display improved considerably, 2 1/2 and 6 versus 4 and 7 1/2.

Pilot G also evaluated the 55 kt, transparency in case using the α display. He still found the glide slope tracking very difficult and actually rated the situation worse than he did without the α display, 5 and 8 - 8 1/2 versus 4 1/2 and 6 1/2. An explanation for the rating decrement in this case is not available.

The main conclusion from this test is that an α display will not allow significant (on the order of 5 kt) reductions in operational speeds. On the other hand, the α display could improve safety by helping the pilot avoid dangerously high α situations. Angle of attack as a flight reference also has the advantage of being independent of weight. However, as demonstrated in the pilot/vehicle analyses of Appendix B, the pilots must be carefully trained not to chase angle of attack. Tight control of angle of attack will seriously degrade the glide slope tracking performance.

SECTION IV

FLARE AND LANDING

A. 1972 TESTS

1. Test Conditions

Flare and landing was one part of the overall approach and landing task. Therefore, the parameters that were varied for the ILS tracking phase (transparency, approach speed, glide slope, winds, etc.) were also parameter variations for flare and landing.

All landings in this series were made from a normal approach attitude. A nose down touchdown attitude resulted in a probable bounce (just as in the actual BR 941S), therefore the pilot was forced to flare to at least level or slightly nose high. The touchdown attitude was typically zero to +2 deg.

The pilot was not given any specific instructions as to touchdown conditions other than to observe runway constraints and the touchdown sink rate limit of the actual BR 941S (-10.5 ft/sec).

2. Data Analysis

The two parameters which were considered most meaningful in describing landing conditions were touchdown sink rate, $\dot{h}_{TD}$, and touchdown position relative to the runway threshold, x_{TD}. These parameters are plotted first in landing-by-landing scatter plots of $\dot{h}_{TD}$ versus x_{TD} then as cumulative distributions of each. In this way the effects of speed, winds, etc. can be separated. The distribution plots are relied upon most heavily to show these effects.

3. Scatter Plots

Fig. IV-1a through h show the degree of correlation in touchdown conditions $\dot{h}_{TD}$ versus x_{TD} for the various configurations, winds, and glide slope conditions flown. The correlation is in general not significant except possibly for the bad wind shear conditions which often resulted in short, hard landings.

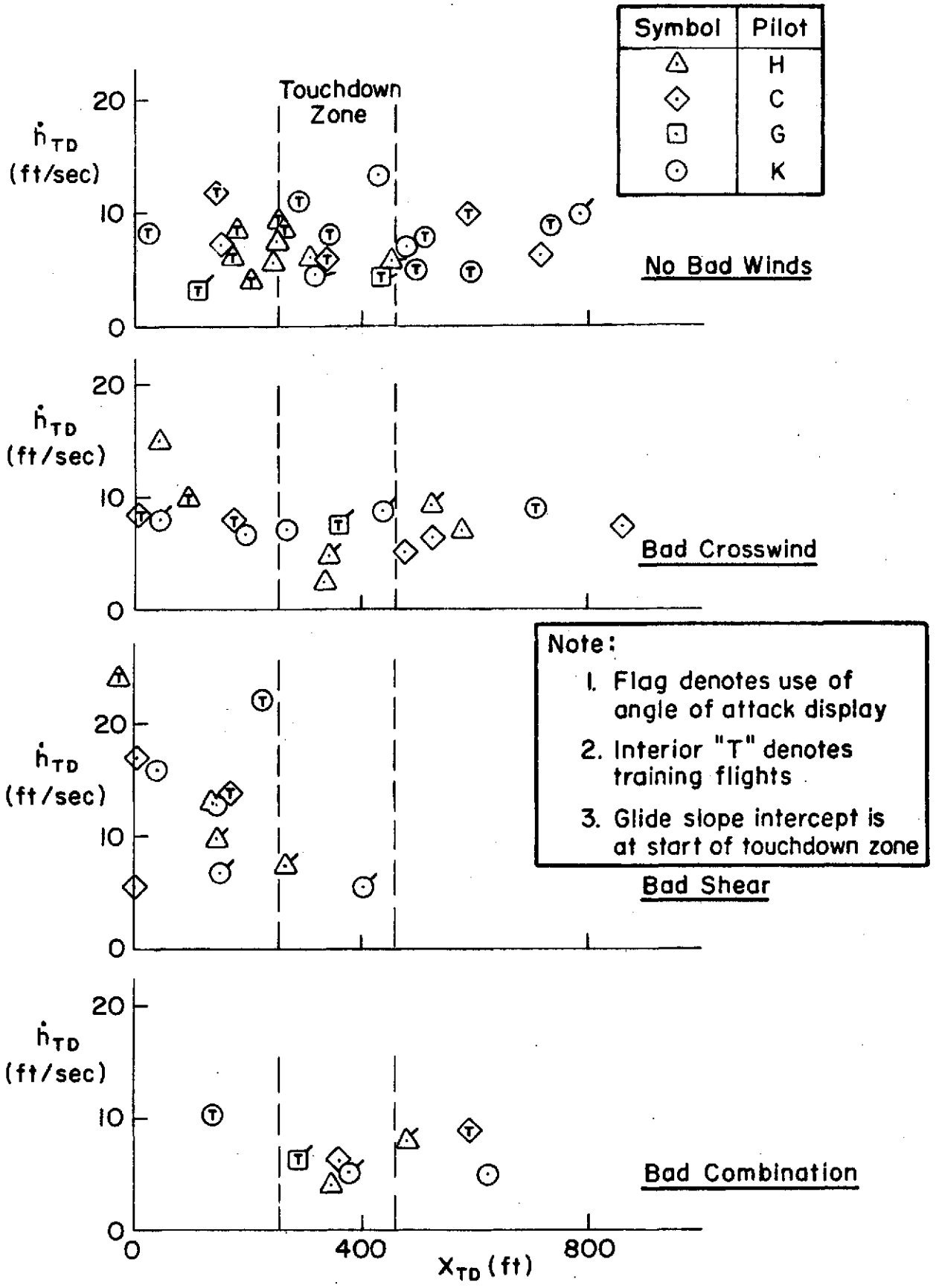

a) 65 kt, T In, γ = -7.5 deg

Figure IV-1. Scatter Plots

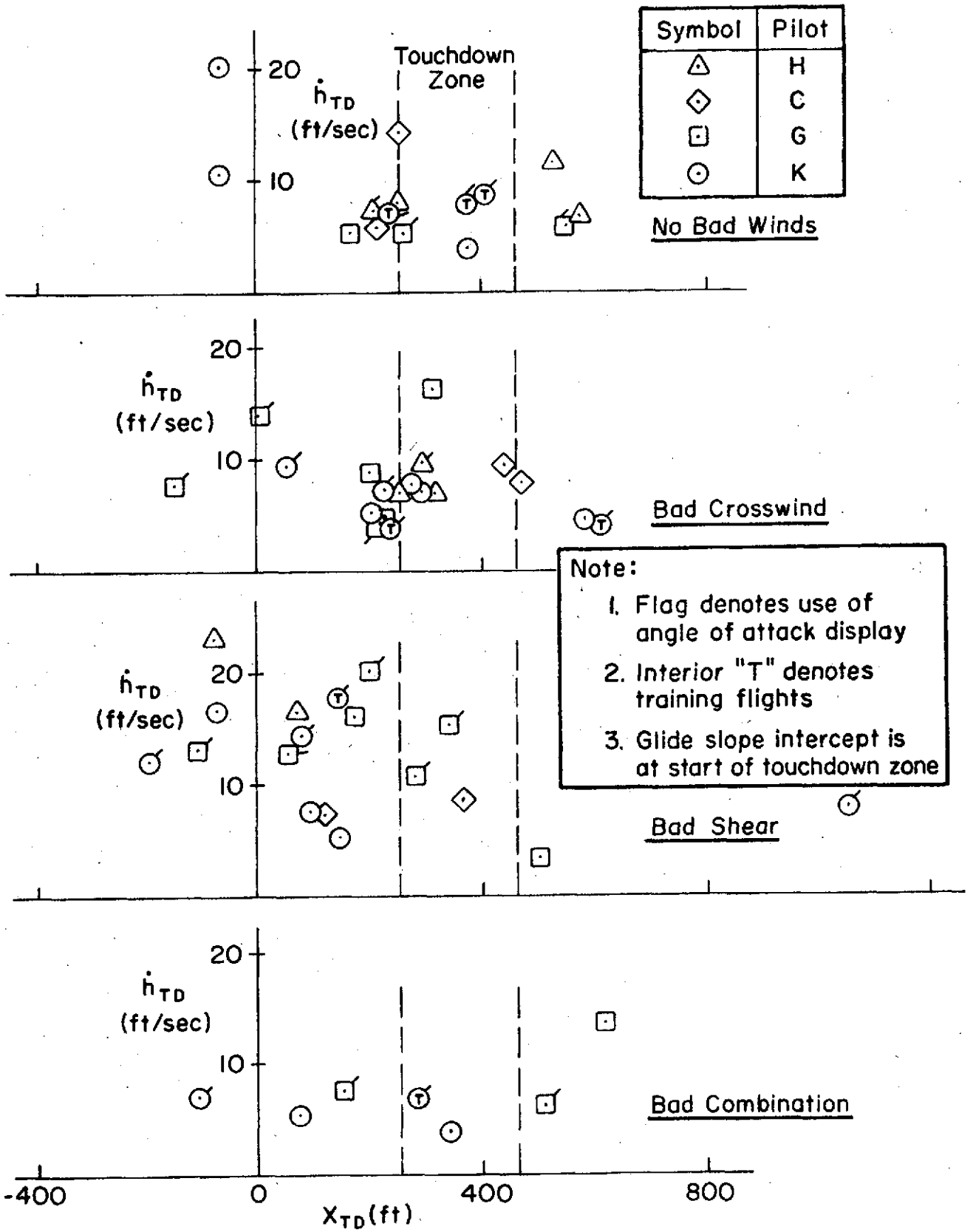

b) 60 kt, T In, γ = −7.5 deg

Figure IV-1. (Continued)

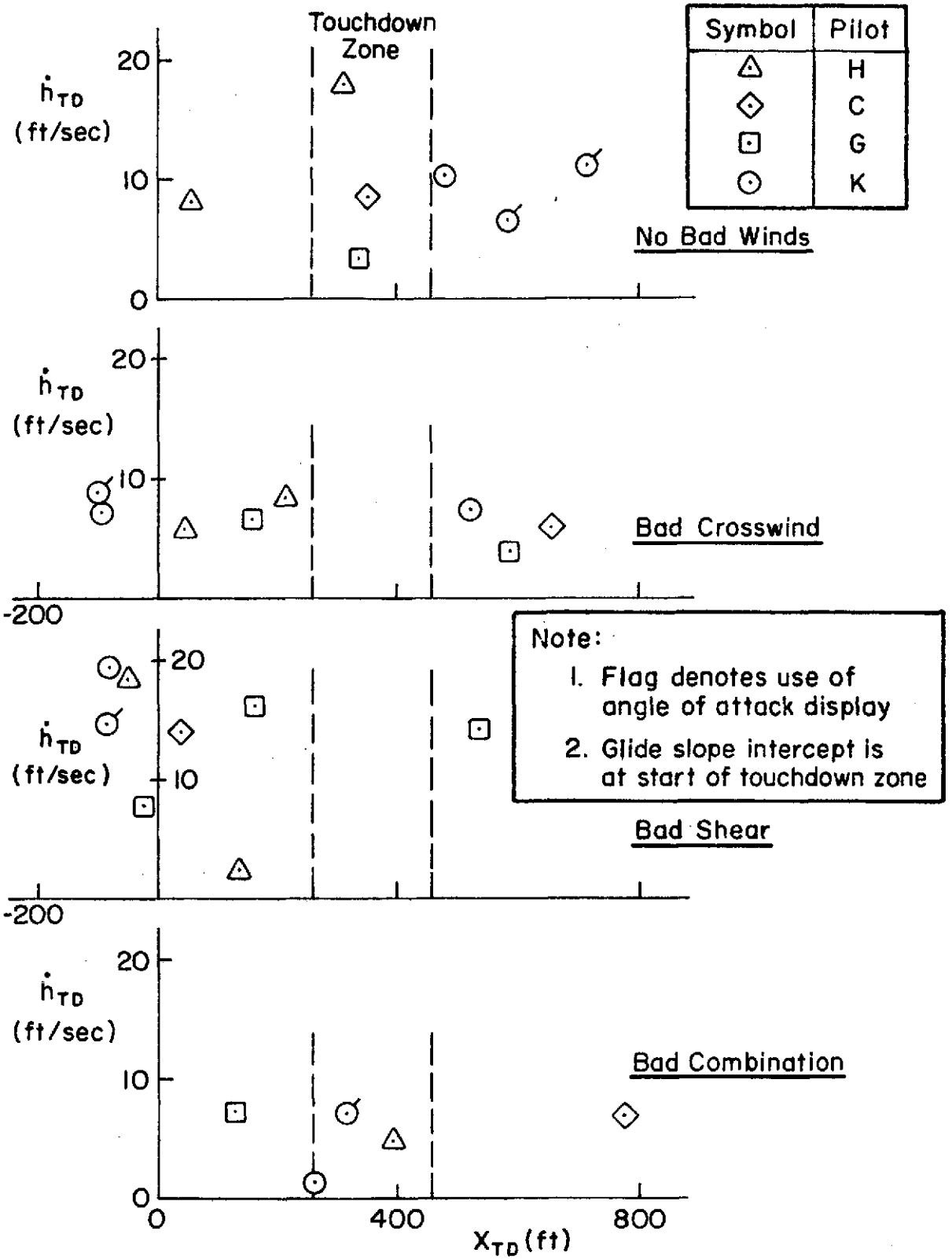

c) 55 kt, T In, γ = -7.5 deg

Figure IV-1. (Continued)

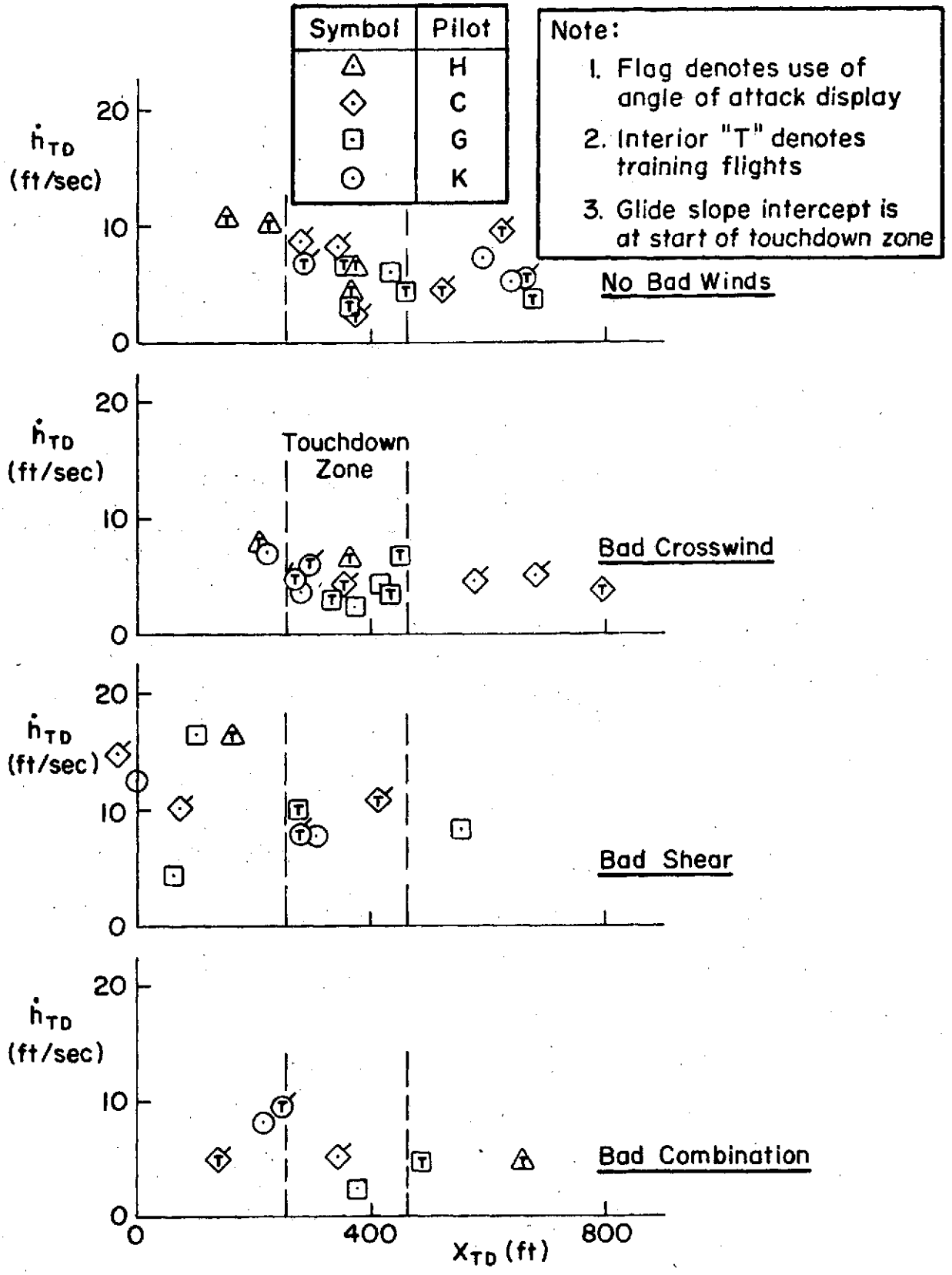

d) 60 kt, T Out, $\gamma = -7.5$ deg

Figure IV-1. (Continued)

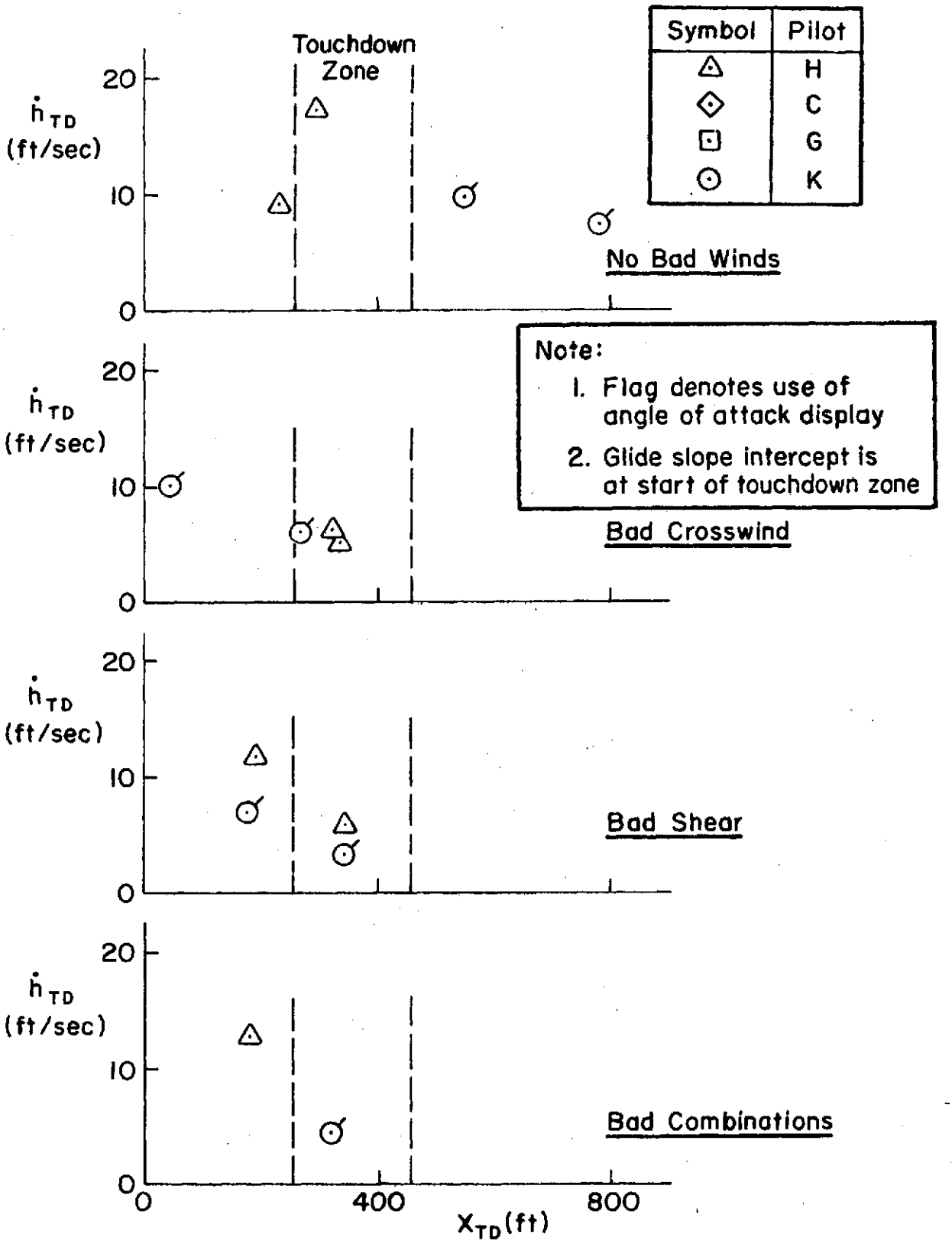

e) 55 kt, T Out, $\gamma = -7.5$ deg

Figure IV-1. (Continued)

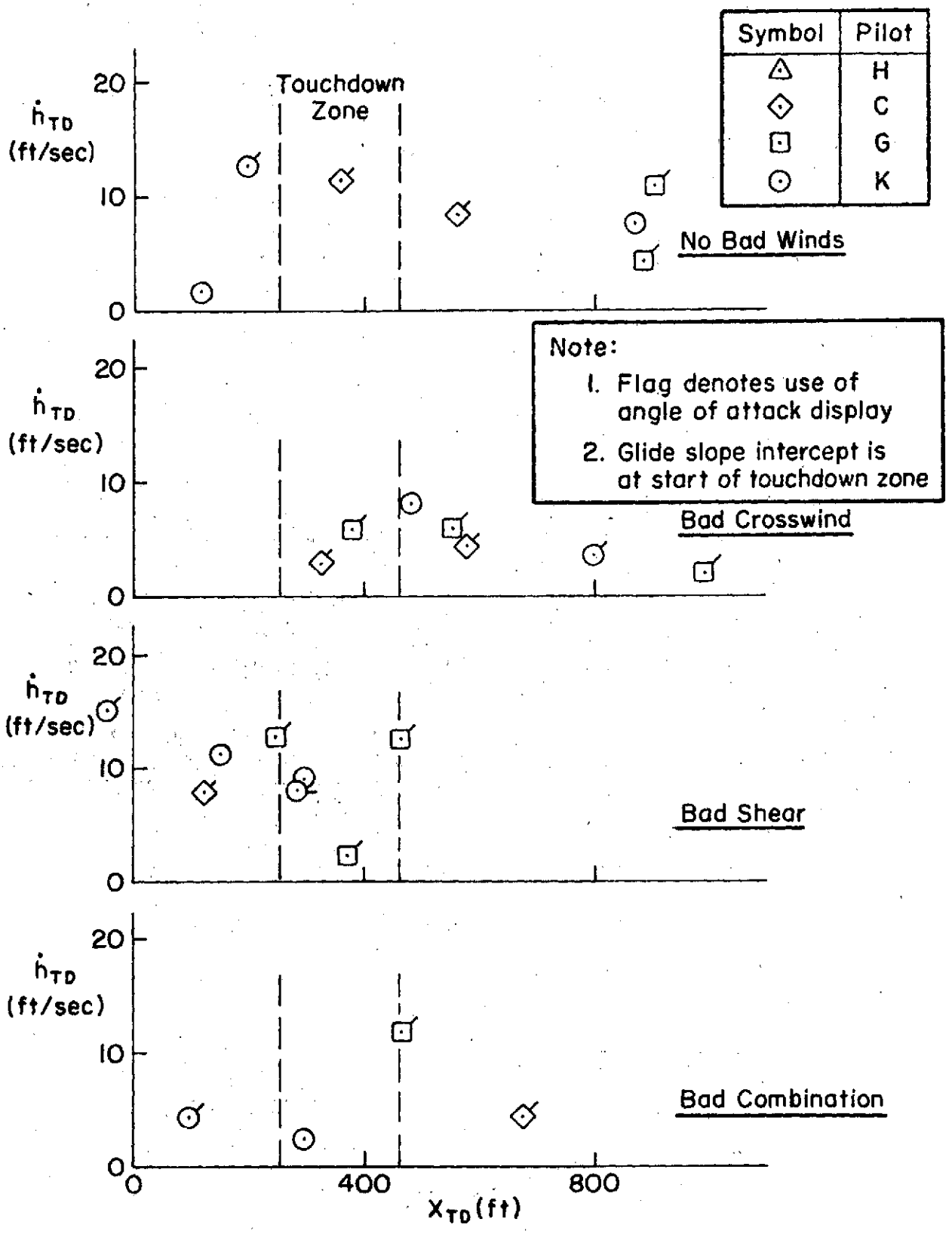

f) 50 kt, T Out, $\gamma = -7.5$ deg

Figure IV-1. (Continued)

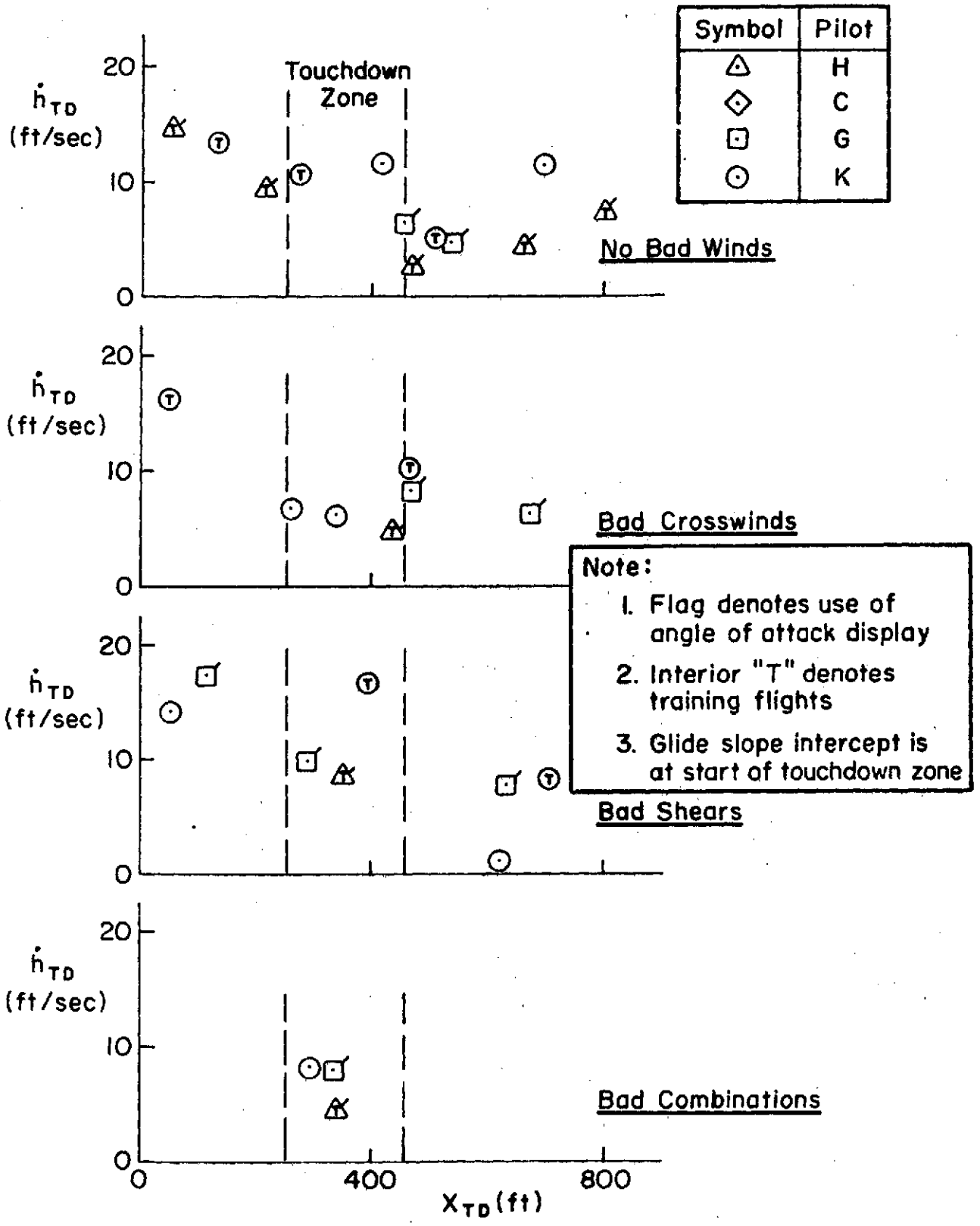

g) 65 kt, T In, $\gamma = -9.5$ deg

Figure IV-1. (Continued)

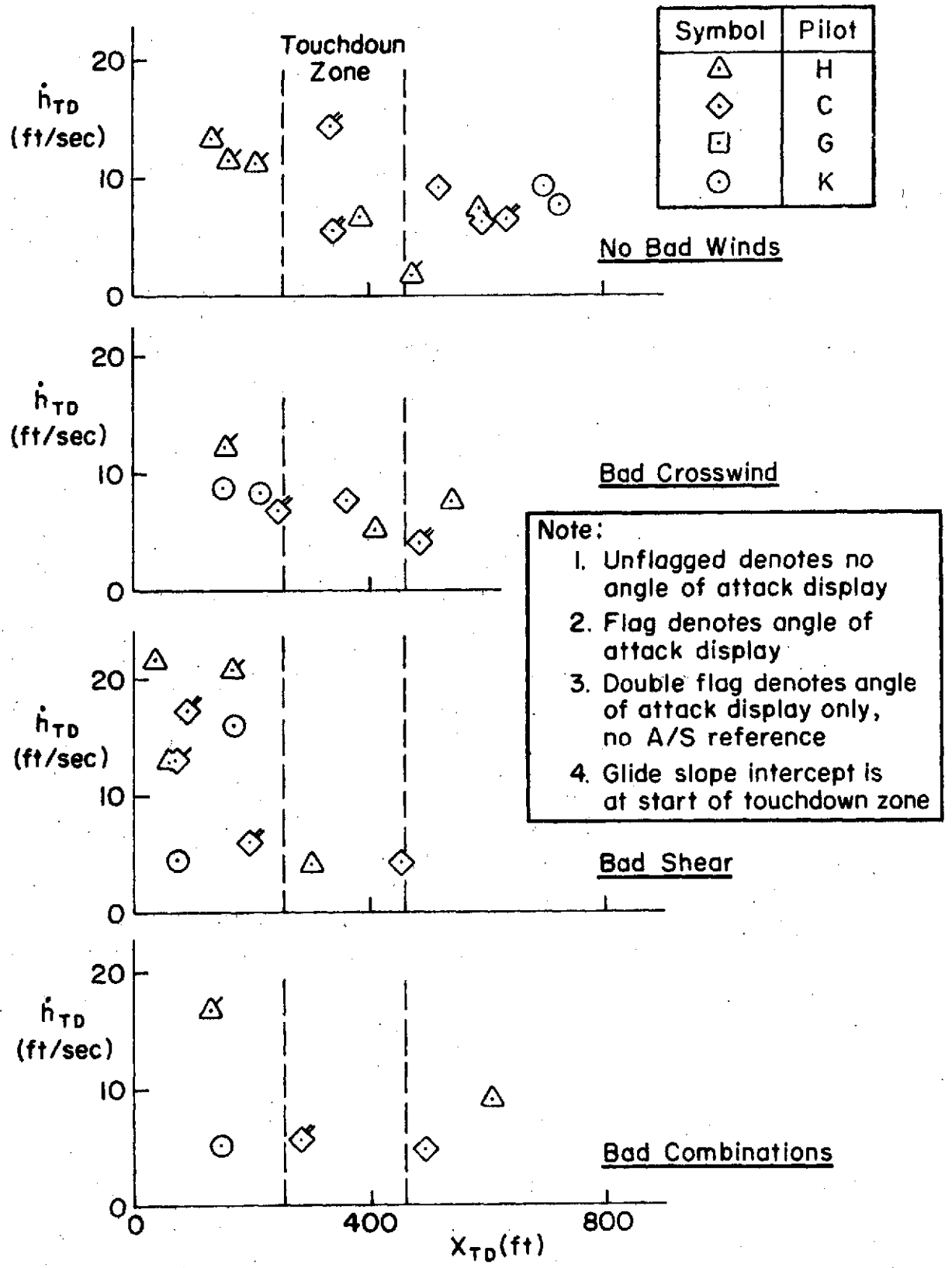

h) 140 kt, T In, γ = -9.5 deg

Figure IV-1. (Concluded)

The scatter plots have a disturbing aspect in their inconsistency in either $\dot{h}_{TD}$ or x_{TD}. This is probably due in part to the lack of specific instructions to the pilot as to desired landing conditions (e.g., a target $\dot{h}_{TD}$ and x_{TD}), as well as a lack of training directed at landings specifically. As a result of these data, pains were taken to correct these deficiencies in the 1973 tests.

4. Distribution Plots

Touchdown position and sink rate statistics are presented in cumulative distribution plots rather than histograms. This makes it easier to determine the percentage of landings within specified boundaries. The cumulative distribution is the fraction of landings at or below the value of x_{TD} or $-\dot{h}_{TD}$. For example, Fig. IV-2a shows that at 65 kt, 10% of the landings were short of the runway threshold and 23% were more than 500 ft down the runway.

a. Speed Effects. Fig. IV-2a through c are the $\dot{h}_{TD}$ and x_{TD} distribution plots for the conditions with no bad wind shears. The effects of velocity are generally rather small for transparency in. For transparency out, the highest speed (60 kt) seems the best. The slower speeds result in either long or harder landings. The trend to short, hard landings in the case of bad wind shears is evident in Fig. IV-2d through f. However, little effect on the approach speed can be detected.

b. Transparency Effects. Fig. IV-3a and b indicate that for conditions with no bad wind shears, removing transparency results in a significant change in x_{TD} and $\dot{h}_{TD}$ at 60 kt, but not at 55 kt. Removing transparency at 60 kt results in a reduction of x_{TD} by approximately 100 ft, an increase from 0 to 11% in the number of runway undershoots and a 1 - 2 ft/sec reduction in $\dot{h}_{TD}$. Considering the trade-off between landing softer but with more short landings, there is no clear advantage to transparency in or out.

Fig. IV-3c and d exhibit the tendencies found earlier for data gathered in bad wind shear conditions, that is, the number of runway undershoots and high sink rate landings both increased significantly. At 60 kt the

Number of Data Points	V_{APP}
20	55 kts
40	60 kts
48	65 kts

$\gamma = -7.5$ deg
Bad Shear Cases Excluded

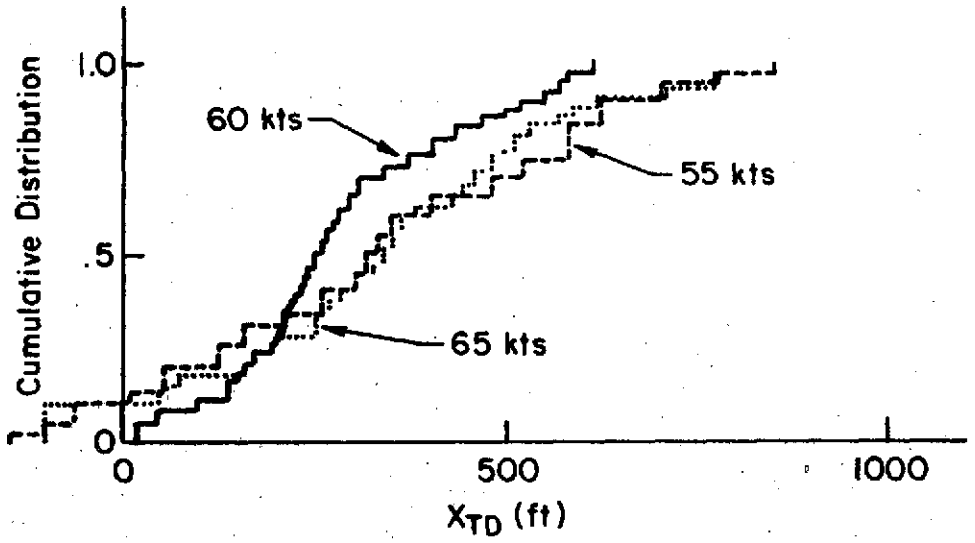

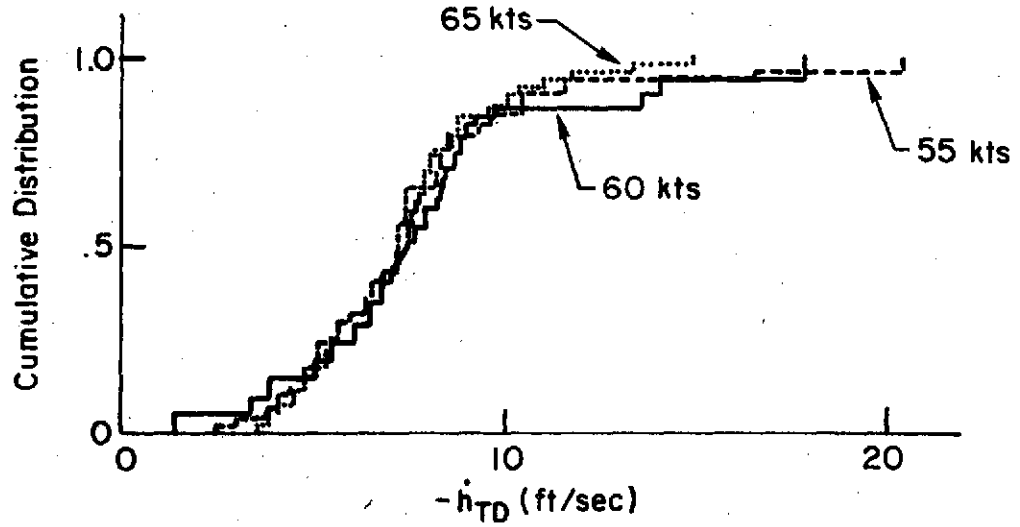

a) Transparency: In

Figure IV-2. Effect of Velocity

Number of Data Points	V_{APP}
18	50 kts
10	55 kts
40	60 kts

$\gamma = -7.5$ deg
Bad Shear Cases Excluded

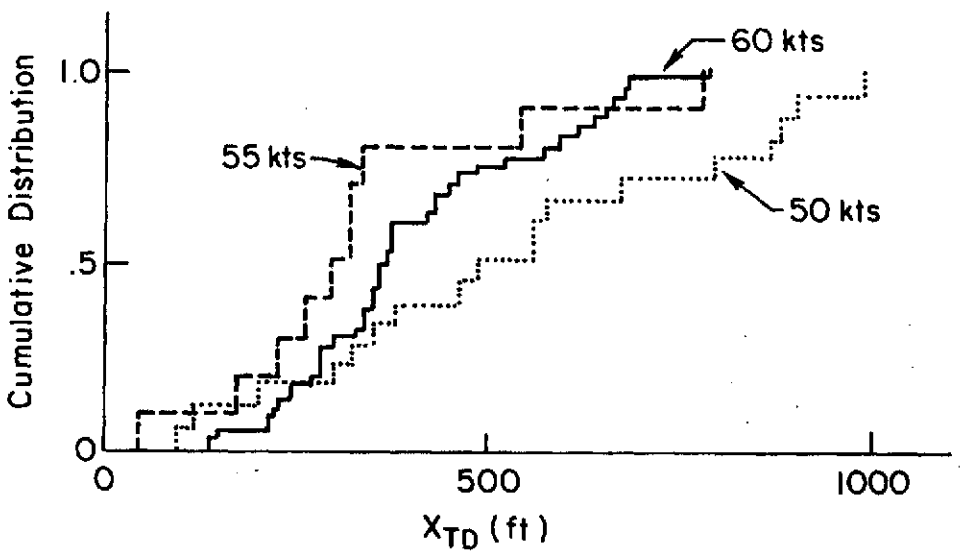

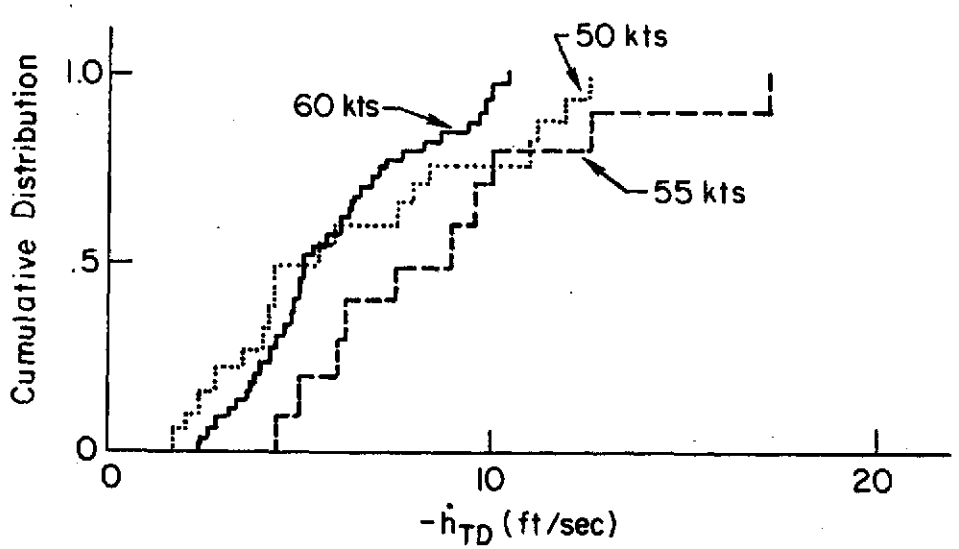

b) Transparency: Out

Figure IV-2. (Continued)

Number of Data Points	V_{APP}
25	60 kts
22	65 kts

$\gamma = -9.5$ deg
Bad Shear Cases Excluded
Transparency In

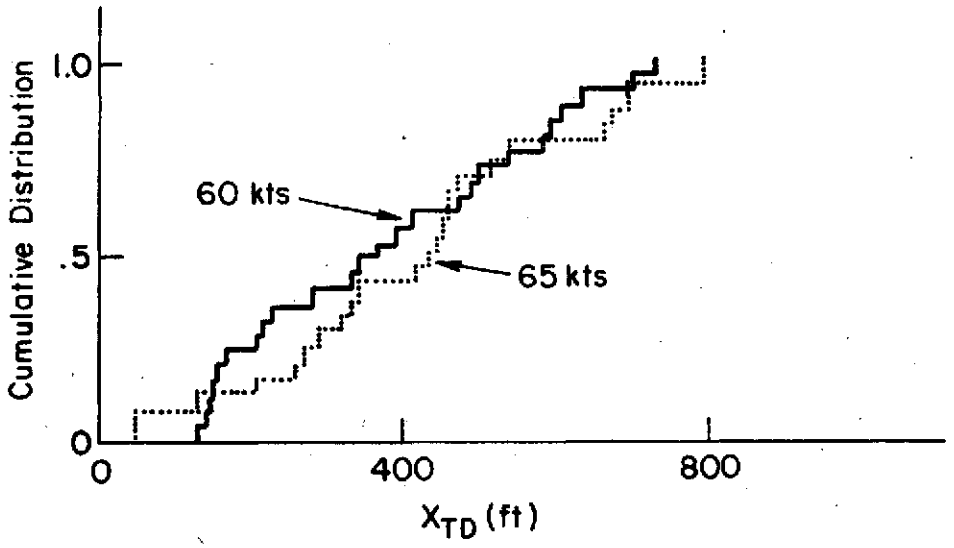

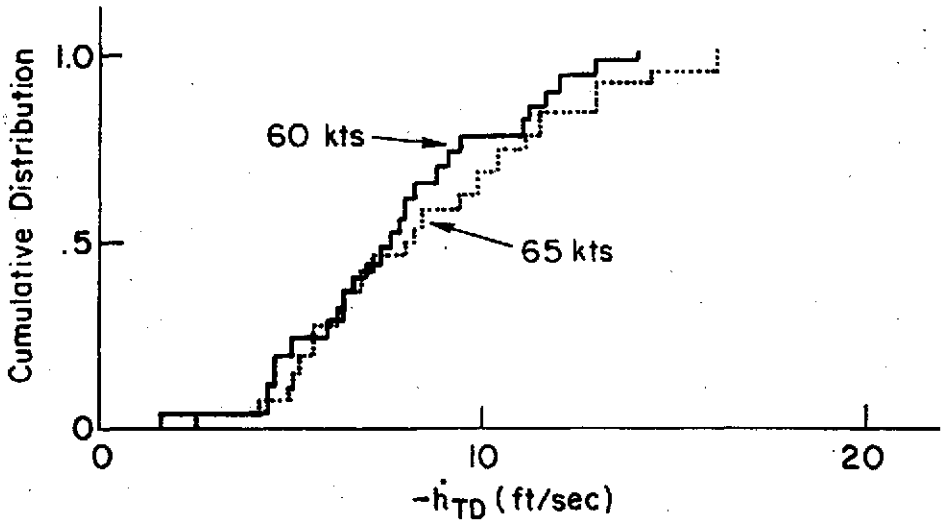

c) Steep Approach

C – 2

Figure IV-2. (Continued)

Number of Data Points	V_{APP}
8	55 kts
19	60 kts
12	65 kts

$\gamma = -7.5$ deg
Bad Shear Cases Only

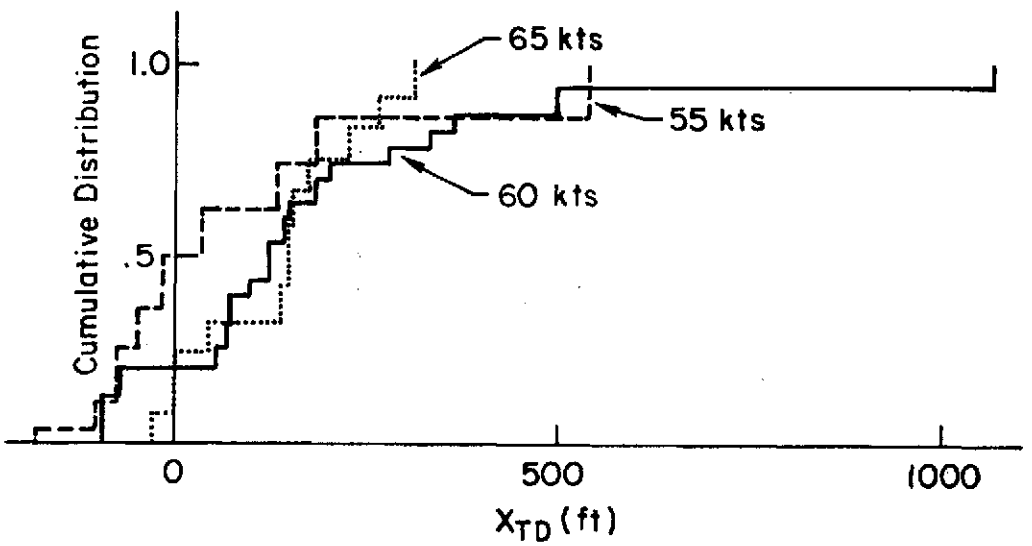

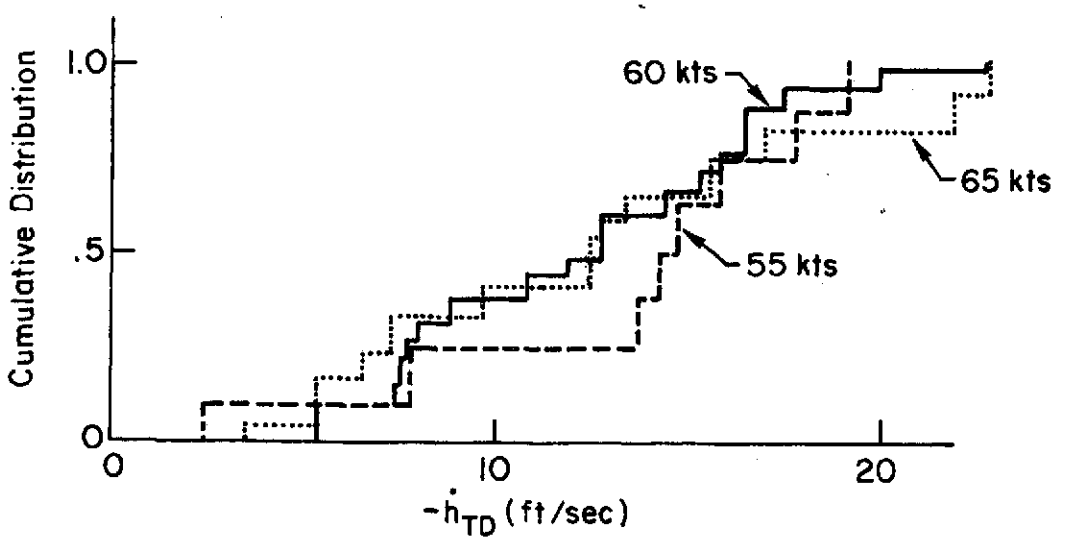

d) Transparency: In

Figure IV-2. (Continued)

Number of Data Points	V_{APP}
8	50 kts
4	55 kts
11	60 kts

$\gamma = -7.5$ deg
Bad Shear Cases Only

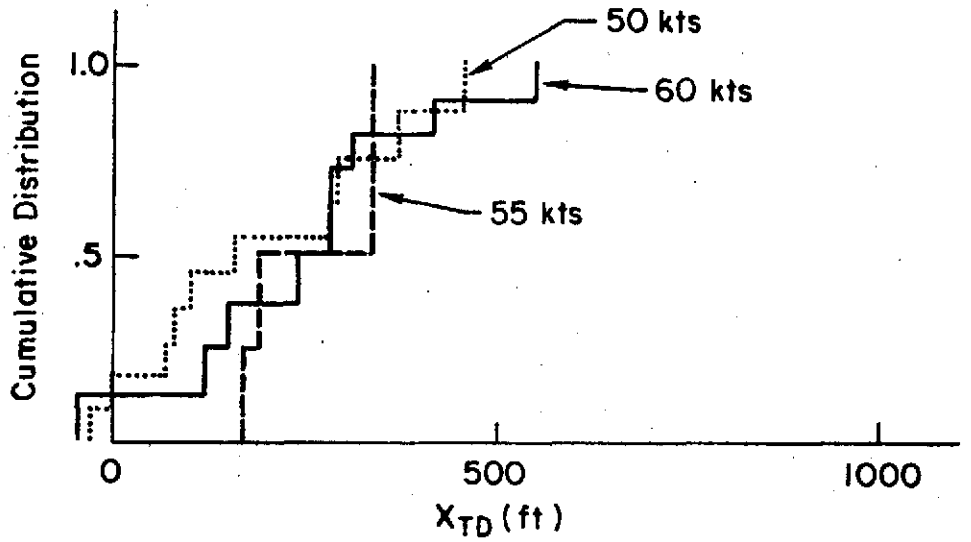

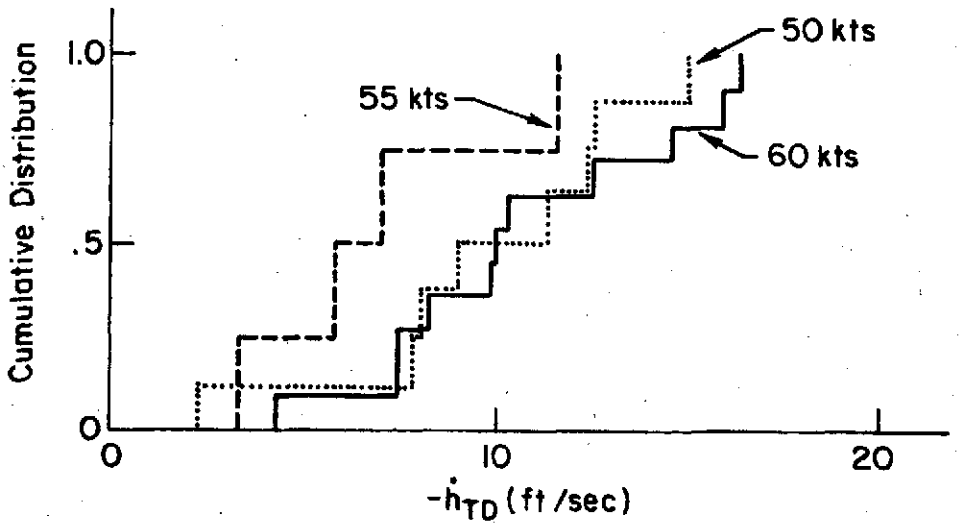

e) Transparency: Out

Figure IV-2. (Continued)

Number of Data Points	V_{APP}
9	65 kts
10	60 kts

γ=-9.5 deg
Bad Shear Cases Only
Transparency In

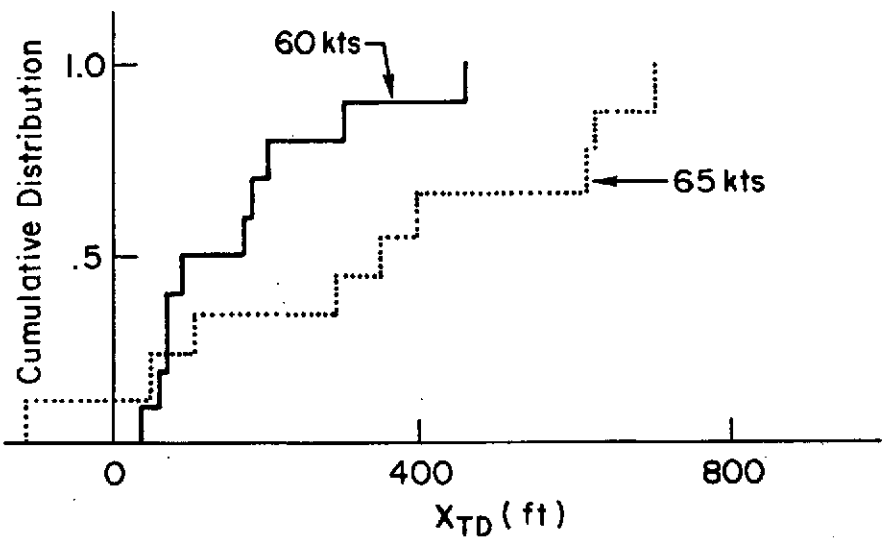

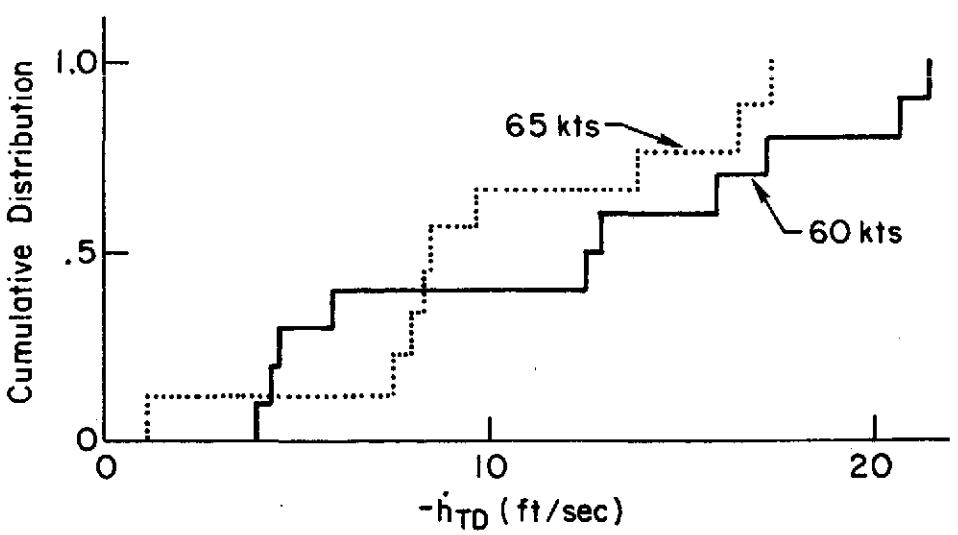

f) Steep Approach

Figure IV-2. (Concluded)

Number of Data Points	Transparency
40	IN
40	OUT

V_{APP} = 60 kts
γ = -7.5 deg
Bad Shear Cases Excluded

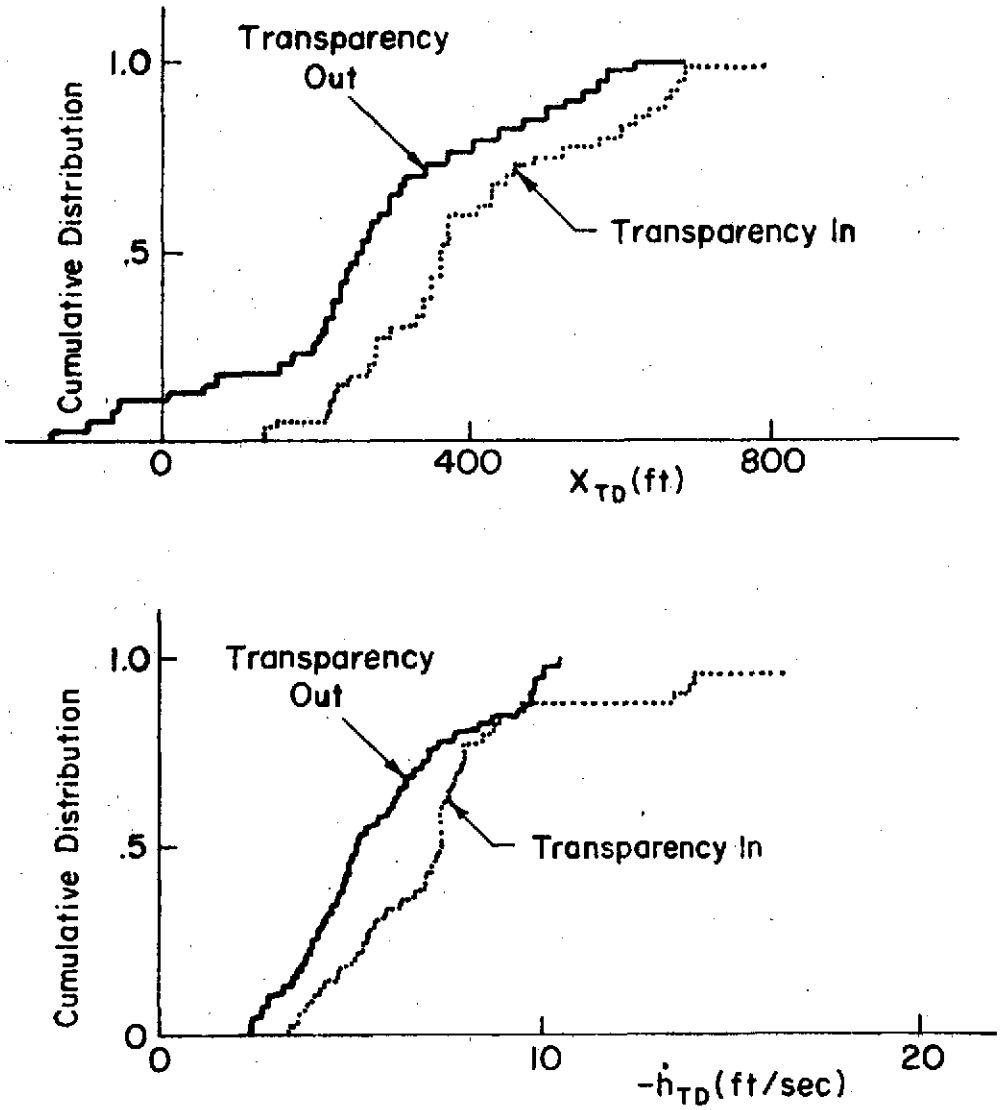

a) V_{APP} = 60 kt; Bad Shear Cases Excluded

Figure IV-3. Effect of Transparency

Number of Data Points	Transparency
20	In
10	Out

V_{APP} = 55 kts
γ = -7.5 deg
Bad Shear Cases Excluded

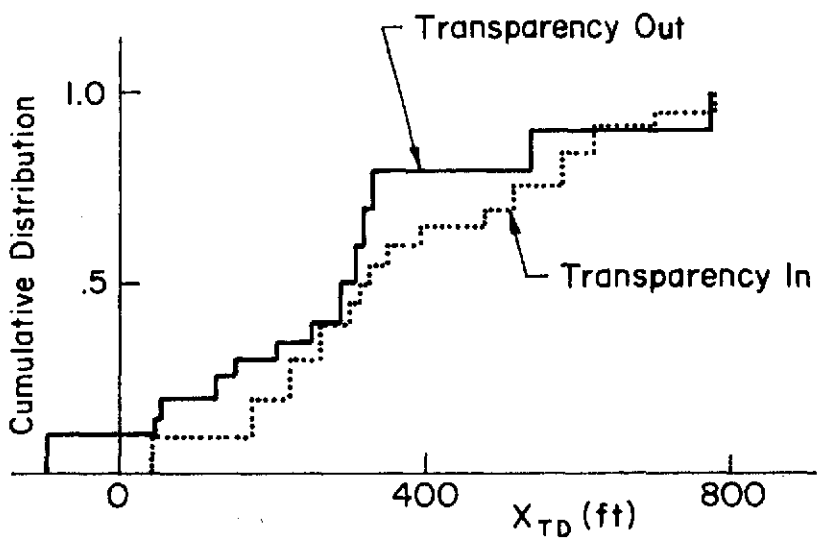

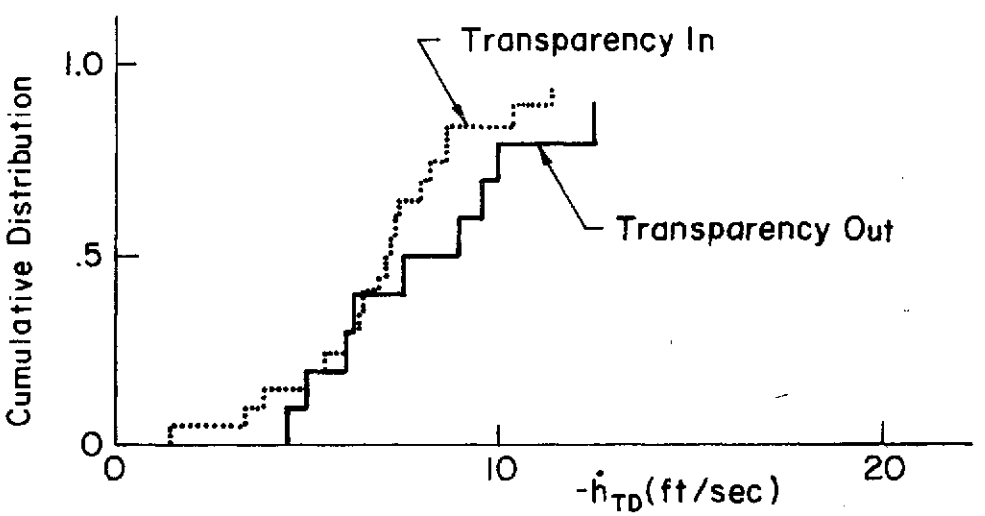

b) V_{APP} = 55 kt; Bad Shear Cases Excluded

Figure IV-3. (Continued)

Number of Data Points	Transparency
19	In
11	Out

V_{APP} = 60 kts
γ = -7.5 deg
Bad Shear Cases Only

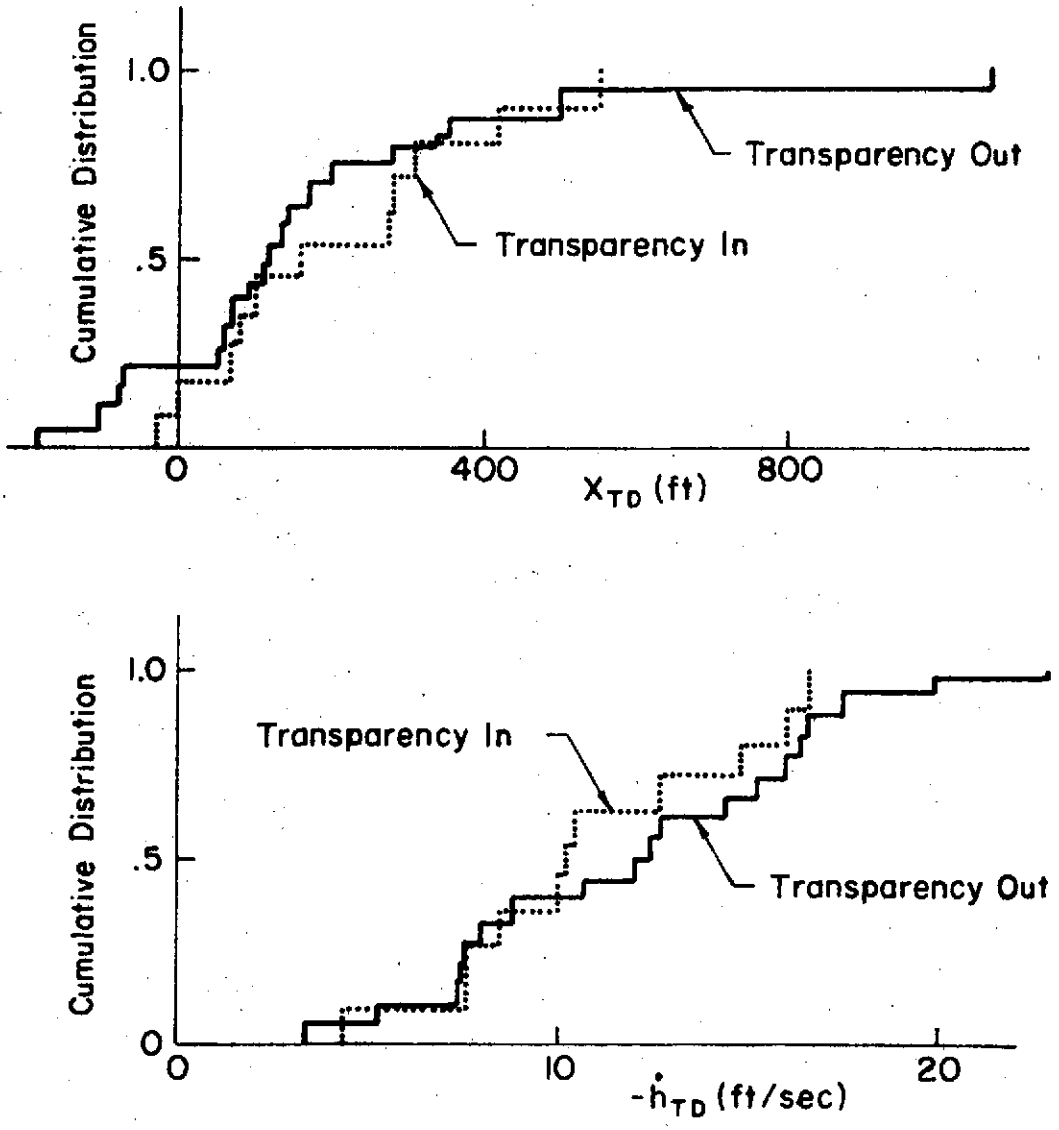

c) V_{App} = 60 kt; Bad Shear Cases Only

Figure IV-3. (Continued)

Number of Data Points	Transparency
8	In
4	Out

V_{APP} = 55 kts
γ = -7.5 deg
Bad Shear Cases Only

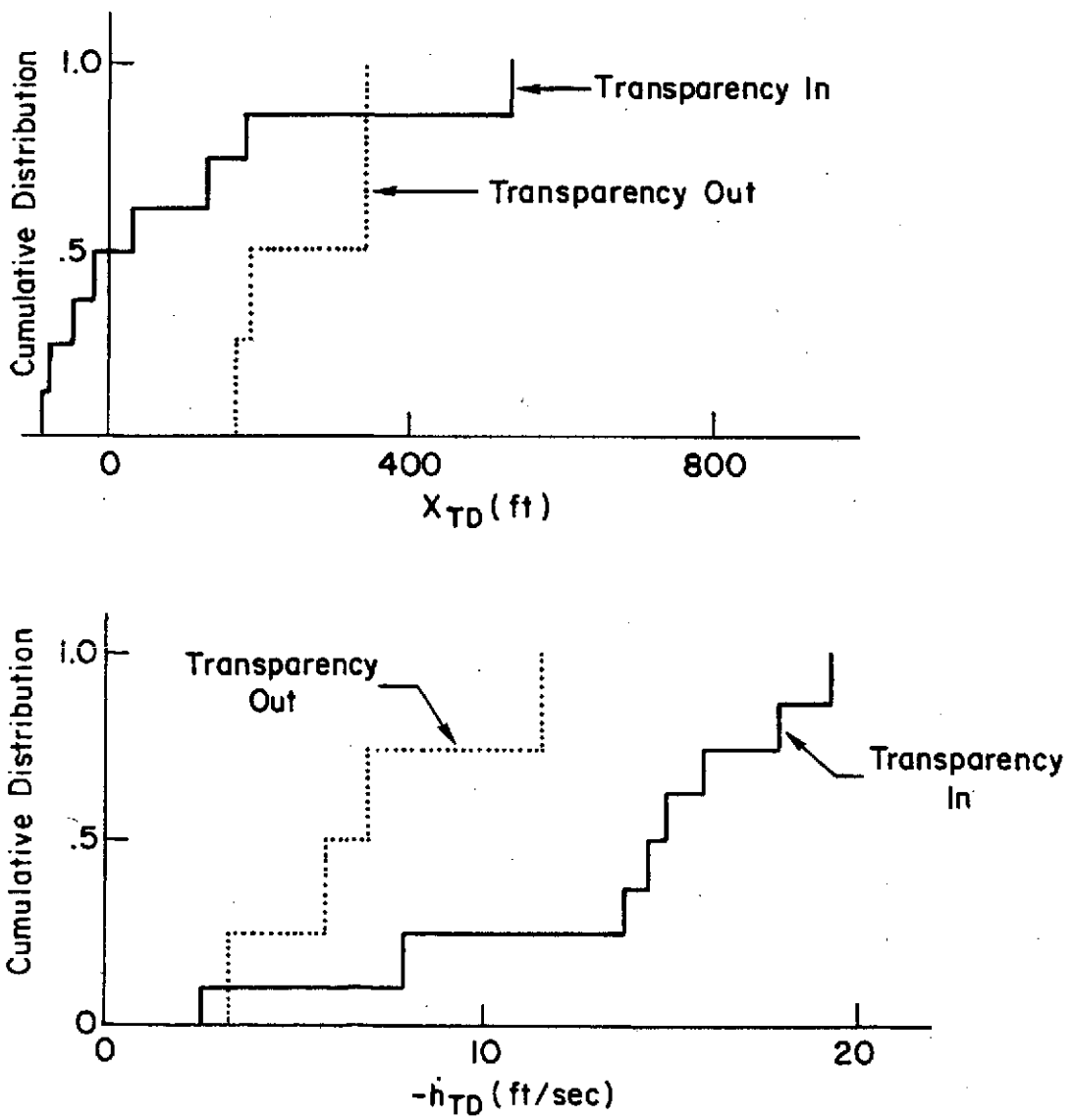

d) V_{APP} = 55 kt; Bad Shear Cases Only

Figure IV-3. (Concluded)

wind shears also had the effect of minimizing, if not removing, the differences in x_{TD} and $\dot{h}_{TD}$ due to the removal or inclusion of transparency. At 55 kt the limited number of data points precludes drawing any firm conclusions.

c. Glide Slope Effects. Fig. IV-4a and b indicate the effect of glide slope differences on x_{TD} and $\dot{h}_{TD}$ with no bad wind shears. At 60 kt, γ = -7.5 deg gives much better dispersion results for x_{TD} than does γ = -9.5 deg. Not only does γ = -9.5 deg result in higher dispersion, but 11% of the landings are undershoots. At 65 kt, γ = -7.5 deg appears to yield only slightly better control of x_{TD}. For both speeds, the variation of glide slope angle did not appear to affect $\dot{h}_{TD}$ to a significant extent. As expected, the inclusion of bad wind shears (Fig. IV-4c and d) increased the number of landing undershoots and high sink rate landings, but did not produce any significant effects due to glide slope angle.

B. 1973 TESTS

1. Test Conditions

The April/May 1973 test conditions and procedures were the same as those used in 1972 with the following exceptions:

- Addition of longitudinal and lateral/directional SAS
- Addition of visual glide slope indicator
- Improved visual display optics
- Pilots were instructed to try to land in the touchdown zone (x = 300 to 500 ft) with moderate sink rates (about 5 ft/sec)
- Approach attitude was always -5 deg (except for a special series of attitude variation tests)
- Pilots were given extensive training directed specifically to landings.

In addition to the landings made in conjunction with the normal approach task a short series of tests were run to investigate the effect of approach pitch attitude and propulsion lags.

Number of Data Points	γ (deg)
22	-9.5
48	-7.5

V_{APP} = 65 kt
Bad Shear Cases Excluded
Transparency In

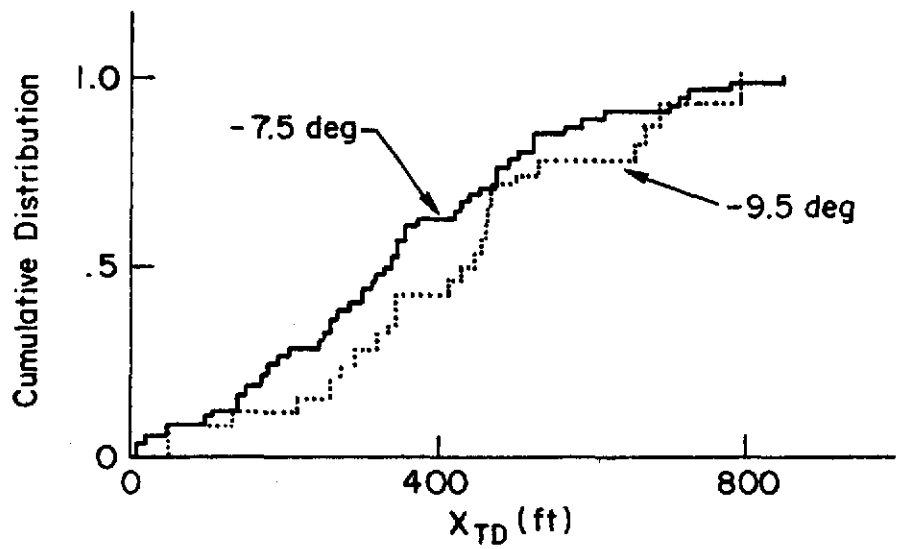

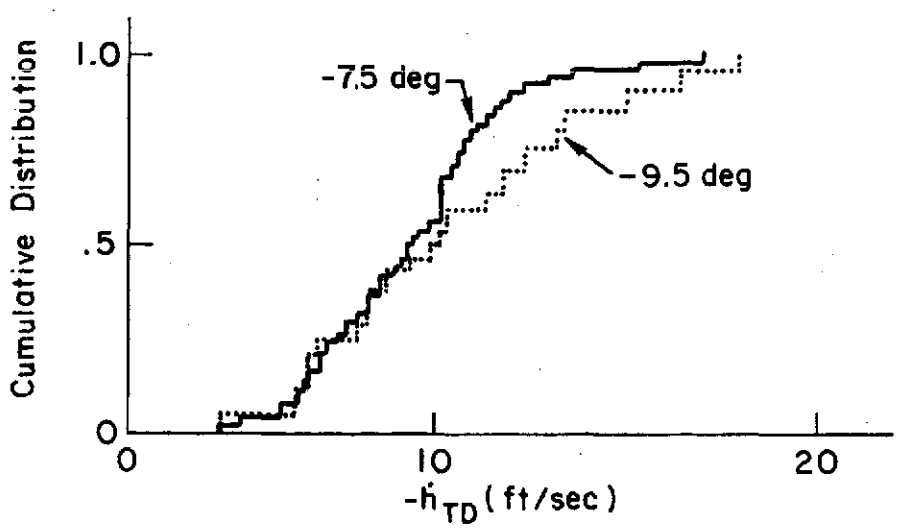

a) V_{APP} = 65 kt; Bad Shear Cases Excluded

Figure IV-4. Effect of Glide Slope

Number of Data Points	γ(deg)
40	-7.5
25	-9.5

V_{APP} = 60 kt

Bad Shear Cases Excluded

Transparency In

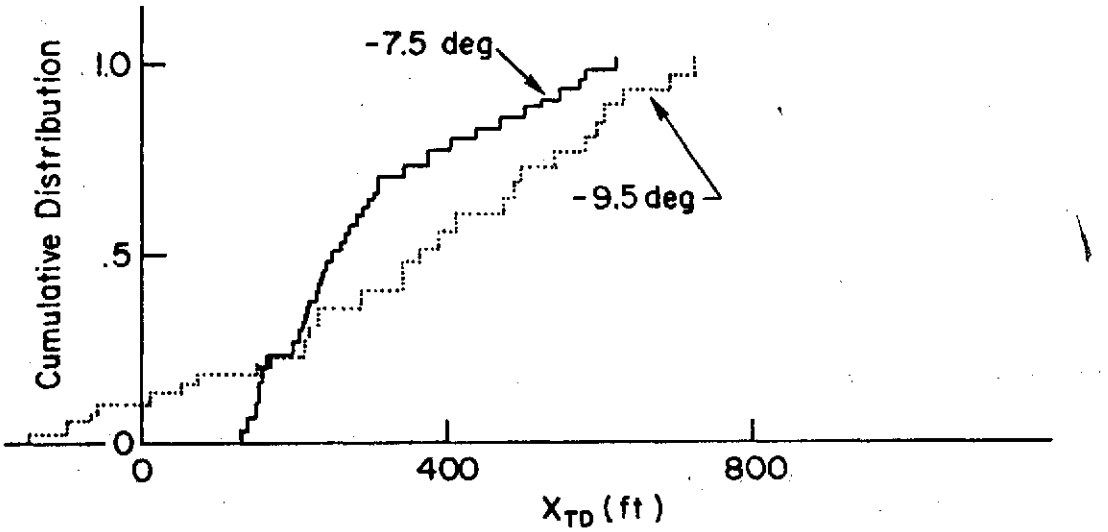

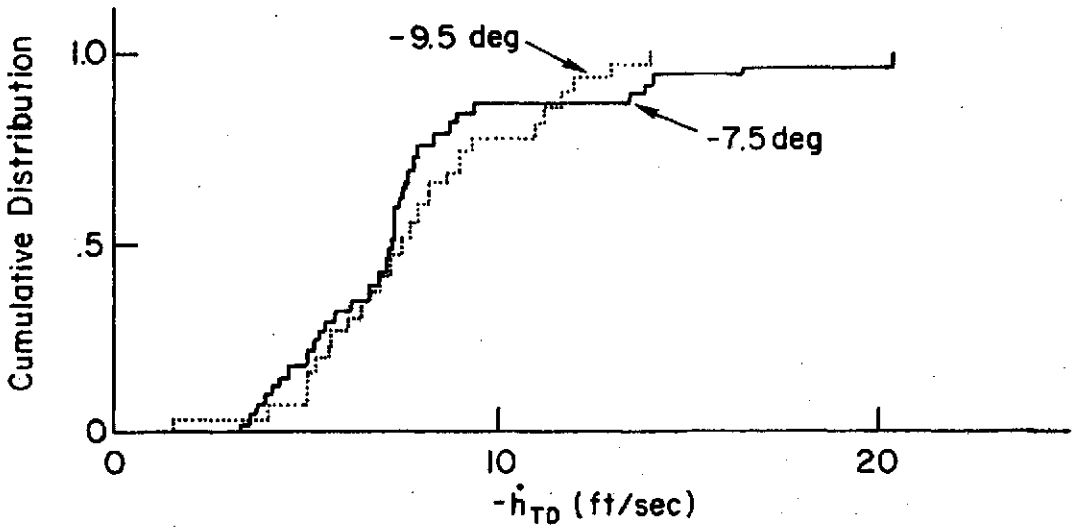

b) V_{APP} = 60 kt; Bad Shear Cases Excluded

Figure IV-4. (Continued)

Number of Data Points	γ deg
9	-9.5
12	-7.5

V_{APP} = 65 kt

Bad Shear Cases Only

Transparency In

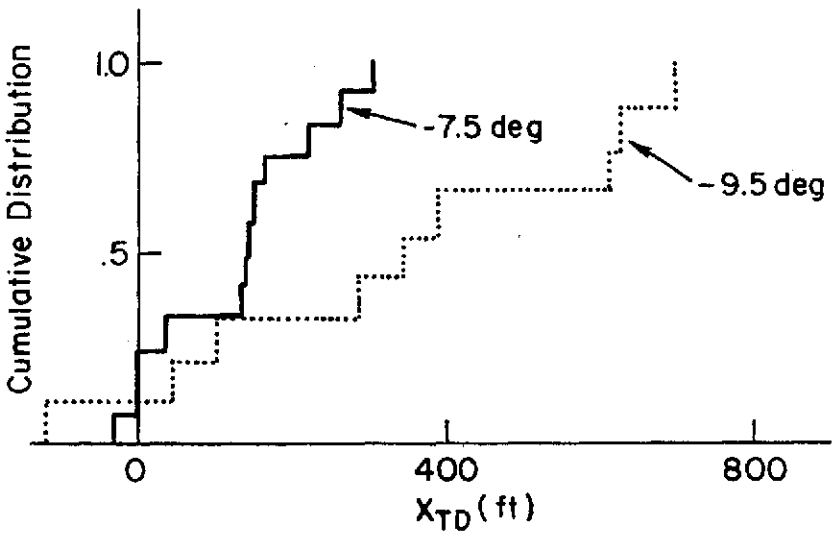

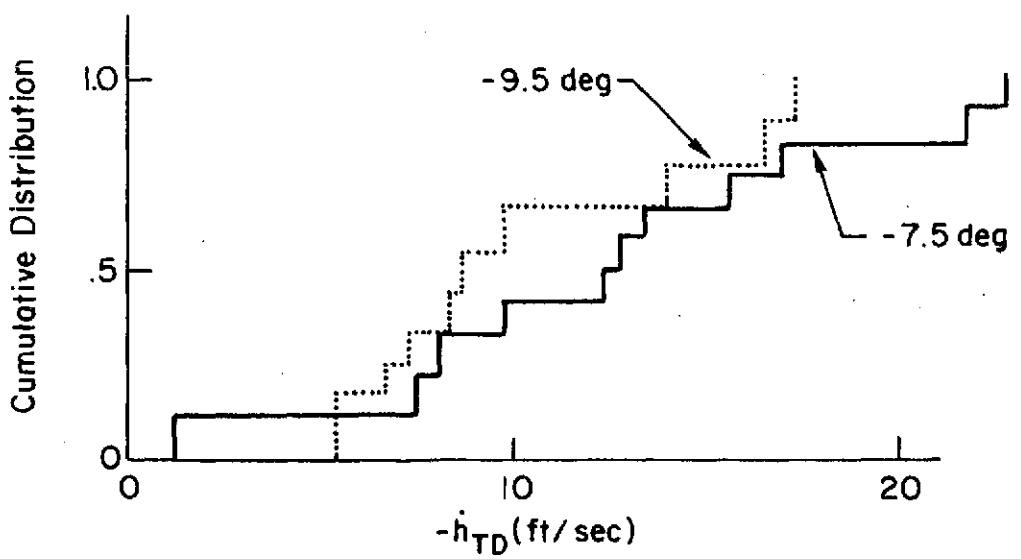

c) V_{APP} = 65 kt; Bad Shear Cases Only

Figure IV-4 (Continued)

Number of Data Points	γ deg
19	-7.5
10	-9.5

V_{APP} = 60 kt

Bad Shear Cases Only

Transparency In

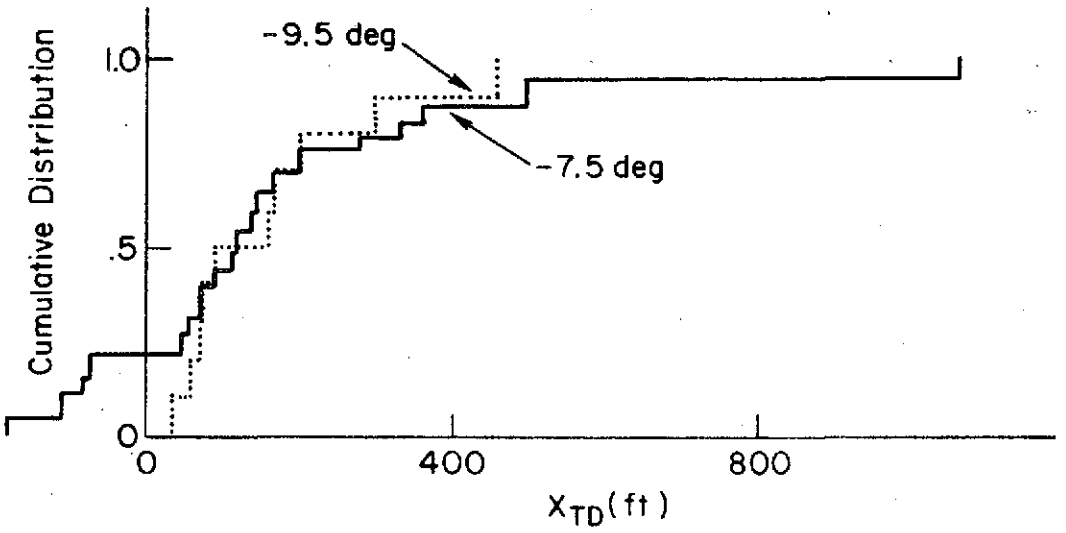

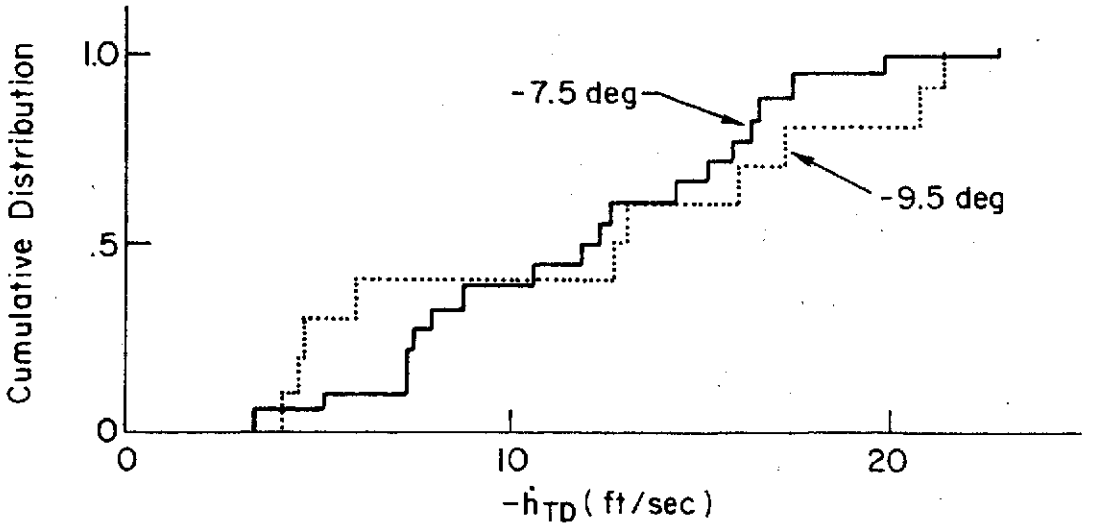

d) V_{APP} = 60 kt; Bad Shear Cases Only

Figure IV-4. (Concluded)

2. Main Test Results

In general, the results of flare and landing tests are broken down in terms of wind and turbulence, configuration (transparency, approach speed), and pilot. Scatter plots of $\dot{h}_{TD}$ versus x_{TD} are shown in Figs. IV-5 and IV-6. Fig. IV-5 shows results obtained in calm air. Each pilot was highly consistent at 65 kt and less so as approach speed was reduced. Also the magnitude of the sink rate degraded with decreasing speed. The effect of transparency appeared small although one pilot (Hardy) seemed to have a tendency to float farther (about 200 ft) with transparency in.

The effects of winds and turbulence are shown in Fig. IV-6a and b. Regardless of configuration or pilot the touchdown dispersion (both $\dot{h}_{TD}$ and x_{TD}) is increased significantly over calm air conditions. For example, the case of transparency out at 60 kt yields the following ranges for 68% of the respective test points for calm air versus turbulence:

	$-\dot{h}_{TD}$ (ft/sec)	x_{TD} (ft)
Calm air	$4.1 \pm .4$	360 ± 110
Turbulence and winds	5.1 ± 2.8	600 ± 235

The effect of the various kinds of mean winds, i.e., cross winds, tailwinds, shears, etc., was not distinguishable. Therefore all are lumped together in Figs. IV-6 and IV-7. The lack of a noticeable effect of the wind shears represents a significant change from the 1972 tests. With the simulation improvements the pilots were apparently able to detect and compensate for the shears.

The distribution plots, Fig. IV-7, show better the effects of configuration. In general, the pilots' performance in terms of $\dot{h}_{TD}$ and x_{TD} was about the same regardless of V_{APP} except for 55 kt. Here the touchdown sink rate increased noticeably (by about 1.5 ft/sec). Transparency seems mainly to affect the high end of the distributions. There are more very hard or very long landings with transparency out.

Pilot comments and ratings correlate well with touchdown sink rate. The pilot ratings given by Hardy (from Appendix D) are tabulated below:

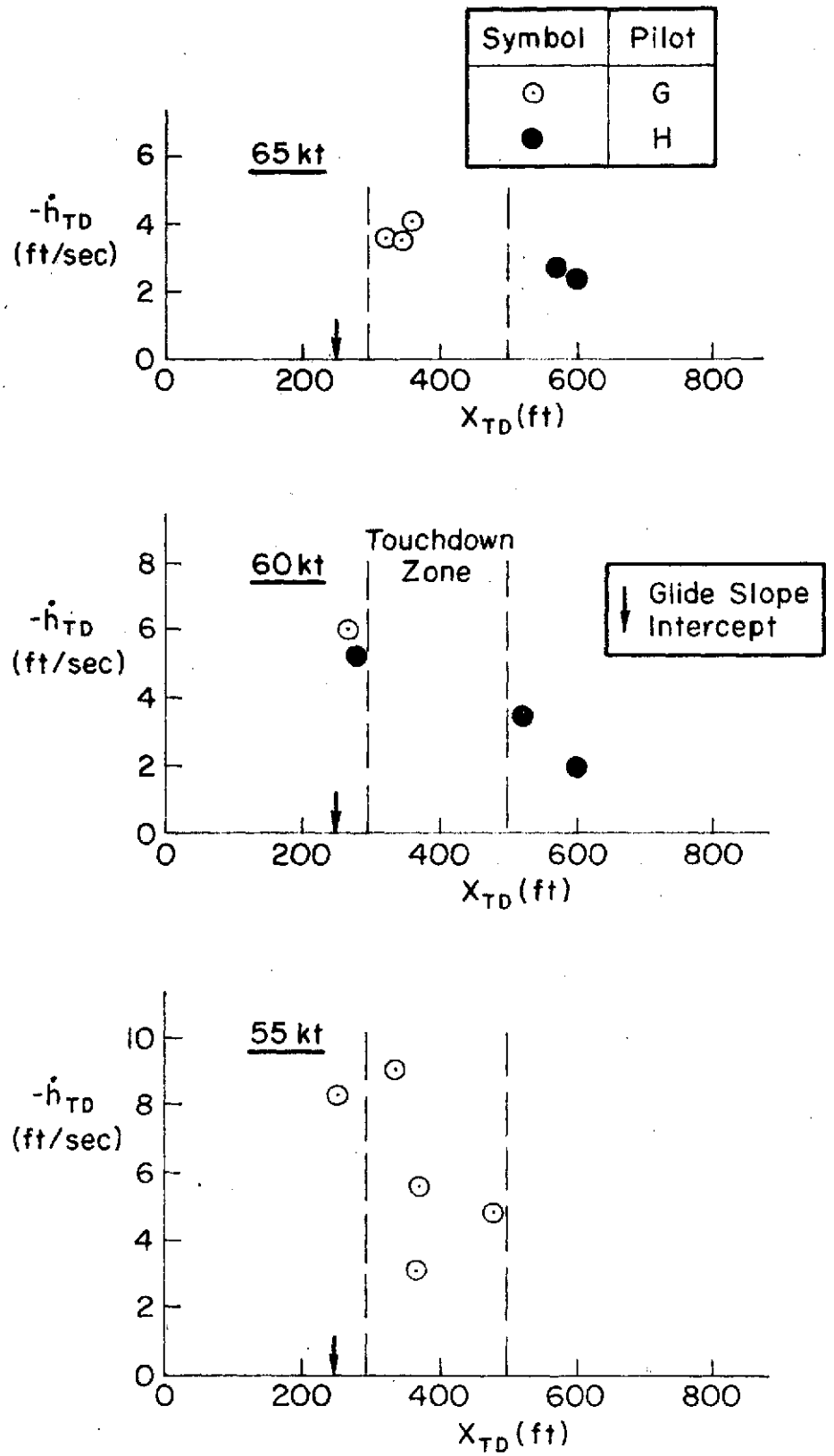

a) Transparency In

Figure IV-5. Touchdown Scatter Plots, Calm Air

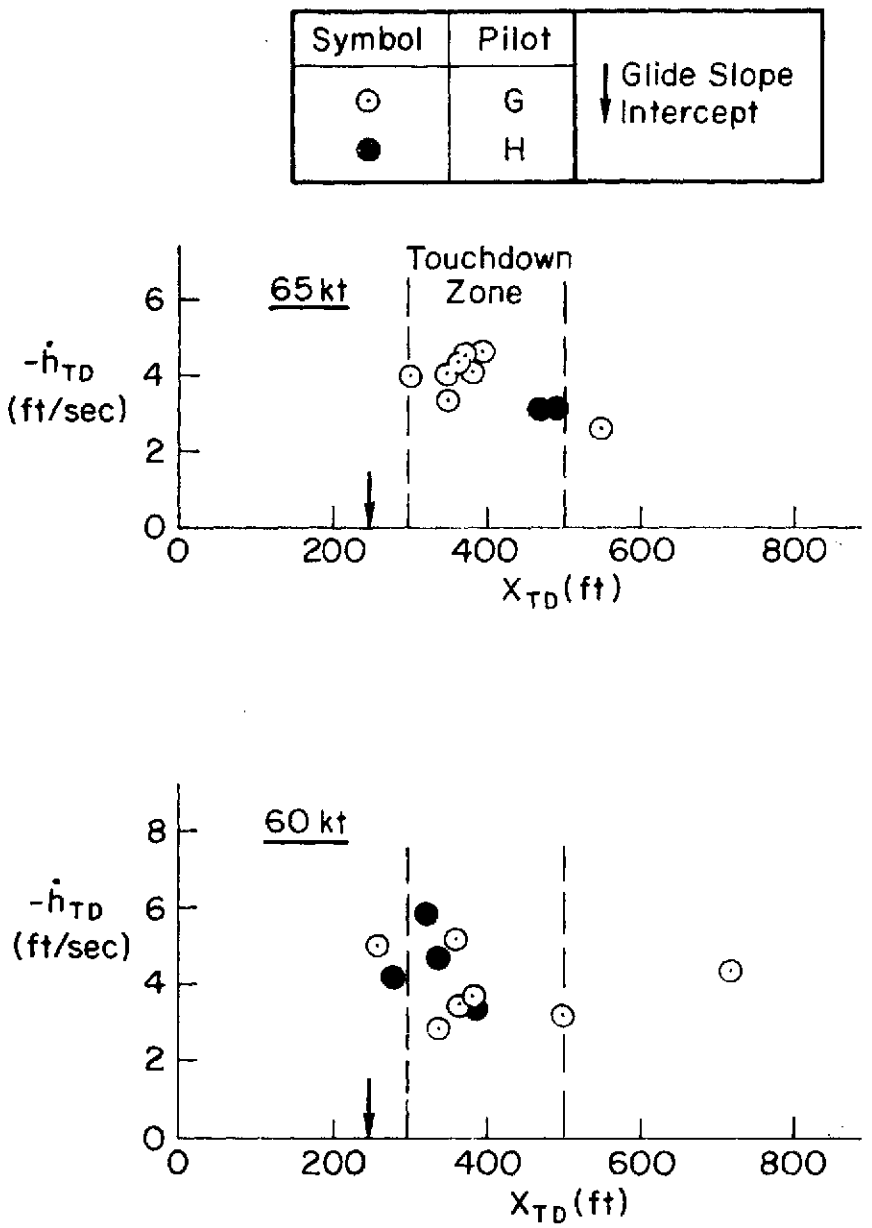

b) Transparency Out

Figure IV-9. (Concluded)

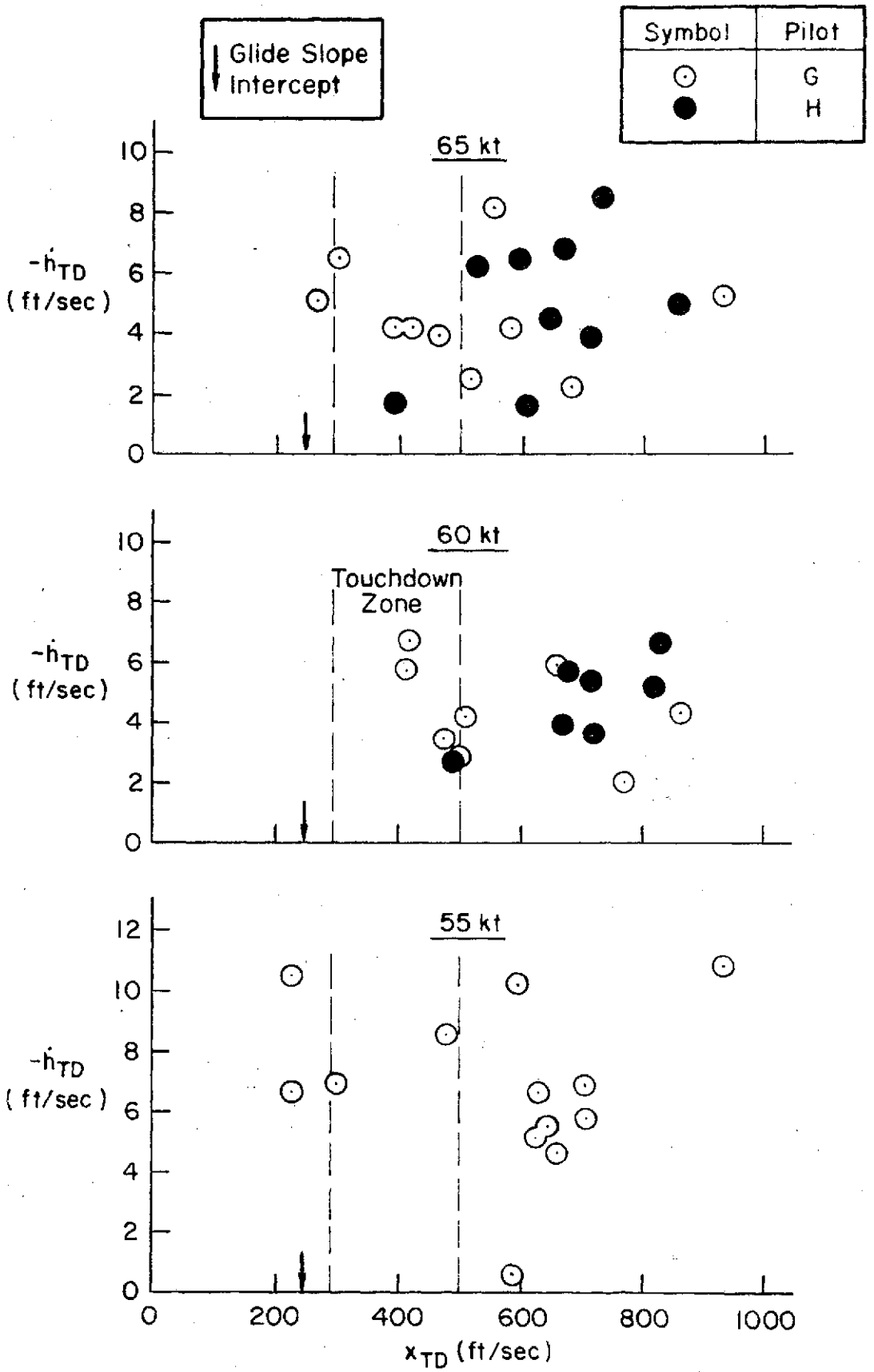

a) Transparency In

Figure IV-6. Touchdown Scatter Plots, with Wind and Turbulence

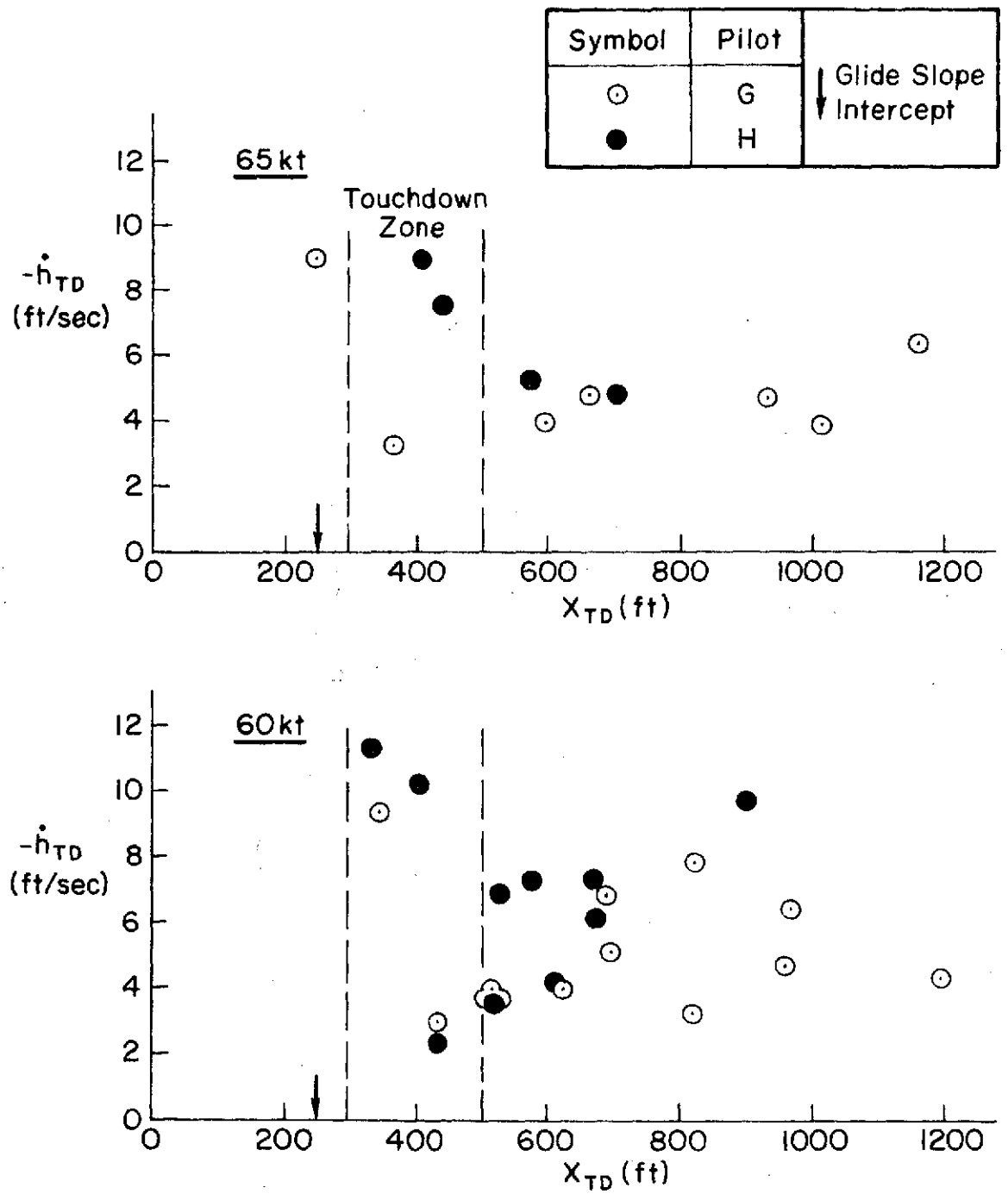

b) Transparency Out

Figure IV-6. (Concluded)

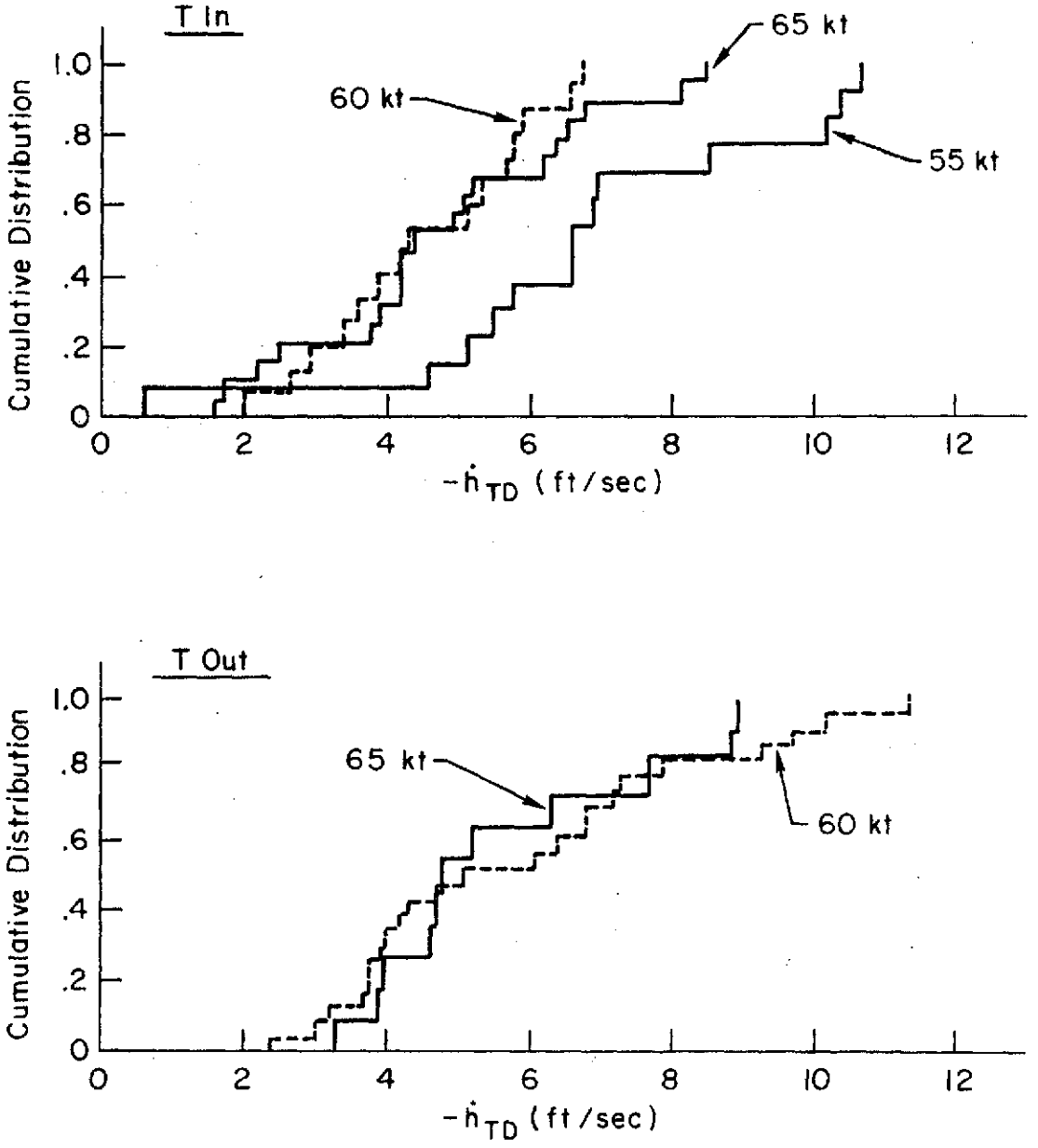

a) Sink Rate

Figure IV-7. Touchdown Distribution Plots with Wind and Turbulence

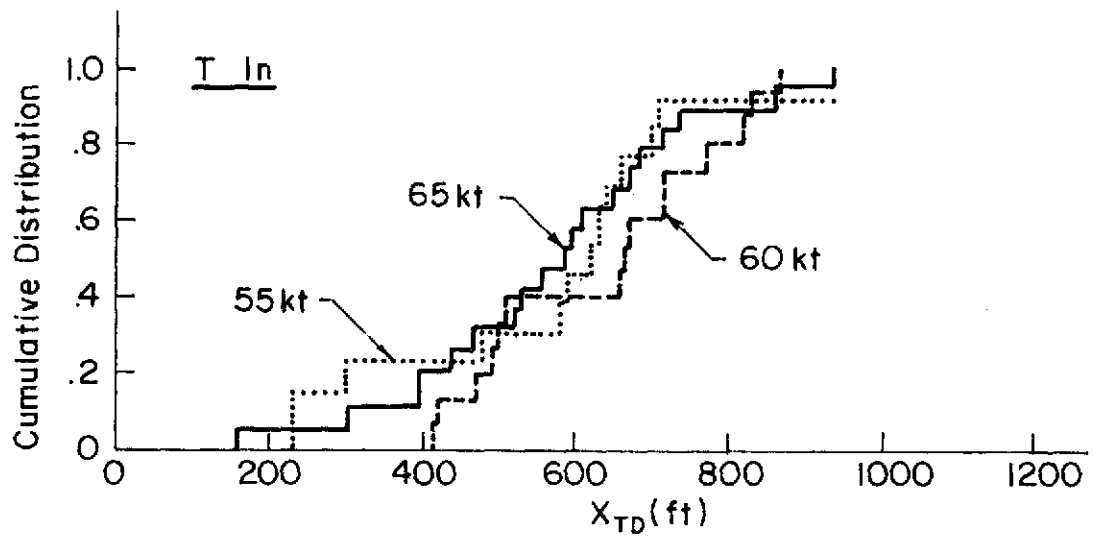

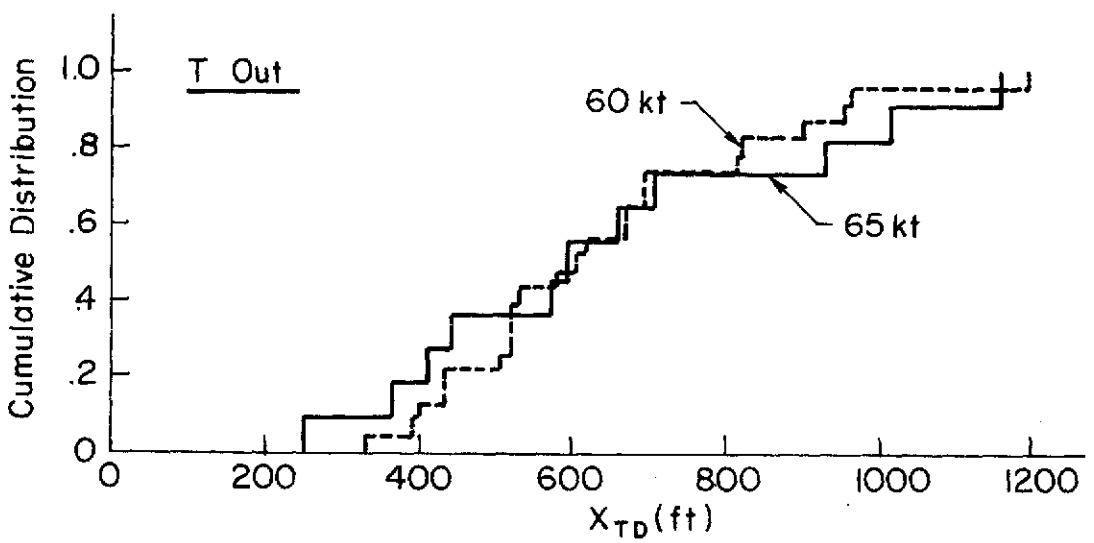

b) Touchdown Distance

Figure IV-7. (Concluded)

V_{APP}	TRANSPARENCY	PILOT RATING (Calm Air)	PILOT RATING (Turbulence)
65	IN	3	5 1/2
60	IN	3 1/2	6
55	IN	5	6 1/2
65	OUT	3 1/2	6
60	OUT	3 1/2	6

Fig. IV-8 shows these ratings plotted against the median touchdown sink rate obtained by both pilots.

The comments of both pilots and the ratings given by Hardy* agree well. Both pilots describe having to cope with varying power to aid in the flare. In general this consisted of a power addition with more power required at the lower speeds. Gough commented on the problem of adding precisely the right amount of power at the lower approach speeds. At 55 kt with transparency in he stated that it was a delicate mix of attitude and throttle increments. At 55 kt without transparency he noted that he added power at the same rate as attitude. In all cases, turbulence significantly worsened the task.

The interpretation of the landing performance data and pilot commentary was aided by the flare analysis of Appendix C. The calm air touchdown performance of Fig. IV-5 is fairly well duplicated in the computer solutions of Fig. C-3 for the nominal flare maneuver. Also shown is the trend of trading $\dot{h}_{TD}$ for increased x_{TD} at the higher speeds and no change in x_{TD} at lower speeds.

The flare analysis explains the pilots' need to add power at the lower speeds. The flare program was used to search for the best obtainable $\dot{h}_{TD}$ without a power change for each of the configurations tested. This is plotted in Fig. IV-9 versus the margin above V_{min} (at the approach power setting). The figure shows that landings at 5 ft/sec or less cannot be made at 55 or 60 kt without adding power. Thus the pilot cannot make a

* Pilot Gough did not rate approach and landing separately.

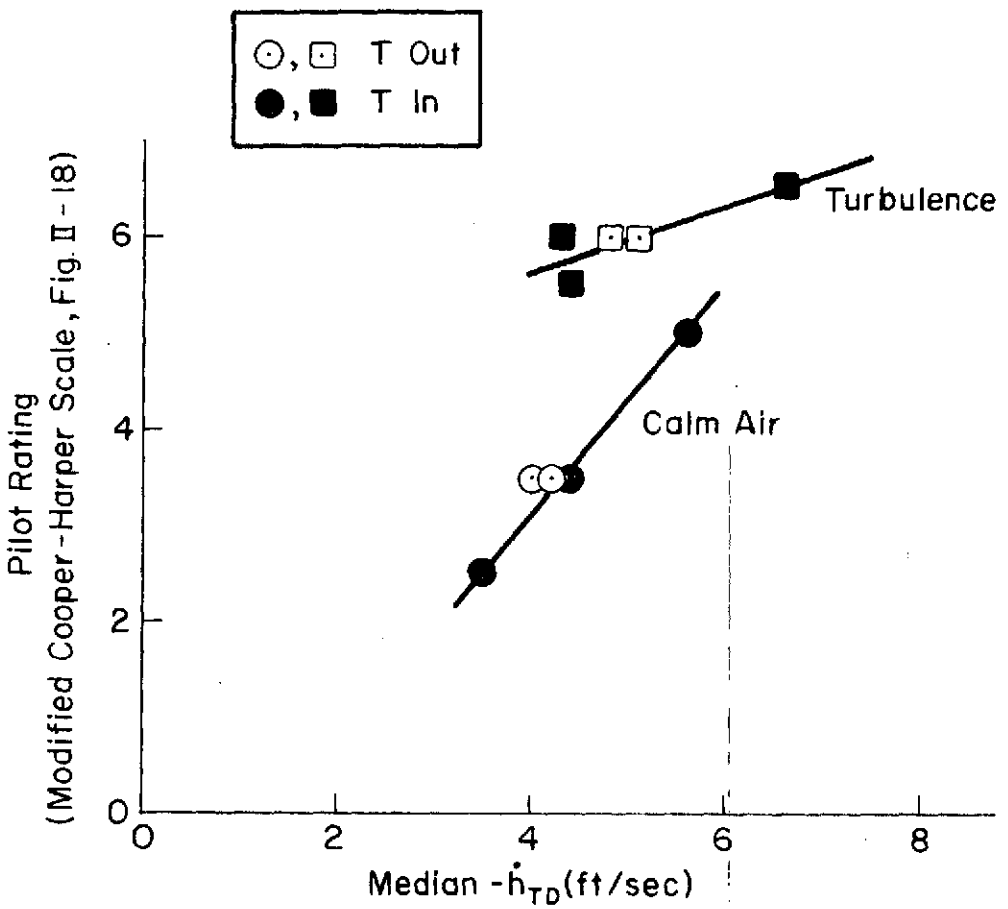

Figure IV-8. Correlation of Pilot Rating to Median $\dot{h}_{TD}$

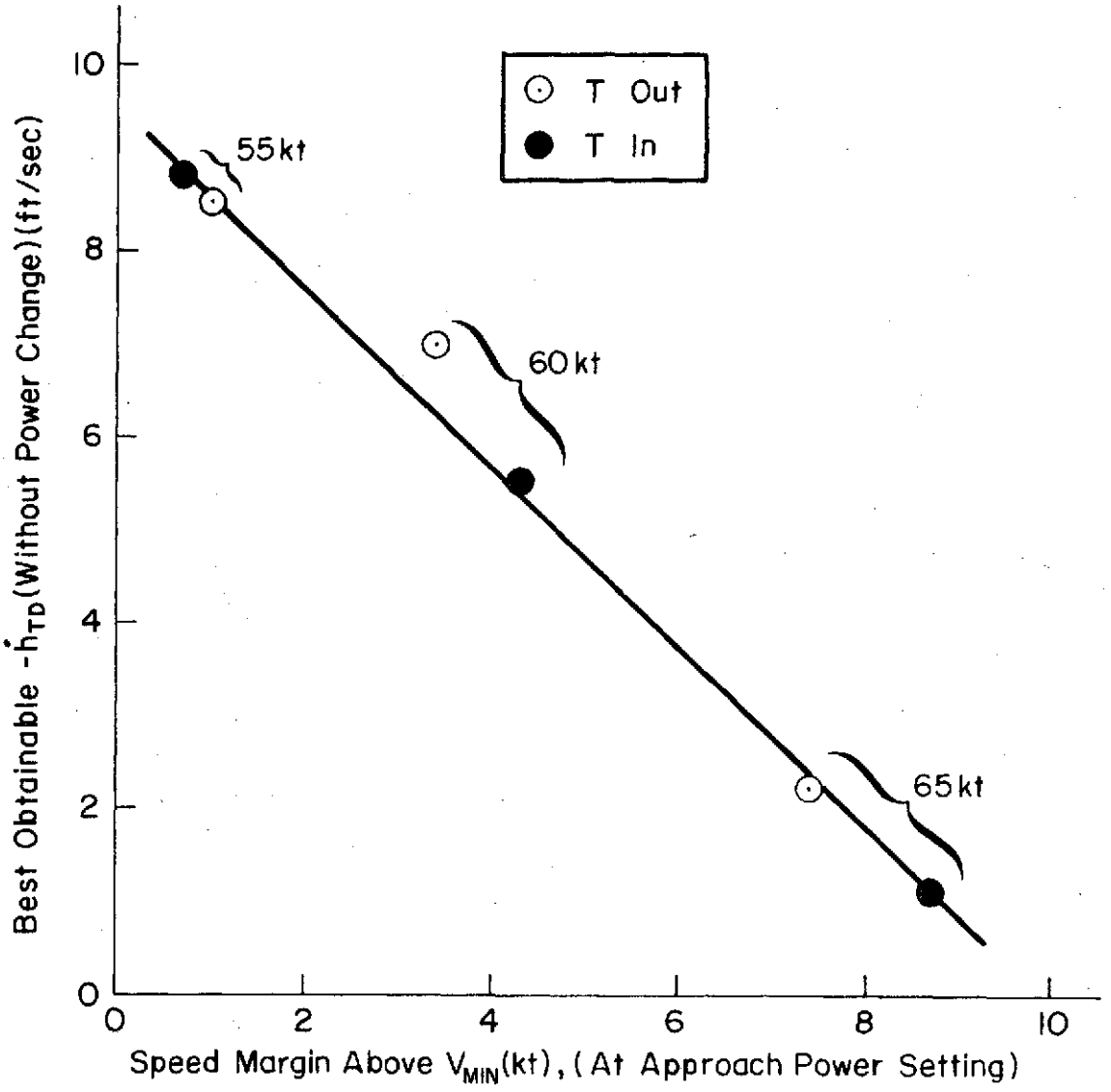

Figure IV-9. Touchdown Sink Rate Potential vs. Speed Margin

satisfactory landing at these speeds, even in calm air, without adding power. The power addition is essential at 55 kt. At 60 kt, transparency in, the power addition is not critical as a sink rate of 5.6 ft/sec is possible without it, but the power addition permits more desirable sink rates at touchdown.

Figure IV-9 also shows that the best $\dot{h}_{TD}$ is well correlated with speed margin. Whether the same relationship holds for other STOL configurations is a matter for further investigation.

The best obtainable $\dot{h}_{TD}$ without changing power also correlates well with the pilot ratings (see Fig. IV-10). This suggests a flare criteria might be based on the best obtainable $\dot{h}_{TD}$ without adding power even if the pilots find it desirable to add a small amount of power in the flare.

3. Comparison with 1972 Results and Flight Data

Results obtained from the 1973 simulation generally agreed well with those obtained during flight tests in the actual airplane during July 1972. Table C-1 gives flight test landing data. A distribution plot of $\dot{h}_{TD}$ for all landings made is included in Fig. IV-11. These landings were made in atmospheric conditions falling somewhere between the calm air and turbulence conditions of the simulation. Thus, Fig. IV-11 shows an excellent agreement between the 1973 simulation and flight data. It also shows a significant difference between the 1972 and 1973 simulations. The simulation improvements made for the 1973 tests clearly improved landing performance to the point that it was very close to actual flight.

4. Variation of Approach Attitude

The effects of varying approach attitude were evaluated by adjusting the wing incidence of the model (see Section II, Part B, No. 2) while maintaining a constant γ_{APP} of -7.5 deg at 60 kt with transparency in. Approach attitudes of -10, +2, and the nominal value of -5 deg, were investigated and the results are depicted in Fig. IV-12a. The touchdown sink rates and distances do not show an obvious effect of approach attitude.

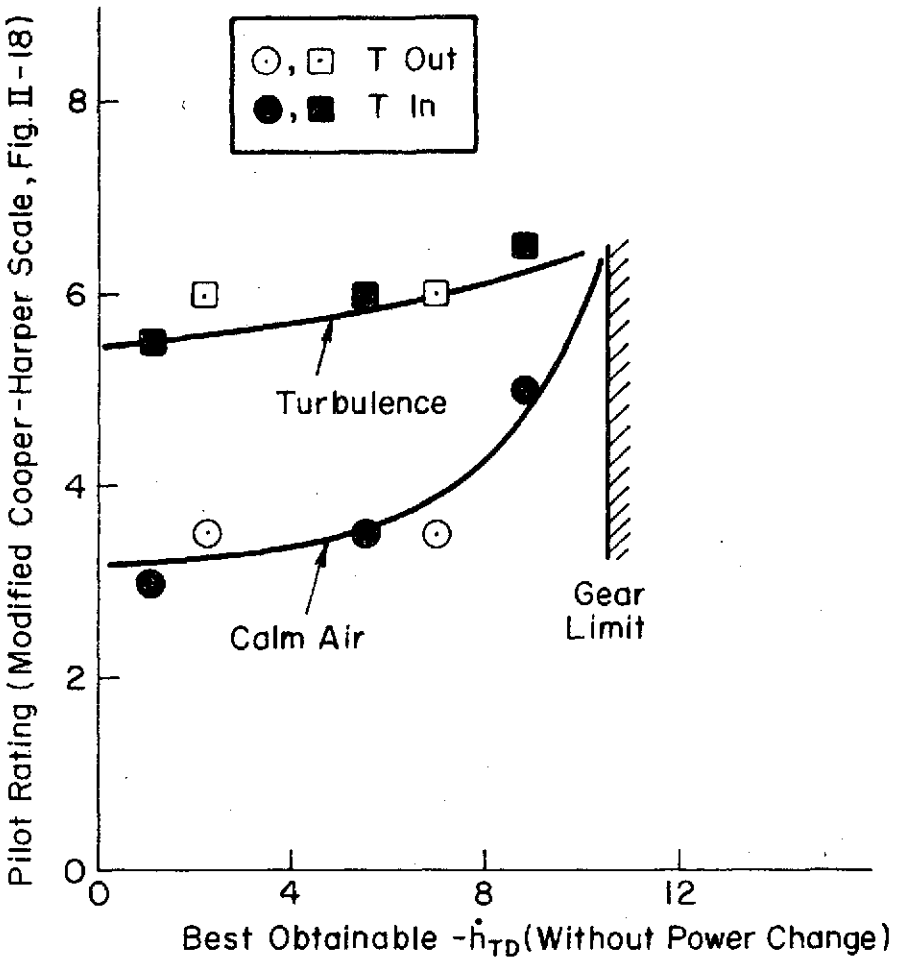

Figure IV-10. Pilot Rating vs. Best Obtainable $\dot{h}_{TD}$

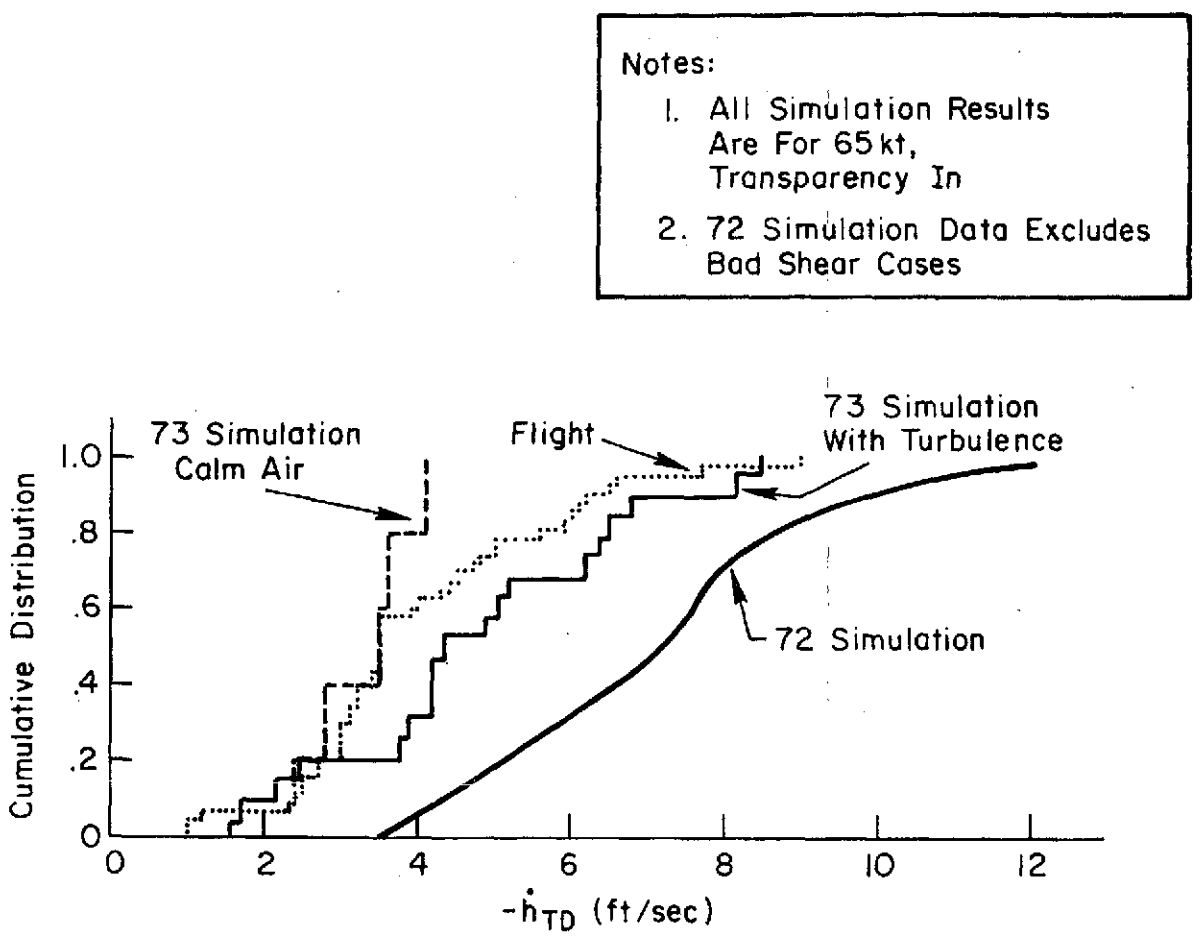

Figure IV-11. Comparison of Flight and Simulation Landing Data

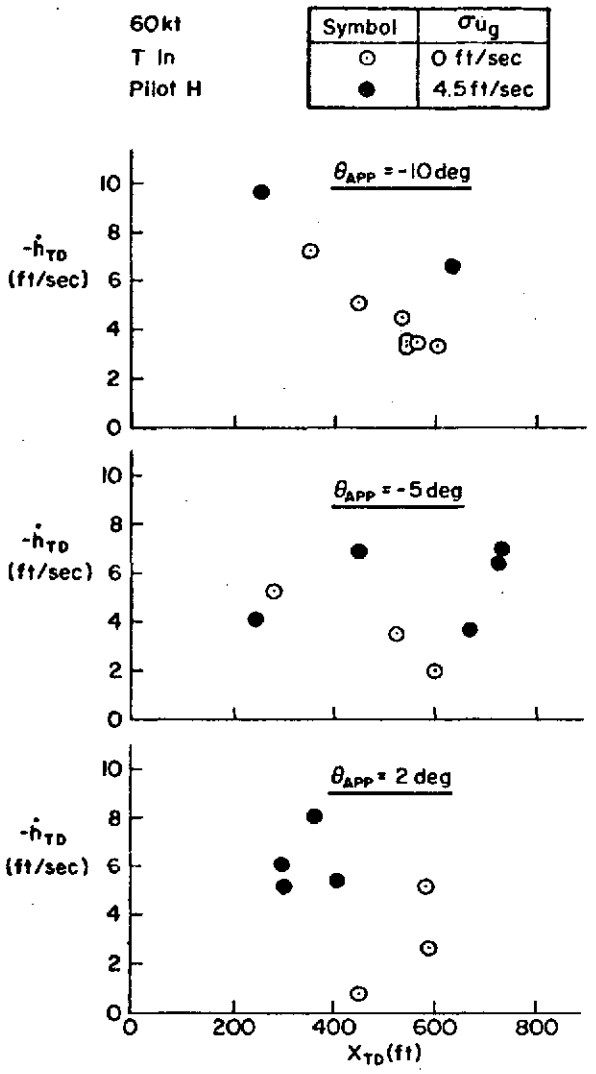

a) Nominal Thrust Lag (1.4 sec)

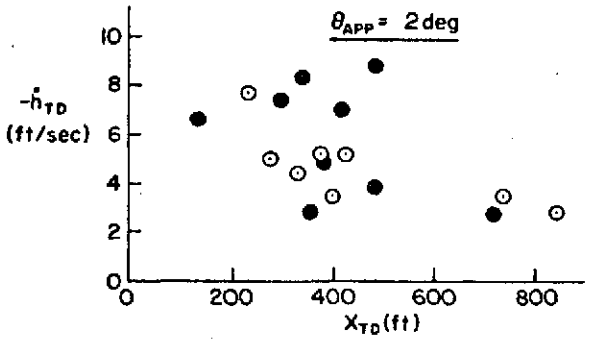

b) Short Thrust Lag (0.5 sec)

Figure IV-12. Landing Data

The pilot comments are more revealing. The pilot (Hardy) felt that the -10 deg approach attitude did not present a problem during flare. The extra rotation required to bring the nose level was useful in arresting the sink rate (as shown in Appendix C). There was no tendency for the aircraft to float or balloon during flare, although he felt this might be a problem at higher speeds. The -10 and -5 deg approach attitudes were given a pilot rating of 3 in calm air and 5 1/2 in turbulent air. The +2 deg approach attitude was more difficult. Power had to be controlled carefully during the flare to keep the pitch attitude from increasing too much. The pilot experimented with two flare techniques: (1) using power only and (2) using low frequency (roughly .2 Hz) power inputs combined with higher frequency (roughly .7 Hz) elevator inputs. The combined technique (pilot rating was 4 in calm air, 6 1/2 in turbulent air) was preferred to the power alone technique which was felt to be unacceptable by the pilot. (Pilot rating was 5 in calm air, 7 1/2 in turbulent air). Additionally, with an approach attitude of +2 deg the runway was only visible near the bottom of the windshield, which the pilot found disturbing.

5. Variation of Thrust Lags

The effective thrust lag (time to reach 63% of the thrust change after a throttle input) was changed from the nominal value of 1.4 sec to 0.5 sec by removing the lags in the engine gas generator model while retaining the dynamics in the propeller/governor model. The results of the change in thrust lag on touchdown performance are depicted in Fig. IV-12b for an approach attitude of +2 deg.

Comparing Fig. IV-12a and b, it is clear that reducing the thrust lags did not significantly affect the touchdown sink rate or distance. The pilot felt that the reduced thrust lags were worth a rating improvement of about 1/2 rating point.

6. Variation of Flare Technique

In an effort to investigate the +2 deg approach attitude power control problems, a series of landings were conducted with another pilot (Kennedy).

For these landings thrust lags of 1.4 and 0.5 sec were used. Fig. IV-13 depicts the results. In calm air with either thrust lag the pilot had little difficulty in making consistent landings, commenting that he was using his sink rate as a prime indicator of how much power to use. He felt this was a reasonable landing technique. It was felt that Kennedy's experience in helicopters is the factor which predisposed him to accept and utilize power as the primary control during the flare. In contrast, Hardy, who has no helicopter experience, termed this control technique unacceptable.

In an attempt to resolve this conflict, Hardy was asked to re-evaluate the power alone flare technique. His final conclusion was that with the shorter thrust lag, the power alone flare technique might be acceptable.

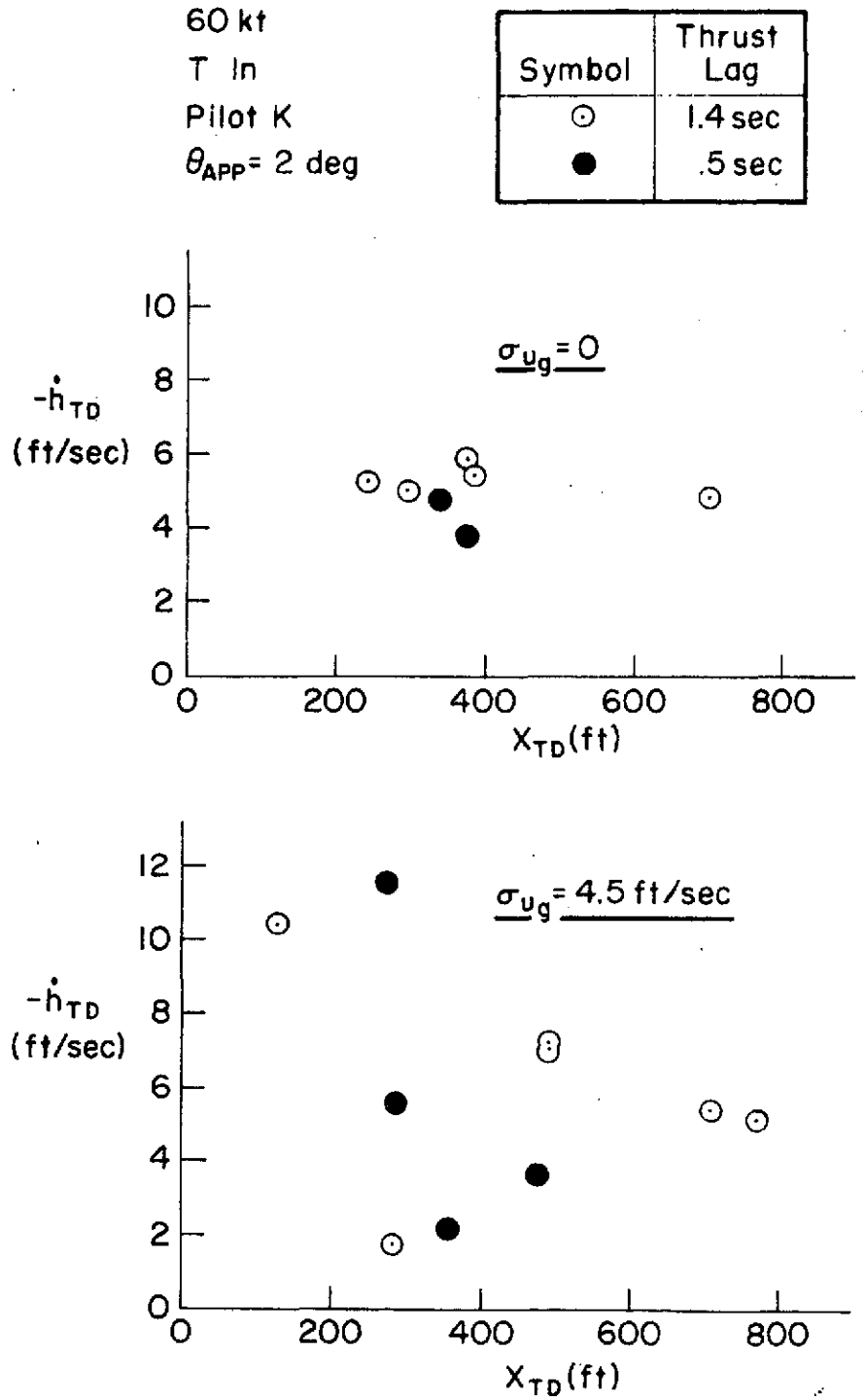

Figure IV-13. Flaring with Power Alone

SECTION V

GO-AROUND DATA

A. 1972 RESULTS

A go-around condition was simulated in 3 of the 10 runs of a landing and approach test sequence. This was done by setting the ceiling below the decision height of 200 ft. Of the 3 scheduled go-arounds 1 was made with all engines operating, 1 had an engine failure near the decision height and 1 had an engine failure at an altitude of 400 ft (while descending). The sequence of 10 runs was presented in a random order so the pilots did not know if they would break out of the clouds or not. Besides the planned go-arounds there were a number of landings which were aborted (pilot's decision) at lower altitudes because a poor landing seemed likely.*

The go-around procedure was:

- Full power and flaps up to 70 deg (flap retraction was done with thumb switch on throttle handle; flap rate was 7 deg/sec; if transparency was in, it was automatically reduced from 12 to 5 deg when the flaps reached 93 deg)
- Stabilize at an airspeed of 60 kt
- Gradually raise flaps to 45 deg and increase airspeed to 70 kt
- Continue straight ahead departure until reaching an altitude of 1100 ft.

All the pilots considered the go-around maneuver quite easy to accomplish. One hand motion simultaneously advanced the throttle and raised the flaps to 70 deg. There were no problems with trim changes or

---

* Data for the unscheduled go-arounds are not included here because of the difficulty in determining when the pilot initiated the go-around maneuver.

lift losses. After a positive rate-of-climb was established the flaps were raised to 45 deg. The pilots had no difficulty with this last maneuver although it generally resulted in a momentary loss in rate-of-climb, frequently to near zero.

Go-around performance was analyzed in terms of two parameters--minimum altitude reached (h_{min}) and minimum plane penetrated (MPP). The MPP was computed by defining a family of planes originating at a point 2100 ft from the runway threshold (100 ft past the upwind end of a 2000 ft runway) at increasing inclinations from the horizon. The value of the MPP was defined by selecting the shallowest plane which was tangent to the aircraft's flight trajectory in the interval $h_{min} < h < 1100$ ft. The computer calculated the MPP from:

$$MPP = \text{Min } \tan^{-1} \frac{h}{x-2100}$$

The geometry for this computer calculation is shown in the sketch below.

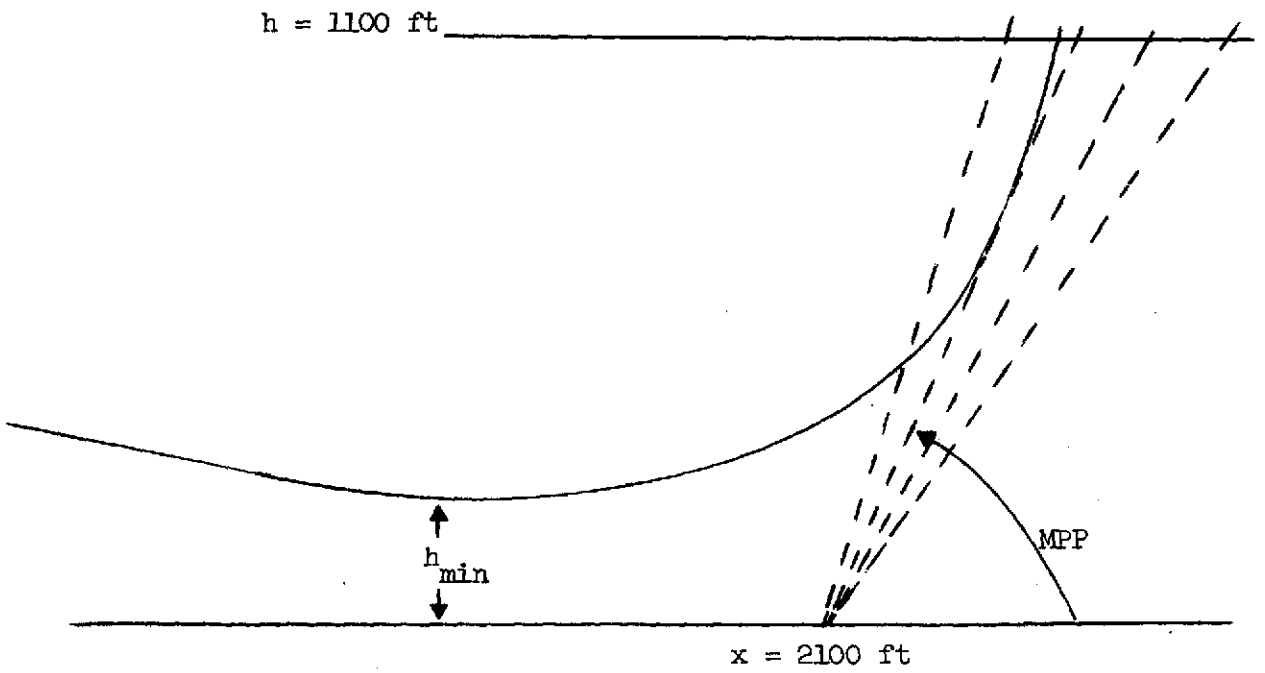

Plots of the minimum wheel height and MPP are given in Fig. V-1. To provide some reference for evaluating the go-around performance, Fig. V-1 also displays an idealized curve which assumes:

- Aircraft was on the glide slope at h_{min}
- At h_{min} there was an instantaneous transition to a 45 deg flap setting and 70 kt airspeed
- The trim γ for this condition was maintained until the end of the run, altitude = 1100 ft.

The geometry for this idealized maneuver is shown in the sketch below.

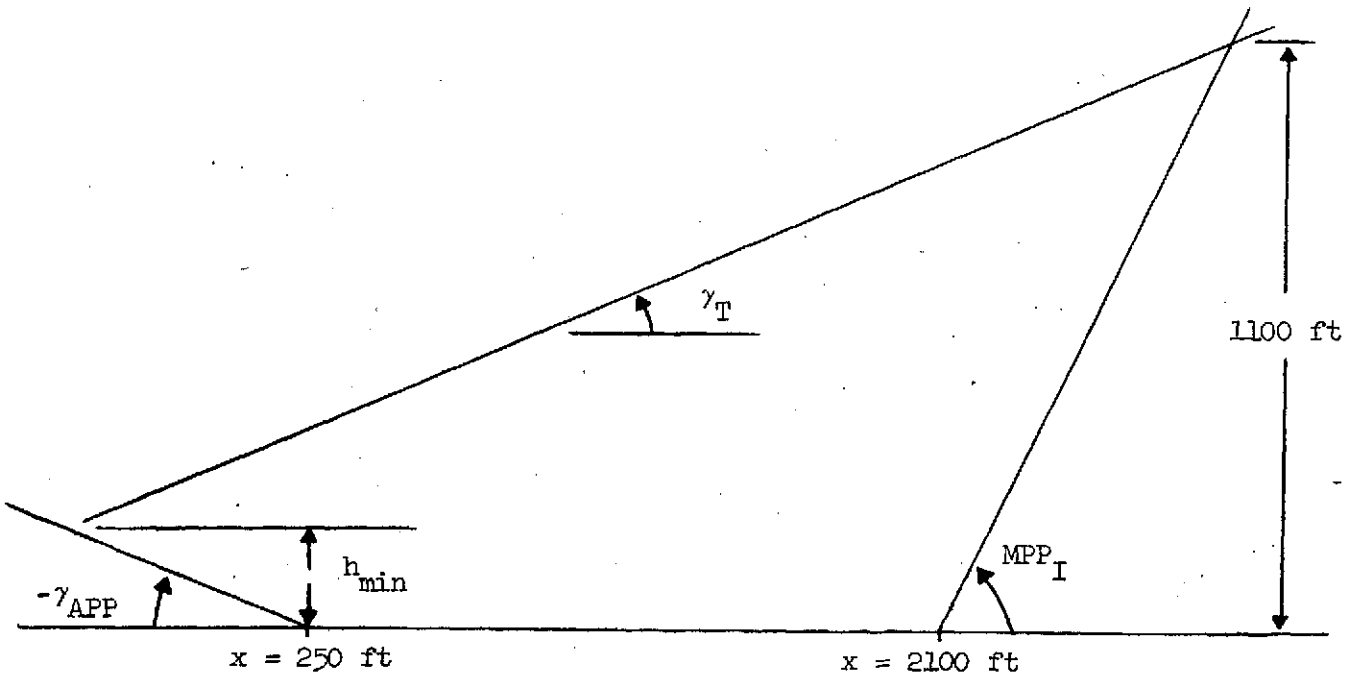

Symbol	V_{APP} (kt)
⊡	65
⊙	60
△	55
◇	50

Notes:

1. Solid Symbols Denote AEO, Open Denote OEI
2. Flagged Symbols Denote Angle-of-Attack Display On

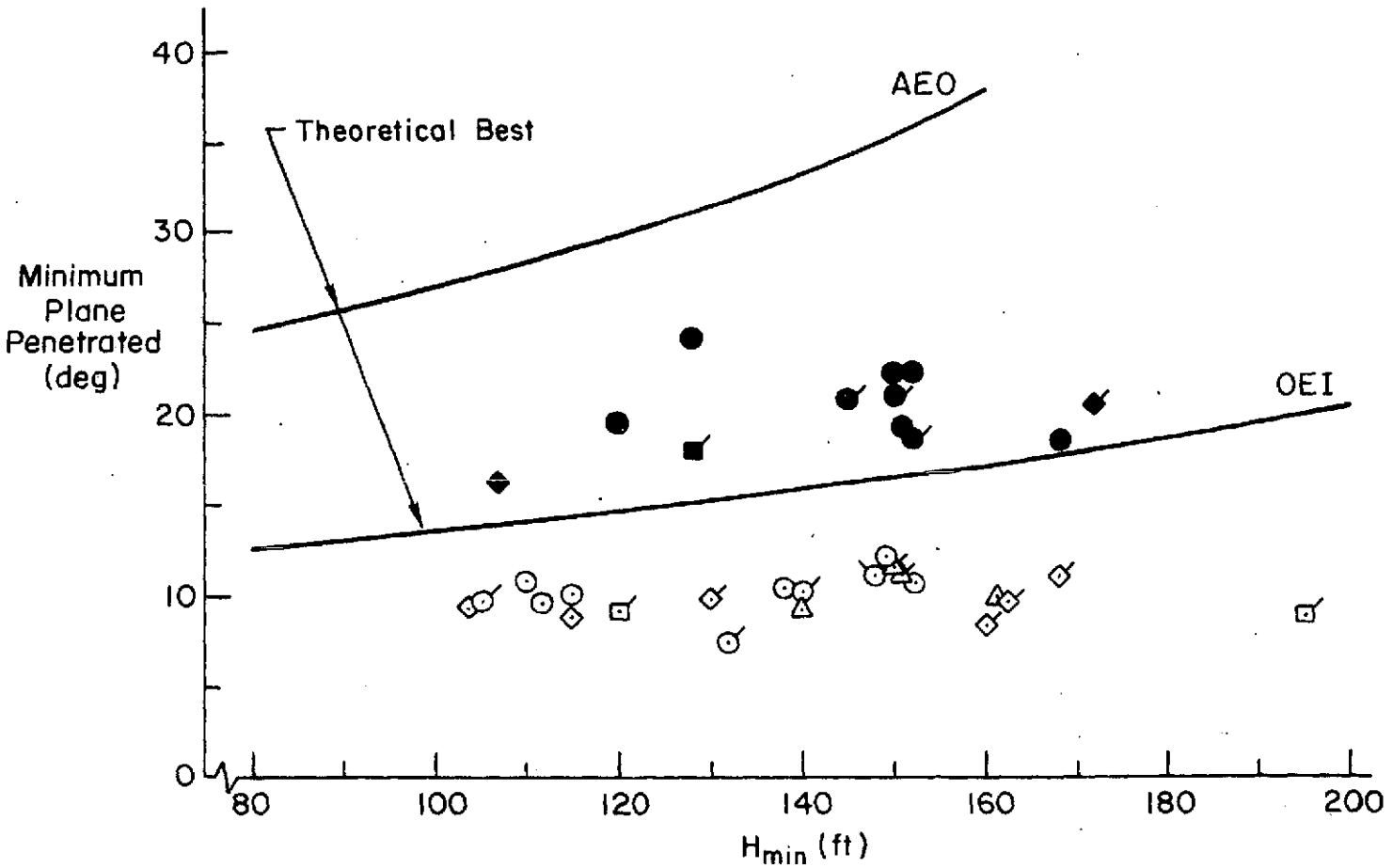

a. Transparency out, $\gamma = -7.5$ deg

Figure V-1. Go-Around

Symbol	V_{APP} (kt)
⊡	65
⊙	60
△	55

Notes:

1. Solid Symbols Denote AEO, Open Denote OEI
2. Flagged Symbols Denote Angle-of-Attack Display On

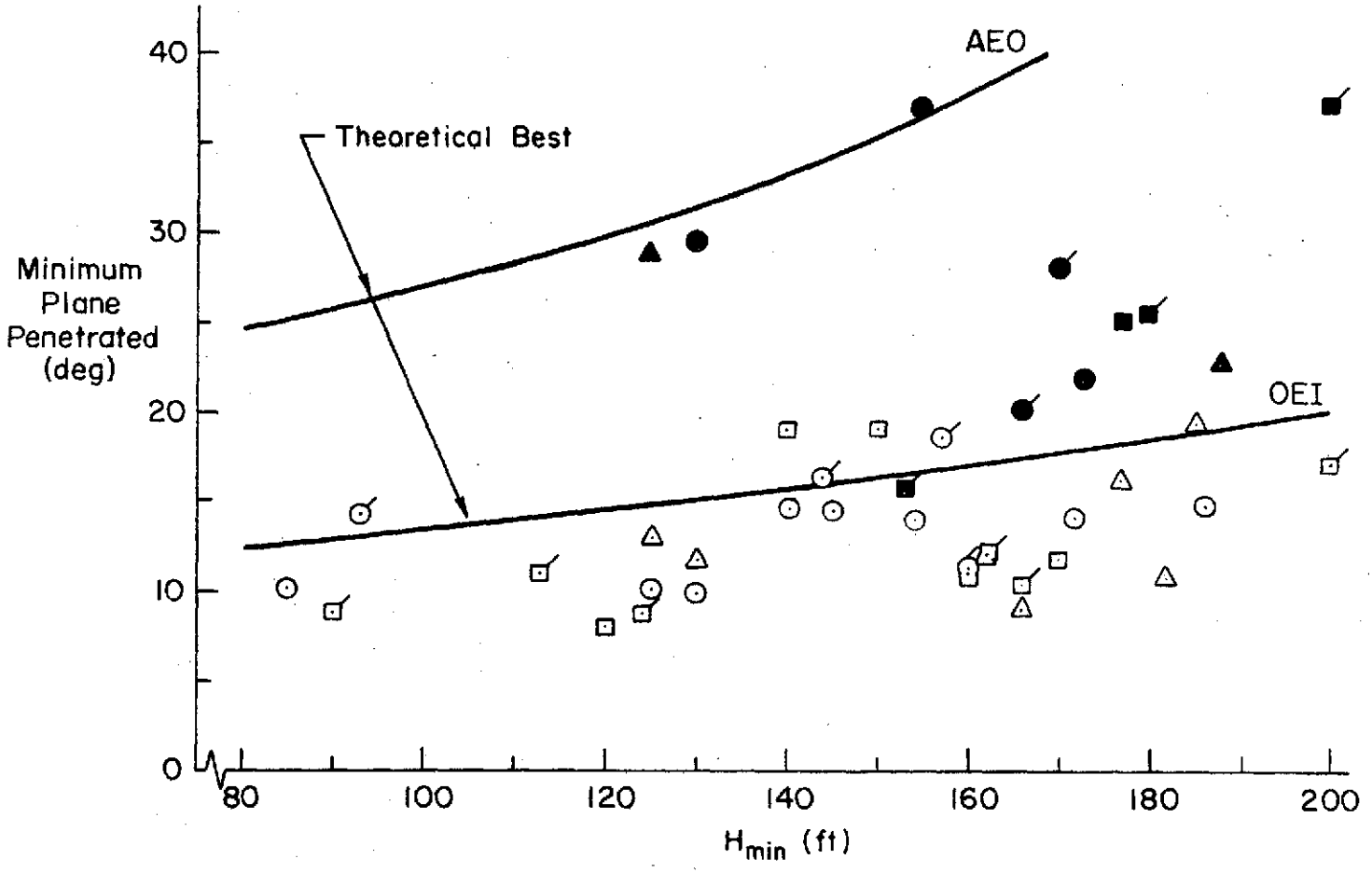

b. Transparency in, $\gamma = -7.5$ deg

Figure V-1. Continued

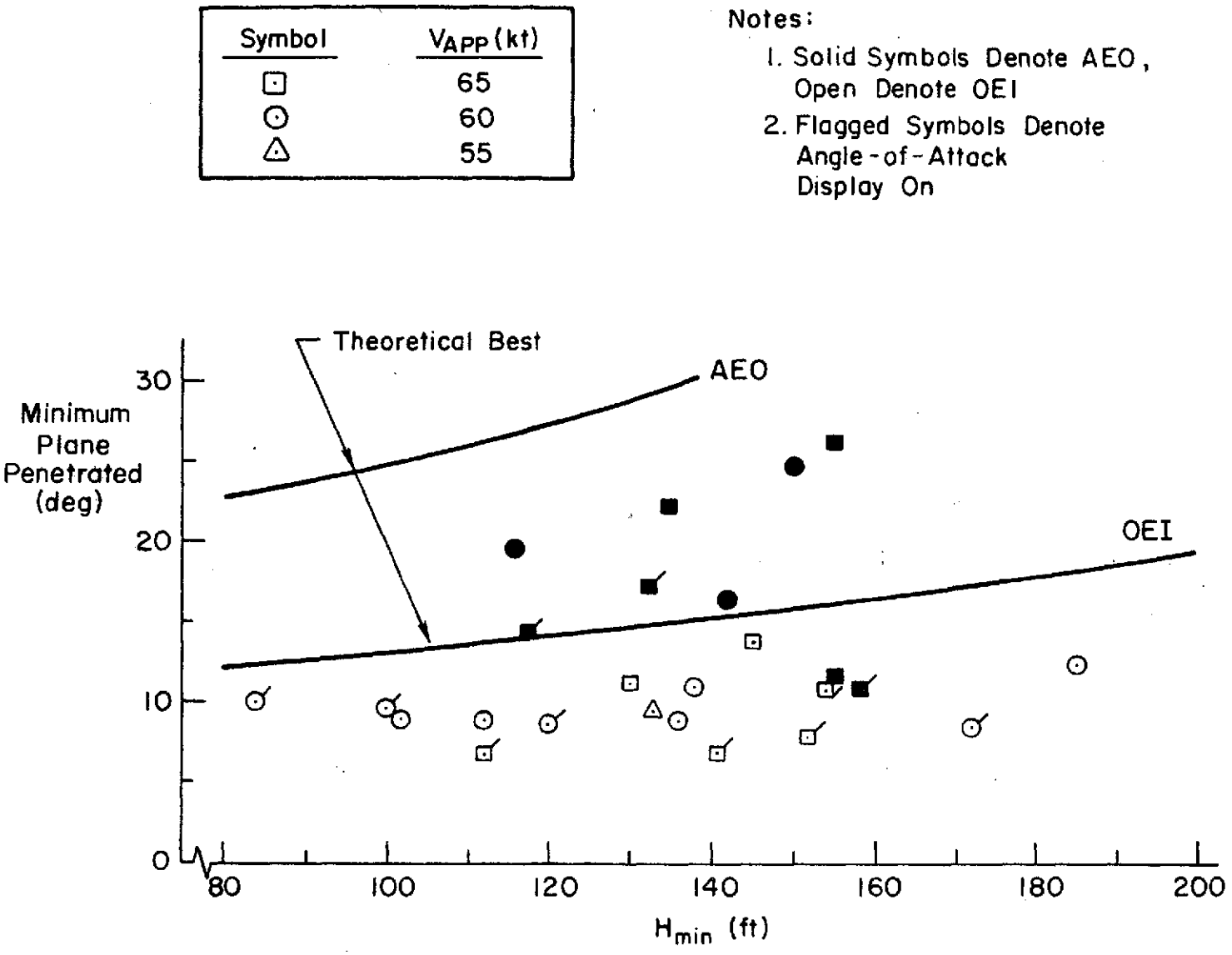

c. Transparency in, $\gamma = -9.5$ deg

Figure V-1. Concluded.

From the sketch it can be shown that the idealized MPP is given by:

$$MPP_I = \tan^{-1}\left[\frac{1100}{(1100 - h_{min})\cot\gamma_T - h_{min}\cot(-\gamma_{APP}) - 1850}\right]$$

$$\text{Where } \gamma_T = \begin{cases} 10.9 \text{ deg AEO} \\ 7.3 \text{ deg OEI} \end{cases}$$

Fig. V-1 indicates that for the conditions evaluated neither approach speed nor the status of the angle of attack display had an appreciable effect on the minimum height or the MPP values. The values which are greater than their theoretical best were obtained when the pilot was significantly above the glide slope at the initiation of the go-around. An examination of the equation for the theoretical best MPP for a given h_{min} indicates that shallower glide slopes should yield greater MPP's. Comparison of data within Fig. V-1 indicate that this is indeed the case. Also greater MPP values are obtained at a given h_{min} for go-arounds initiated with transparency in than those initiated with transparency out (Fig. V-1, a and b). The better performance for transparency in is due to the faster thrust response available. In the initial application of full power and retraction of flaps to 70 deg, the first 2 deg of flap motion removes most of the transparency and produces a very rapid thrust increase as the pitch of the outboard propellers is increased.

The data are shown as cumulative distribution plots of h_{min} and MPP in Fig. V-2. Here the increased go-around performance with transparency in at $\gamma = -7.5$ is apparent, as is the decrease in performance when the glide slope is steepened to -9.5 deg. The following analysis gives a possible means of estimating the effect of varying glide slope angle about a nominal value.

If we were to assume a step normal acceleration starting at go-around initiation then an approximate expression for h_{min} would be:

$$h_{min} \doteq h_o - \frac{V^2 \gamma_{G/S}^2}{2g\, n_z}$$

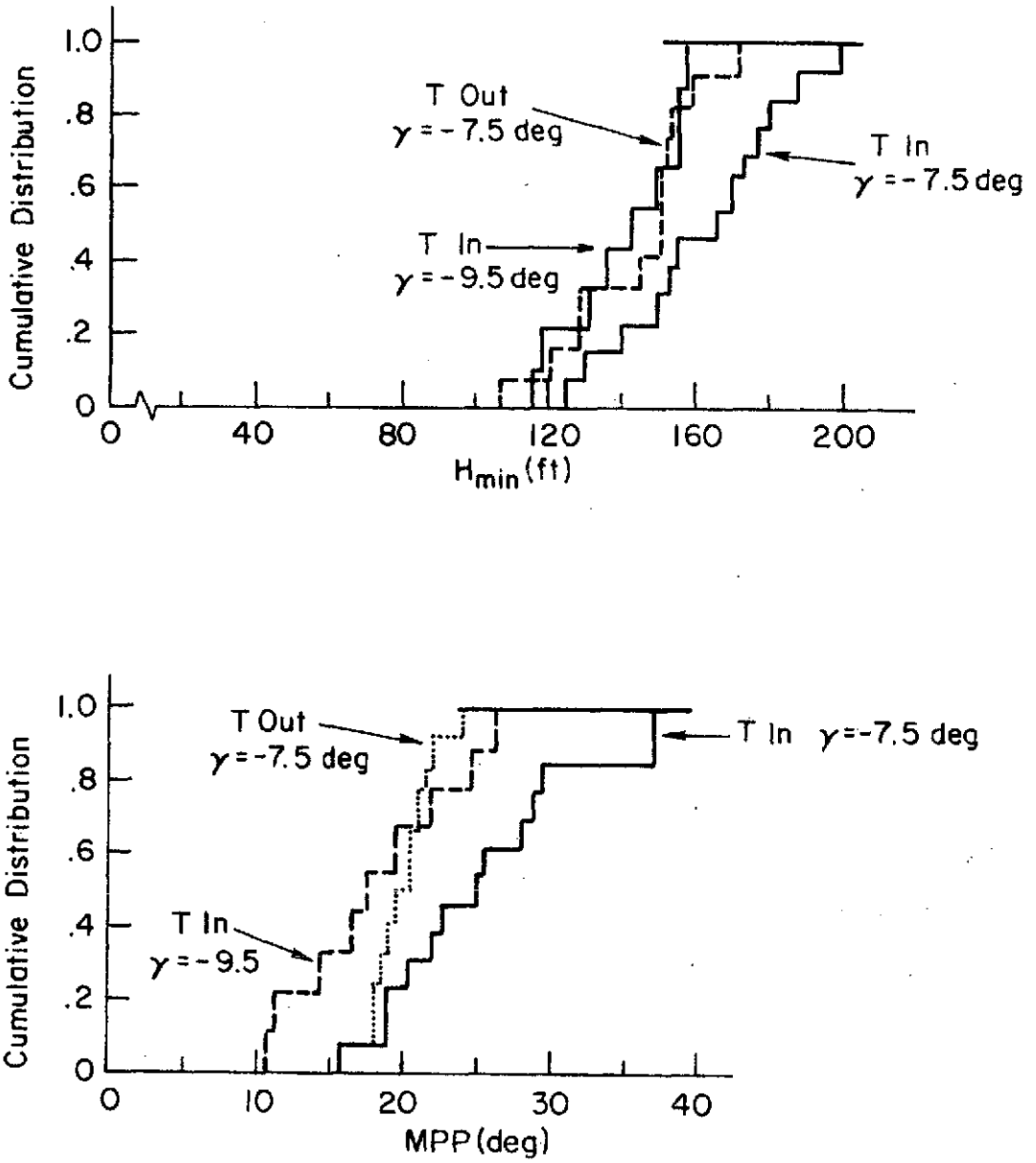

a. AEO

Figure V-2. Cumulative Distributions

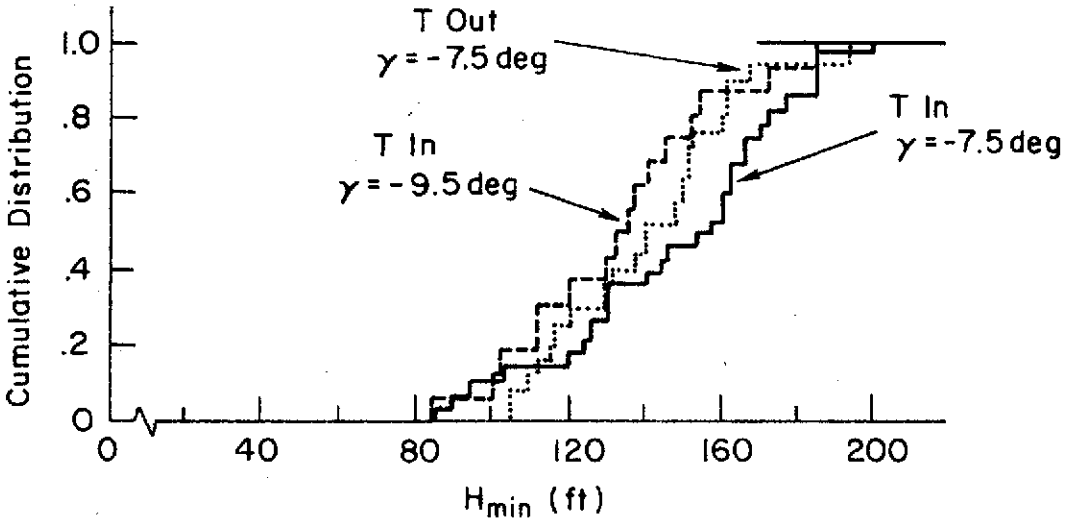

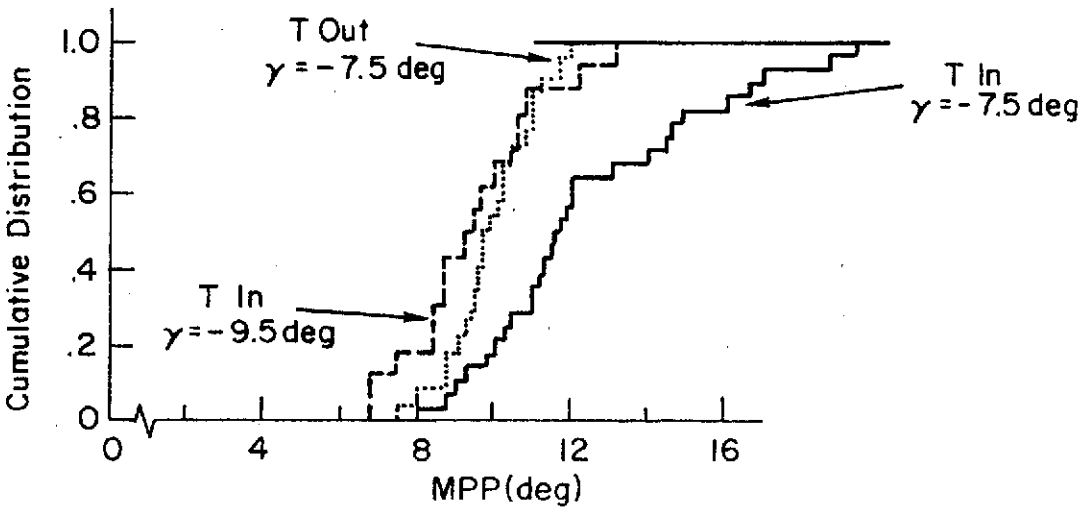

b. OEI

Figure V-2. Concluded

Then based on this the effect of airspeed and glide slope angle would be:

$$\frac{\Delta h_{min}}{h_o - h_{min}} = - \frac{2\Delta V}{V} - \frac{2\Delta \gamma_{G/S}}{\gamma_{G/S}}$$

i.e., if the speed were varied from 60 kt to 65 kt, the altitude excursion would be 16% beyond the nominal and if the glide slope were varied from -7.5 deg to -9.5 deg, the altitude excursion would be 53% beyond the nominal.

This approximate relationship seems to correspond well to the glide slope angle variation shown in Fig. V-2. For transparency in at $\gamma_{G/S}$ = -7.5 deg the median $h_o - h_{min}$ is 34 ft. Using the above expression we would expect an increase of 53% or $h_o - h_{min}$ = 52 ft. The actual median value for -9.5 deg is 57 ft.

Perhaps the most significant aspect of the go-around data shown in Fig. V-2 is the low altitudes which were frequently reached OEI. Roughly 20 - 30% of the go-arounds resulted in minimum altitudes of 120 ft or less (decision height was 200 ft). Thus a decision height no less than 200 ft seems indicated if ground contact is to be avoided.

The MPP data are more favorable. For the -7.5 deg approaches, the minimum MPP never got below 7 deg. This performance is largely due to the geometry of the go-around situation. Go-around as initiated prior to the runway threshold and the MPP starts 100 ft past the upwind end of the runway. Thus the pilot has roughly 3500 ft of range or 30 - 35 sec of flight time from go-around initiation to the start of the MPP.

B. 1973 RESULTS

Verifying the 1972 go-around conclusions was not a primary objective of the 1973 tests. Of the 19 go-arounds recorded in the 1973 testing, only 6 were initiated at the decision height of 200 ft (because of low ceiling) and can be compared with the 1972 data. Fig. V-3 presents this data. The results are similar to the 1972 data and do not give any reason for altering the conclusions already reached.

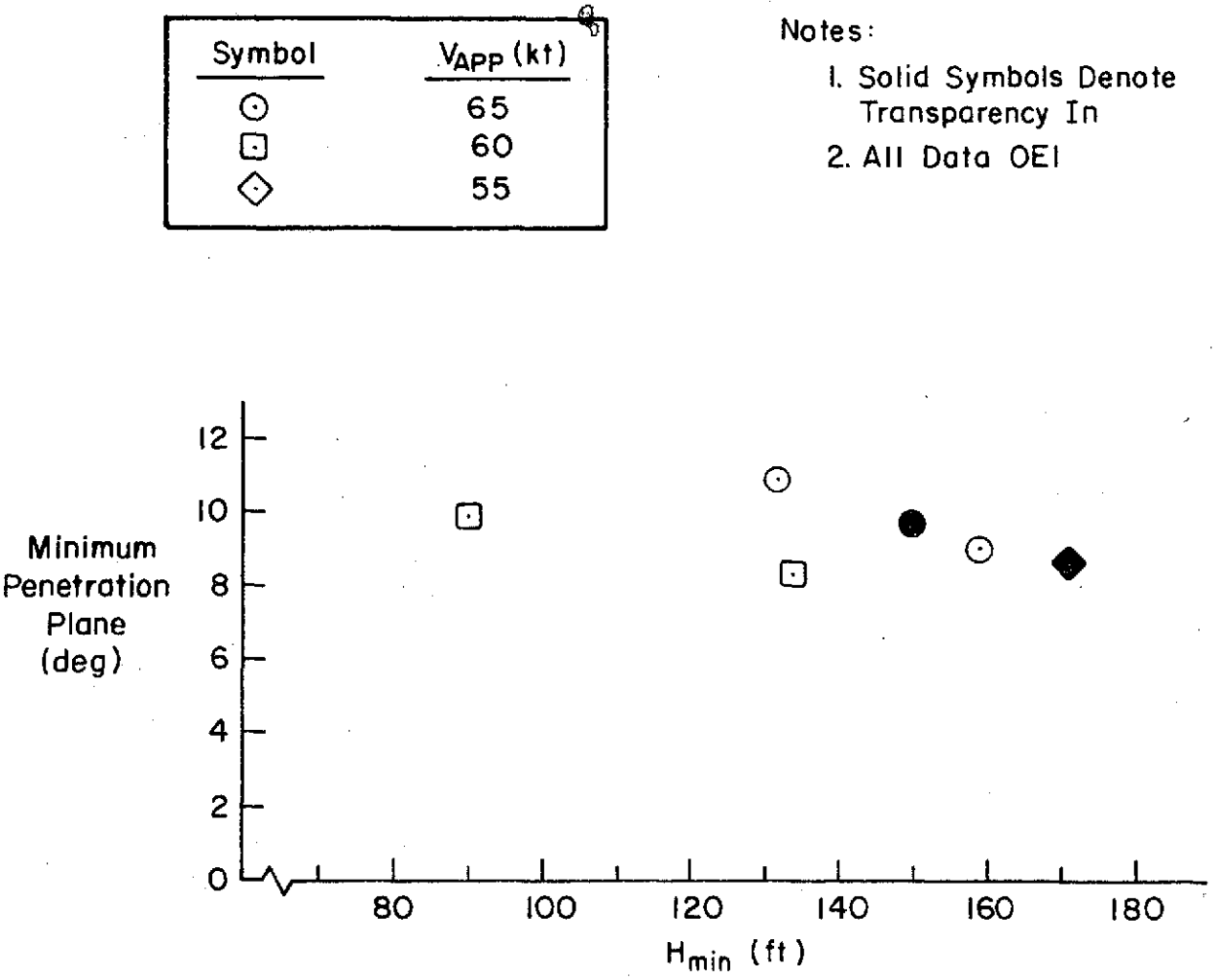

Figure V-3. 1973 Go-Around Data

SECTION VI

TAKEOFF DATA

A. TEST CONDITIONS

All the takeoff tests were conducted during the October/November 1972 simulation. A weight of 52,000 lb and a flap setting of 45 deg were used. These conditions were selected so that the OEI climb gradient would be only slightly greater than obstacle clearance plane proposed in Ref. 3 (15:1 slope or 4 deg). The basic idea was to evaluate a loading condition near the maximum which might be expected in operation. This should represent the most critical condition regarding takeoff performance.

B. V_{MU} TESTING

Tests to determine the minimum takeoff velocity (V_{MU}) were conducted by rotating the aircraft as soon as possible and measuring the distance to lift-off (x_{LOF}), the velocity at lift-off (V_{LOF}), the distance to a 35 ft height (x_{35}), and the velocity at a 35 ft height (V_{35}). The results, Fig. VI-1, indicate that regardless of rotation speed, the aircraft will lift off at an airspeed of approximately 66 kt with a ground roll of approximately 1000 ft.

C. OEI TAKEOFFS

Takeoffs with engine failures* occurring prior to rotation were conducted with V_R = 65 kt and V_2 = 74 kt. Examination of Fig. VI-2 indicates that a balanced field length of 1900 ft, with a V_1 of 65 kt, is appropriate for this condition. This compares with a length of 1840 ft given in Ref. 2 for V_R = 71 kt and V_2 = 80 kt. The data also indicate that an engine failure occurring near 0 kt instead of 65 kt adds only

---

* Failure occurred at an airspeed of V_{EC}.

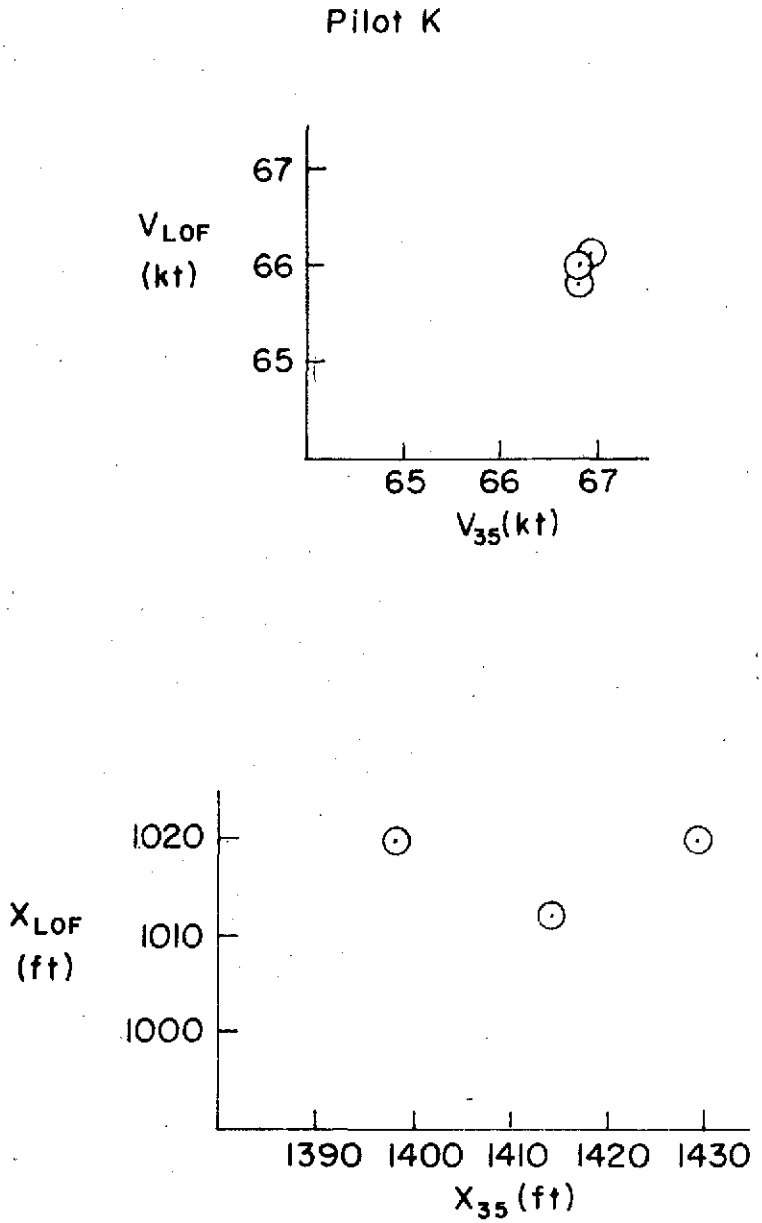

Figure VI-1. V_{MU} Test

Note:

1. ⊙ Distance Required to Accelerate to V_{EC} and Stop
2. ⊡ Distance to H = 35 ft
3. Pilot K
4. Flags Denote Multiple Points
5. V_R = 65 kt V_2 = 74 kt

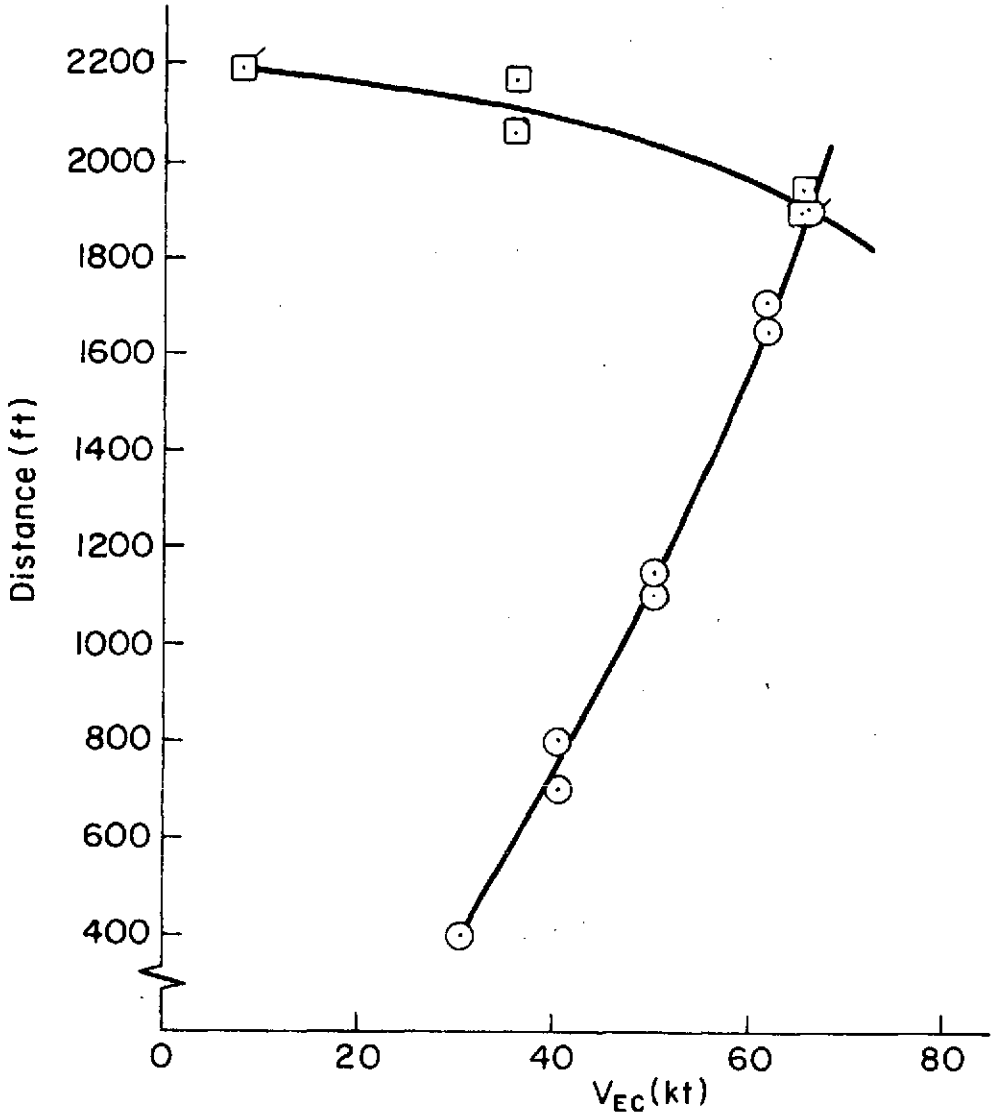

Figure VI-2. Balanced Field Test

300 ft to x_{35}. Thus the penalty for selecting V_1 = 0 would be quite small.

Fig. VI-3 shows the effects of the engine failure on x_{LOF}, V_{LOF}, and V_{35}. It is apparent from this figure that an engine failure prior to rotation does not affect the pilot's ability to reach V_2 by 35 ft. It is also clear that the variation of x_{LOF} and x_{35} with V_{EC} are similar in that varying V_{EC} from 7.5 to 65 kt results in decreases of x_{LOF} and x_{35} of approximately 300 ft. Also, for each V_{EC}, $x_{35} - x_{LOF} \doteq 600$ ft, so that at $V_{EC} = V_1 = 65$ kt, almost 1/3 of the balanced field length is required for the aircraft to go from liftoff to a height of 35 ft.

D. ABUSES

The effect of 5 and 10 kt OEI early rotation and AEO maximum practical rate abuses (V_R -5, V_R -10, and MPR respectively) were studied for nominal rotation speeds* of 55, 60, 65, and 75 kt. For the V_R -5 and V_R -10 abuses the engine failure occurred 5 kt prior to the nominal V_R. The results are presented in Fig. VI-4 with AEO data as a baseline. Examination of Fig. VI-4 a and b indicates that V_{LOF} and V_{35} are not sensitive to these abuses and confirms that for normal rotation rates, the minimum AEO V_{LOF} occurs at approximately 66 kt. With high rotation rates (MPR) V_{LOF} could go down to almost 63 kt. Note that at the lower rotation speeds the speed at 35 ft was always above V_2. This may be due to the lag (1 sec time constant) in the indicated airspeed.

Fig. VI-4c indicates that the OEI V_R -5 and V_R -10 abuses generally increased x_{LOF}, while the AEO MPR abuses slightly reduce x_{LOF}, relative to the AEO baseline case. As would be expected, the OEI V_R -10 abuses generally caused larger increases in x_{LOF} than did the V_R -5 abuses. For the OEI V_R -5 and V_R -10 abuses, it is impossible to determine precisely how much of the increase in x_{LOF} was due to the engine loss, and how much was due to the early rotation.

---

* For a V_R -5 abuse and a nominal rotation speed of 65 kt, the pilots would rotate at 60 kt.

Note:

1. Pilot K
2. Flags Denote Multiple Point
3. $V_R = 65$, $V_2 = 74$ kt

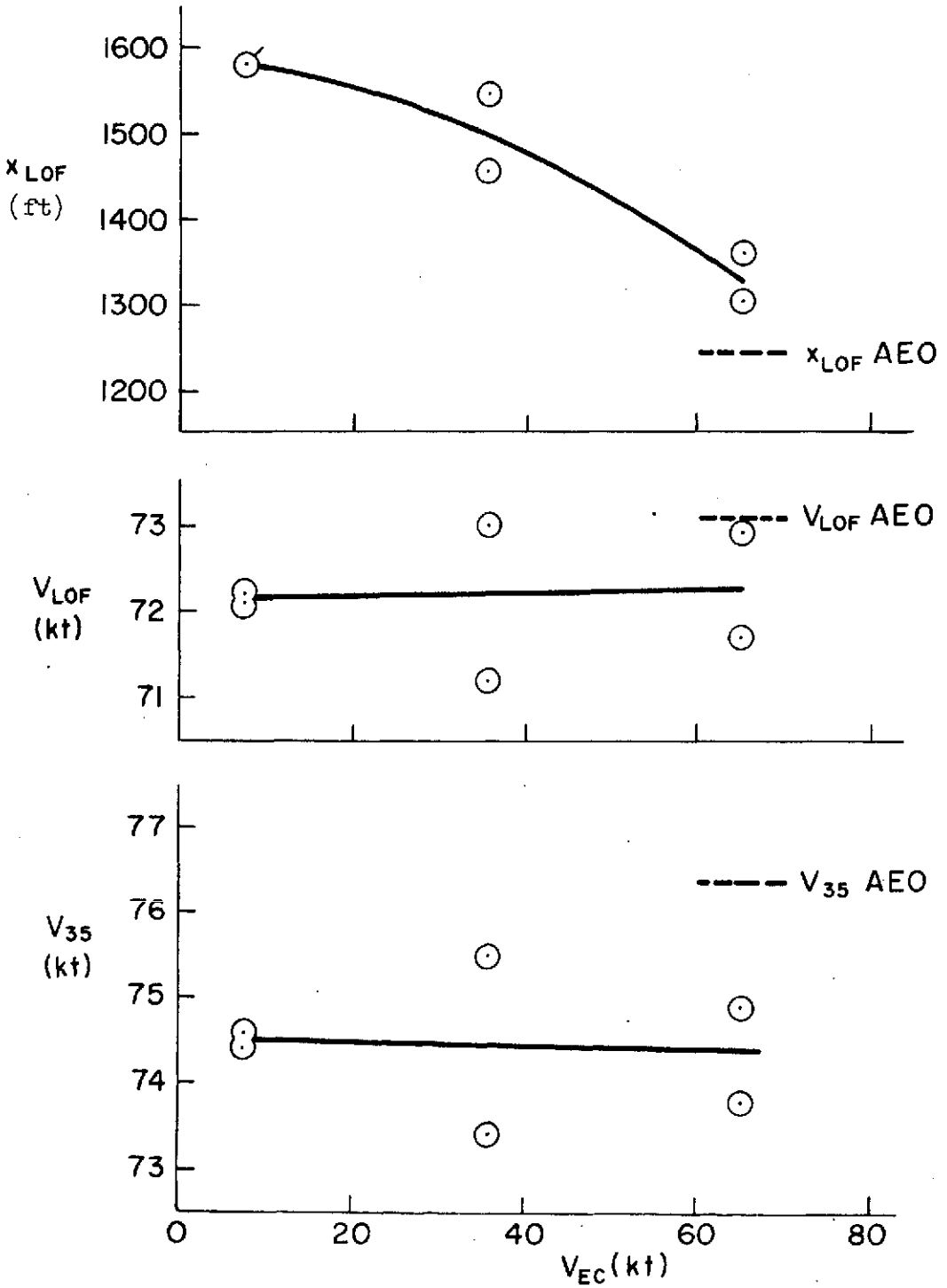

Figure VI-3. OEI Takeoff Data

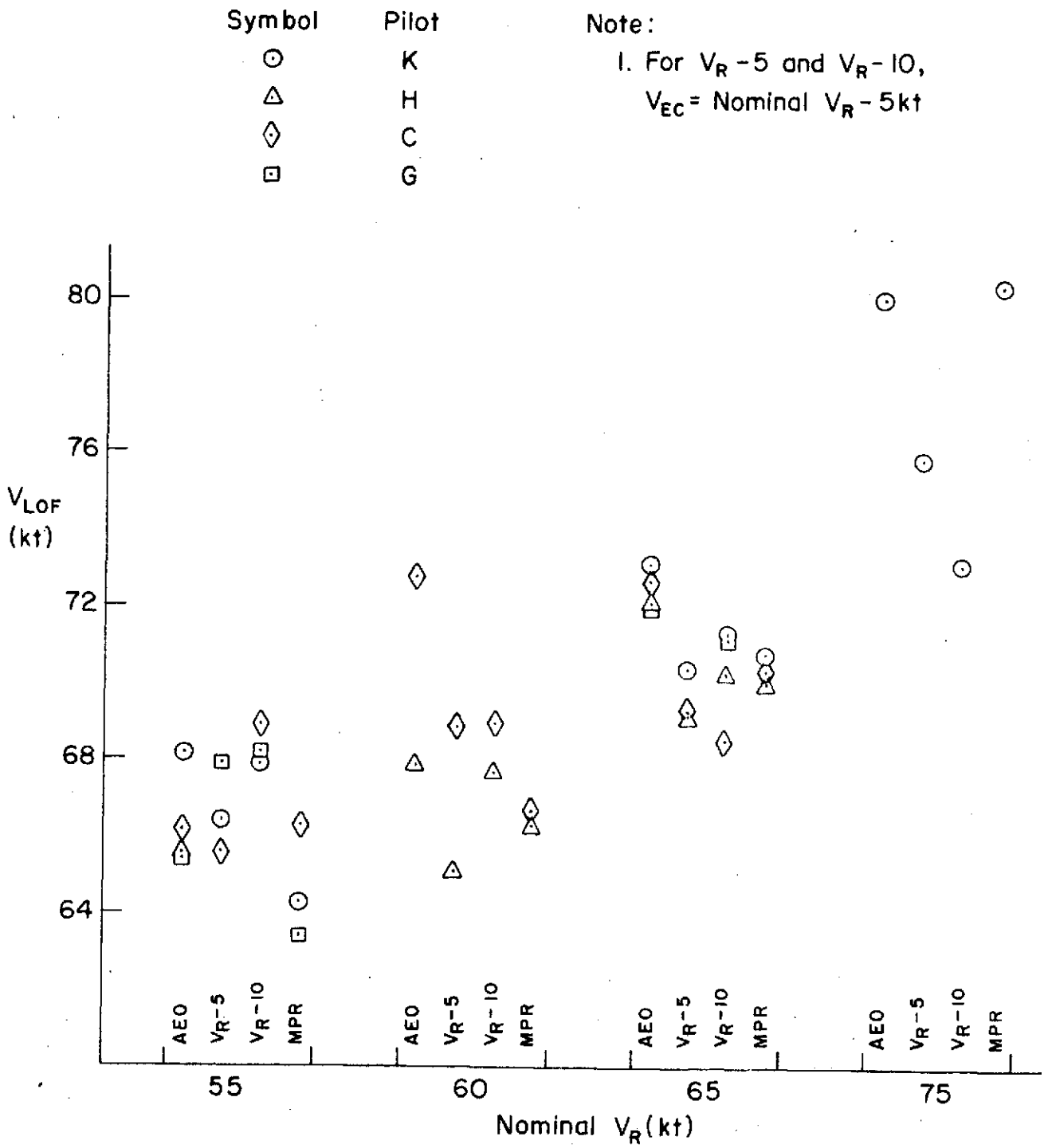

a. V_{LOF}

Figure VI-4. Effects of Takeoff Abuses

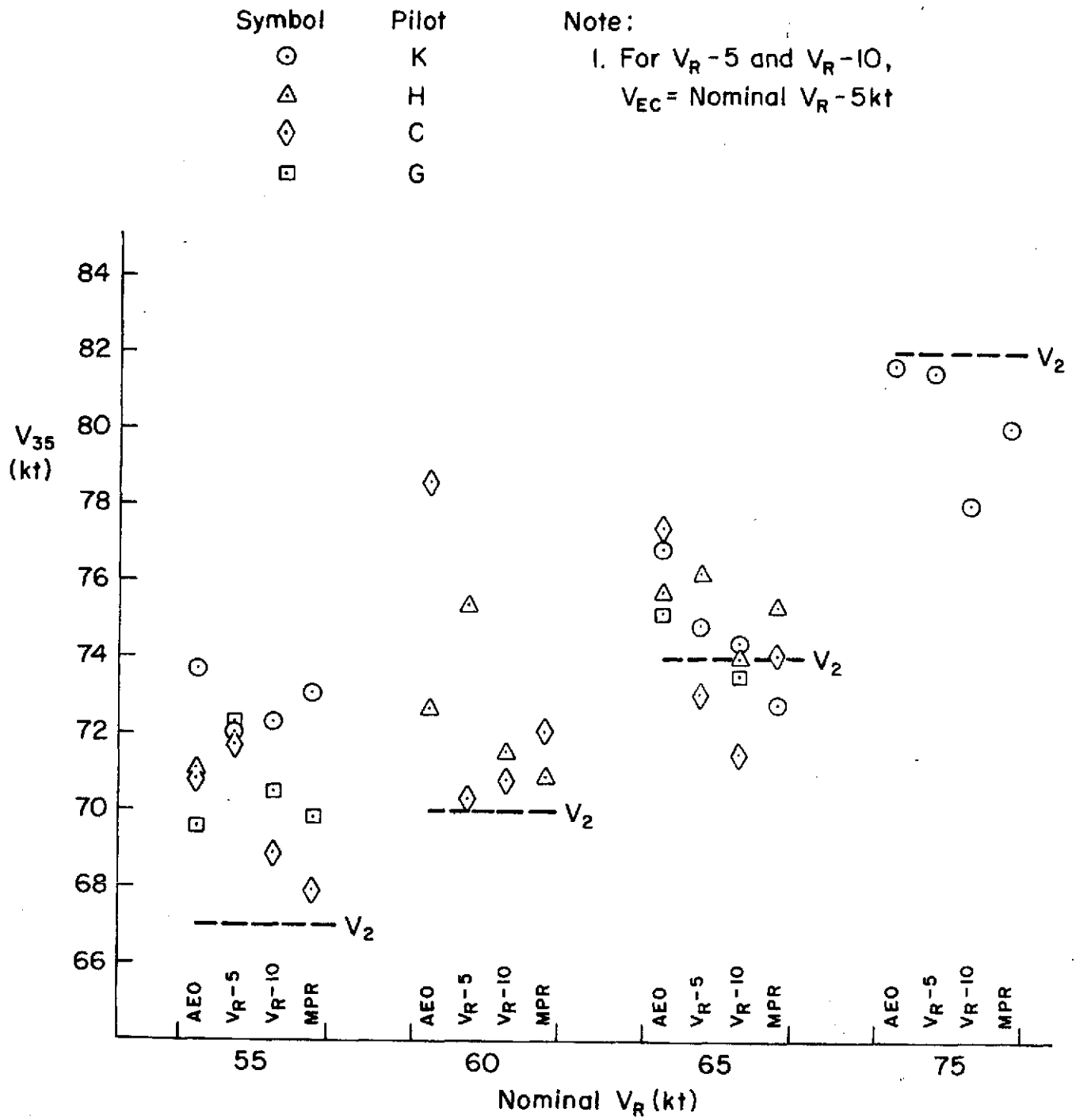

b. V_{35}

Figure VI-4. Continued

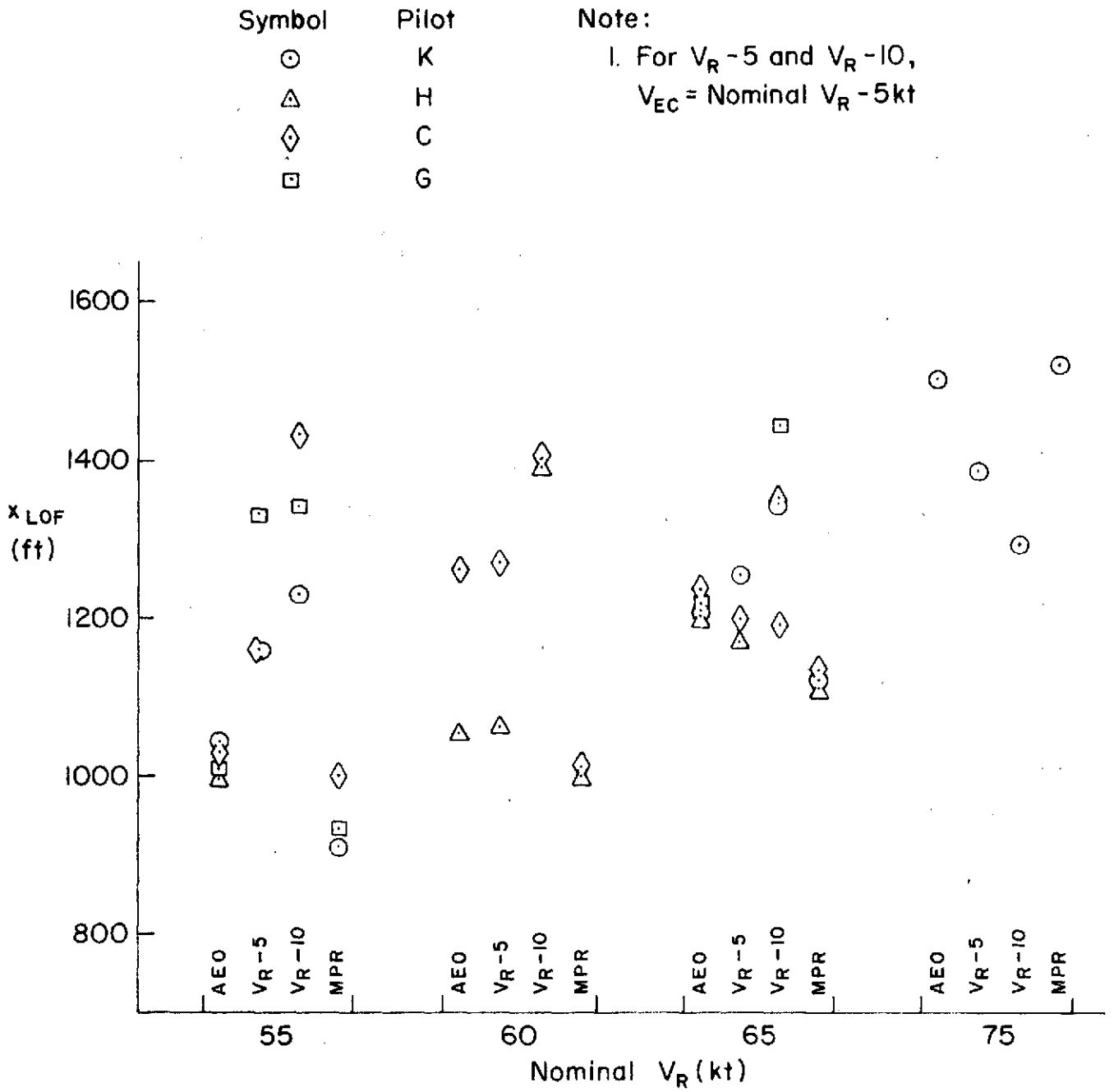

c. X_{LOF}

Figure VI-4. Continued

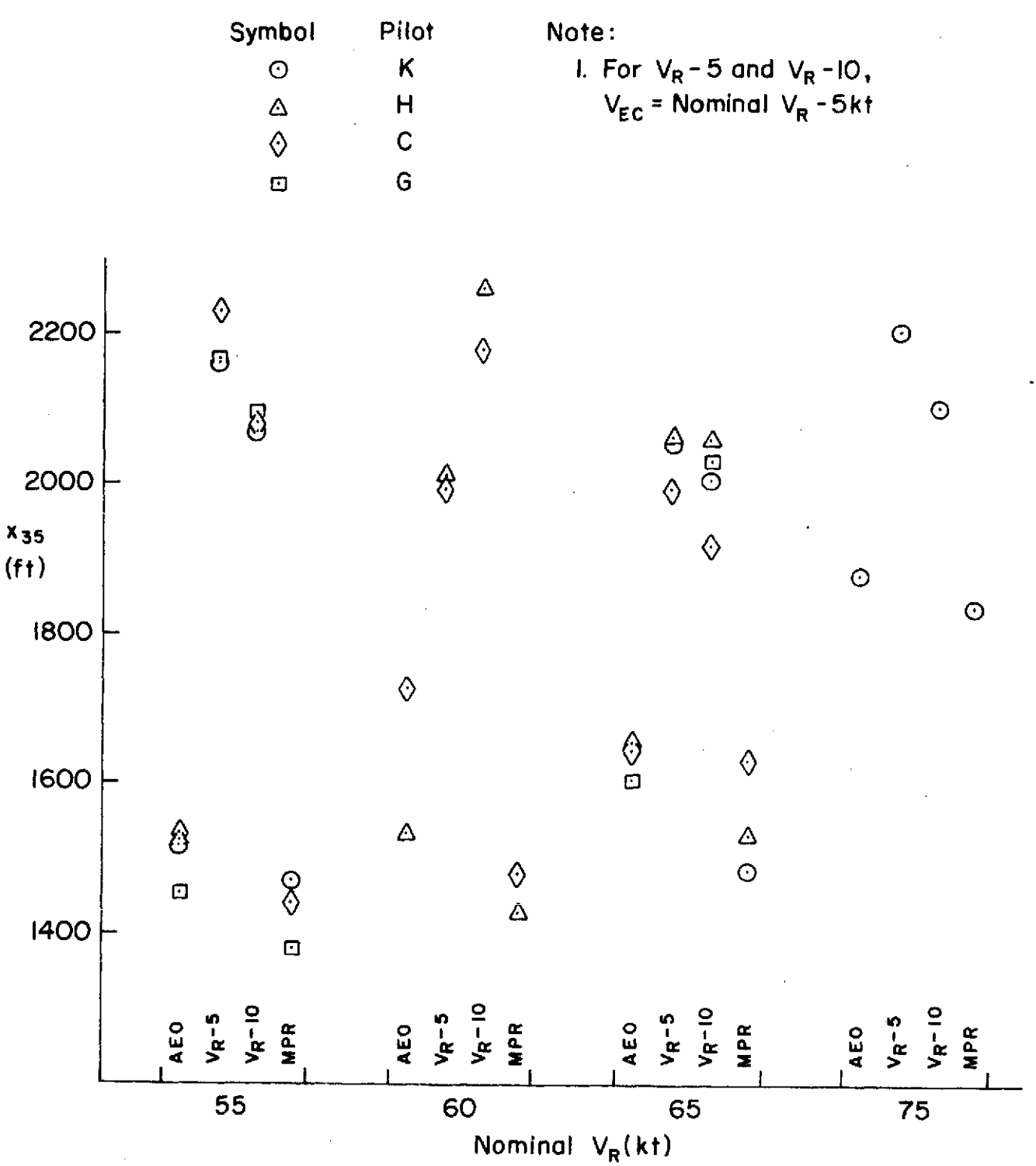

d. X_{35}

Figure VI-4. Concluded

Data presented in Fig. VI-4d indicate the same general trends in x_{35} as in x_{LOF}. The OEI V_R -5 and V_R -10 abuses increase x_{35} relative to the AEO baseline case, while the MPR abuses reduce it. Again, it is impossible to determine precisely how much of the increase in x_{35} for the OEI V_R -5 and V_R -10 abuses was due to the engine loss and how much was due to the early rotation. The scatter of the data precludes the possibility of precise numbers, but the MPR abuses decrease both x_{LOF} and x_{35} by approximately 10%, while V_R -5 and V_R -10 abuses increase x_{LOF} and x_{35} by as much as 45%.

Interpolation of x_{LOF} in Fig. VI-4c yields an AEO liftoff distance of approximately 1300 ft at a V_R of 71 kt, as opposed to the 1210 ft given in Ref. 2. Similarly, interpolation of x_{35} in Fig. VI-4d gives a distance to 35 ft of approximately 1700 ft at a V_R of 71 kt, as opposed to the 1570 ft given in Ref. 2.

E. MINIMUM PLANE PENETRATED

The minimum plane penetrated, MPP, was calculated for a 2000 ft runway (i.e., plane starts at x = 2100 ft). The results are presented in Fig. VI-5. Also presented are the theoretical MPP's based upon the average x_{LOF} and trim γ for each V_2. The theoretical MPP assumes a climb at γ_{TRIM} from liftoff to an altitude of 1100 ft (end of run) and thus

$$MPP_I = \tan^{-1}\left[\frac{1100}{1100 \cot \gamma_{TRIM} - (2100 - x_{LOF})}\right]$$

In examining the data of Fig. VI-5, the data for V_2 = 67 kt and OEI must be considered separately---that speed is the minimum possible with OEI and a slight speed increase significantly increases γ_{TRIM}. That is the reason for the low value of the theoretical MPP and the good performance relative to the theoretical limit.

For the other OEI data, we see that the measured MPP's were always less than the theoretical values. Differences of 1 deg were not uncommon

Symbol	Pilot
⊙	K
△	H
◇	C
⊡	G

V_2 (kt)	V_{EC} (kt)
67	50
70	55
74	60
82	70

Notes:

1. Numbers in Parentheses Indicate Number of Data Points
2. Solid Symbols Denote No Turbulence
3. Data Covers V_R - 5 and V_R - 10 Abuses
4. ---- Indicates Theoretical Best MPP Based on γ_{TRIM} and Average x_{LOF}
5. —— Indicates γ_{TRIM}
6. Nominal Turbulence = σ_{ug} = 3 ft/sec

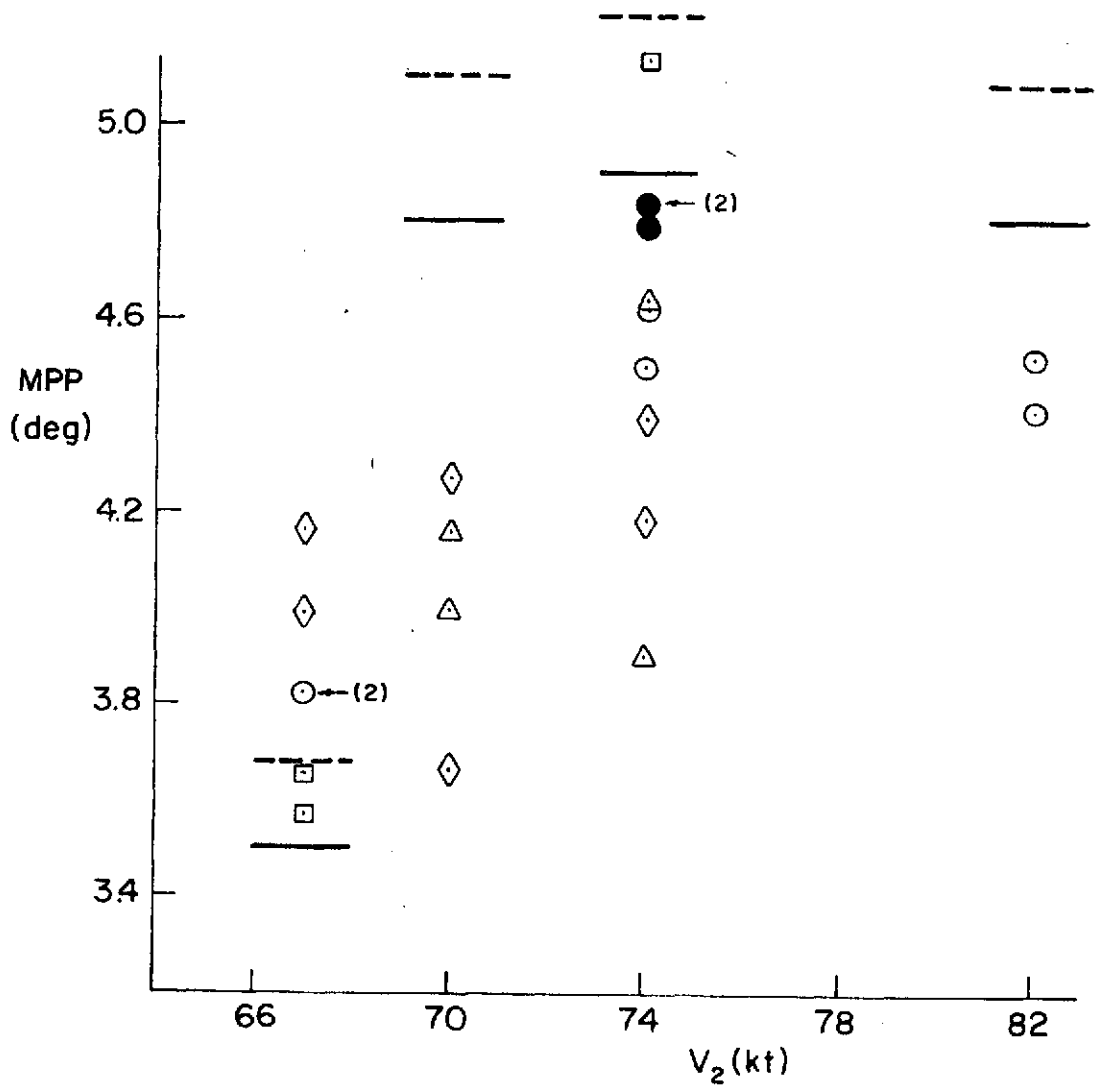

a. OEI

Figure VI-5. Minimum Plane Penetrated

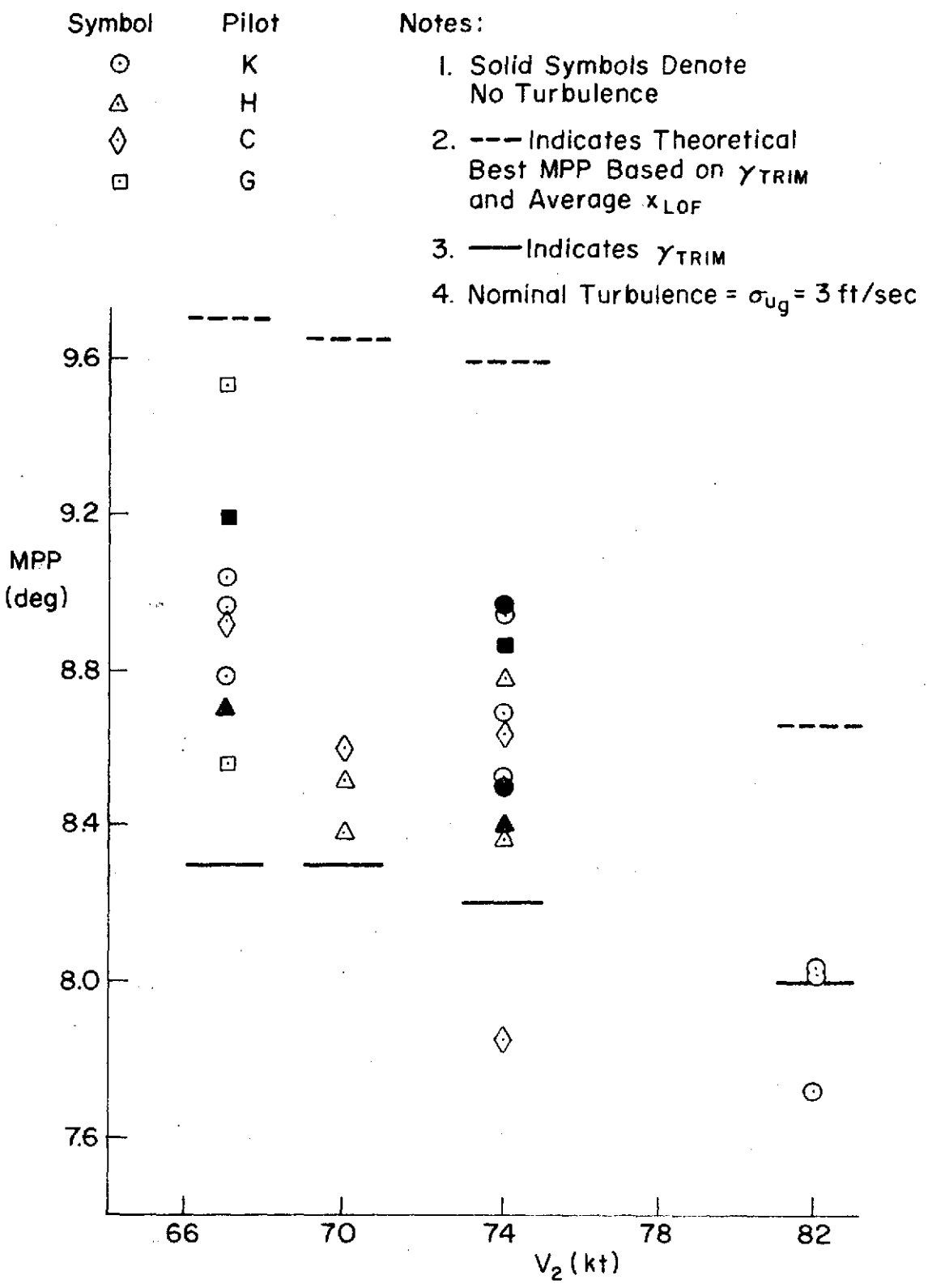

b. AEO

Figure VI-5. Concluded

and a value of 1.4 deg was obtained. Furthermore, with one exception the measured MPP's were less than the trim climb angle, γ_{TRIM}.

The AEO data are of less concern from a safety standpoint but are presented in Fig. VI-5b for comparison. For these cases there is more separation between the theoretical MPP's and the γ_{TRIM}'s because of the smaller x_{LOF}'s. With two exceptions, these two limiting values bracket the measured MPP's.

F. PILOT COMMENTS

The takeoffs never presented a problem to the pilots. Even in the worst abuse cases the aircraft was easy to handle. The aircraft would not lift off before it had adequate flying speed. Even with OEI it was easy to accelerate to V_2 after an early rotation.

The only difficulty encountered by any of the pilots was climbing out at low airspeed with OEI. One pilot 'crashed' while trying to climb at 67 kt, OEI. He inadvertently got to an angle of attack above that for $C_{L_{max}}$. Not recognizing the situation, he pulled the nose up because his airspeed was too high. This just increased the speed further.

This pilot rated an OEI climb at V_2 = 67 kt as impossible, marginal at V_2 = 70 (pilot rating = 6), and easy to fly at V_2 = 74 kt (pilot rating = 3.5). Obviously some margin between V_2 and the minimum speed is required. These results suggest a 10% margin might be adequate.

SECTION VII

SUMMARY OF RESULTS

The following is a summary list of the findings of the 1972 and 1973 simulation experiments reported in the preceding sections and the results of the analyses contained in Appendices B and C.

A. ILS TRACKING

- Pilot opinion of the ILS task was a more conservative indicator than was actual tracking performance (RMS deviation from the glide slope).
- The glide slope tracking task increased in difficulty as the approach speed was lowered.
- The lowest target approach speed which was rated acceptable for the simulated task was 60 kt transparency in and 60 - 65 kt transparency out.
- The limit approach speed was slightly higher for transparency out, and this was reflected in the closed loop analysis as well as pilot opinion.
- In general, the relative pilot ratings for ILS tracking corresponded to the results of the pilot/vehicle analyses.
- The pilot lead required to obtain a good glide slope loop closure increases as approach speed is reduced.
- Glide slope tracking performance was not dependent on SAS although the SAS did reduce pilot workload.
- At extremely low speeds a reverse $d \longrightarrow \theta$, $u \longrightarrow \delta_T$ technique is required which is completely unacceptable even though good tracking performance is attainable.
- The effect of increasing glide slope angle over the nominal 7.5 deg was not significant to ILS task.

- An angle of attack display will not allow a substantial reduction in approach speed but could improve safety by helping the pilot to avoid excessive angles of attack.
- If an angle of attack display is used, pilots must be trained not to track it tightly.

B. FLARE AND LANDING

- Consistent, well controlled touchdowns can be made in the simulator when the aircraft characteristics permit it.
- For acceptable flare and landing characteristics, the approach speed limit is approximately 60 kt with transparency in and 60 - 65 kt with transparency out.
- At the minimum acceptable approach speeds noted above, a slight power addition just prior to the flare maneuver was required. This open loop power addition was considered to be an acceptable technique by the pilots.
- Pilot acceptability correlated with the airplane's potential touchdown sink rate without the use of power.
- The above airframe characteristic correlated with speed margin above V_{min} (power fixed) for this particular model and set of conditions.
- For the limiting speeds noted above, the speed margins are 6 - 15 percent.
- Significant changes in $\dot{h}_{TD}$ performance occurred in cases where pilot rating changed significantly (e.g., 55 kt).
- Touchdown performance in the simulator compared favorably with that obtained in flight with the actual airplane with the same pilots.
- A more nose-down approach attitude (-5 to -10 deg) did not adversely affect the pilots, but with a nose-up approach attitude (2 deg) the pilot had to add power to avoid losing sight of the runway.

- A thrust lag reduction from 1.4 to 0.5 sec did not significantly affect landing performance but improved pilot ratings by 1/2 point.
- Flare using power alone (or as the primary control) may be an acceptable technique but pilot acceptance will be strongly influenced by his flight background.
- In this particular model, the limit speed for ILS tracking was also the limit for flare and landing.

C. GO-AROUND

- A configuration change such as used on this airplane is reasonable for go-around situations.
- During a significant number of go-arounds the minimum altitude was 80 to 100 ft below the decision height.
- Altitude loss following go-around initiation was far more sensitive to the 2 deg increased glide slope than to the approach speed variation.
- A significant degradation in go-around performance with transparency out was noted and attributed to the longer thrust buildup time relative to that with transparency in.

D. TAKEOFF

- For a balanced field, the decision speed, V_1, was very close to the rotation speed, V_R.
- The takeoff performance was quite insensitive to V_1; the distance to an altitude of 35 ft increased only 300 ft (1900 - 2200 ft) in going from $V_1 = V_R = 65$ kt to $V_1 = 0$.
- The aircraft was very forgiving of the takeoff abuses in that early rotations did not result in dangerous situations -- the aircraft would not lift off until it reached adequate flying speed. This characteristic would allow reduction or elimination of the required margins between V_{LOF} and V_{MU}.

- Although early rotations and engine failures did not cause pilot control problems, they did greatly increase takeoff distances (by as much as 45%); therefore in setting takeoff performance standards, early rotation abuses with engine failures must be considered.
- Climb performance of 1.4 deg less than the theoretical value was measured; these data provide an indication of the margins which must be provided between demonstrated climb performance and actual obstacle clearance planes.
- A margin between V_2 and the minimum speed on the order of 10% was necessary.

REFERENCES

1. Zuccaro, J. L., The Flight Simulator for Advanced Aircraft - A New Aeronautical Research Tool, AIAA Paper 70-359, March 1970.

2. Model 188 STOL Pilot Training Manual, McDonnell-Douglas Report No. G509, 3 September 1968, Revised February 1969.

3. Planning and Design Criteria for Metropolitan STOL Ports, FAA AC 150/5300-8, November 1970.

4. Craig, Samuel J. and Robert K. Heffley, An Investigation of Parameters and Factors Governing Manual Control of STOL Aircraft in Landing Approach, AIAA Paper 72-987, September 1972.

5. Military Specification, Flying Qualities of Piloted Airplanes, MIL-F-8785B (ASG), 7 August 1969, Amended 31 March 1971.

APPENDIX A

SIMULATION MODEL CHARACTERISTICS

This Appendix contains general information describing the simulator model used in both the 1972 and 1973 simulation periods. A complete description of the model is given in Volume III of this report.

Table A-1 lists longitudinal dimensional stability derivatives for each of the approach configurations evaluated. These derivatives are taken with respect to the body-fixed stability axis system.

Table A-2 gives longitudinal transfer functions for elevator and throttle control. The engine response is not included. Throttle transfer functions can be made to include engine lags by adding the following transfer function:

$$\frac{N_G}{N_{G_c}} = \frac{e^{-.5s}}{.9s + 1}$$

For example the transfer function for rate of climb due to throttle including lags would be:

$$\frac{\dot{h}}{N_{G_c}} = \frac{N^{\dot{h}}_{N_G}(s)}{\Delta(s)} \quad \frac{e^{-.5s}}{.9s + 1}$$

Fig. A-1 shows small perturbation dynamic responses obtained on the simulator. The simulation included a pitch stabilization system similar to that a pilot would provide and similar to the pitch SAS used in the 1973 tests. Fig. A-1 includes flight path, speed, and angle of attack responses to the following inputs:

- 3% step in N_{G_c}
- 3 deg step in attitude
- -5 kt/100 ft wind shear

In this figure 95/12 means 95 deg flap and 12 deg transparency, 95/0 means 95 deg flap and zero transparency.

TABLE A-1

BR 941S
LONGITUDINAL STABILITY DERIVATIVES
APPROACH CONFIGURATIONS
45000 lbs at .27$\bar{c}$; 95 deg flaps

	TRIM CONDITION									
T (deg)	12	12	12	ZERO	ZERO	ZERO	ZERO	12	12	12
γ_o (deg)	-7.5	-7.5	-7.5	-7.5	-7.5	-7.5	-7.5	-9.5	-9.5	-9.5
V_{T_o} (kt)	55	60	65	50	55	60	65	55	60	65
θ_o (deg)	-4.6	-8.7	-11.3	2.73	-1.32	-5.7	-9.6	-3.0	-8.5	-11.7
N_G (% RPM)	94.7	93.2	92.5	93.4	89.4	86.0	84.6	93.9	91.2	90.2
	DIMENSIONAL DERIVATIVES (Stability Axis)									
X_u (1/sec)	-.144	-.128	-.118	-.098	-.109	-.116	-.119	-.161	-.147	-.137
Z_u (1/sec)	-.416	-.364	-.334	-.416	-.408	-.409	-.397	-.435	-.377	-.345
X_w (1/sec)	.165	.092	.024	.219	.192	.162	.129	.182	.111	.040
Z_w (1/sec)	-.211	-.488	-.686	-.106	-.211	-.377	-.557	-.053	-.393	-.613
g/U_o (1/sec)	.347	.318	.294	.382	.347	.318	.294	.347	.318	.294
$\tan^{-1}\left[\frac{-Z_{N_G}}{X_{N_G}}\right]$ (deg)	79.0	80.3	80.5	90.3	86.1	81.6	76.9	79.3	80.3	80.3
M_u(1/sec-ft)	.00194	.00187	.00174	.00305	.00238	.00188	.00159	.00176	.00173	.00162
M_w(1/sec-ft)	-.00250	-.00367	-.00450	-.00260	-.00292	-.00342	-.00396	-.00208	-.00344	-.00434
$M_{\dot{w}}$(1/ft)	-.00281	-.00281	-.00281	-.00280	-.00280	-.00281	-.00281	-.00280	-.00281	-.00281
M_q(1/sec)	-.682	-.744	-.807	-.620	-.682	-.744	-.807	-.682	-.744	-.807
$Z_{\dot{w}}$(1/1)	-.0125	-.0125	-.0125	-.0125	-.0125	-.0125	-.0125	-.0125	-.0125	-.0125
Z_q(ft/sec-rad)	-3.04	-3.32	-3.60	-2.77	-3.04	-3.32	-3.60	-3.04	-3.32	-3.60
M_{δ_e} (1/sec^2-rad)	-.972	-1.16	-1.36	-.803	-.972	-1.16	-1.36	-.972	-1.16	-1.36
Z_{δ_e} (ft/sec^2-rad)	-4.45	-5.30	-6.22	-3.68	-4.45	-5.30	-6.22	-4.45	-5.30	-6.22
X_{N_G} (ft/sec^2-%)	.168	.162	.164	-.004	.044	.072	.095	.151	.116	.114
Z_{N_G} (ft/sec^2-%)	-.861	-.952	-.979	-.811	-.652	-.486	-.410	-.798	-.679	-.667
$\frac{\partial N_G}{\partial \delta_T}$ (%/in)	3.3	3.5	3.6	3.5	3.9	4.2	4.3	3.4	3.8	3.9

TABLE A-2

BR 941S - LONGITUDINAL TRANSFER FUNCTIONS
(Approach Configuration)

TRIM CONDITION					
T (deg)	12	12	12	ZERO	ZERO
γ_o (deg)	-7.5	-7.5	-7.5	-7.5	-7.5
V_{T_o} (kt)	55	60	65	50	55
DENOMINATOR					
Δ	[.14;.35][.97;.62]	[.13;.31][.90;.86]	[.13;.29][.90;1.02]	[.06;.40][.97;.52]	[.10;.36][.92;.64]
ELEVATOR NUMERATORS					
$N^{\theta}_{\delta_e}$	-.96[.55;.31]	-1.14[.97;.31]	-1.34(.13)(.65)	-.79[.30;.32]	-.96[.48;.32]
$N^{u}_{\delta_e}$	15.7(.35)	25.7(.65)	39.2(.72)	10.3(.16)	13.3(.40)
$N^{w}_{\delta_e}$	-92.[.24;.38]	-119.[.24;.34]	-152.[.24;.32]	-69.[.17;.40]	-92.[.19;.38]
$N^{\dot{h}}_{\delta_e}$	4.4(-.3)(-1.3)(2.4)	5.2(-.02)(-2.7)(3.7)	6.1(.01)(-3.5)(3.7)	3.60(1.8)[-.63;.8]	4.4(-.26)(-1.3)(2.4)
$N^{\dot{d}}_{\delta_e}$	4.4(-.44)(-1.1)(2.3)	5.2(-.07)(-2.6)(3.6)	6.1(-.03)(-3.4)(4.4)	3.63(1.6)[-.53;.85]	4.4(-.37)(-1.1)(2.3)
THROTTLE NUMERATORS					
$N^{\theta}_{N_G}$	.0024(.10)(1.15)	.0026(.17)(1.44)	.0027(.20)(1.68)	.0023(-.13)(1.2)	.0018(-.007)(1.24)
$N^{u}_{N_G}$	.168(-.89)[.91;.66]	.162(-.69)[.85;.98]	.163(-.53)[.87;1.25]	-.0038(46.)[.83;.62]	.044(-2.8)[.84;.69]
$N^{w}_{N_G}$	-.85(.85)[.10;.27]	-.94(.89)[.095;.26]	-.97(.93)[.11;.24]	-.80(.79)[-.11;.35]	-.64(.83)[-.02;.30]
$N^{\dot{h}}_{N_G}$	.82(.74)[.60;.37]	.91(.68)[.59;.46]	.93(.63)[.61;.53]	.80(.64)[.50;.34]	.63(.64)[.62;.37]
$N^{\dot{d}}_{N_G}$	.85(.73)[.63;.35]	.94(.65)[.65;.44]	.97(.56)[.69;.53]	.80(.63)[.51;.31]	.64(.63)[.66;.34]
ELEVATOR-THROTTLE COUPLING NUMERATORS					
$N^{\theta\, u}_{\delta_e N_G}$	-.161(-.64)	-.185(-.07)	-.219(.52)	.0030(46.5)	-.042(-2.65)
$N^{\theta\, w}_{\delta_e N_G}$	.83(.23)	1.09(.19)	1.31(.18)	.64(.10)	.63(.14)
$N^{u\, w}_{\delta_e N_G}$	16.7(-1.54)	20.8(-1.63)	26.4(-1.55)	-.014[.25;.38]	5.0(-4.1)
$N^{\theta\, \dot{h}}_{\delta_e N_G}$	-.80(.25)	-1.05(.20)	-1.27(.17)	-.64(.12)	-.61(.16)
$N^{u\, \dot{h}}_{\delta_e N_G}$	-.73(-4.3)(5.0)	-.84(-5.8)(6.6)	-1.0(-6.9)(7.7)	.014[.013;25.]	-.19(-6.7)(7.3)
STEADY STATE PARTIAL DERIVATIVES					
$[\frac{\partial \gamma}{\partial V}]_{N_G}(\frac{\text{deg}}{\text{kt}})$	.91	.18	.08	2.95	.82
$[\frac{\partial \gamma}{\partial V}]_{\theta}(\frac{\text{deg}}{\text{kt}})$	-1.9	-15.4	1.8	-.5	-.8
$[\frac{\partial \gamma}{\partial \theta}]_{N_G}(\frac{\text{kt}}{\text{deg}})$	-.6	-1.6	-2.5	-.2	-.6

TABLE A-2

BR 941S - LONGITUDINAL TRANSFER FUNCTIONS (Concluded)
(Approach Configuration)

			TRIM CONDITION		
T (deg)	ZERO	ZERO	12	12	12
γ_o (deg)	-7.5	-7.5	-9.5	-9.5	-9.5
V_{T_o} (kt)	60	65	55	60	65
			DENOMINATOR		
Δ	[.12;.32][.90;.80]	[.15;.30][.89;.95]	(.31)(.73)[.15;.37]	[.17;.32][.91;.80]	[.17;.29][.89;.98]
			ELEVATOR NUMERATORS		
$N^{\theta}_{\delta_e}$	-1.14[.72;.33]	-1.34[.96;.34]	-.96[.34;.30]	-1.14[.84;.31]	-1.34(.17)(.56)
$N^{u}_{\delta_e}$	17.8(.70)	23.9(.93)	13.8(.03)	23.4(.56)	36.8(.68)
$N^{w}_{\delta_e}$	-119.[.21;.36]	-152.[.22;.34]	-92.[.27;.40]	-119.[.27;.35]	-152.[.28;.32]
$N^{\dot{h}}_{\delta_e}$	5.2(-.04)(-2.3)(3.2)	6.09(.03)(-3.1)(4.0)	4.3(1.6)[-.35;.97]	5.2(-.03)(-2.4)(3.3)	6.1(.03)(-3.3)(4.2)
$N^{\dot{d}}_{\delta_e}$	5.2(-.09)(-2.2)(3.2)	6.14(-.01)(-3.0)(4.0)	4.4(1.4)[-.25;1.0]	5.2(-.10)(-2.2)(3.2)	6.1(-.03)(-3.1)(4.1)
			THROTTLE NUMERATORS		
$N^{\theta}_{N_G}$	.0014(.10)(1.40)	.0011(.19)(1.57)	.0022(.07)(1.0)	.0019(.17)(1.4)	.0019(.21)(1.6)
$N^{u}_{N_G}$	.072(-1.06)[.83;.82]	.095(-.54)[.84;.98]	.151(-1.1)[.99;.56]	.116(-.76)[.85;.90]	.114(-.55)[.86;1.2]
$N^{w}_{N_G}$	-.48(.88)[.08;.26]	-.41(.94)[.18;.23]	-.79(.84)[.17;.25]	-.67(.88)[.15;.25]	-.66(.92)[.17;.23]
$N^{\dot{h}}_{N_G}$	.47(.64)[.68;.43]	.39(.66)[.68;.50]	.75(.76)[.69;.34]	.64(.69)[.62;.45]	.63(.65)[.62;.53]
$N^{\dot{d}}_{N_G}$	.48(.60)[.74;.41]	.41(.60)[.75;.49]	.79(.75)[.70;.31]	.67(.65)[.69;.43]	.66(.57)[.71;.52]
			ELEVATOR-THROTTLE COUPLING NUMERATORS		
$N^{\theta\ u}_{\delta_e N_G}$	-.082(-.73)	-.127(-.018)	-.145(-.92)	-.132(-.27)	-.153(.36)
$N^{\theta\ w}_{\delta_e N_G}$	.56(.18)	.55(.21)	.77(.24)	.78(.21)	.90(.20)
$N^{u\ w}_{\delta_e N_G}$	9.4(-1.87)	15.1(-1.13)	14.9(-1.57)	14.8(-1.62)	18.4(-1.50)
$N^{\theta\ \dot{h}}_{\delta_e N_G}$	-.55(.20)	-.53(.22)	-.73(.28)	-.74(.23)	-.86(.19)
$N^{u\ \dot{h}}_{\delta_e N_G}$	-.37(-5.1)(5.9)	-.58(-5.0)(5.8)	-.66(-3.8)(4.5)	-.60(-5.4)(6.2)	-.69(-6.5)(7.4)
			STEADY STATE PARTIAL DERIVATIVES		
$[\frac{\partial\gamma}{\partial V}]_{N_G}(\frac{deg}{kt})$	.24	.03	18.5	.26	.07
$[\frac{\partial\gamma}{\partial V}]_{\theta}(\frac{deg}{kt})$	-1.6	-46.	-1.5	-4.4	2.8
$[\frac{\partial V}{\partial\theta}]_{N_G}(\frac{kt}{deg})$	-1.0	-1.5	-.05	-1.2	-2.0

Note: The following identities hold true for stability axis transfer functions $N^{u\ \dot{d}}_{\delta_e N_G} = \frac{-N^{\dot{d}\ \dot{h}}_{\delta_e N_G}}{\sin\theta_o} \doteq N^{u\ \dot{h}}_{\delta_e N_G}$ and $N^{\theta\ \dot{d}}_{\delta_e N_G} = \frac{N^{w\ \dot{d}}_{\delta_e N_G}}{U_o} = N^{w\ \theta}_{\delta_e N_G}$

FIG. A-1 -- TIME RESPONSES

a. FLIGHT PATH RESPONSE TO A +3% GAS GENERATOR RPM STEP

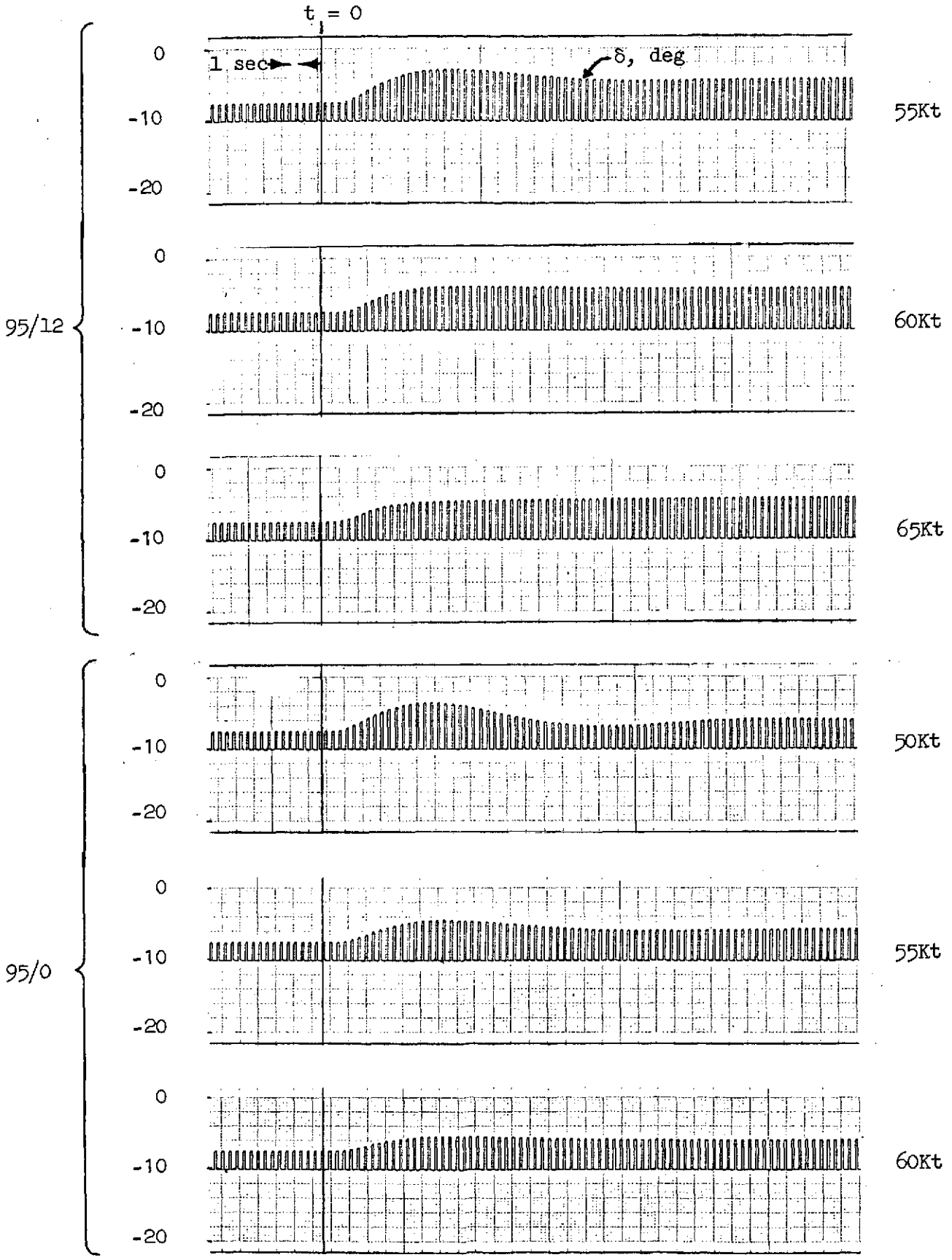

FIG. A-1 (Continued)

b. SPEED RESPONSE TO A +3% GAS GENERATOR RPM STEP

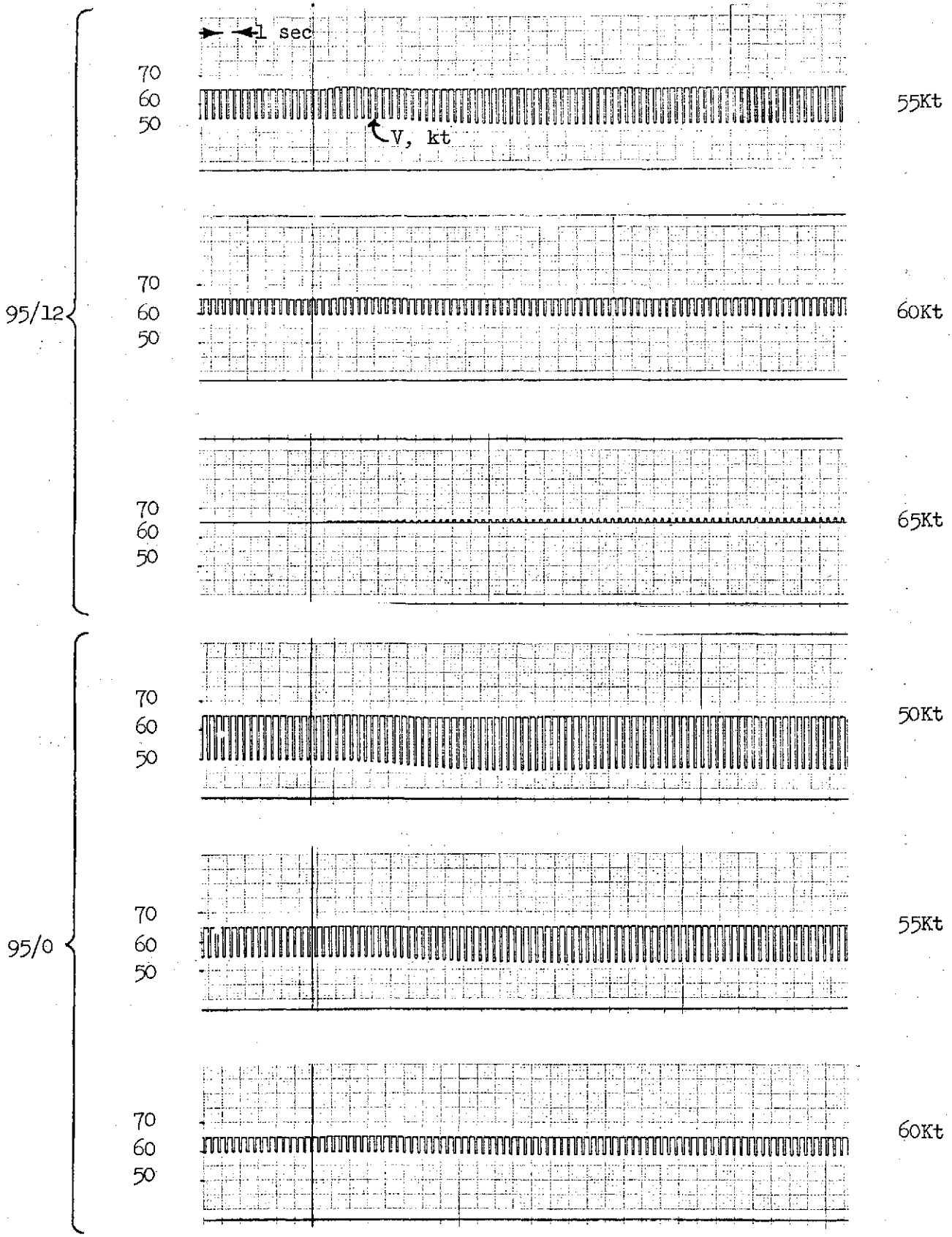

FIG. A-1 (Continued)

c. ANGLE OF ATTACK RESPONSE TO A +3% GAS GENERATOR RPM STEP

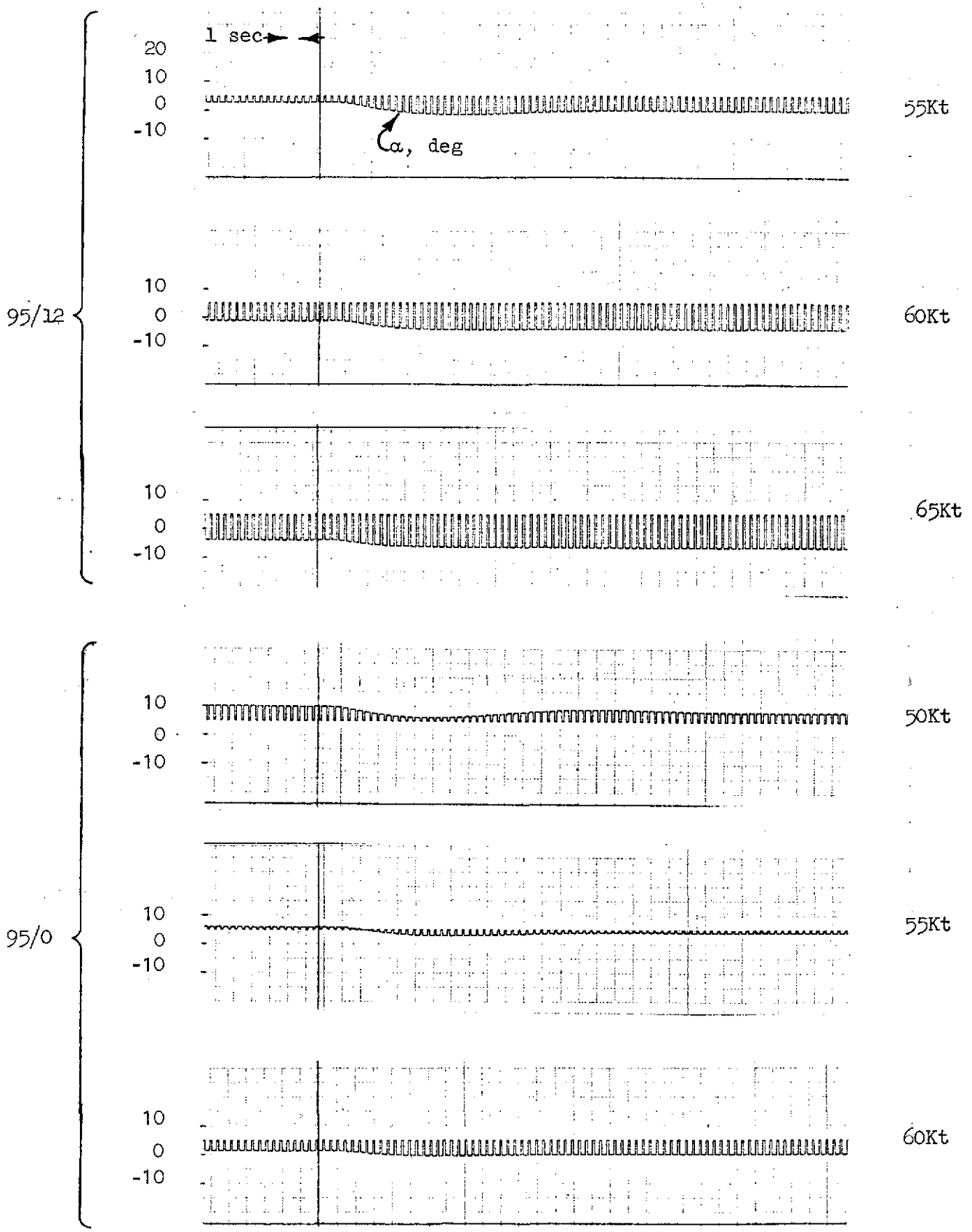

FIG. A-1 (Continued)

d. ALTITUDE RESPONSE TO A +3% GAS GENERATOR RPM STEP

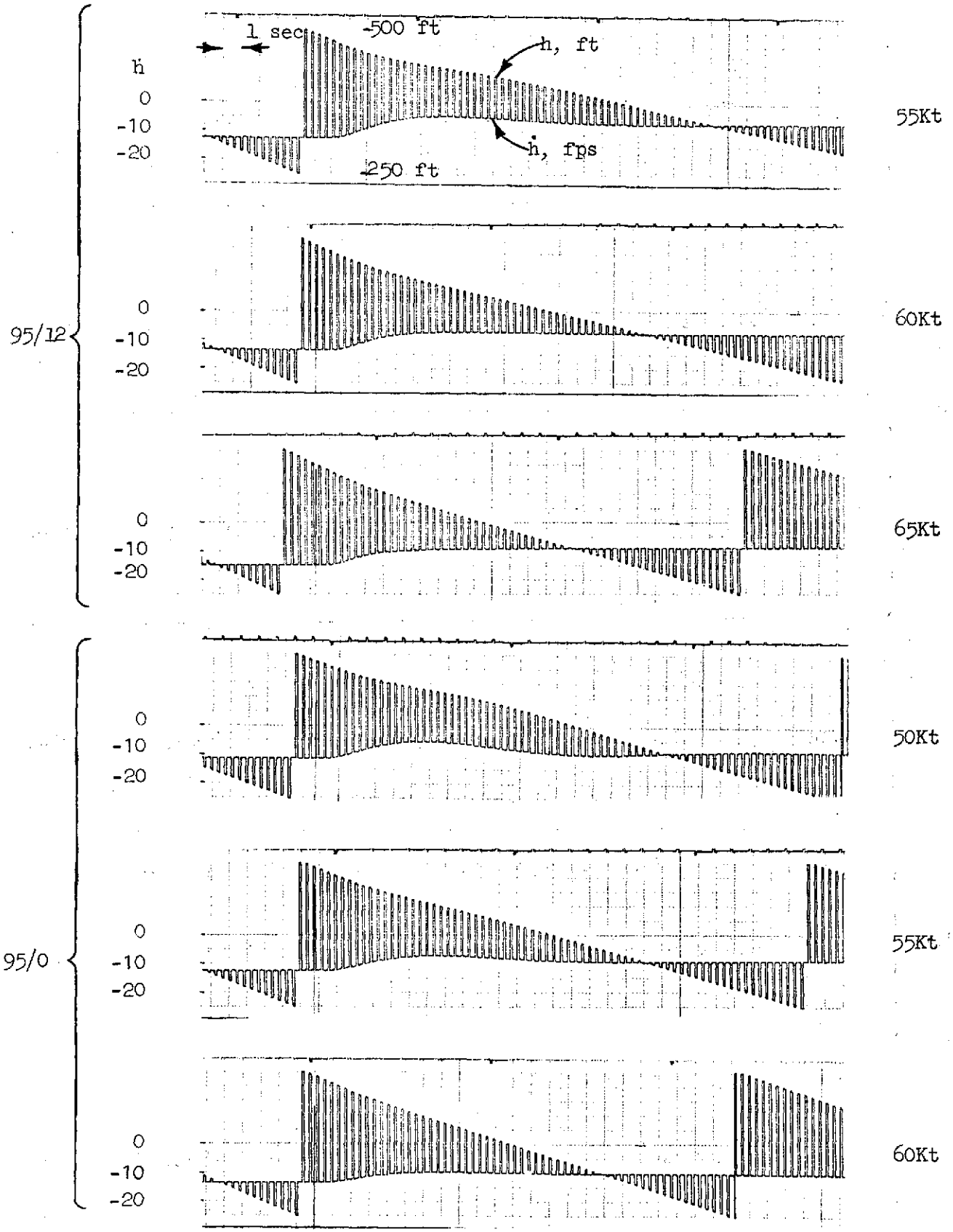

FIG. A-1 (Continued)

e. FLIGHT PATH RESPONSE TO A +3° ATTITUDE STEP

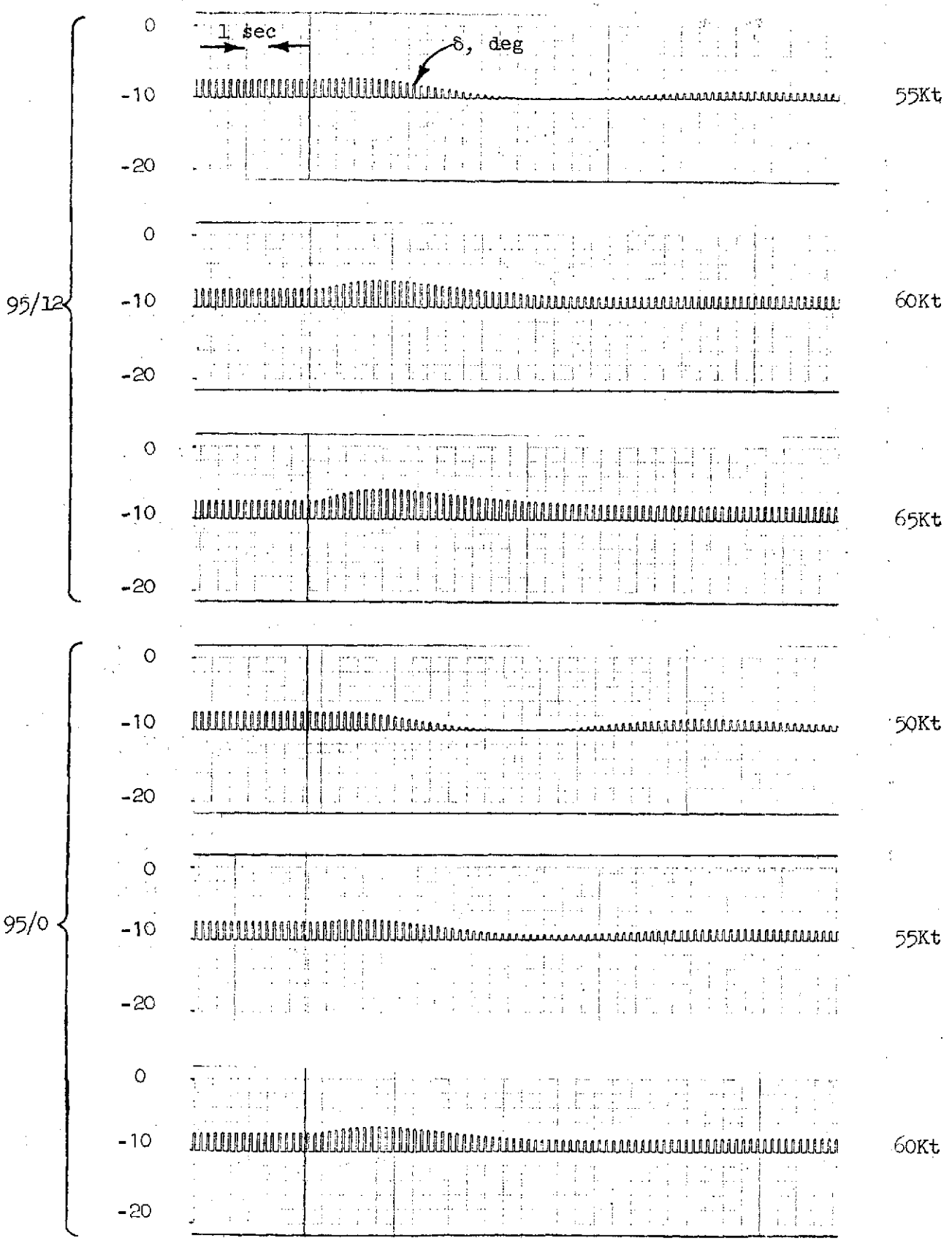

FIG. A-1 (Continued)

f. SPEED RESPONSE TO A +3° ATTITUDE STEP

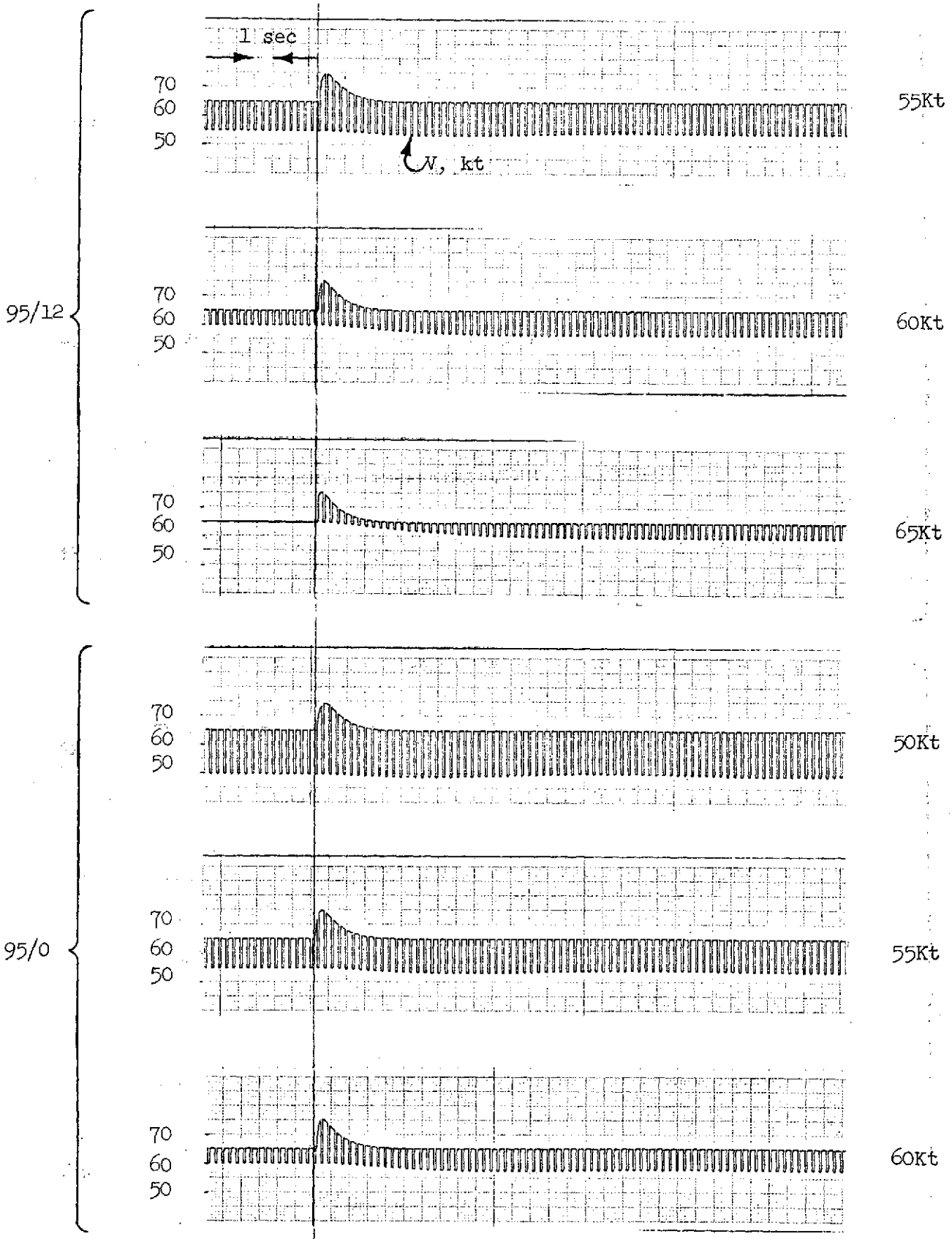

FIG. A-1 (Continued)

g. ANGLE OF ATTACK RESPONSE TO A +3° ATTITUDE STEP

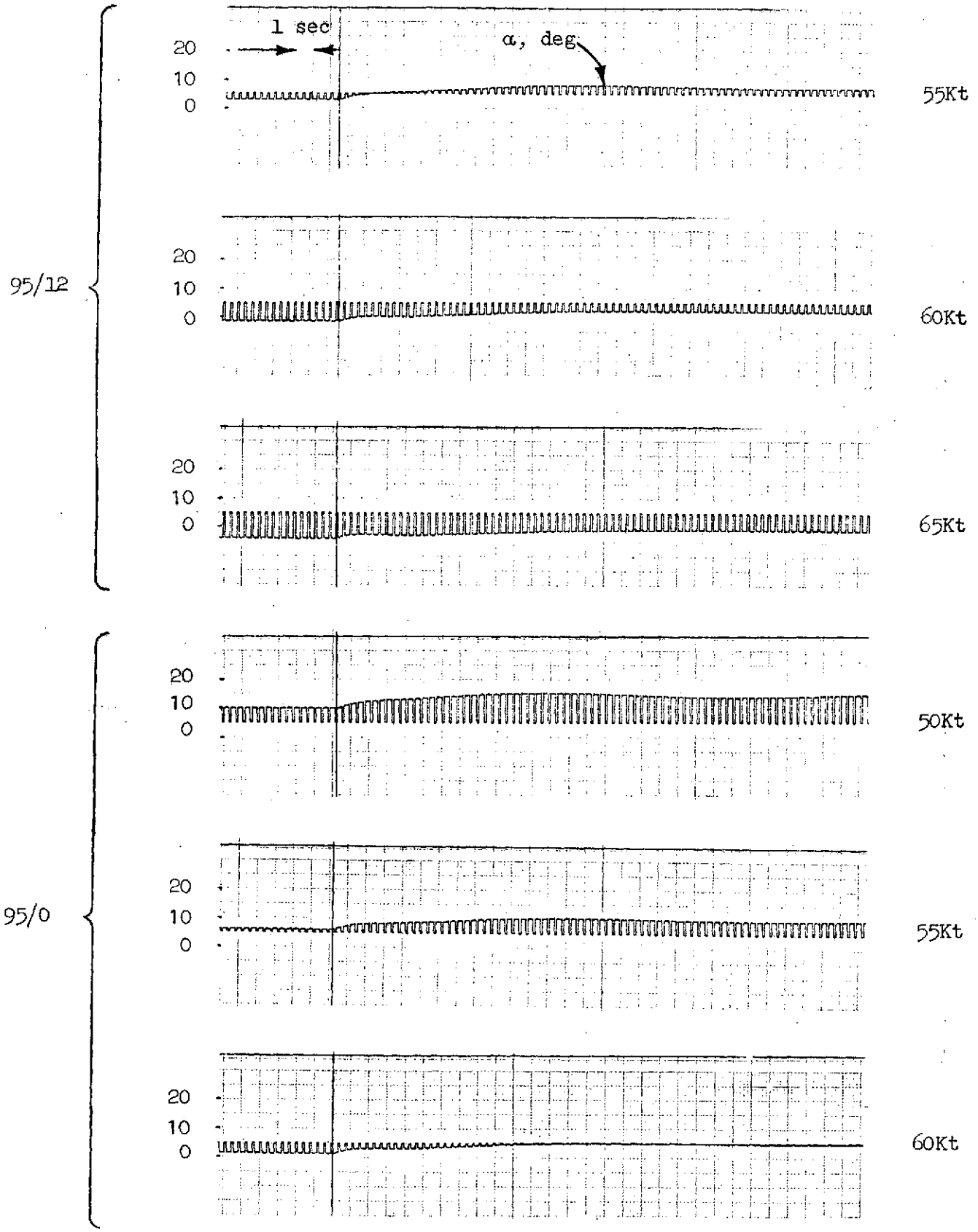

FIG. A-1 (Continued)

h. FLIGHT PATH RESPONSE TO A -5KT/100FT SHEAR

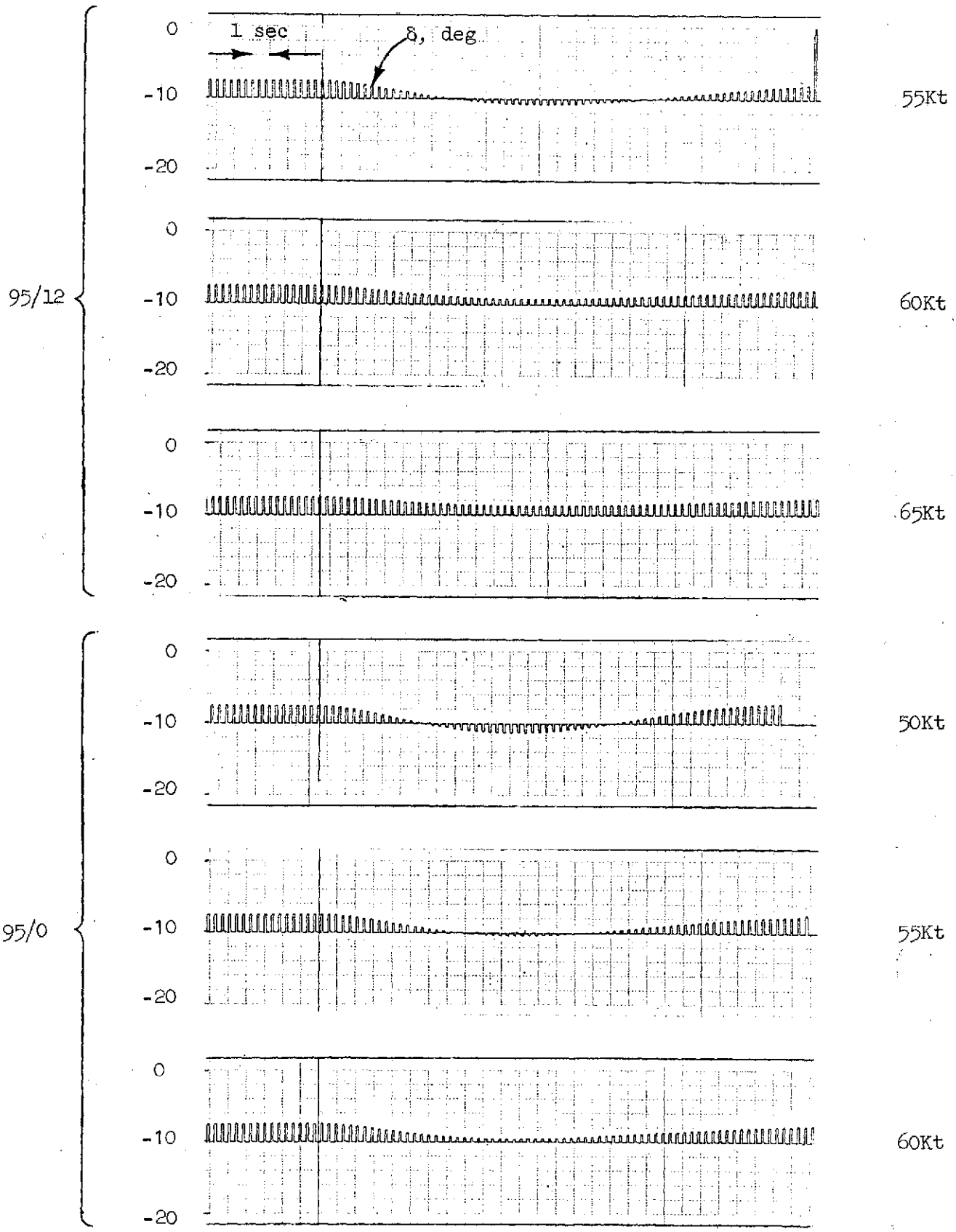

FIG. A-1 (Continued)

i. SPEED RESPONSE TO A -5KT/100FT SHEAR

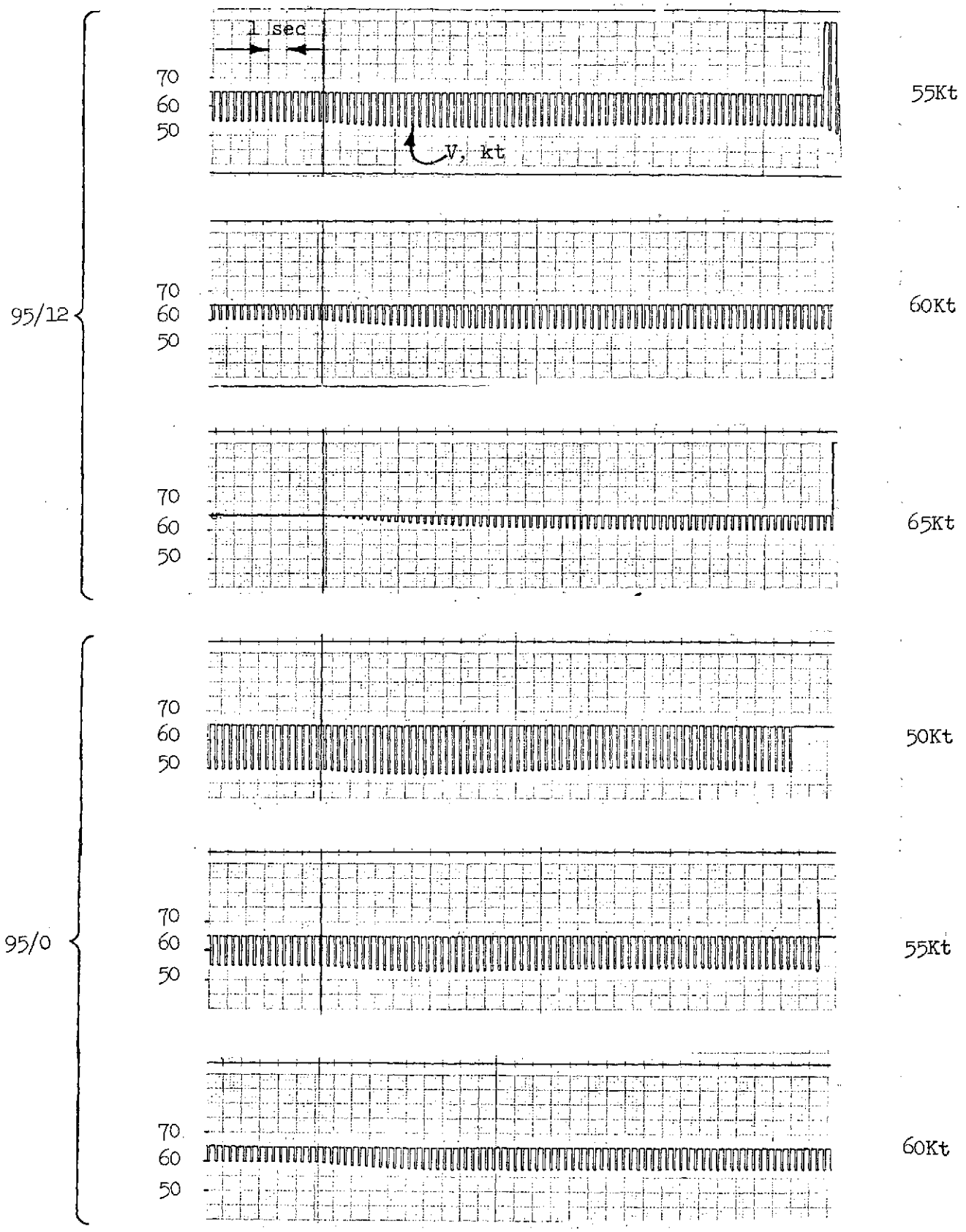

FIG. A-1 (Concluded)

j. ANGLE OF ATTACK RESPONSE TO A -5KT/100FT SHEAR

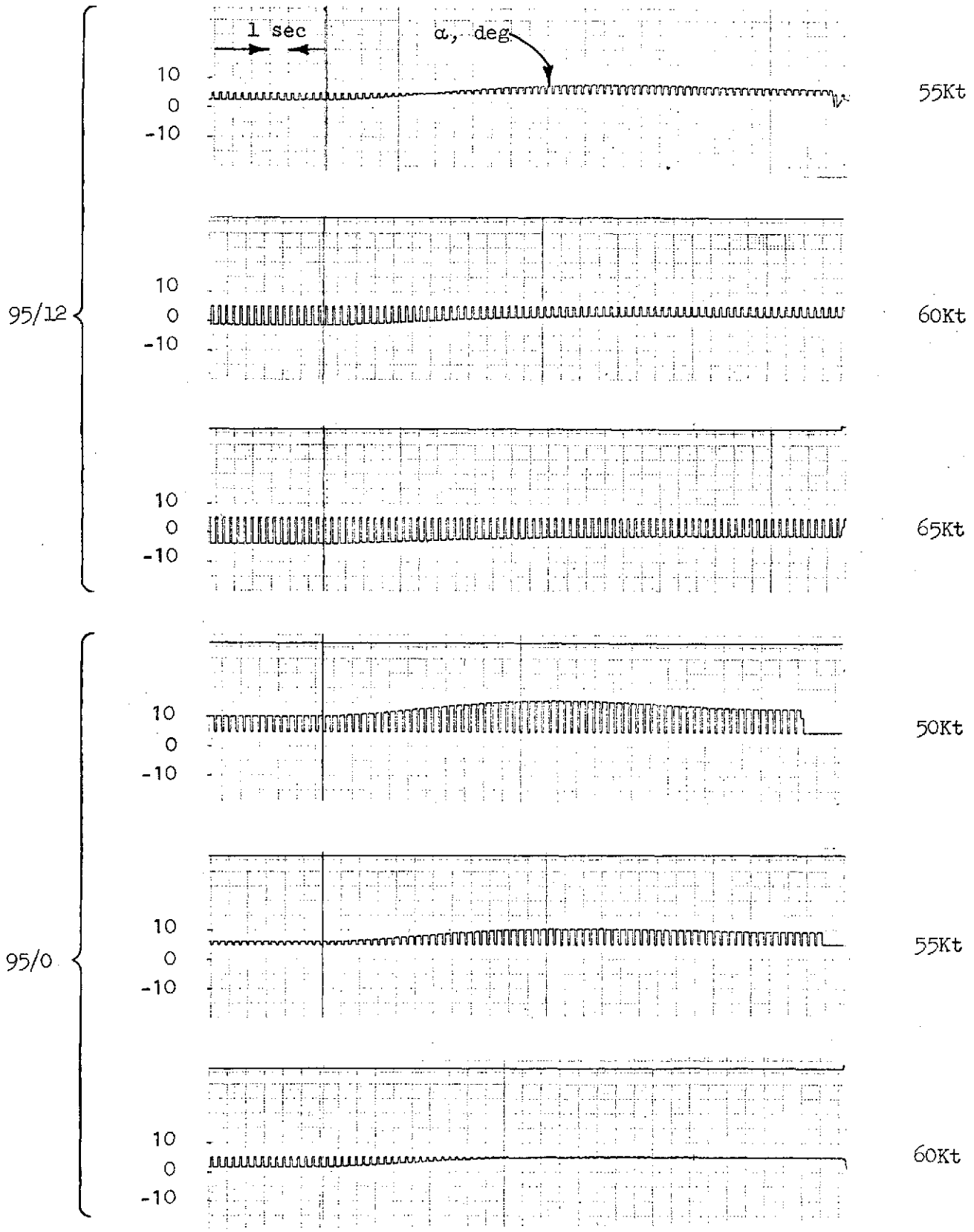

Fig. A-2 describes the γ - V performance envelopes for the configurations used during the simulations. These include:

FLAP	TRANSPARENCY	GROSS WEIGHT	USE
45 deg	ZERO	52000 lb	Takeoff
45 deg	ZERO	45000 lb	Initial condition for approach task
70 deg	5 deg	45000 lb	Prior to glide slope intercept
95 deg	ZERO	45000 lb	Approach
95 deg	12 deg	45000 lb	Approach

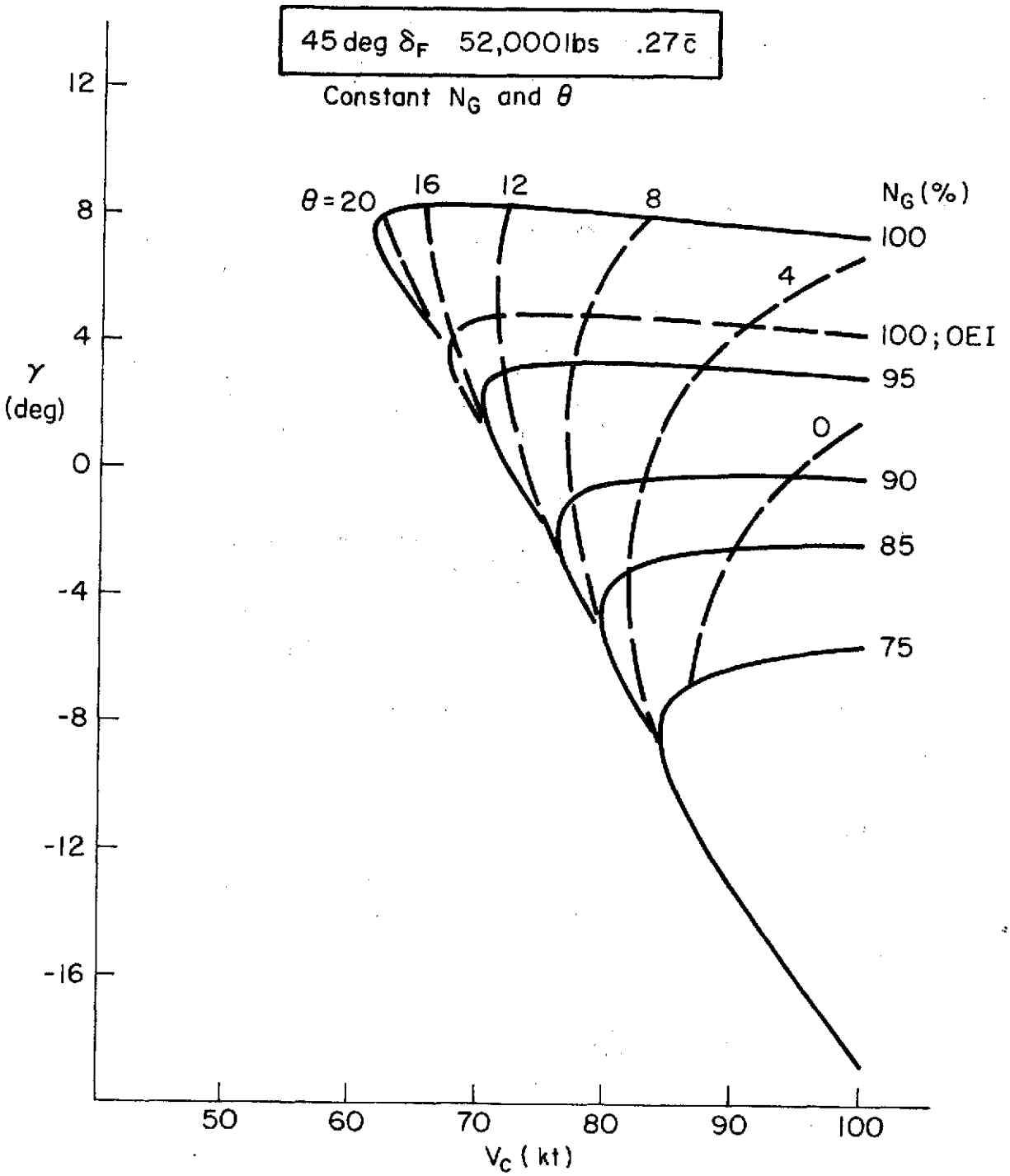

a) Takeoff

Figure A-2. Performance Curves

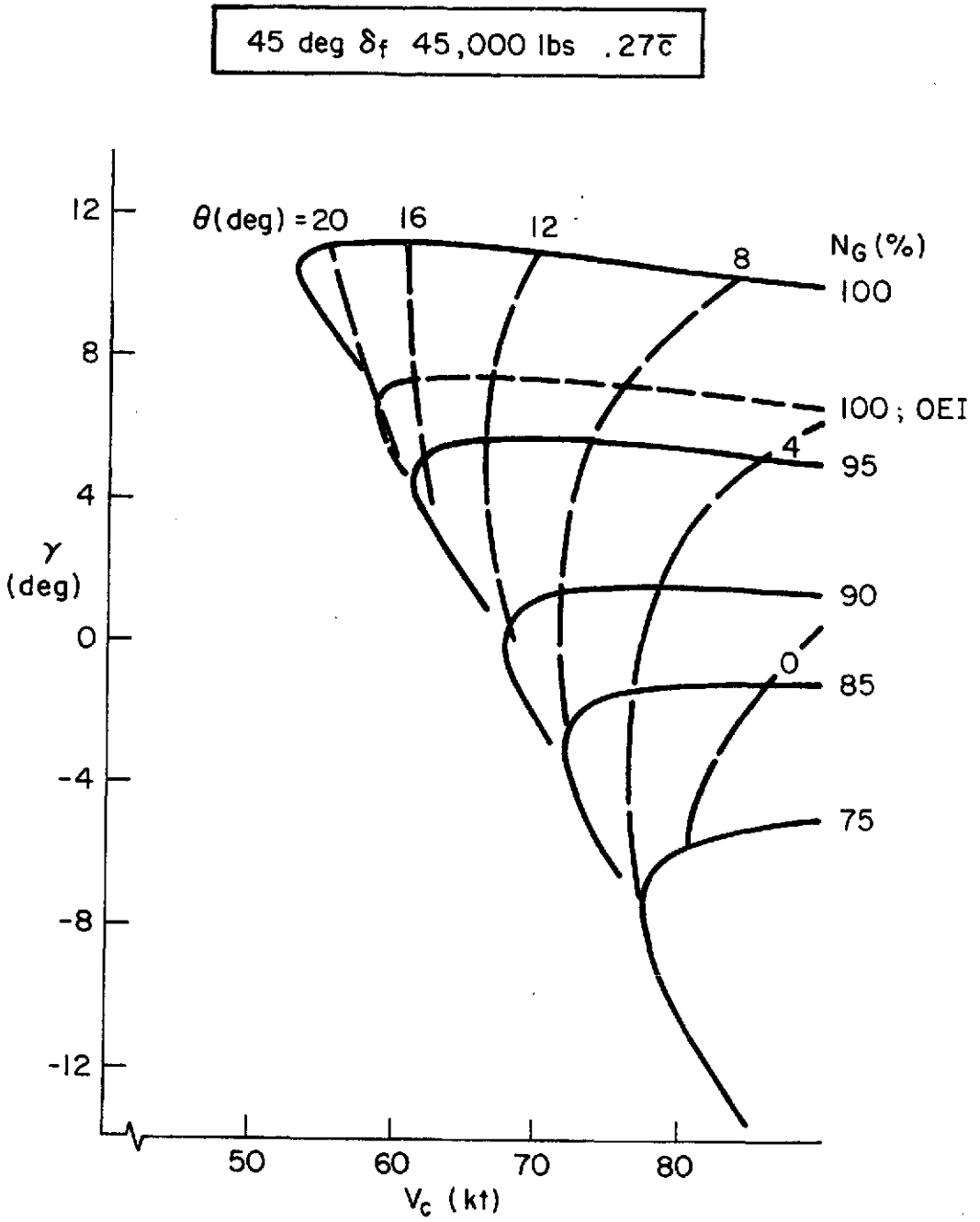

b) Initial Condition for Approach Task

Figure A-2. (Continued).

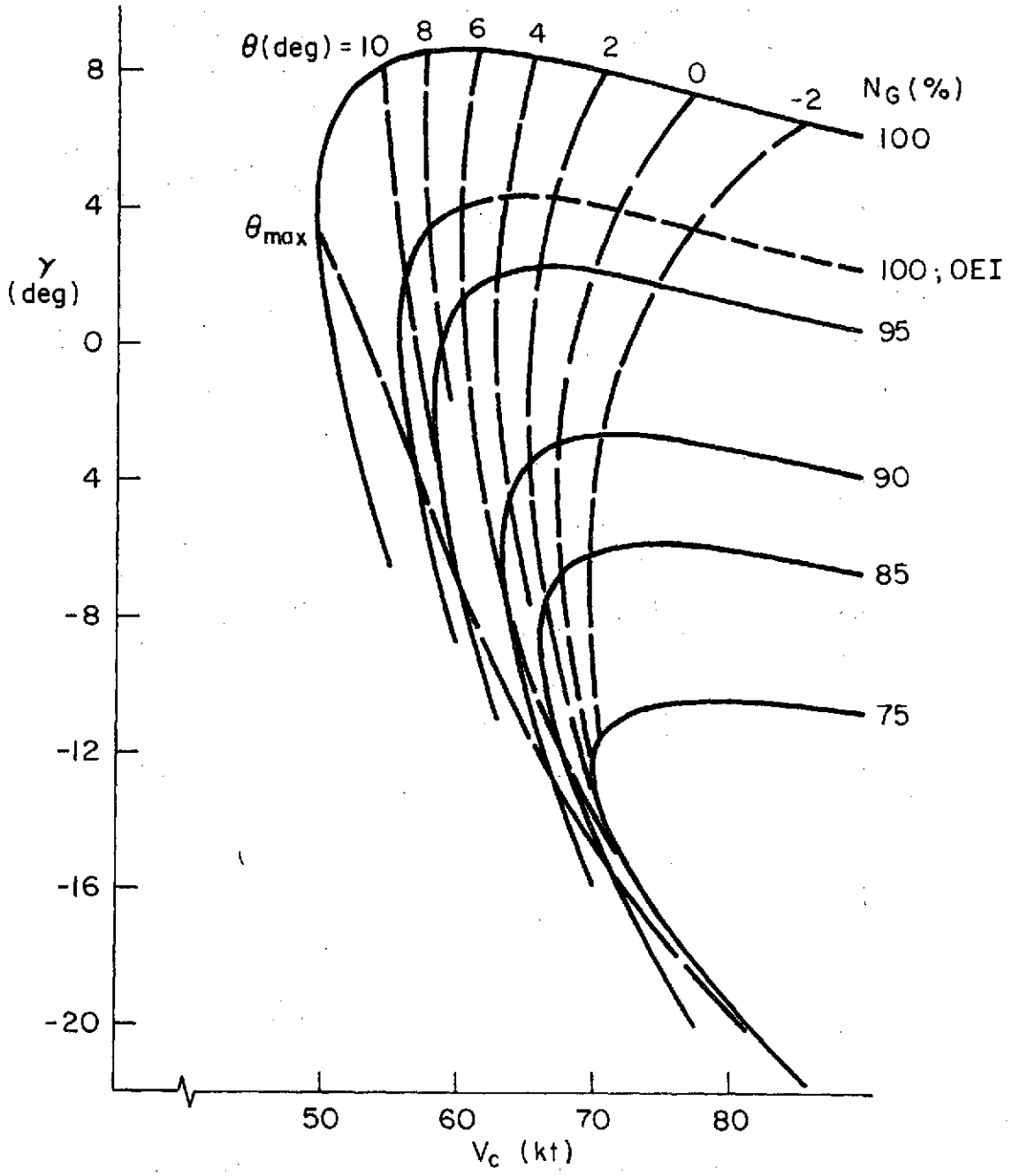

c) Intermediate Flap Setting

Figure A-2. (Continued)

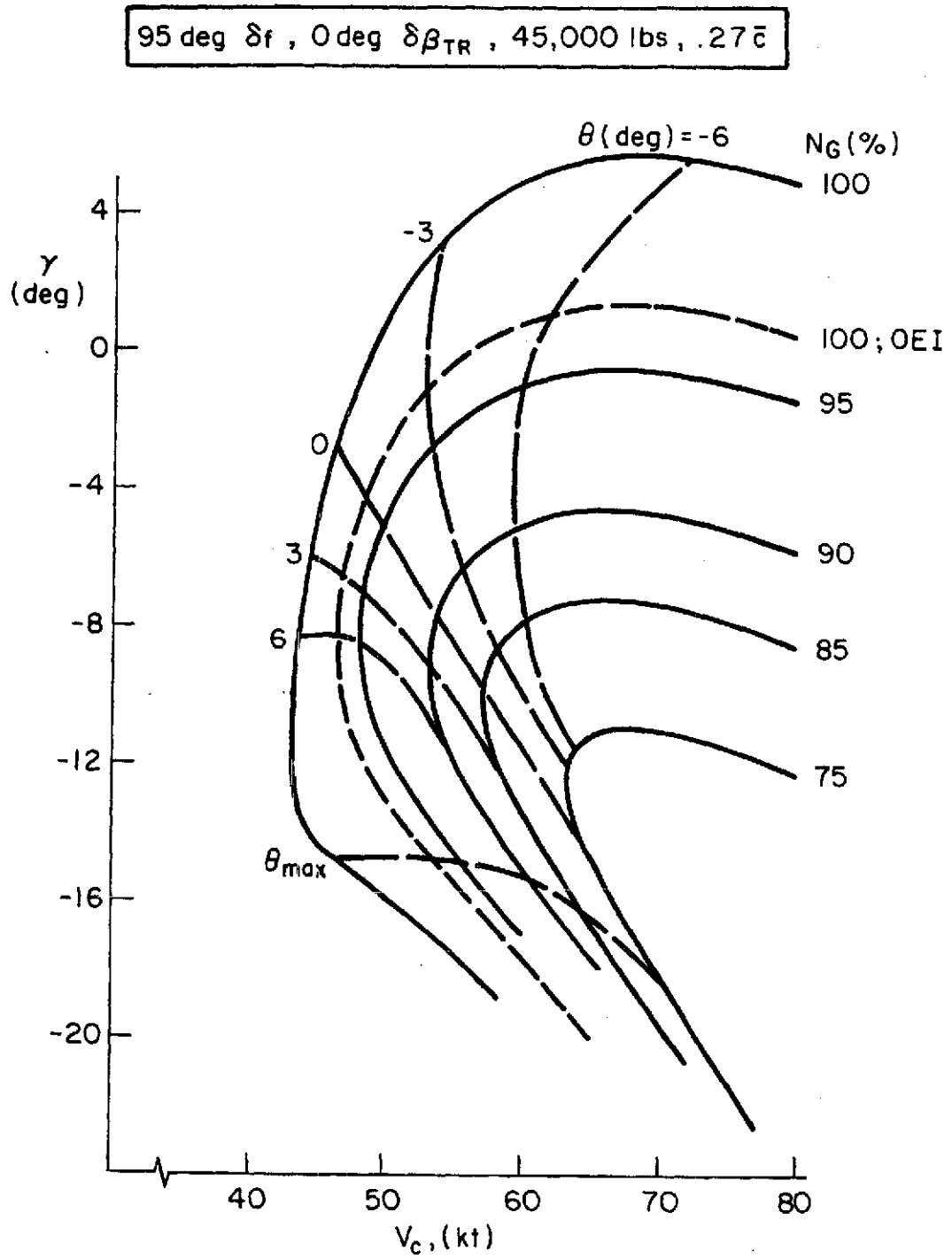

d) Approach Without Transparency

Figure A-2. (Continued)

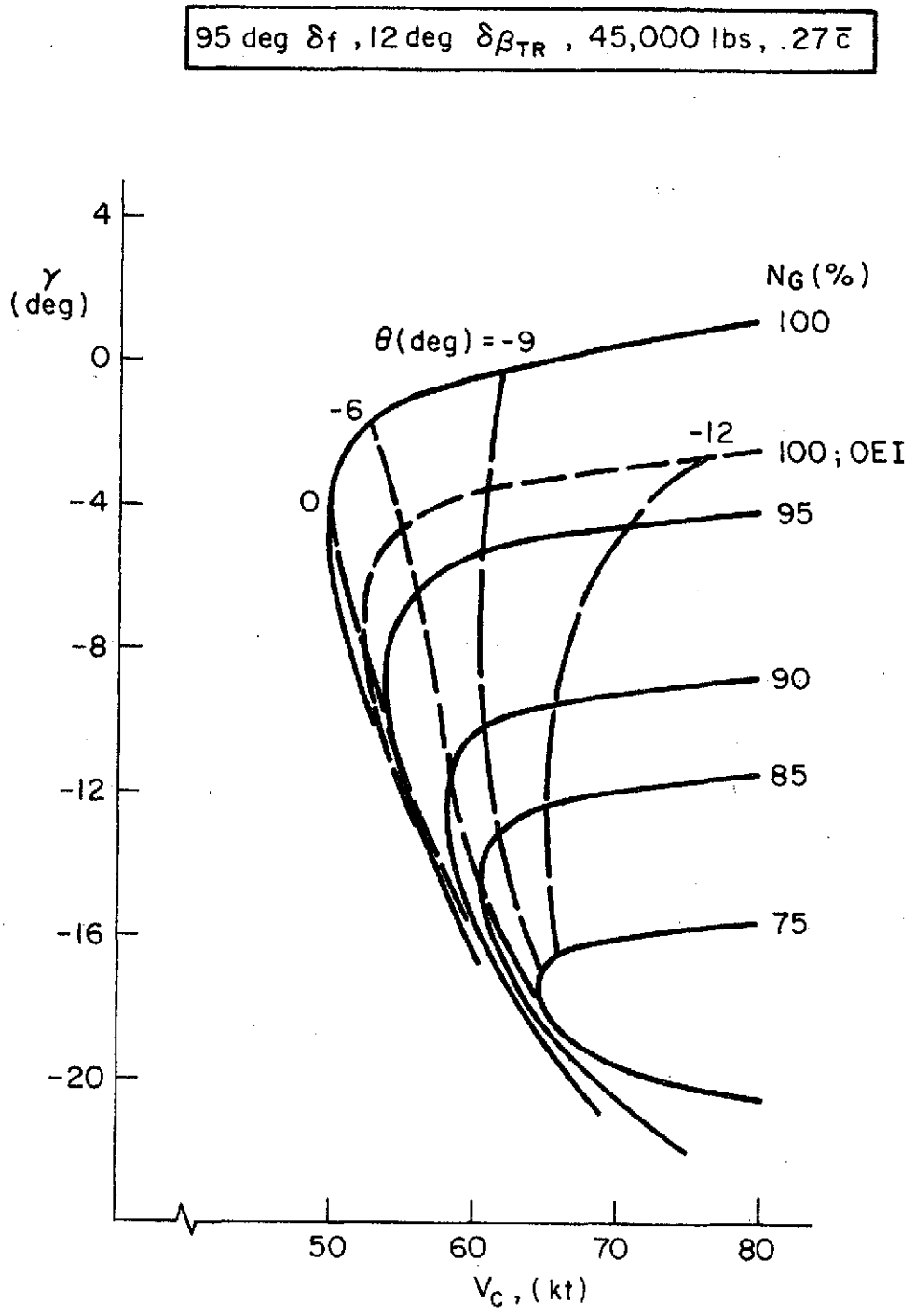

e) Approach With Transparency

Figure A-2. (Concluded)

APPENDIX B
PILOT/VEHICLE ANALYSES

The objective of the following analyses is to describe the manual path control characteristics of the various approach configurations used in the simulator experiments. The effects of approach speed, transparency in or out, and variations in piloting technique (involving use of speed and angle of attack control) are explored.

In order to provide a basis of comparison, certain ground rules are established. First, an automatic attitude stabilization scheme is assumed. This consists of an attitude command/attitude hold SAS*. This provides a θ/θ_c response over the range of speeds examined of:

$$\frac{\theta}{\theta_c} = \frac{3^2 \times 6.5}{[.7,3](6.5)}$$

Fig. B-1 shows a step response to θ/θ_c. Similar performance would be expected if the pilot were manually stabilizing attitude.

In addition to use of an attitude SAS, the pilot model for glide slope control is assumed to be a gain with lead compensation (Fig. B-2). The gain is set to give a .3 rad/sec crossover frequency and the lead is set at one second. These values are considered realistic for the task being analyzed based on observed performance during the October/November 1972 test series.

The following variations in piloting technique (glide slope controlled with throttle) were considered:

- No airspeed regulation
- Crossfeed of throttle to attitude to minimize speed variation

---

* The SAS used in the analyses is identical to that used in the 1973 simulations except for the feedback gain. A gain of -5 deg/deg was used in the analyses and in the initial simulation checkout. Because of pilot complaints of excessively rapid response the gain was lowered to -2.5 deg/deg. The slight reduction in attitude response does not affect the results of the analyses.

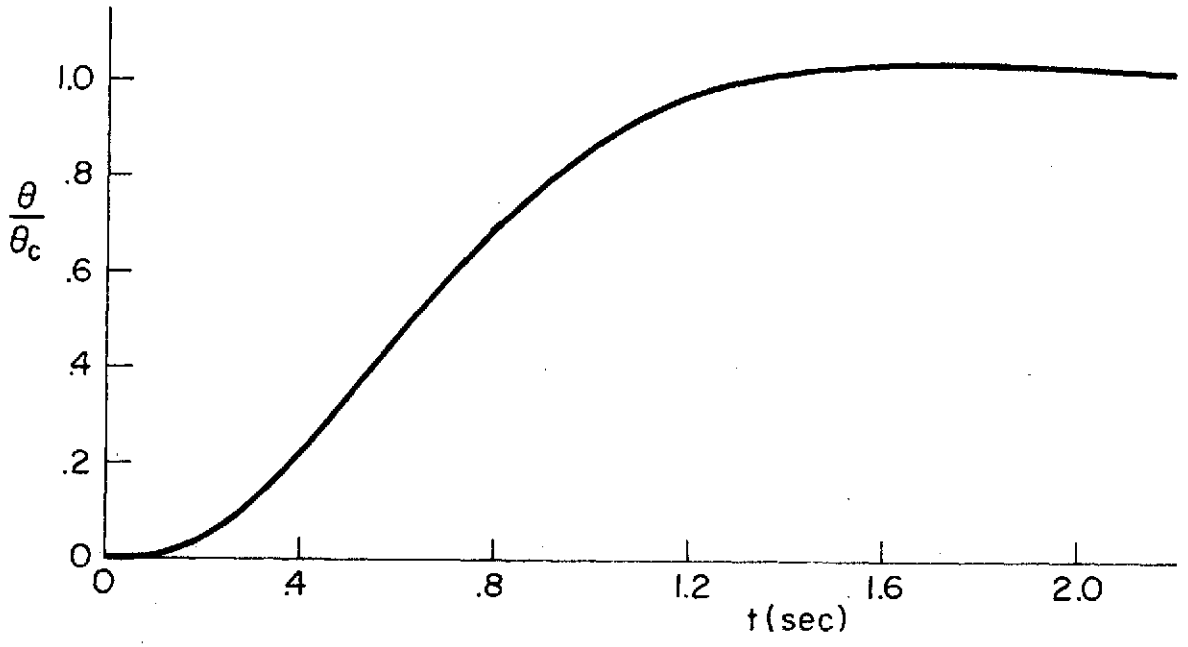

Figure B-1. SAS Attitude Response to Step Input

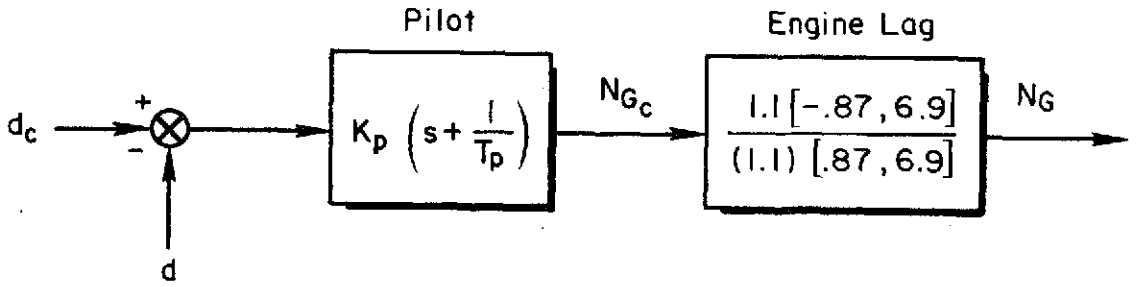

Figure B-2. Pilot Model for Glide Slope Control

- Closed loop control of airspeed
- Closed loop control of angle of attack

Each of the above cases was analyzed using the linear stability derivatives and transfer functions shown in Appendix A.

The loop closures for each approach condition and piloting technique are shown in subsequent figures. Each figure contains a system block diagram, a Bode plot, a root locus, and a closed loop step time response. This gives an overall view of the closed loop control problem for each case.

1. Glide Slope Control Without Airspeed Regulation

Figs. B-3 through B-7 show the effects of decreasing approach speed, first with transparency in then out. The 65 kt, transparency in case (Fig. B-3) shows a well behaved case in that the closed loop flight path oscillation is well damped. This is indicated by the short (4 sec) settling time and the high frequency at which the controlled system would become unstable (ω_{180} = 1.05 rad/sec) if the pilot gain were increased.

As the approach airspeed is reduced, the closed loop response becomes more oscillatory implying the need for increased pilot lead and the ensuing increase in pilot workload. The change from 60 kt to 55 kt is more dramatic than that between 65 kt and 60 kt.

The effect of transparency on glide slope control is fairly small but apparent. Transparency out performance for the 60 kt case appears to be somewhere between the 55 and 60 kt cases, transparency in. The 55 kt case, transparency out, is much worse than 55 kt, transparency in, because of poor dc gain in the closure. Overall, it seems that adding transparency is roughly equivalent to adding 2 - 3 kt of airspeed.

2. Glide Slope Control With a Throttle-to-Attitude Crossfeed

This form of flight path control is the antithesis of the one above. Where previously no airspeed regulation was exercised now we will examine the case of near ideal constraint of airspeed. The 'ideal' crossfeed used in this analysis is:

BLOCK DIAGRAM

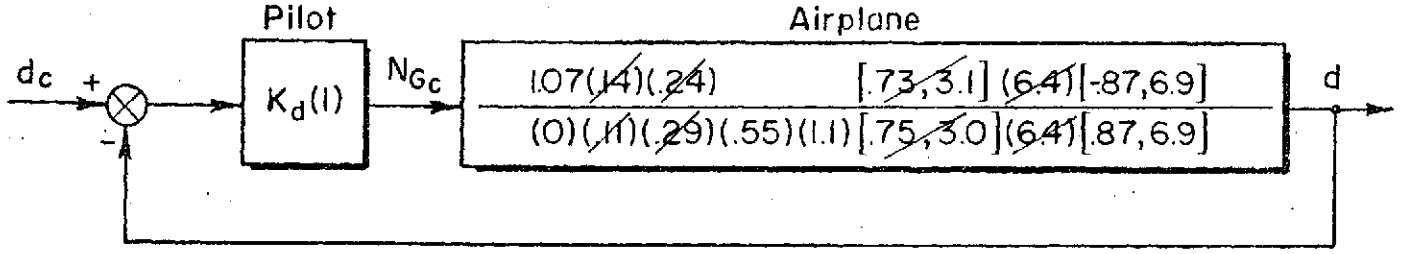

CLOSED LOOP DENOMINATOR

$\Delta' = [.99,.18][.56,.45](1.06)[.74,3.0](6.4)[.86,7.0]$

STEP RESPONSE

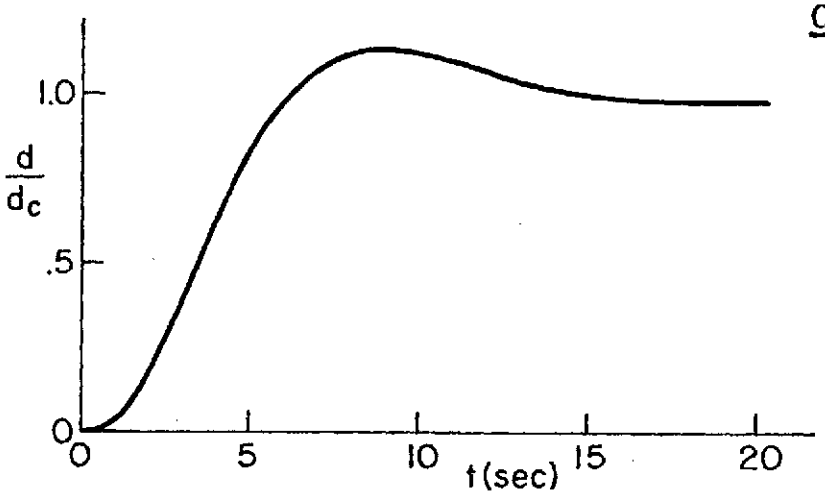

CLOSURE

Crossover .3rad/sec
Gain -14.16 dB = .196% rpm/ft
Phase Margin 53.8 deg
Period of Oscillation 17sec
Settling Time 4sec
ω_{180} = 1.05 rad/sec

ROOT LOCUS

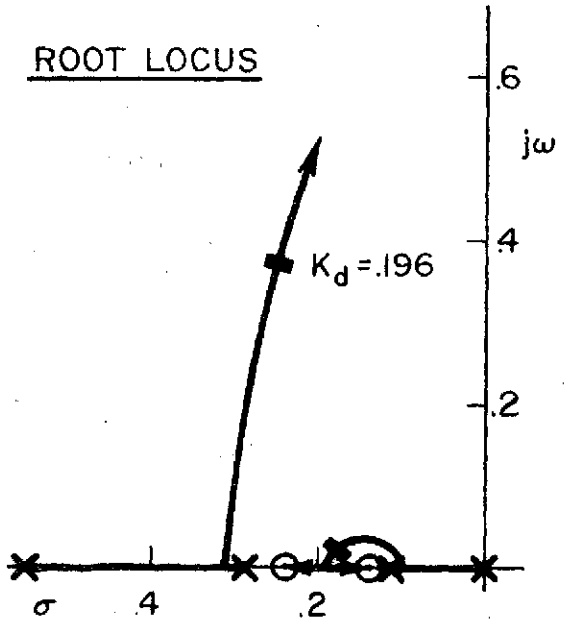

BODE

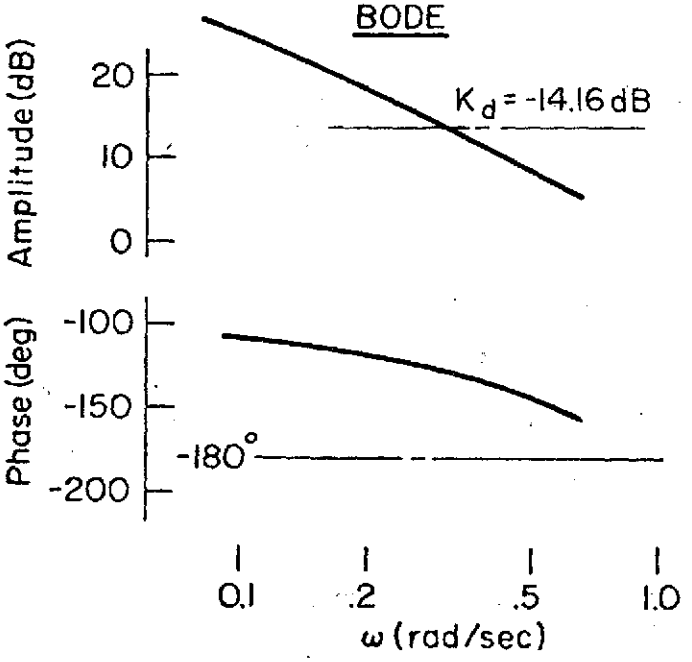

Figure B-3. Glide Slope Loop Closure, No Airspeed Regulation, Transparency In, 65 kt

BLOCK DIAGRAM

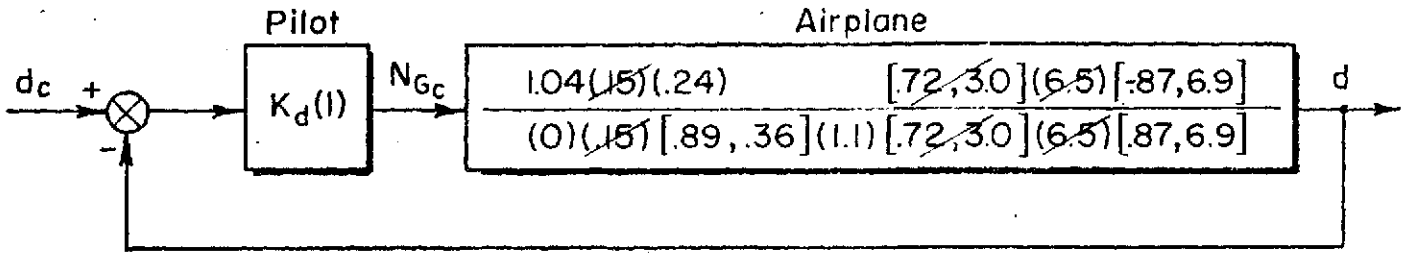

CLOSED LOOP DENOMINATOR

$$\Delta' = (.17)(.18)[.43,.43](1.08)[.72,3.0](6.5)[.86,7.0]$$

STEP RESPONSE

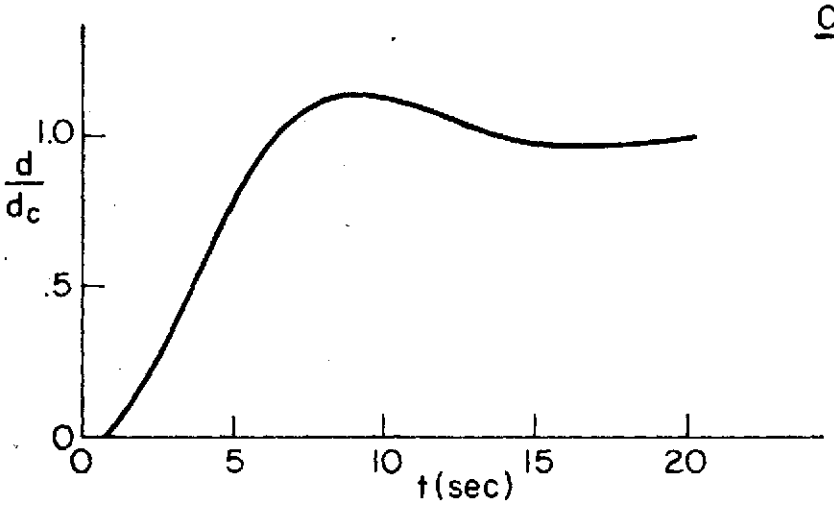

CLOSURE

Crossover .3 rad/sec
Gain -16.2 dB = .155 % rpm/ft
Phase Margin 54 deg
Period of Oscillation 16 sec
Settling Time 5.4 sec
ω_{180} = 0.91 rad/sec

ROOT LOCUS

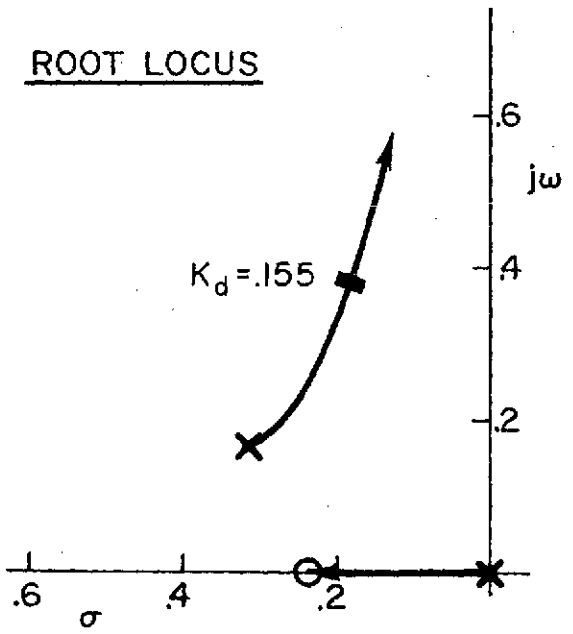

BODE

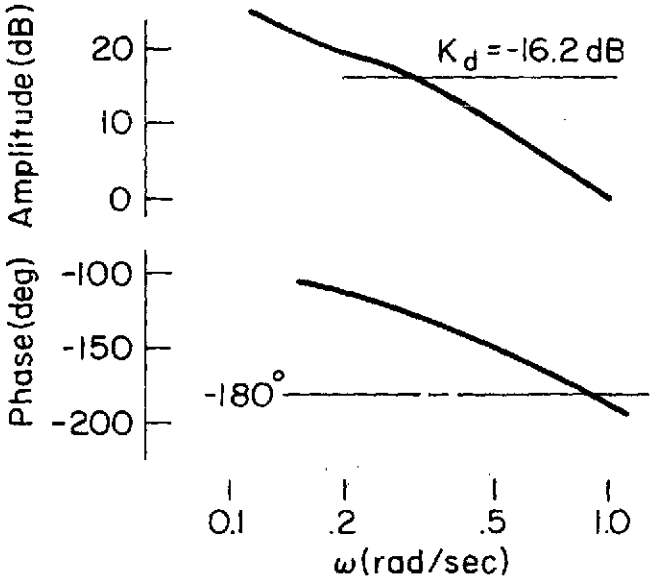

Figure B-4. Glide Slope Loop Closure, No Airspeed Regulation, Transparency In, 60 kt

BLOCK DIAGRAM

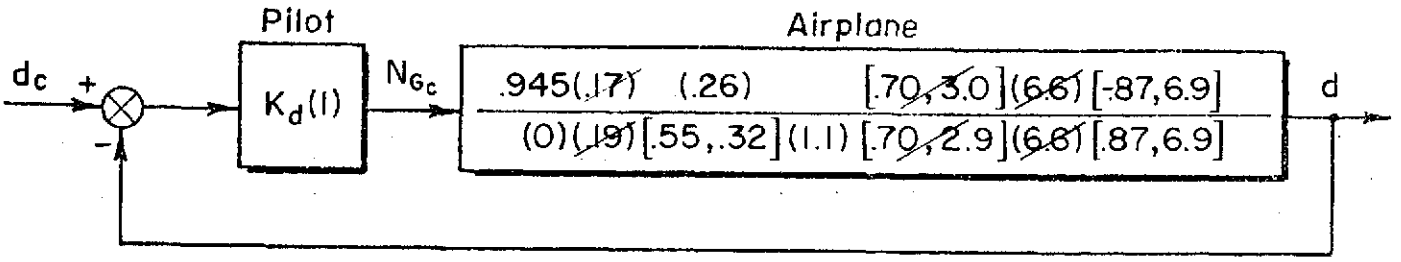

CLOSED LOOP DENOMINATOR

$\Delta' = (.12)(.20)[.24,.39](1.1)[.70,3.0](6.6)[.86,7.0]$

STEP RESPONSE

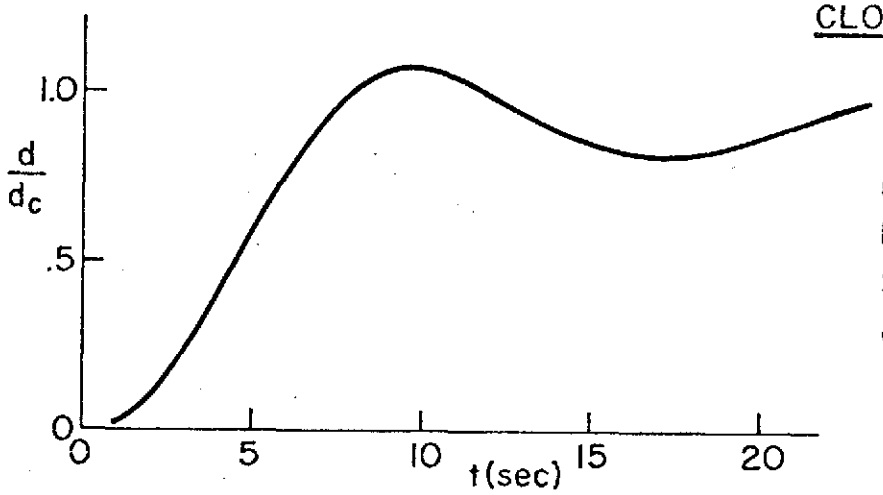

CLOSURE

Crossover .3 rad/sec
Gain -20.4dB = .095 %rpm/ft
Phase Margin 52 deg
Period of Oscillation 16.5 sec
Settling Time 10.5 sec
ω_{180} = 0.65 rad/sec

ROOT LOCUS

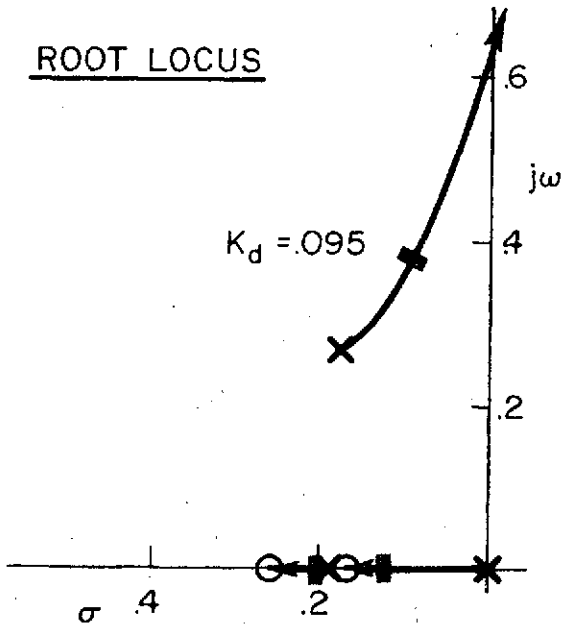

BODE

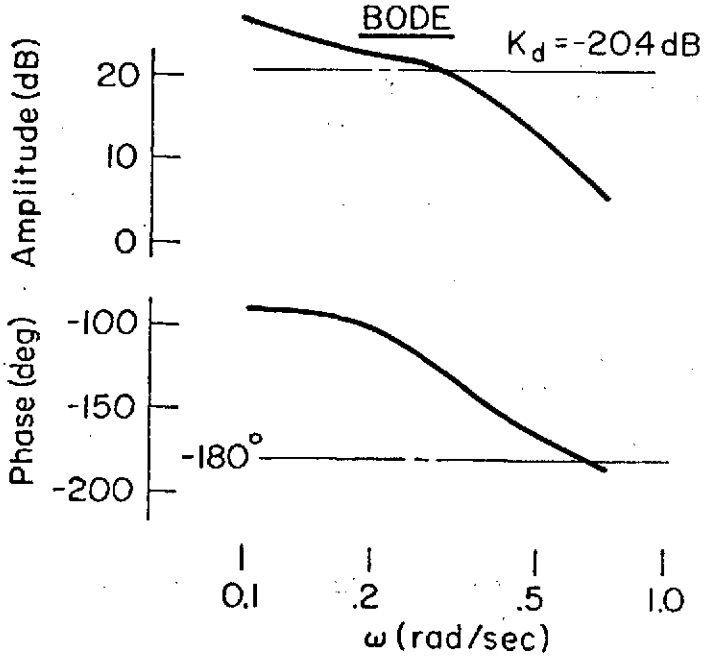

Figure B-5. Glide Slope Loop Closure, No Airspeed Regulation, Transparency In, 55 kt

BLOCK DIAGRAM

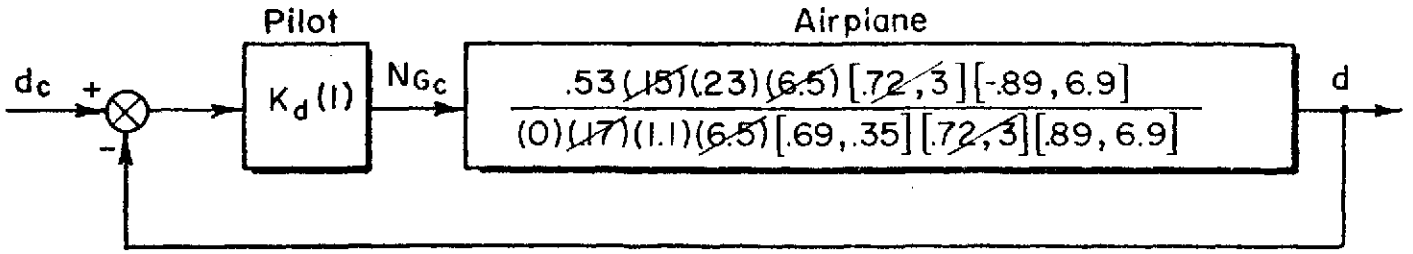

CLOSED LOOP DENOMINATOR

$$\Delta' = (.12)(.19)(1.09)(6.5)[.35,.44][.72,3][.86,7]$$

STEP RESPONSE

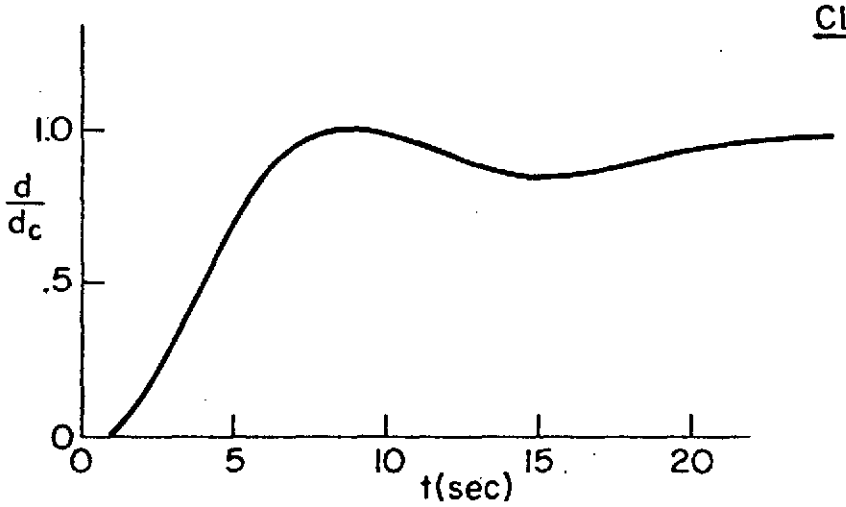

CLOSURE

Crossover .3 rad/sec
Gain .25 % rpm/ft
Phase Margin 52 deg
ω_{180} = .82 rad/sec

ROOT LOCUS

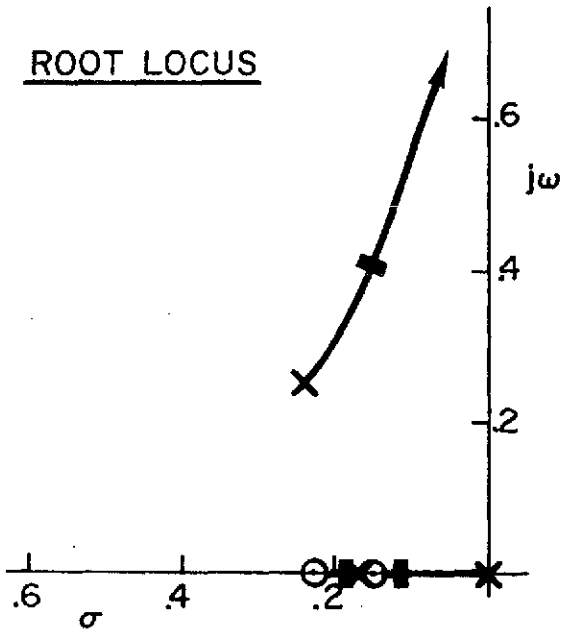

BODE

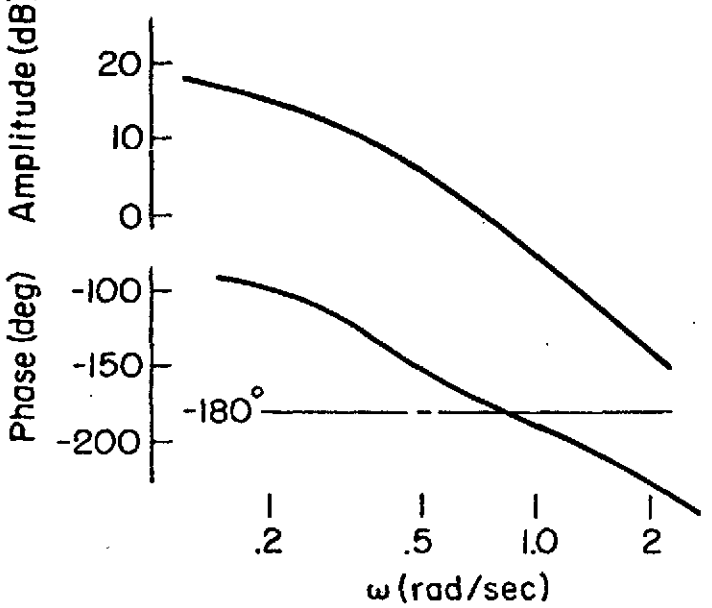

Figure B-6. Glide Slope Loop Closure, No Airspeed Regulation, Transparency Out, 60 kt

BLOCK DIAGRAM

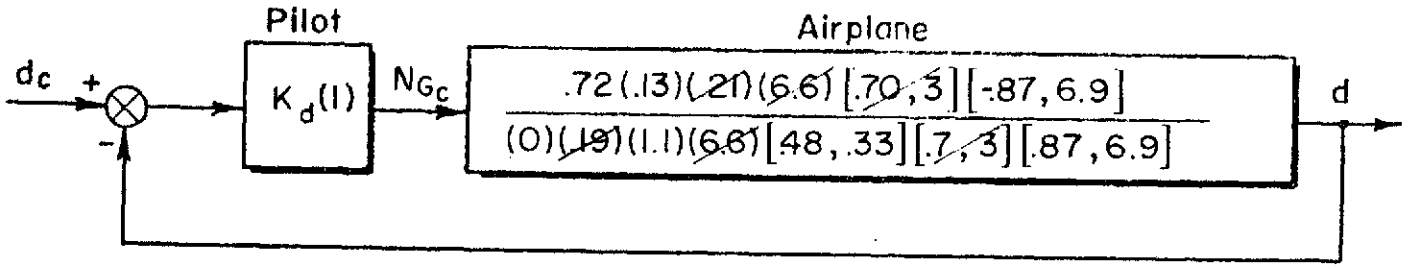

CLOSED LOOP DENOMINATOR

$\Delta' = (.07)(.19)(1.1)(6.6)[.25,.42][.70,3][.86,7]$

STEP RESPONSE

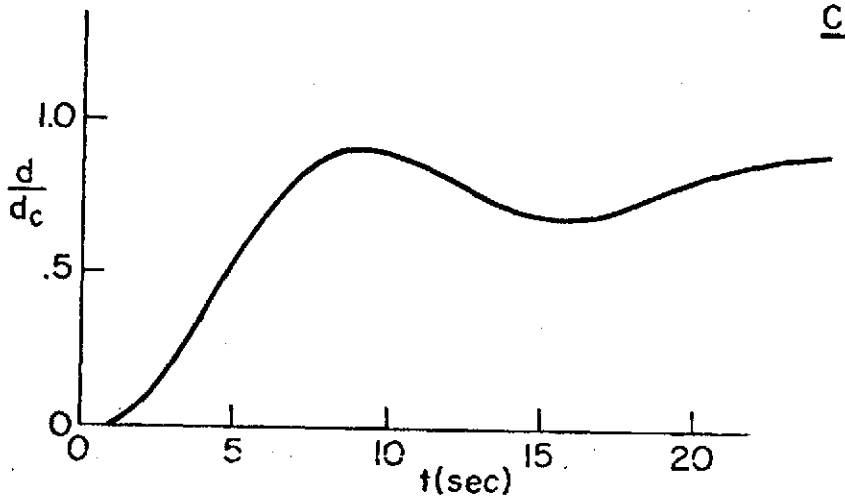

CLOSURE

Crossover .3 rad/sec
Gain .13 % rpm/ft
Phase Margin 67 deg
ω_{180} = .70 rad/sec

ROOT LOCUS

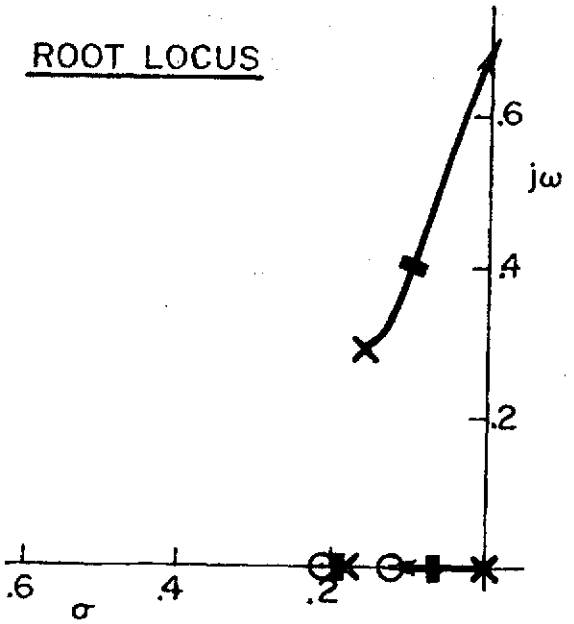

BODE

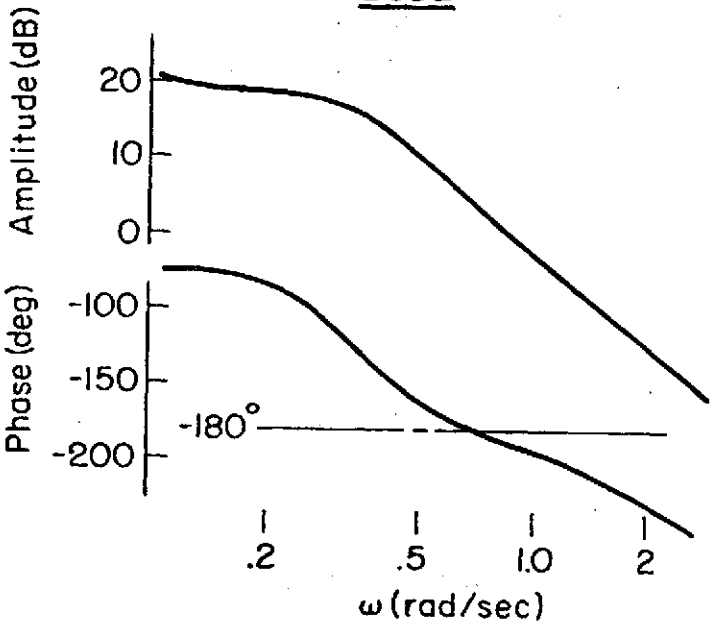

Figure B-7. Glide Slope Loop Closure, No Airspeed Regulation, Transparency Out, 55 kt

$$Y_x = \frac{N^u_{\delta_e} N^{\theta}_{N_G}}{N^u_{\delta_e}}$$

and

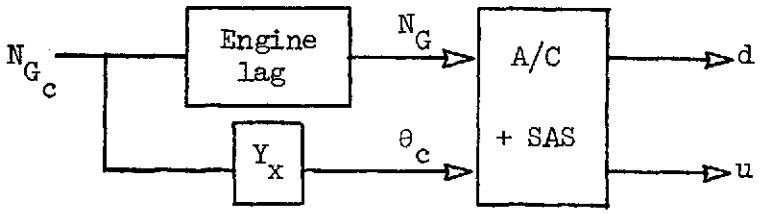

The Y_x crossfeed does not exactly cancel speed perturbations because of the lack of instantaneous attitude control (i.e. $\frac{\theta}{\theta_c}(s) \neq 1$) and engine lags (i.e. $\frac{N_G}{N_{G_c}}(s) \neq 1$). However the 'ideal' crossfeed is sufficiently good to indicate how flight path control characteristics are changed by good speed control. Also the form of the crossfeed tells us something about the difficulty involved in using it. If the crossfeed differs significantly from a simple gain then the pilot might find it too complicated to use. This leads us to also consider a simplified crossfeed consisting only of the dc gain of Y_x. If the simplified crossfeed gives a result similar to that of the ideal then we have an indication of how appropriate a crossfeed technique would be for a given configuration.

Figs. B-8 through B-12 show glide slope loop closures for varying approach speeds and transparency in and out. In general, the crossfeed improves glide slope control and reduces the effects of airspeed and transparency. With the crossfeed in, the effects of transparency are very small. The crossfeed effects on glide slope control show up most strongly in the neutral stability frequency, ω_{180}. The crossfeed always produces significant increase in this parameter.

The nature of the ideal crossfeeds used above is shown in Fig. B-13. The $\frac{\theta}{N_G}(t)$ required for a step throttle input is shown for each of the approach configurations. In all cases an initial nose up attitude is

BLOCK DIAGRAM

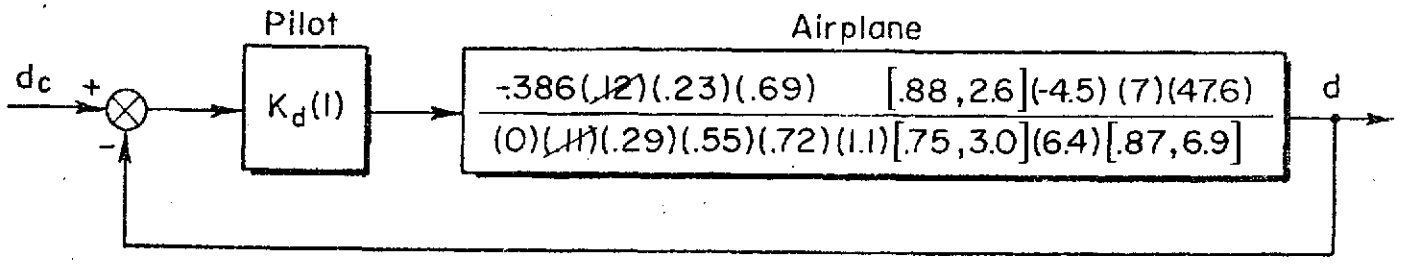

CLOSED LOOP DENOMINATOR

$\Delta' = (.13)(.18)[.64,.50](.7)(1.07)[.75,3.0](6.5)[.86,7.0]$

STEP RESPONSE

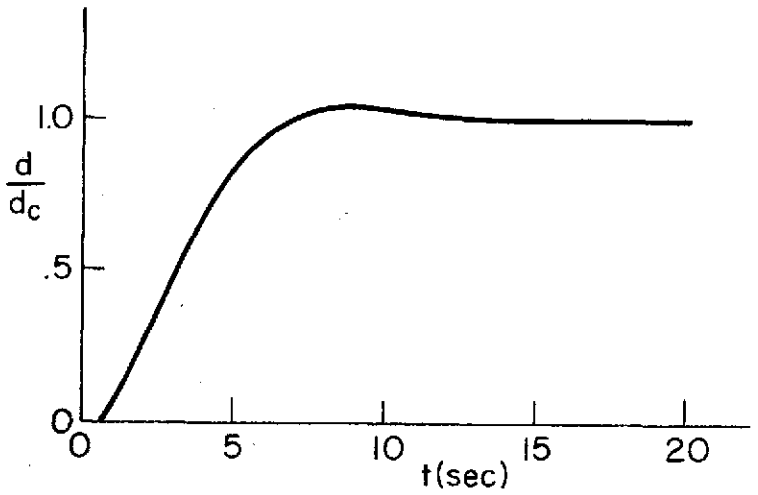

CLOSURE

Crossover .3 rad/sec
Gain -15.6 dB = .166 % rpm/ft
Phase Margin 63.9 deg
Period of Oscillation 16.4 sec
Settling Time 3.1 sec
ω_{180} = 1.4 rad/sec
Y_x = .32 (.52)/(.72)

ROOT LOCUS

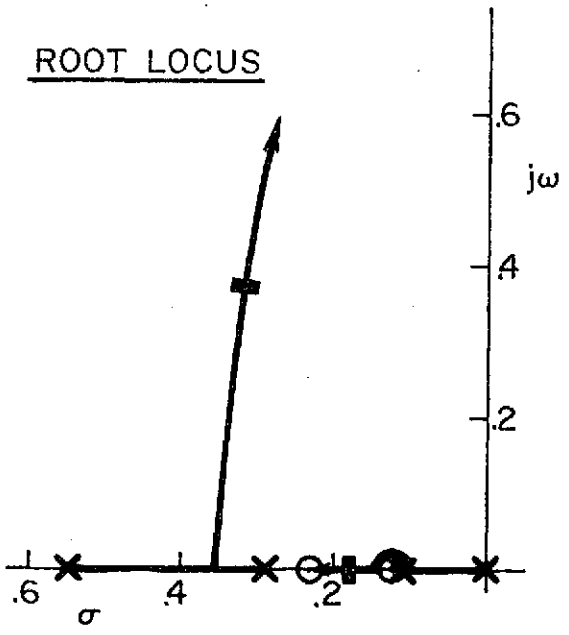

BODE

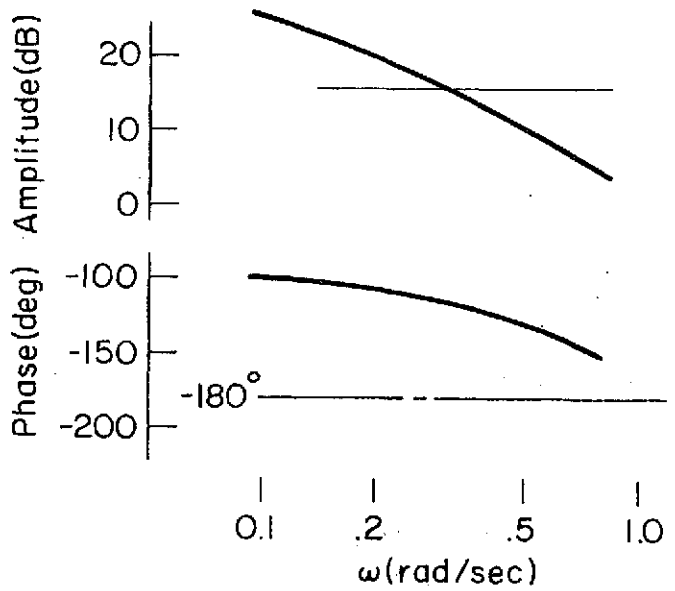

Figure B-8. Glide Slope Loop Closure, Ideal Crossfeed, Transparency In, 65 kt

BLOCK DIAGRAM

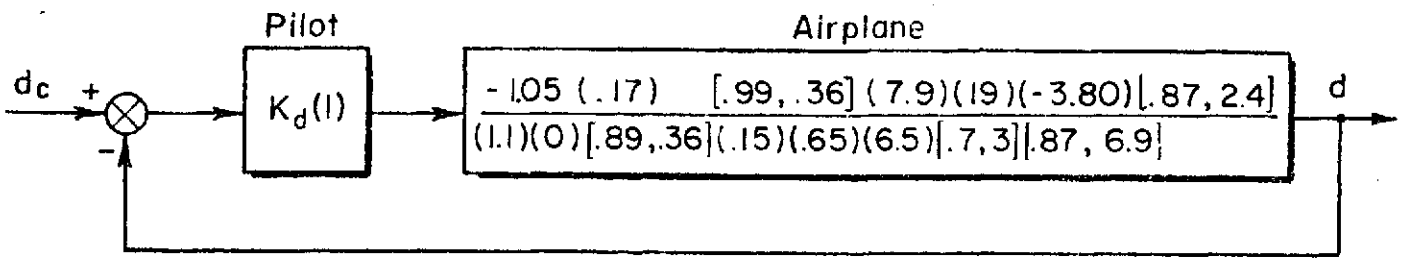

CLOSED LOOP DENOMINATOR

$\Delta' = [.99;\ .20][.57;\ .45](.52)(1.08)[.72;\ 2.9](6.6)[.86;\ 7.0]$

STEP RESPONSE

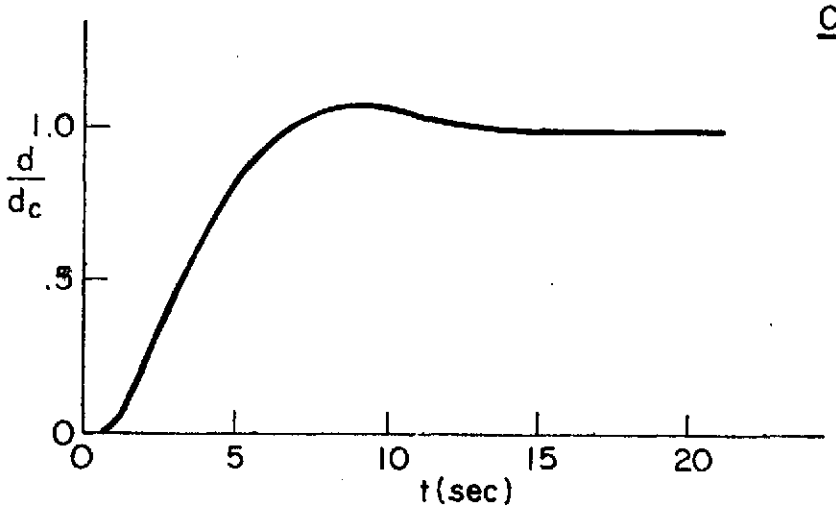

CLOSURE

Crossover .3 rad/sec

Gain −15.5 dB = .168% rpm/ft

Phase Margin 60 deg

$Y_x = .458\frac{(-.07)}{(.65)}$

$\omega_{180} = 1.5$ rad/sec

ROOT LOCUS

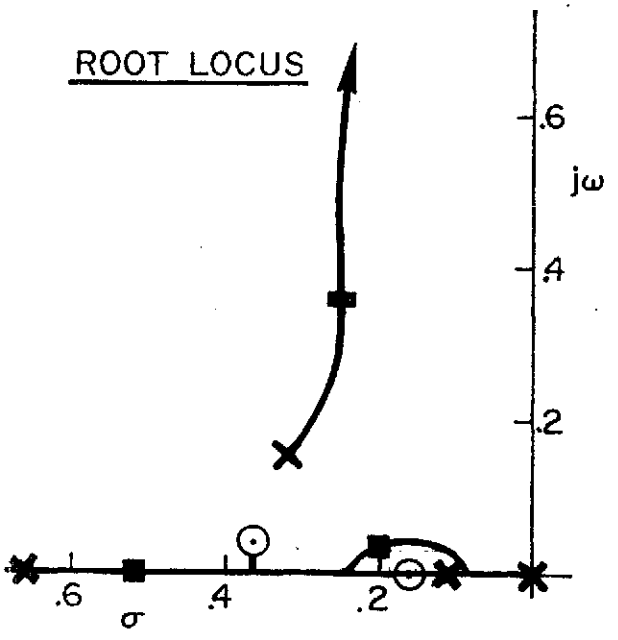

BODE

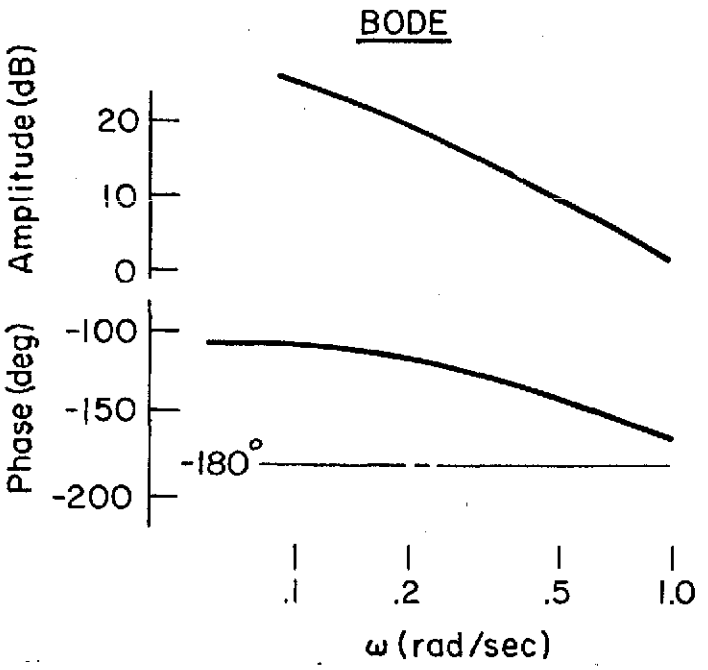

Figure B-9. Glide Slope Loop Closure, Ideal Crossfeed, Transparency In, 60 kt.

BLOCK DIAGRAM

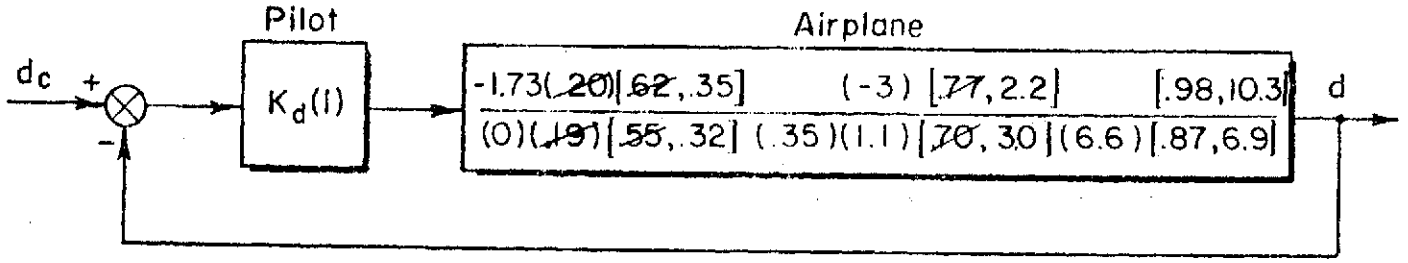

CLOSED LOOP DENOMINATOR

$\Delta' = (.20)[.72,.32](1.1)[.28,.35][.70,2.9](6.7)[.86,7.0]$

STEP RESPONSE

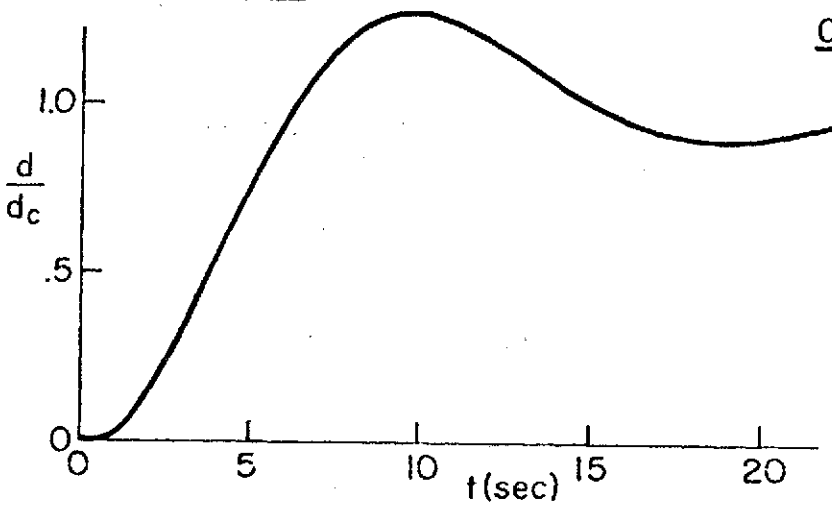

CLOSURE

Crossover .3 rad/sec

Gain −17.9 dB = .127 %rpm/ft

Phase Margin 39.3 deg

Period of Oscillation 18.5 sec

Settling Time 9.5 sec

ω_{180} = 1.04 rad/sec

$Y_x = .587\ \frac{(-.64)}{(.35)}$

ROOT LOCUS

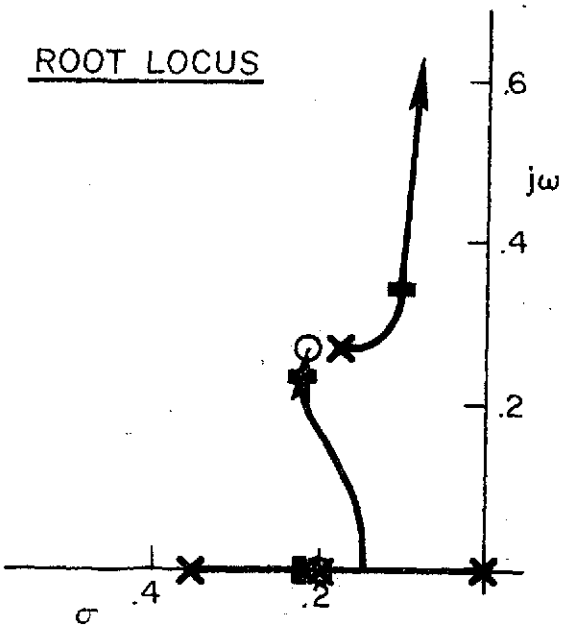

BODE

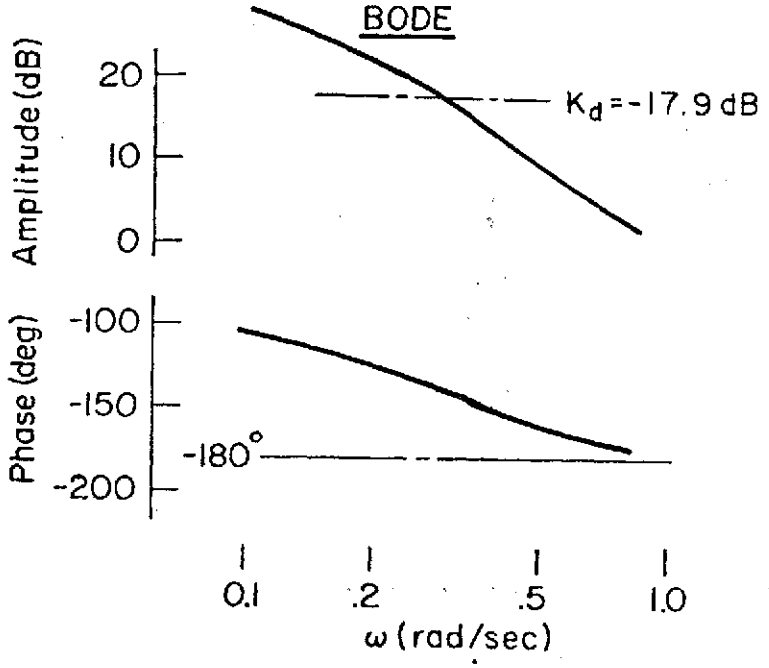

Figure B-10. Glide Slope Loop Closure, Ideal Crossfeed, Transparency In, 55 kt

BLOCK DIAGRAM

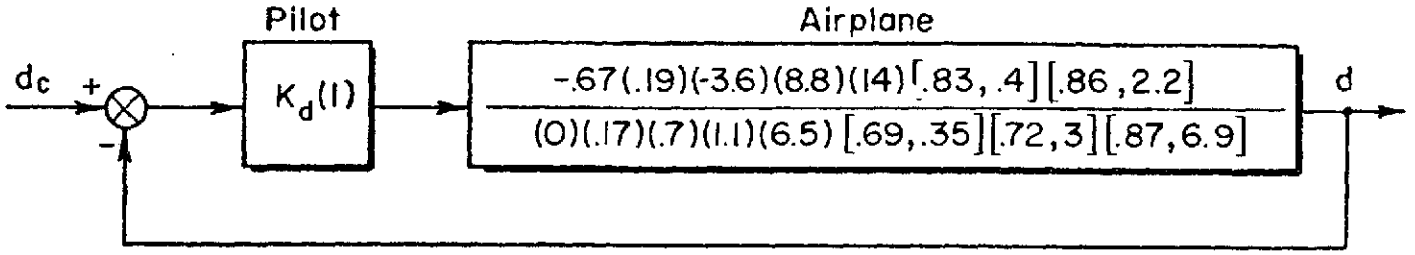

CLOSED LOOP DENOMINATOR

$$\Delta' = (.53)(1.1)(6.6)[.99,.24][.45,.44][.72,2.9][.86,7]$$

STEP RESPONSE

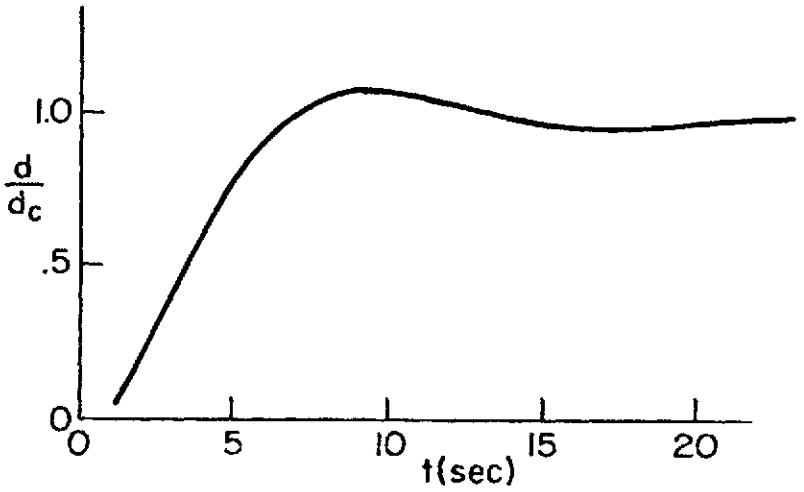

CLOSURE

Crossover .3 rad/sec
Gain .345 % rpm/ft
Phase Margin 57 deg
ω_{180} = 1.6 rad/sec
$Y_x = .264 \frac{(-73)}{(.70)}$

ROOT LOCUS

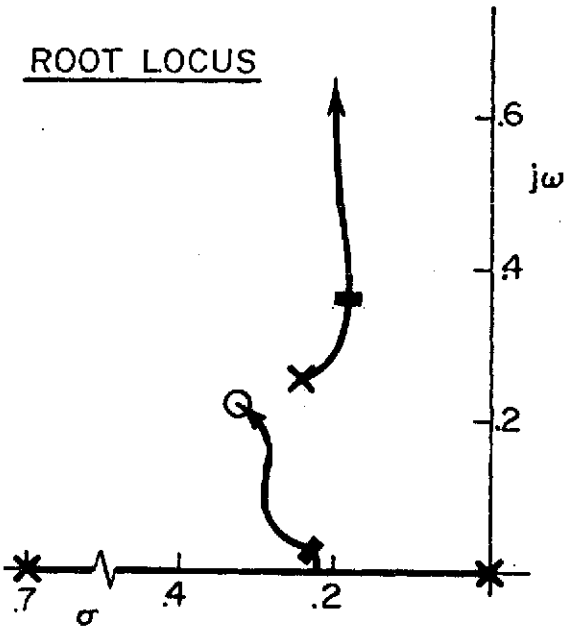

BODE

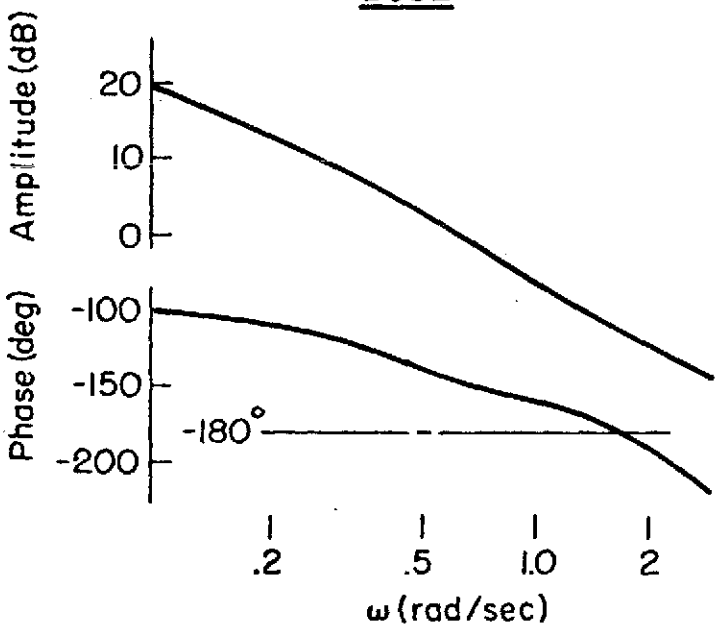

Figure B-11. Glide Slope Loop Closure, Ideal Crossfeed, Transparency Out, 60 kt

BLOCK DIAGRAM

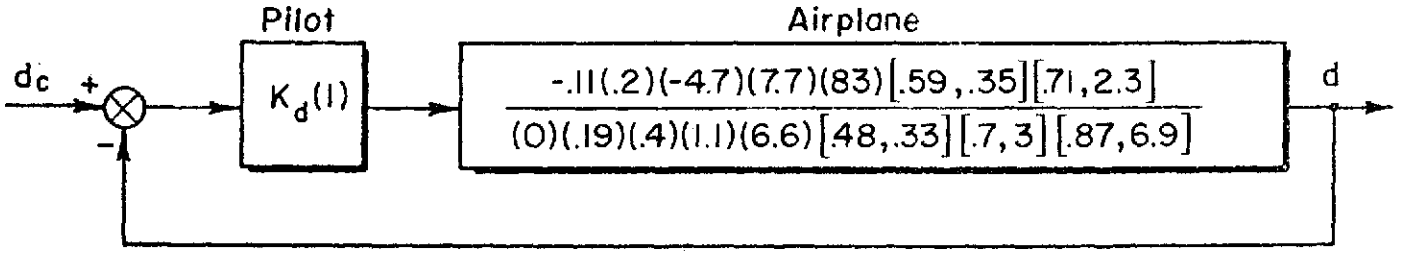

CLOSED LOOP DENOMINATOR

$\Delta = (.2)(1.1)(6.7)[.76,.32][.27,.36][.69,2.9][.86,7]$

STEP RESPONSE

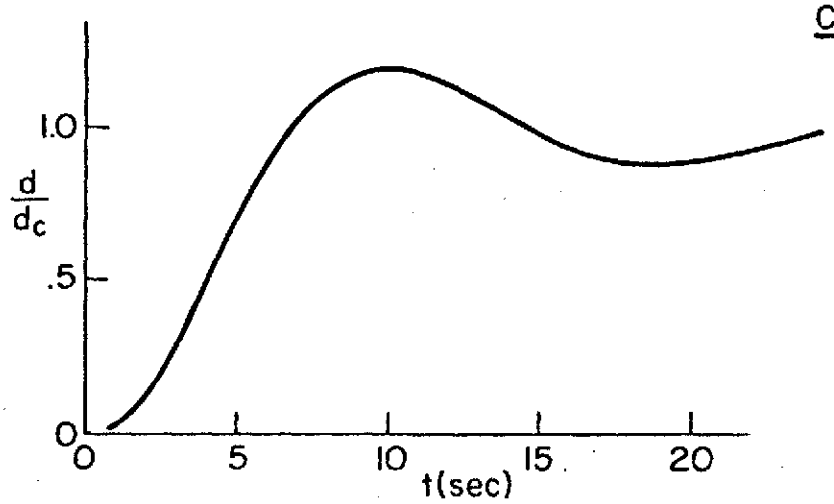

CLOSURE

Crossover .3rad/sec
Gain .186 % rpm/ft
Phase Margin 43 deg
ω_{180} = 1.0 rad/sec
$Y_x = .180 \frac{(-2.67)}{(.4)}$

ROOT LOCUS

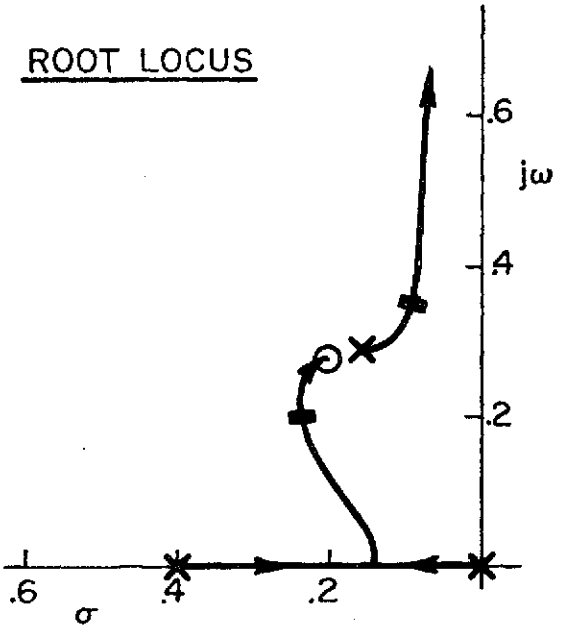

BODE

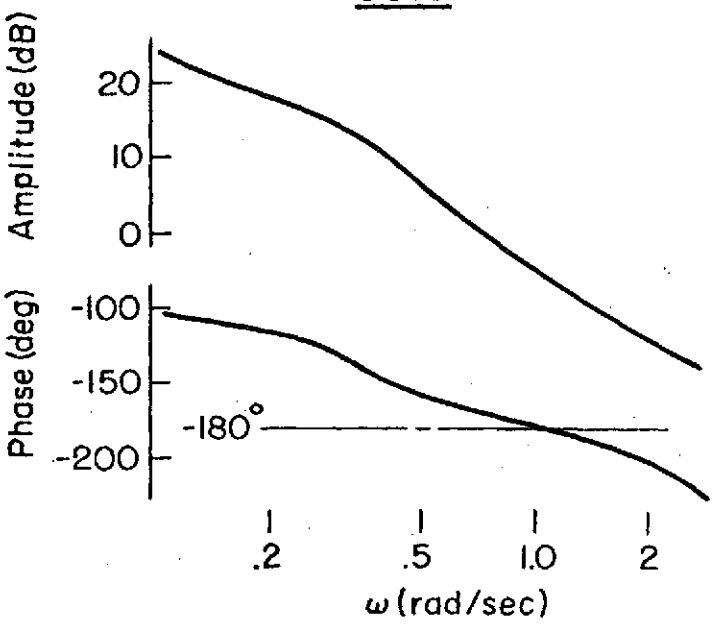

Figure B-12. Glide Slope Loop Closure, Ideal Crossfeed, Transparency Out, 55 kt

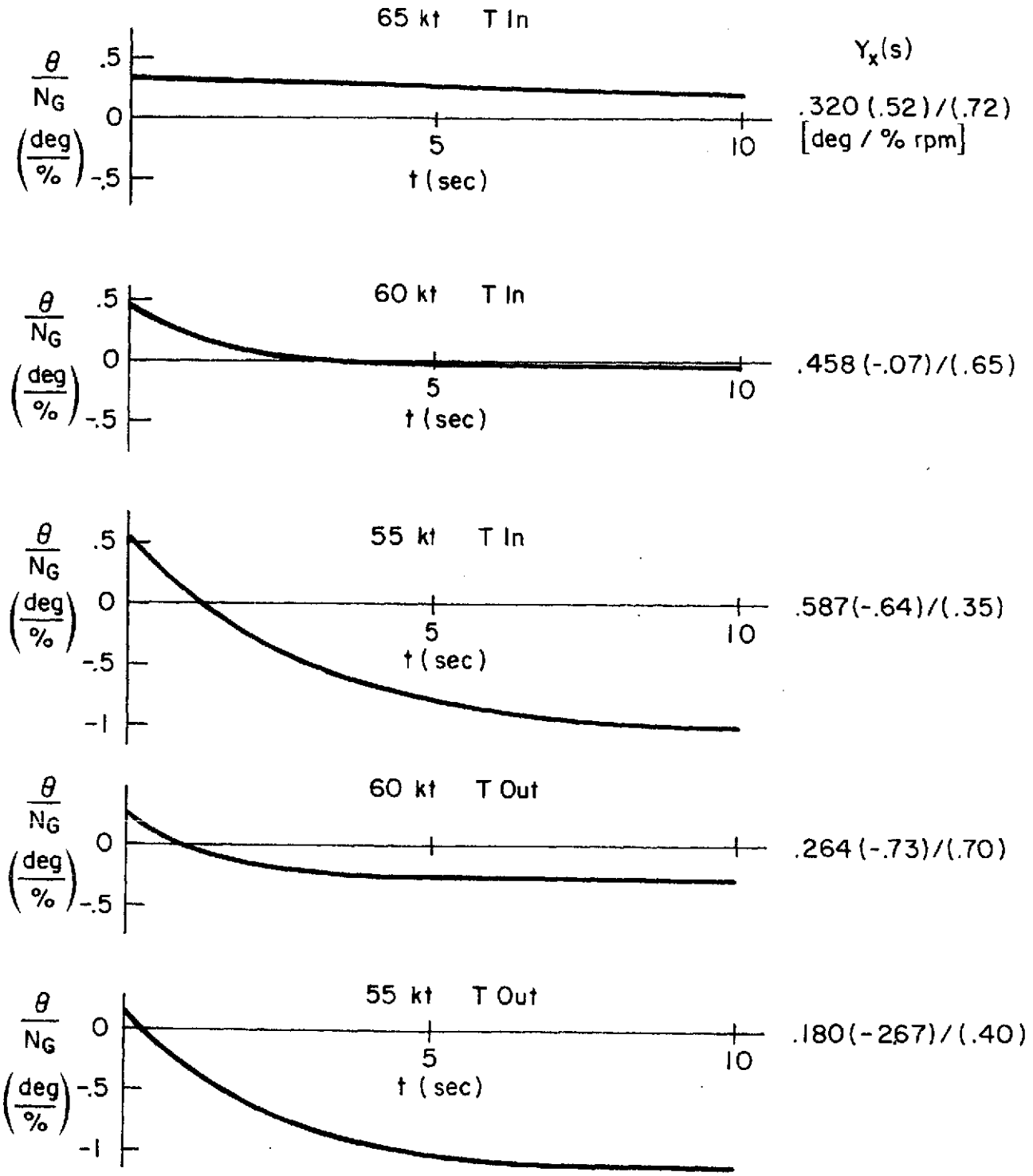

Figure B-13. Ideal Attitude Crossfeed Due to Throttle Step

required for a power increase. However, depending upon the approach speed, some or all of the initial attitude change must be taken out. At 65 kt the crossfeed is nearly a simple gain, but at 55 kt the pilot must initially pitch up then down. The latter is clearly a more difficult piloting technique to use. The washed-out crossfeed (V = 60 kt, T = 12 deg) is probably at or beyond pilot capabilities. The crossfeeds requiring attitude reversals are most likely unrealistic for a pilot to do.

Note that the crossfeeds for transparency out are more difficult than for transparency in. Therefore the pilots should still prefer the transparency in configuration.

Because of the complexity of most of the ideal crossfeeds, the use of a simplified crossfeed was examined. The simplified crossfeed cases shown in Figs. B-14 through B-17 consist of a Y_x equal to the dc gain of the ideal crossfeed. The result is degraded closed loop glide slope response (lower damping) than with the ideal crossfeed and becoming worse with decreasing approach speed. Thus difficulty in generating the ideal crossfeed is accompanied by the inadequacy of a simplified crossfeed.

3. Glide Slope Control in the Presence of Closed Loop Airspeed Control

The third control technique to be analyzed is the use of a $u \longrightarrow \theta$ feedback loop along with the $d \longrightarrow N_G$ loop. This is perhaps the model which most closely coincides with the technique actually used by the pilots in this simulator experiment. The loop structure assumed in the analysis consists of a speed feedback through attitude with a crossover frequency of .5 rad/sec. A pure gain was assumed initially. However, closed loop control of airspeed in each case did require pilot compensation. If a pure gain were used ($Y_{p_u} = K_u$) there would be insufficient dc gain in the feedback. This would show up as a closed loop u/u_c step response that had a steady state value of something less than unity. In order to fix this the pilot must use integral feedback as well as proportional. Therefore, the airspeed control block diagram would appear as:

BLOCK DIAGRAM

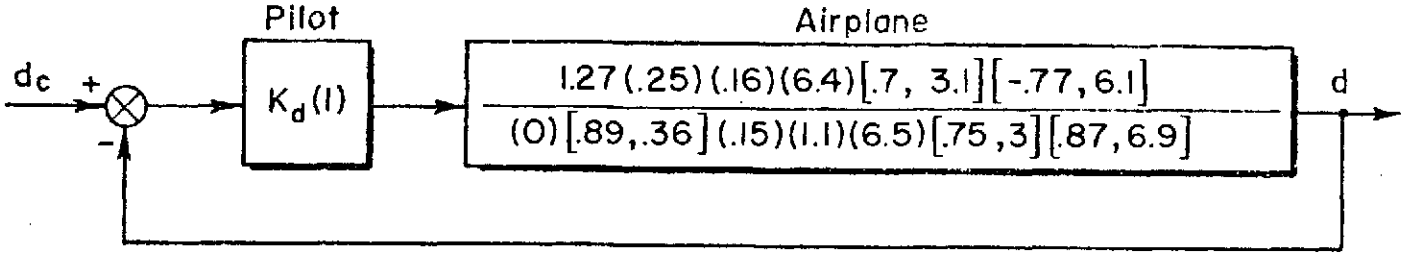

CLOSED LOOP DENOMINATOR

$$\Delta' = (1.1)(6.5)[.998,.18][.42,.43][.72,3][.86,6.9]$$

STEP RESPONSE

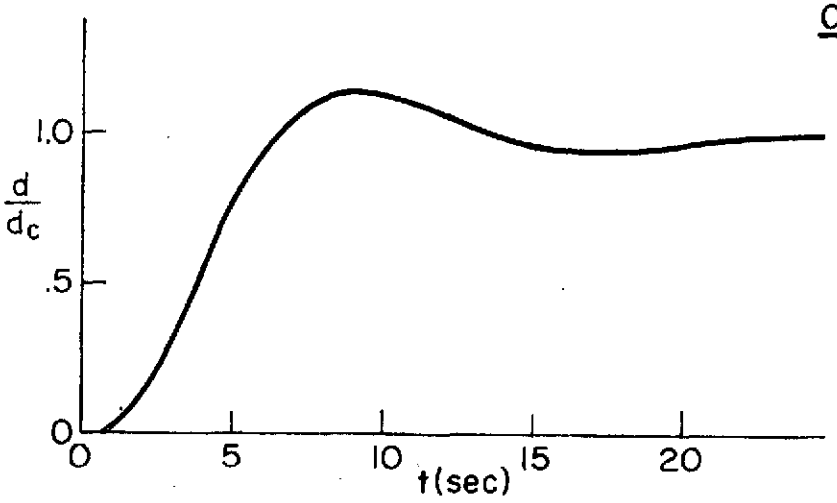

CLOSURE

Crossover .30 rad/sec
Gain -16.1dB = .157 % rpm/ft
Phase Margin 52 deg
ω_{180} = .89 rad/sec
Y_x = .049 deg/% rpm

ROOT LOCUS

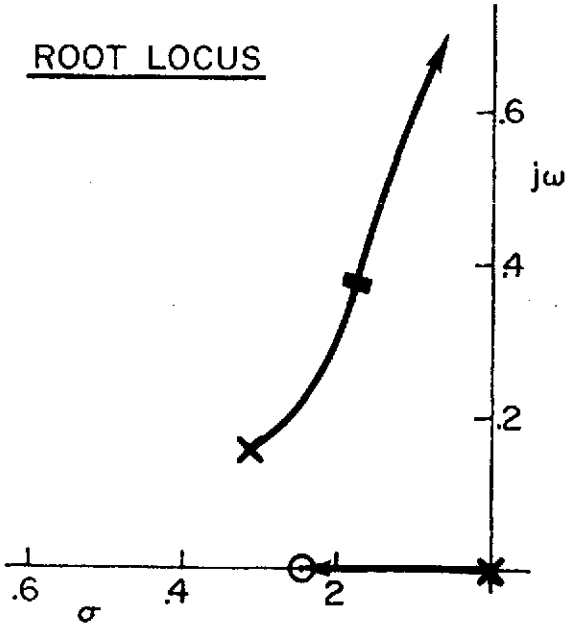

BODE

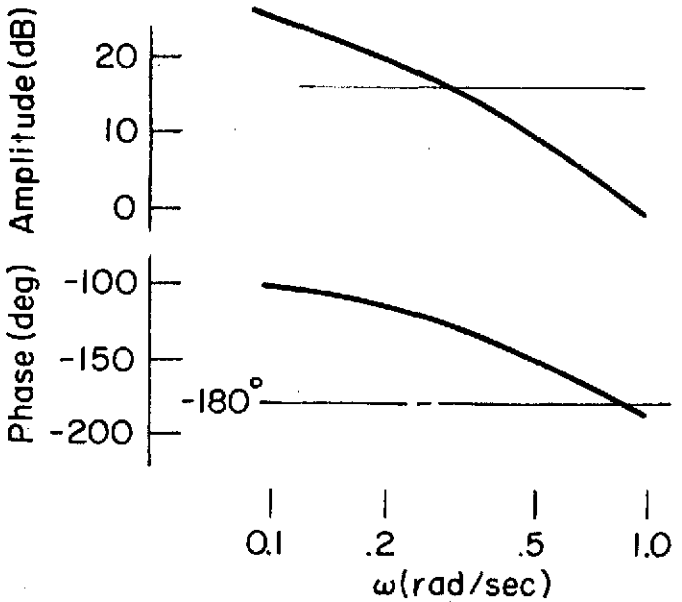

Figure B-14. Glide Slope Loop Closure, Simplified Crossfeed, Transparency In, 60 kt

BLOCK DIAGRAM

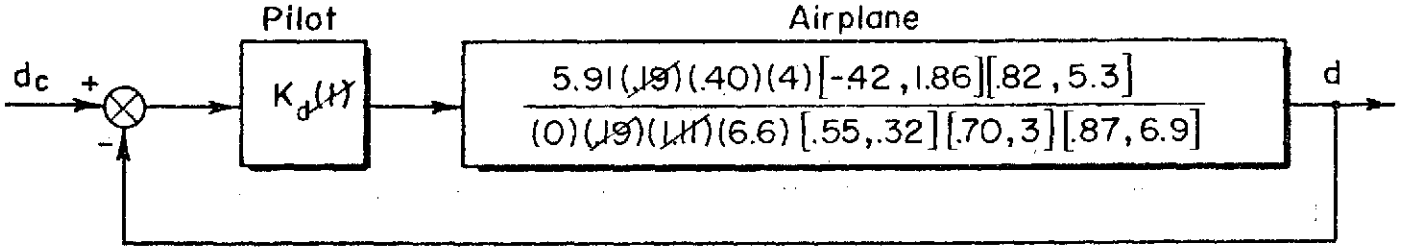

CLOSED LOOP DENOMINATOR

$\Delta' = (1.1)(6.5)[.99,.20][.16,.36][.71,3][.87,6.97]$

STEP RESPONSE

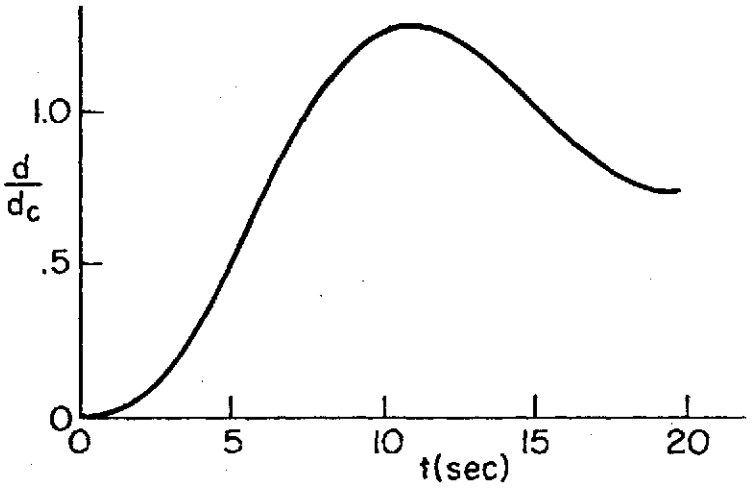

CLOSURE

Crossover .30 rad/sec

Gain .087 % rpm/ft

Phase Margin 32.5 deg

ω_{180} = .44 rad/sec

Y_x = -1.09 deg/% rpm

ROOT LOCUS

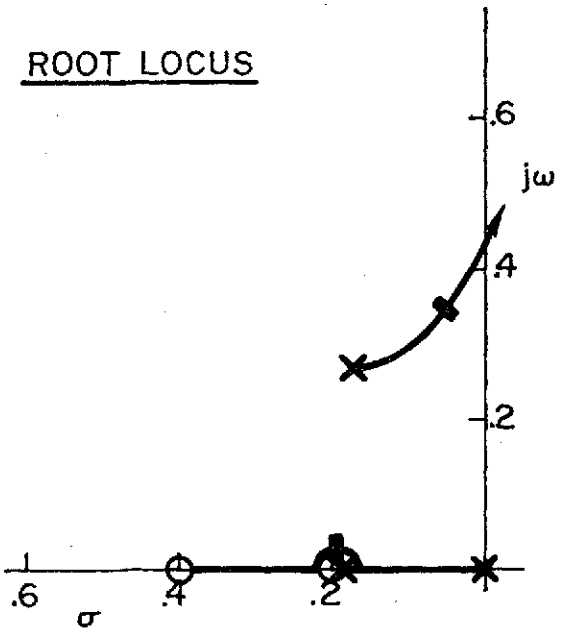

BODE

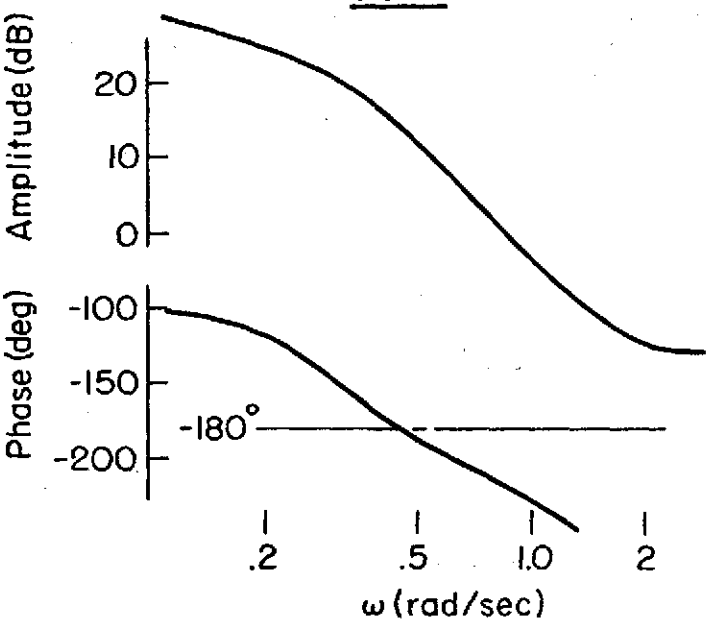

Figure B-15. Glide Slope Loop Closure, Simplified Crossfeed, Transparency In, 55 kt

BLOCK DIAGRAM

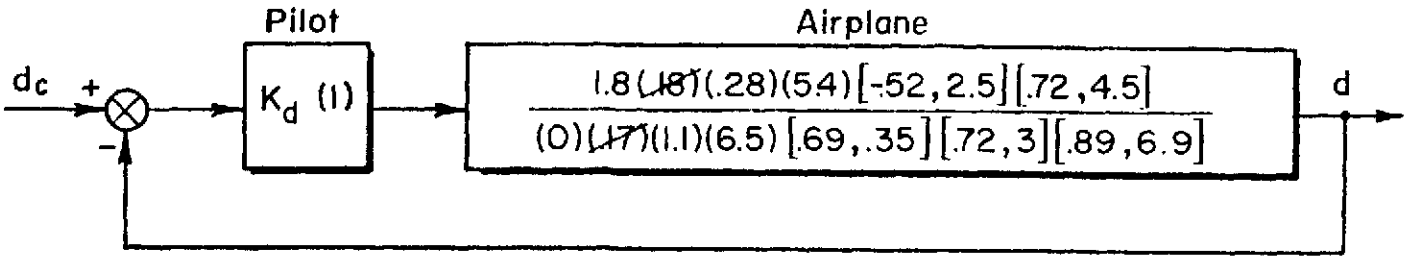

CLOSED LOOP DENOMINATOR

$$\Delta' = (1.1)(6.5)[.99, .18][.27, .40][.72, 3.1][.86, 7]$$

STEP RESPONSE

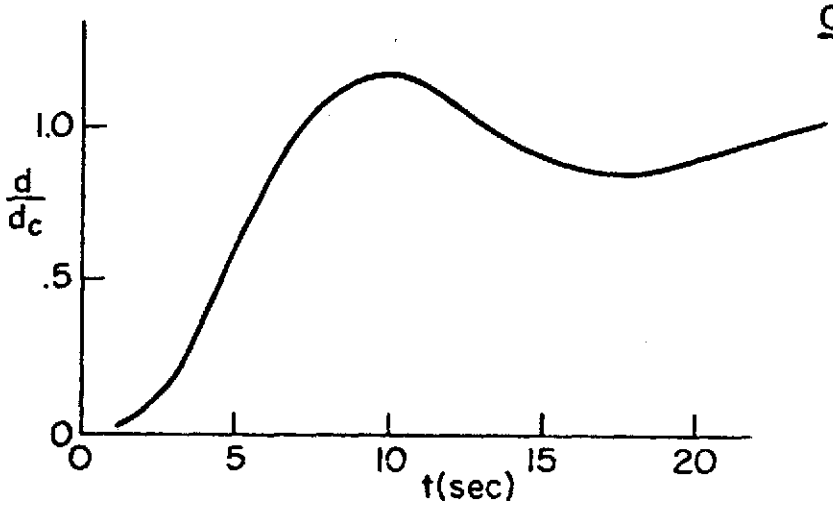

CLOSURE

Crossover .3 rad/sec
Gain .284 % rpm/ft
Phase Margin 46 deg
ω_{180} = .6 rad/sec
Y_x = -.277 deg/%

ROOT LOCUS

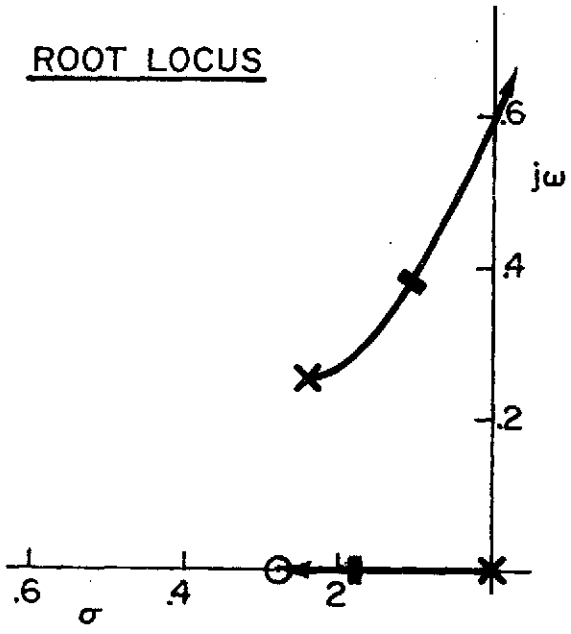

BODE

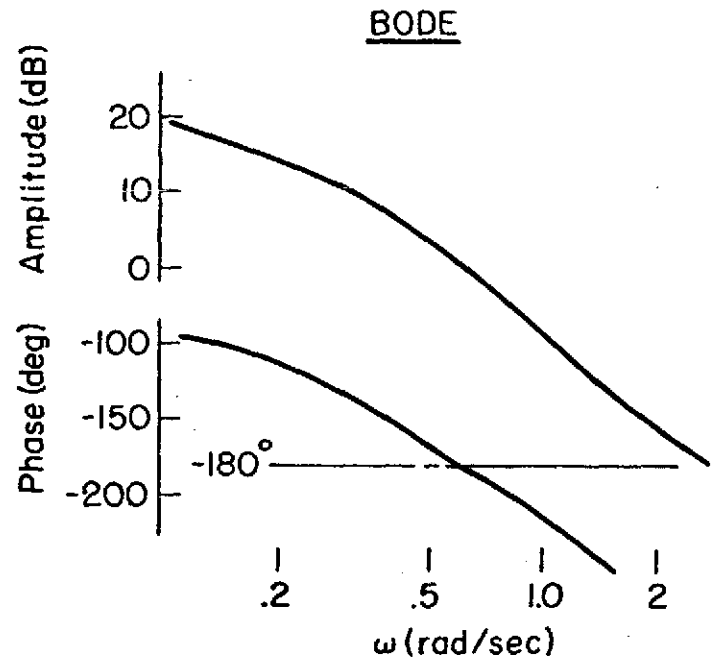

Figure B-16. Glide Slope Loop Closure, Simplified Crossfeed, Transparency Out, 60 kt

C-3

BLOCK DIAGRAM

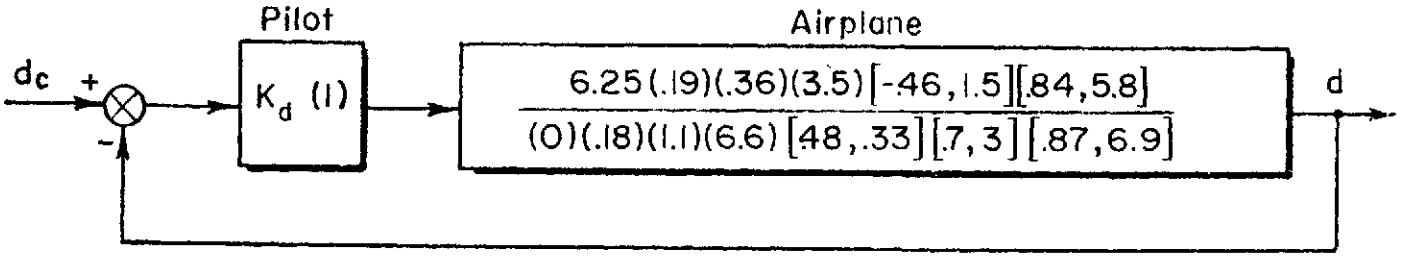

CLOSED LOOP DENOMINATOR

$\Delta = (1.1)(6.5)[.99,.19][.082,.38][.71,3.1][.86,7]$

STEP RESPONSE

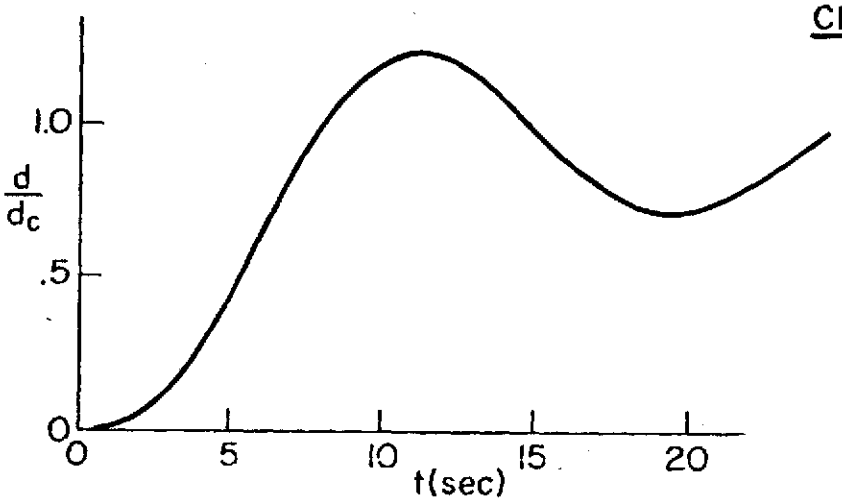

CLOSURE

Crossover .3 rad/sec
Gain .120 % rpm/ft
Phase Margin 35 deg
ω_{180} = .43 deg/sec
Y_x = -1.2 deg/%

ROOT LOCUS

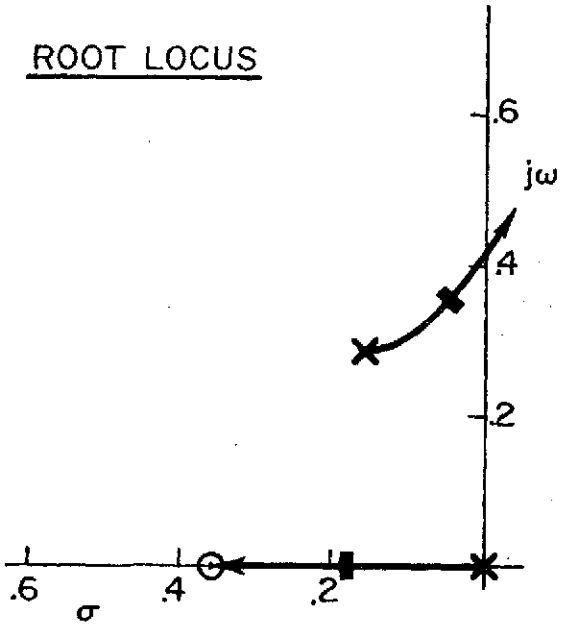

BODE

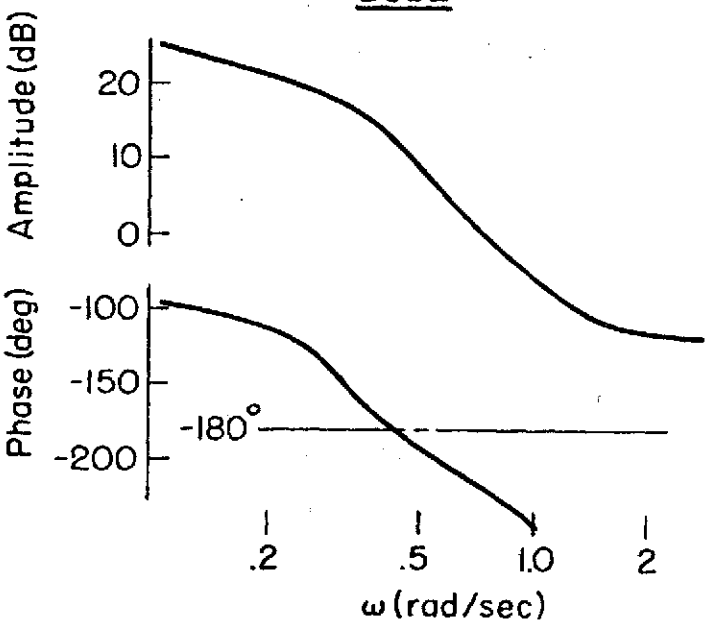

Figure B-17. Glide Slope Loop Closure, Simplified Crossfeed, Transparency Out, 55 kt

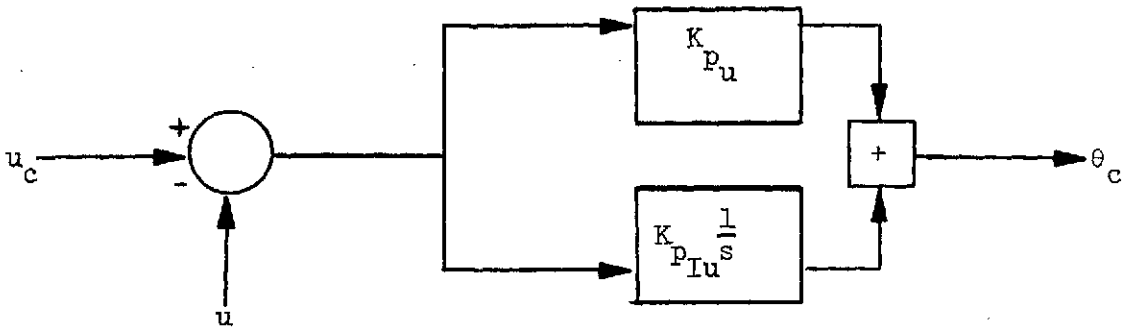

$$\text{and} \quad K_{p_u} + K_{p_{Iu}} \frac{1}{s} = \frac{K_{p_u}\left(s + \frac{K_{p_{Iu}}}{K_{p_u}}\right)}{s}$$

In all cases the value $K_{p_{Iu}}/K_{p_u}$ = .1 rad/sec was sufficient to obtain adequate results.

Figs. B-18 through B-27 show the loop closures for each case including both the airspeed and glide slope loops. Contrary to the previous control techniques, decreasing airspeed is not especially significant to degradation of the glide slope control. Rather, glide slope control characteristics are relatively constant with V_{APP}. The use of transparency does have a beneficial effect in terms of better damping. This is true in both 60 kt and 55 kt cases.

Thus, as approach speed is reduced good glide slope control becomes more dependent on airspeed regulation. This raises the pilot workload to maintain good glide slope tracking performance. Furthermore, the transparency in configuration has better glide slope control with or without airspeed regulation.

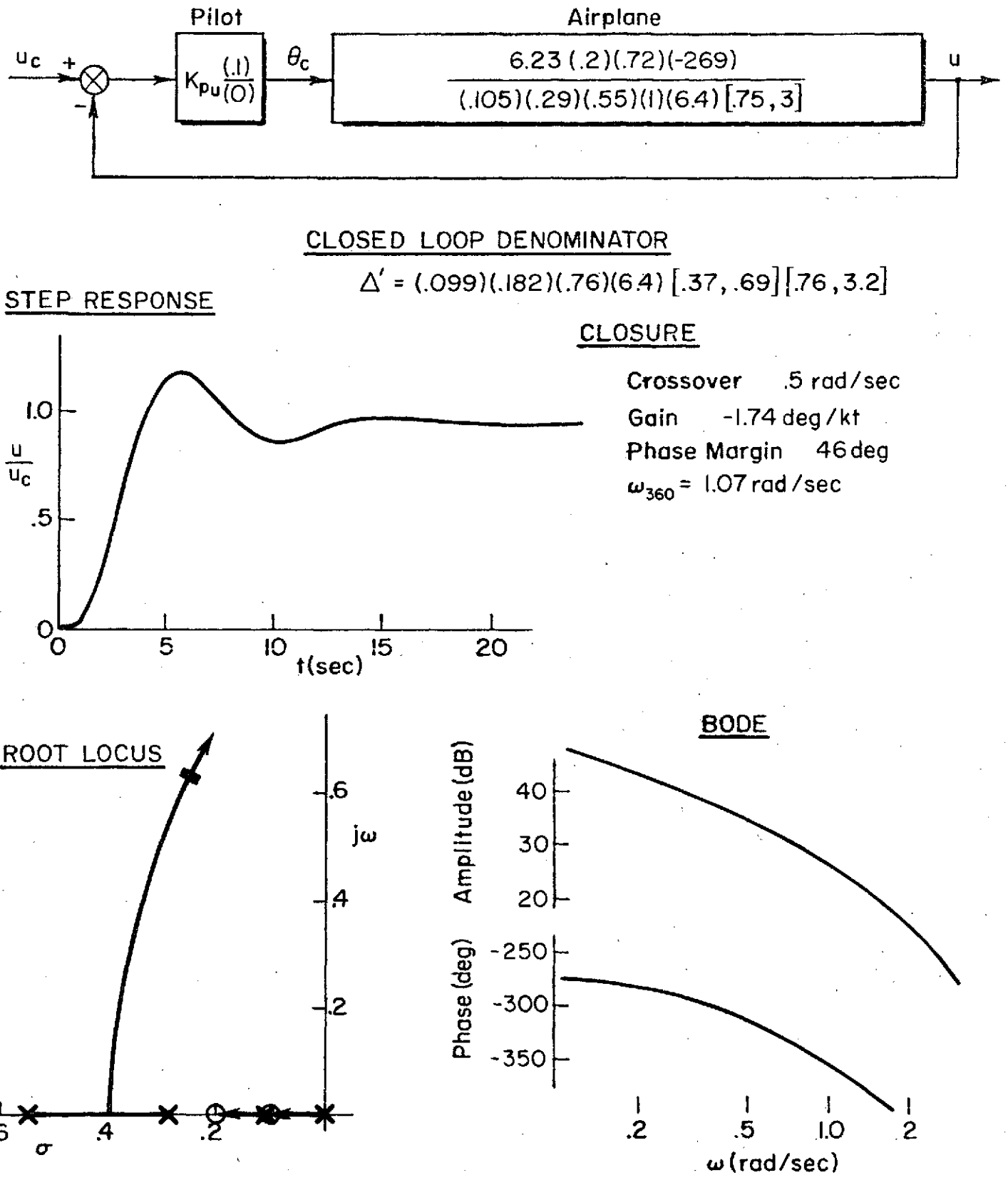

Figure B-18. Airspeed Loop Closure, Transparency In, 65 kt

BLOCK DIAGRAM

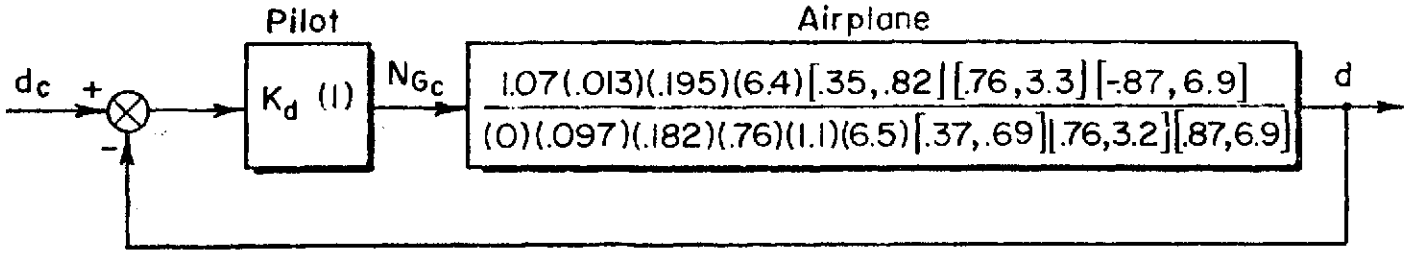

CLOSED LOOP DENOMINATOR

$\Delta' = (.091)(.204)(1.05)(6.5)[.70,.56][.35,.59][.76,3.2][.86,7]$

STEP RESPONSE

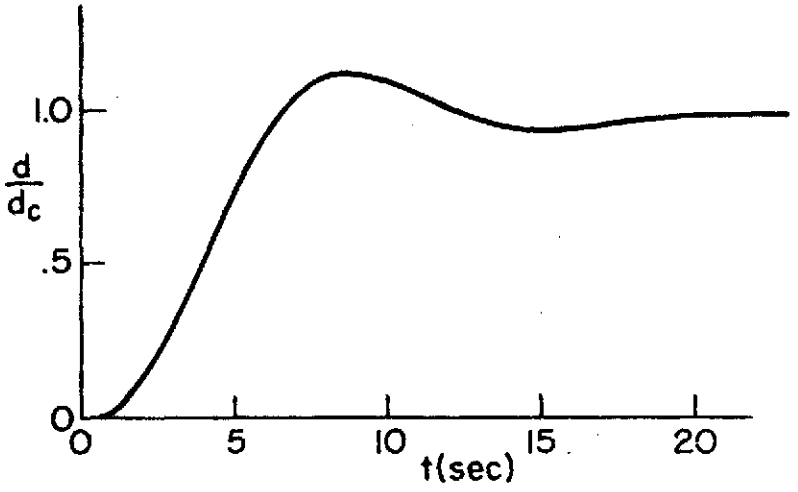

CLOSURE

Crossover .5 rad/sec

Gain .163 % rpm/ft

Phase Margin 55 deg

$\omega_{180} = .74$ rad/sec

$Y_{p_u} = -1.74 \frac{(1)}{(0)}$ deg/kt

$\omega_u = .5$ rad/sec

ROOT LOCUS

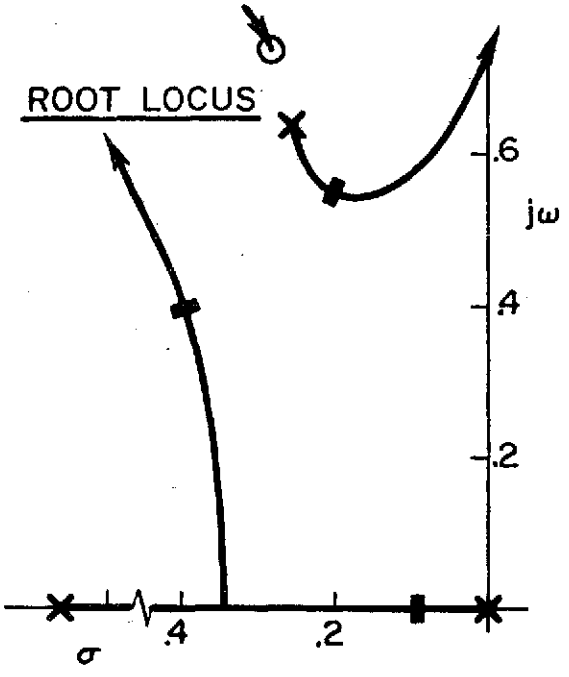

BODE

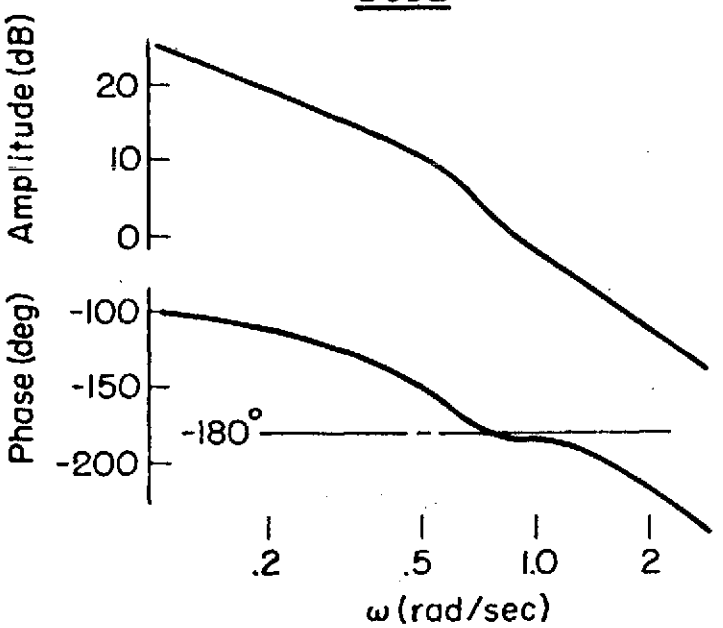

Figure B-19. Glide Slope Loop Closure, Transparency In, 65 kt

BLOCK DIAGRAM

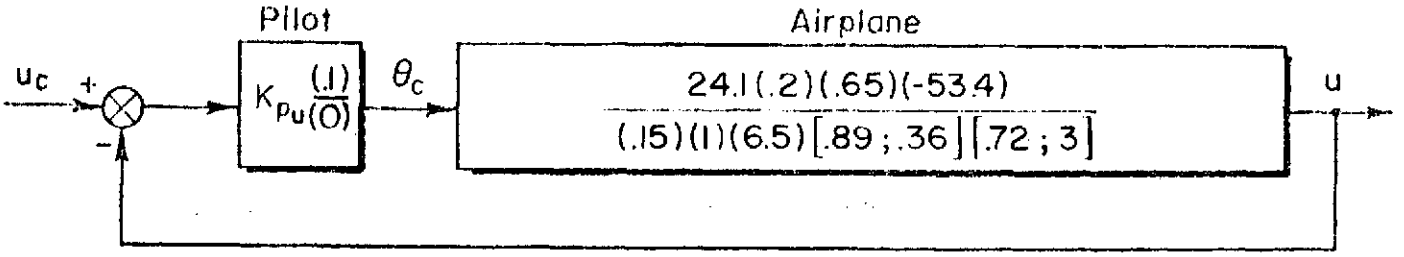

CLOSED LOOP DENOMINATOR

$\Delta = (.088)(.186)(.74)(6.5)[.33;.65][.74,3.15]$

STEP RESPONSE

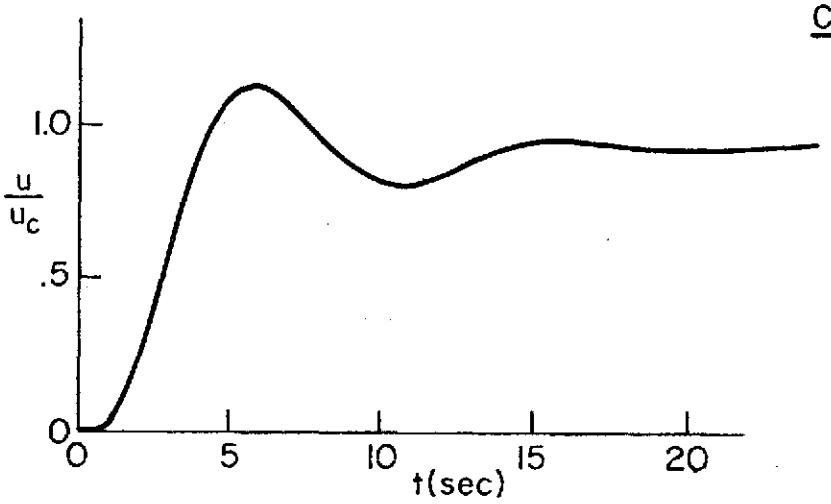

CLOSURE

Crossover .5 rad/sec

Gain .020 rad/fps = -1.94 deg/kt

Phase Margin 45 deg

ω_{360} = 1.01 rad/sec

ROOT LOCUS

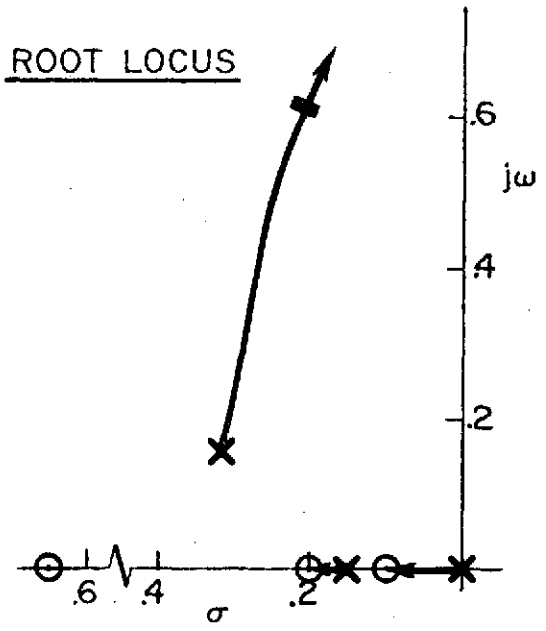

BODE

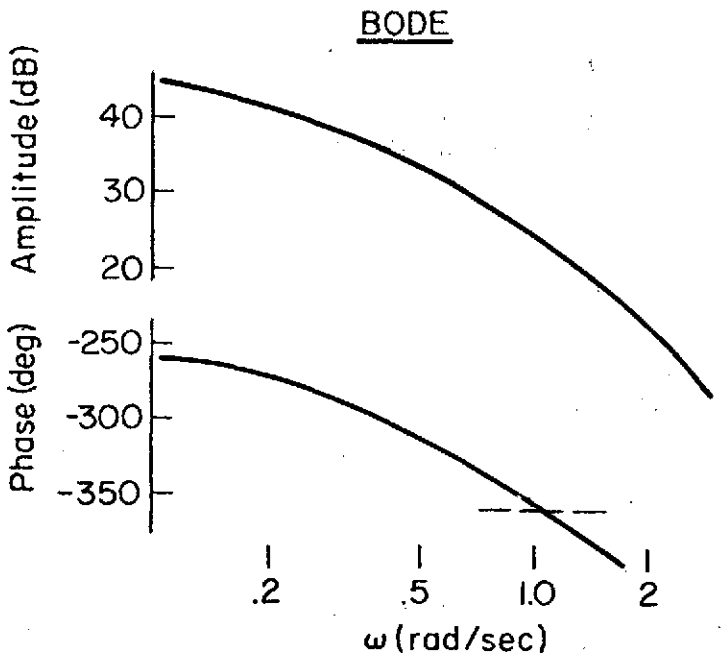

Figure B-20. Airspeed Loop Closure, Transparency In, 60 kt

BLOCK DIAGRAM

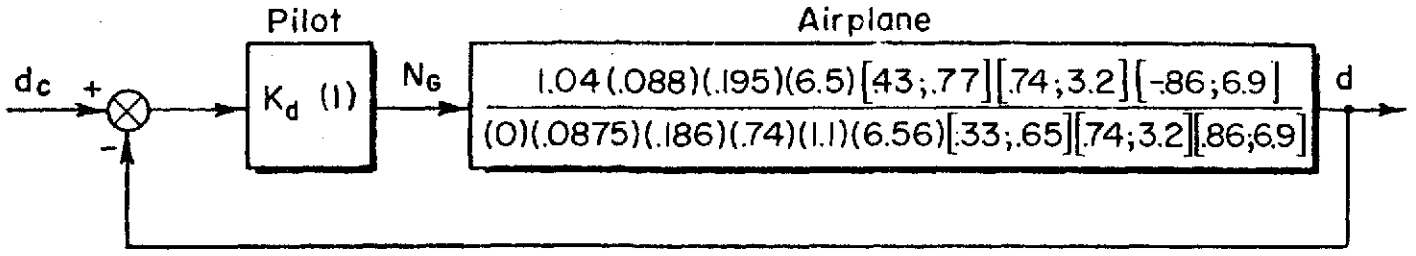

CLOSED LOOP DENOMINATOR

$$\Delta' = (.089)(.2)(1.06)(6.5)[.84;49][.23;.61][.74;3.2][.86;7]$$

STEP RESPONSE

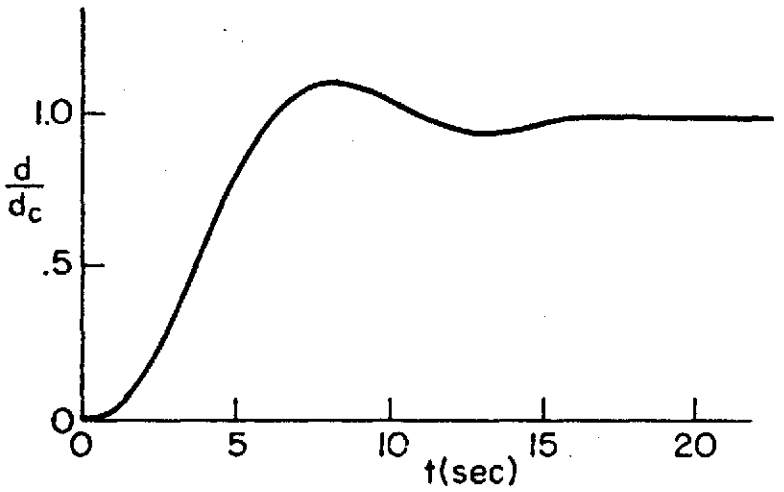

CLOSURE

Crossover .30 rad/sec

Gain .160 % rpm/ft

Phase Margin 60 deg

ω_{180} = .74 rad/sec

$Y_{p_u} = -1.94 \frac{(.1)}{(0)}$ deg/kt

ω_{c_u} = .5

ROOT LOCUS

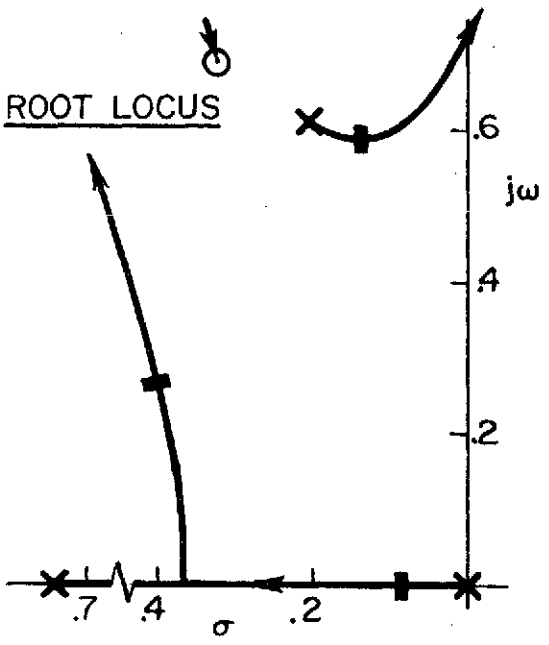

BODE

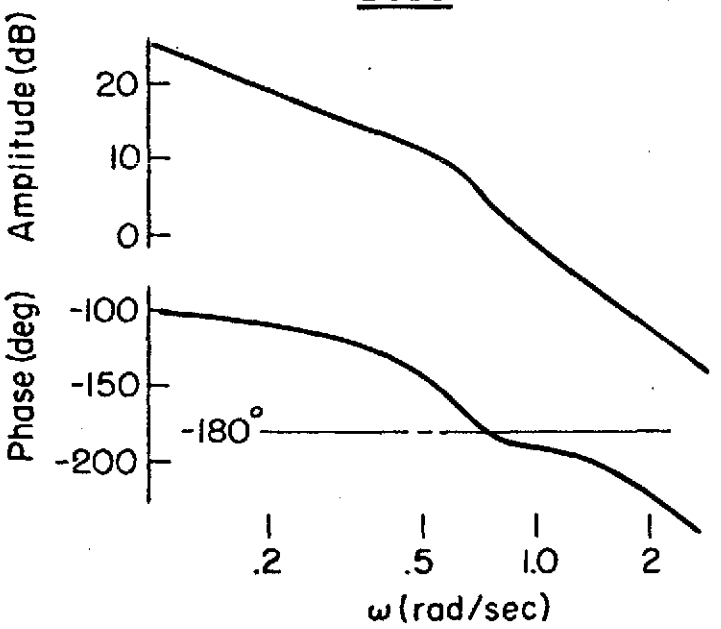

Figure B-21. Glide Slope Loop Closure, Transparency In, 60 kt

BLOCK DIAGRAM

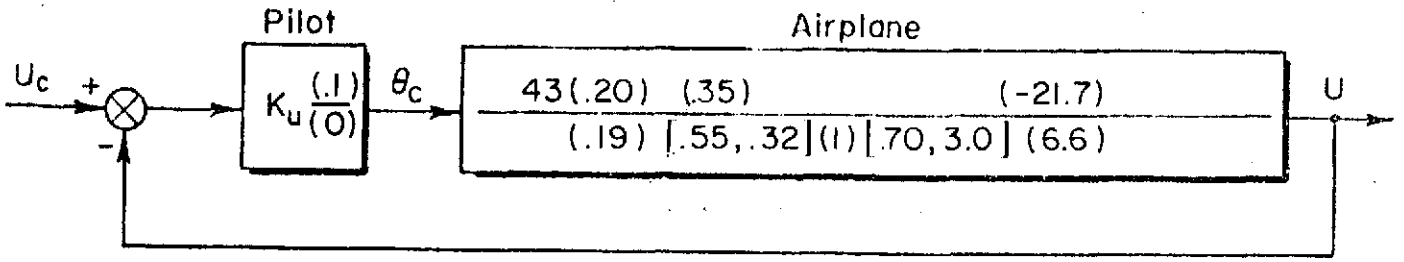

CLOSED LOOP DENOMINATOR

$\Delta' = (.06)(.19)(.55)[.33, .62][.72, 3.1](6.6)$

STEP RESPONSE

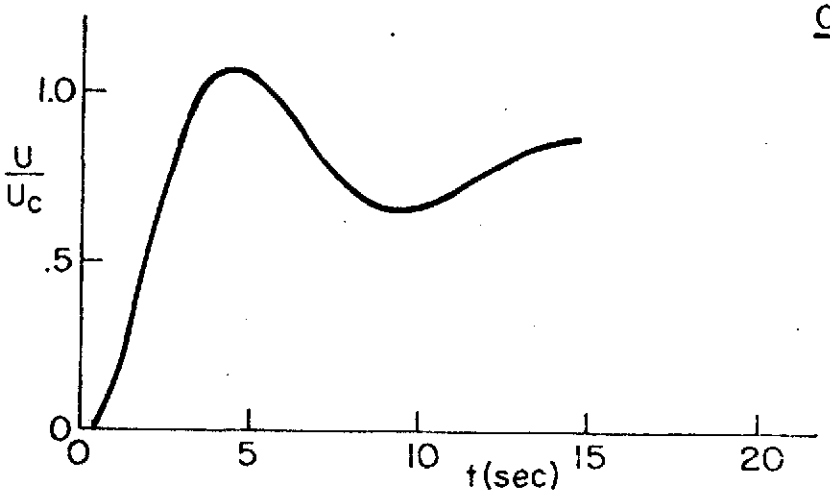

CLOSURE

Crossover .5 rad/sec

Gain -32 dB = 2.42 deg/kt

Phase Margin 50 deg

ROOT LOCUS

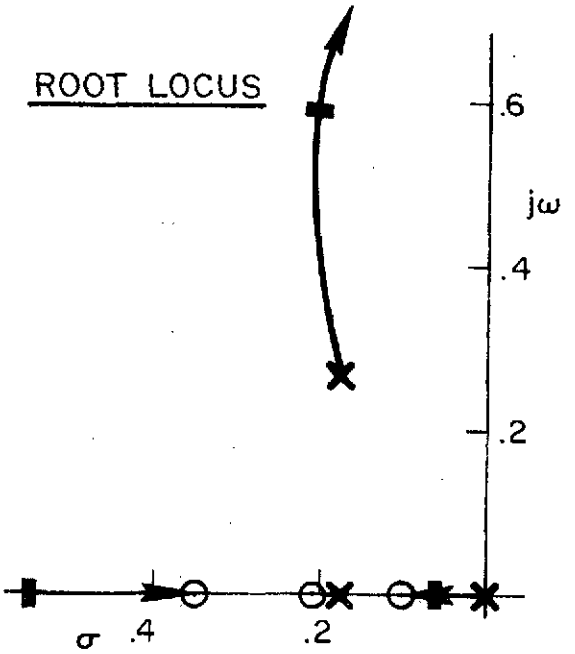

BODE

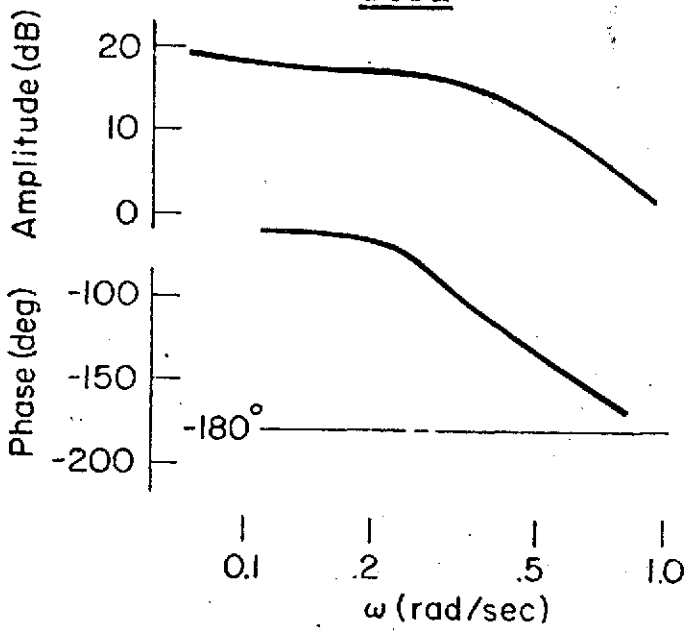

Figure B-22. Airspeed Loop Closures, Transparency In, 55 kt

BLOCK DIAGRAM

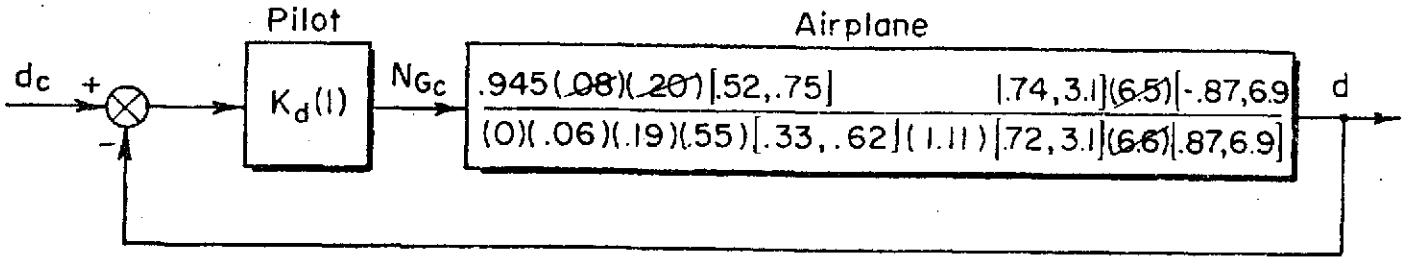

CLOSED LOOP DENOMINATOR

$\Delta' = (.085)(.2)[.77,.43][.19,.60](1.1)[.72,3.1](6.6)[.86,7]$

STEP RESPONSE

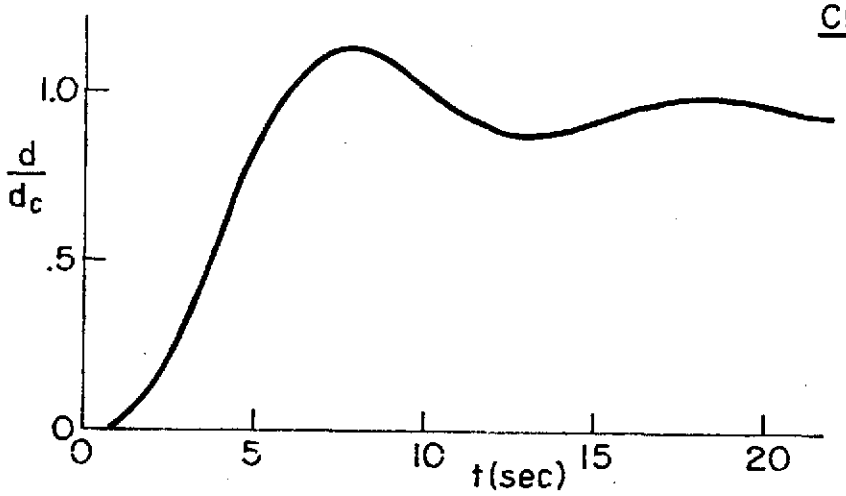

CLOSURE

Crossover − .3 rad/sec

Gain − −17. dB = .141 %rpm/ft

Phase Margin − 55 deg

ω_{180} = 0.65 rad/sec

$Y_{p_u} = 2.42 \frac{(.1)\,\text{deg}}{(0)\,\text{kt}}$

ROOT LOCUS

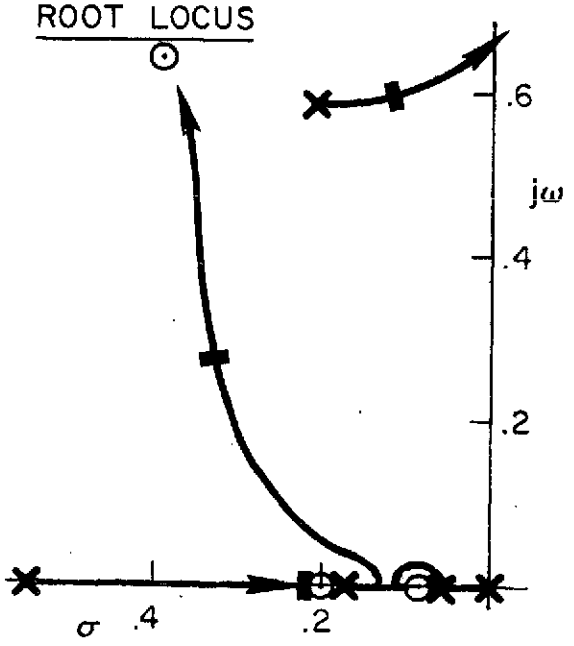

BODE

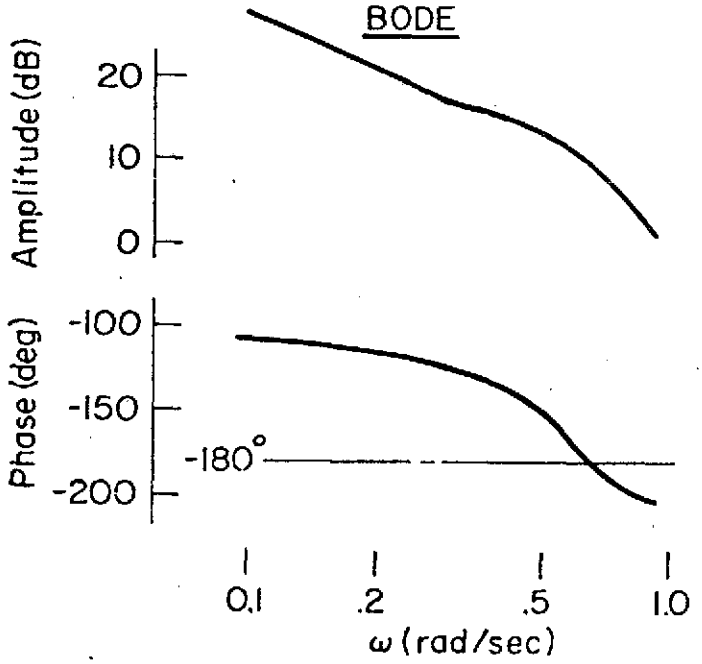

Figure B-23. Glide Slope Loop Closure, Transparency In, 55 kt

BLOCK DIAGRAM

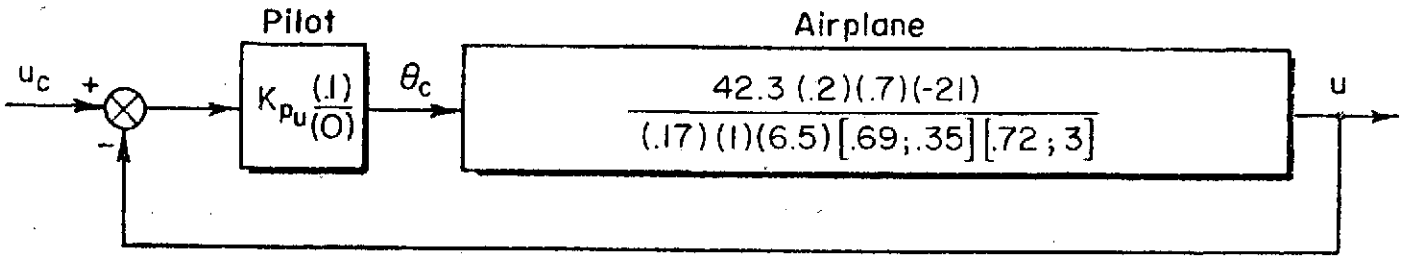

CLOSED LOOP DENOMINATOR

$\Delta' = (.078)(.19)(.83)(6.6)[.24;.60][.73;3.1]$

STEP RESPONSE

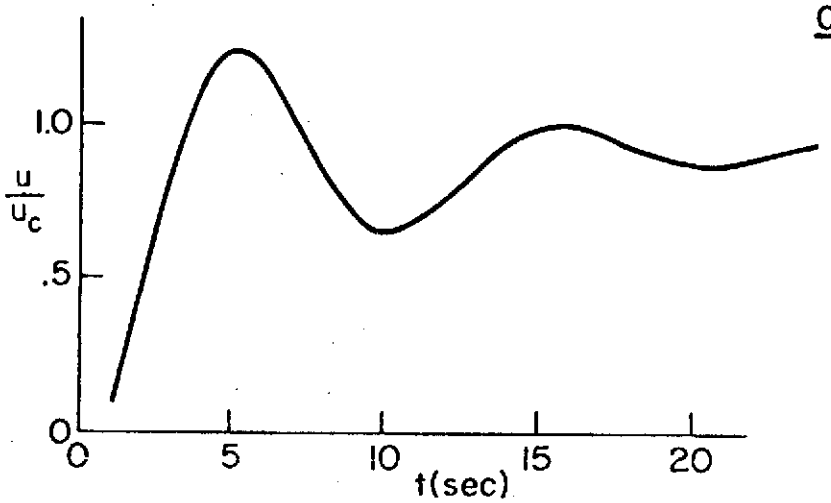

CLOSURE

Crossover .5 rad/sec

Gain -.023 rad/fps = -2.23 deg/kt

Phase Margin 37.2 deg

ω_{360} = .88 rad/sec

ROOT LOCUS

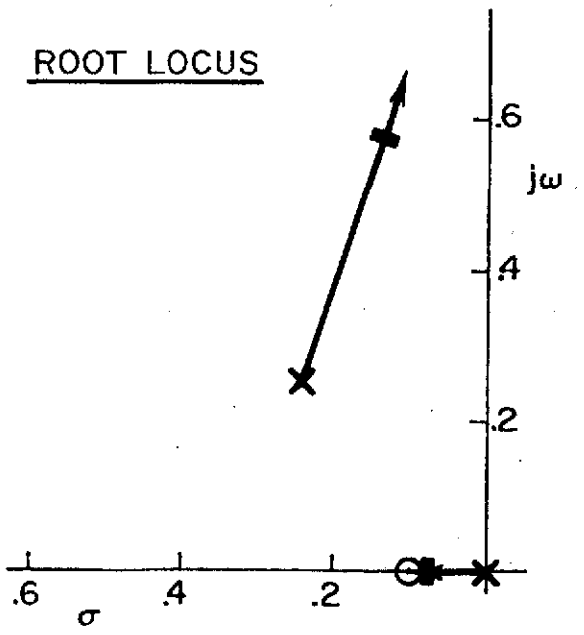

BODE

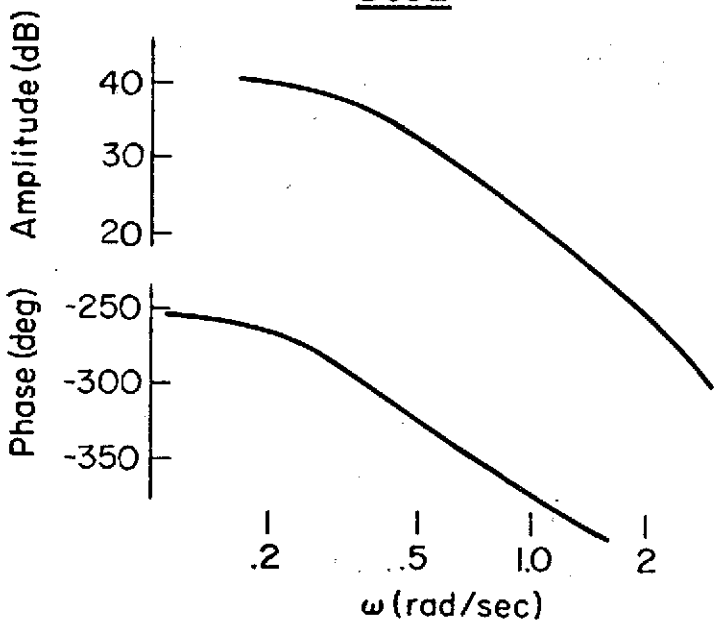

Figure B-24. Airspeed Loop Closure, Transparency Out, 60 kt

BLOCK DIAGRAM

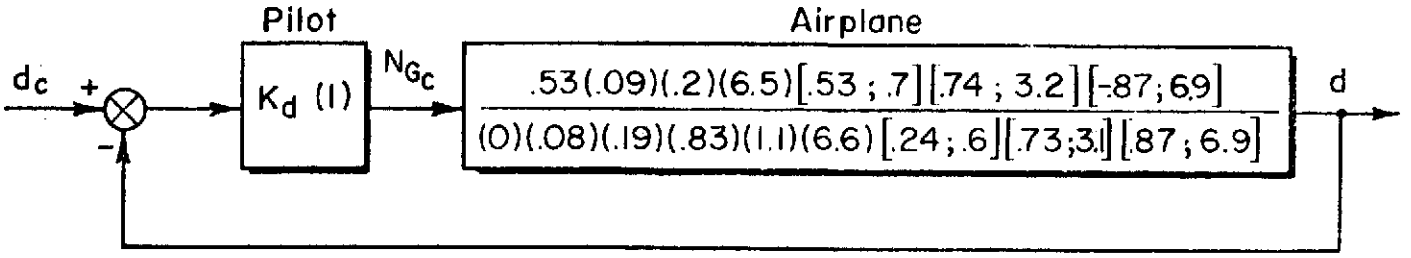

CLOSED LOOP DENOMINATOR

$\Delta' = (.091)(.21)(.31)(.60)(1.06)(6.6)[.10; .62][.73;3.1][.86; 7]$

STEP RESPONSE

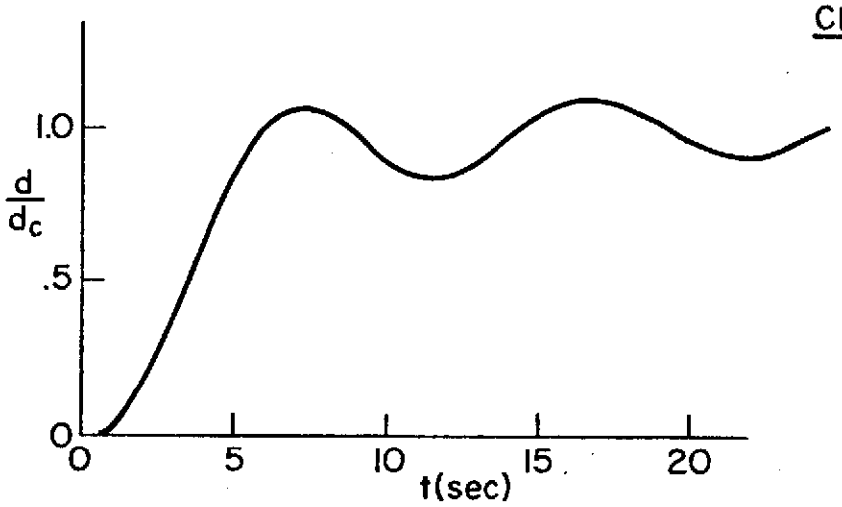

CLOSURE

Crossover .3 rad/sec
Gain .332 % rpm/ft
Phase Margin 72 deg
ω_{180} = .7 rad/sec
$Y_{p_u} = -2.23 \frac{(.1)}{(0)}$ deg/kt
ω_{c_u} = .5 rad/sec

ROOT LOCUS

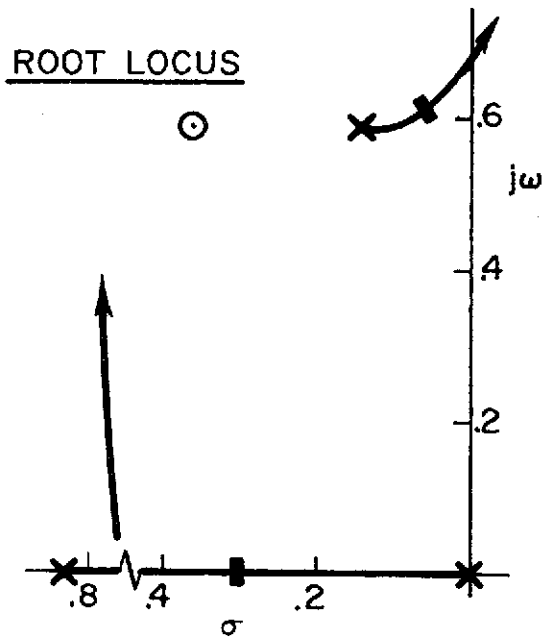

BODE

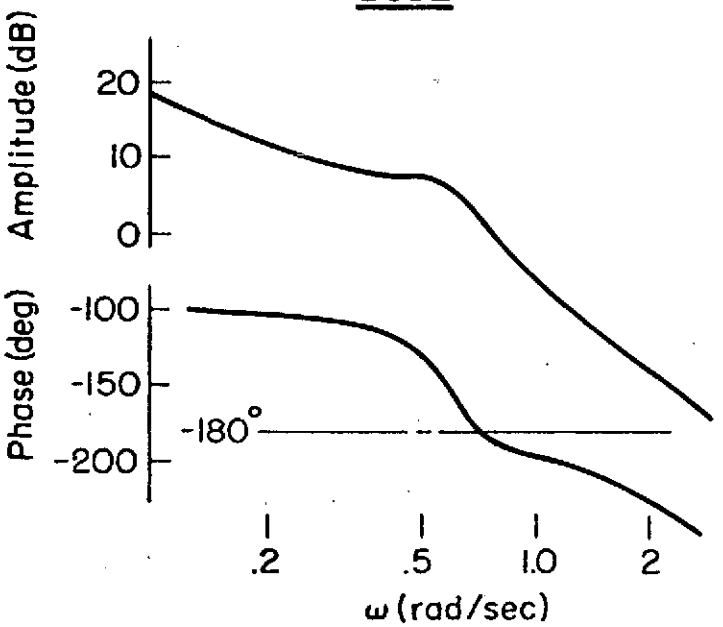

Figure B-25. Glide Slope Loop Closure, Transparency Out, 60 kt

BLOCK DIAGRAM

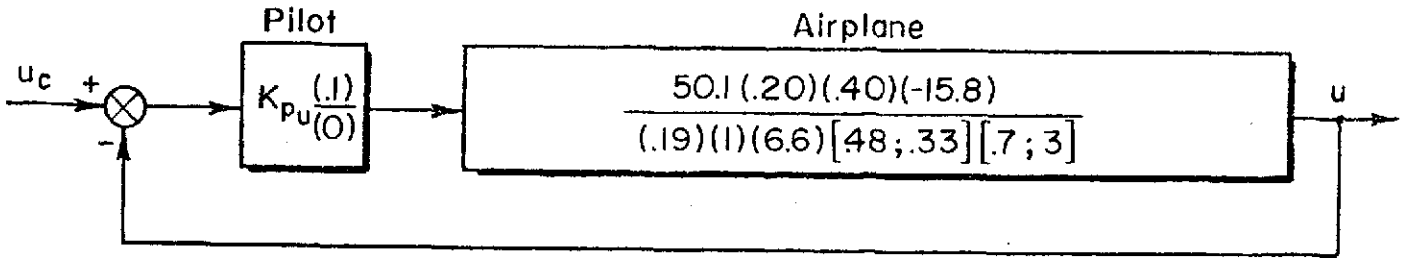

CLOSED LOOP DENOMINATOR

$\Delta' = (.062)(.19)(.64)(6.7)[.26;.59][.71;3.1]$

STEP RESPONSE

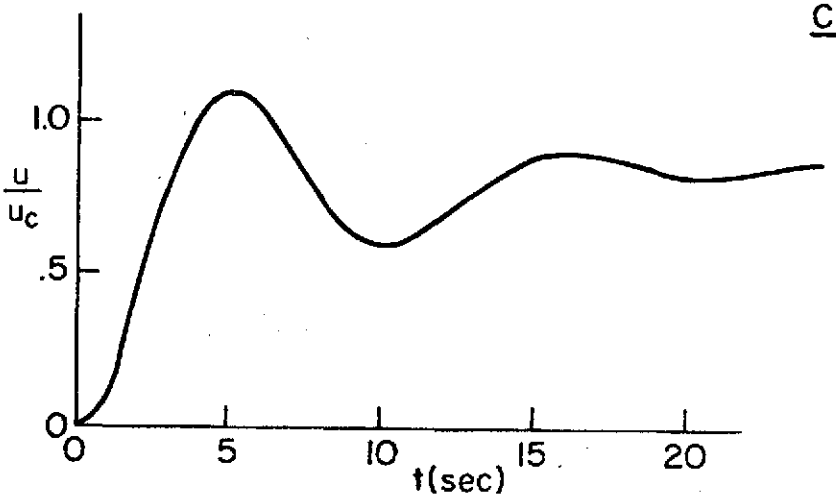

CLOSURE

Crossover .5 rad/sec
Gain -2.62 deg/kt
Phase Margin 41 deg
ω_{360} = .93 rad/sec

ROOT LOCUS

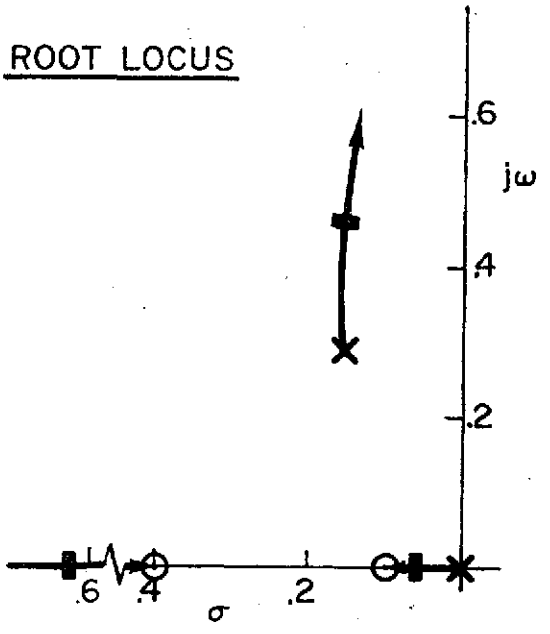

BODE

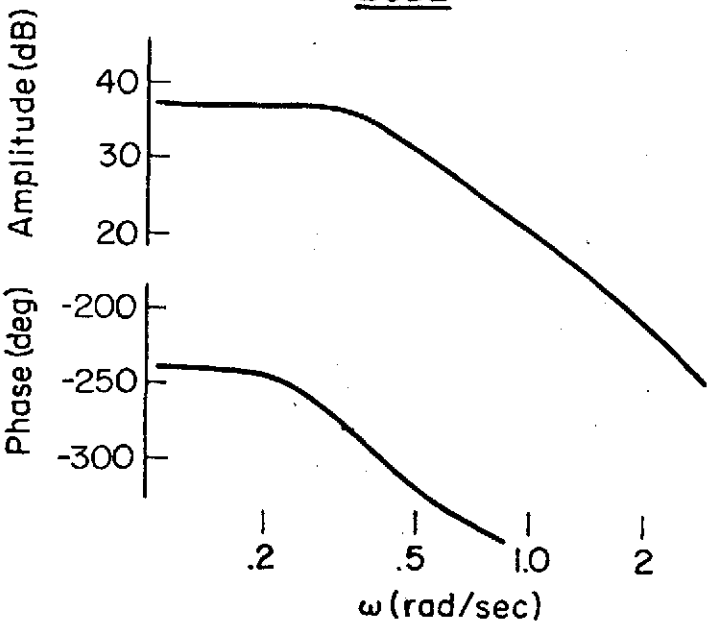

Figure B-26. Airspeed Loop Closure, Transparency Out, 55 kt

BLOCK DIAGRAM

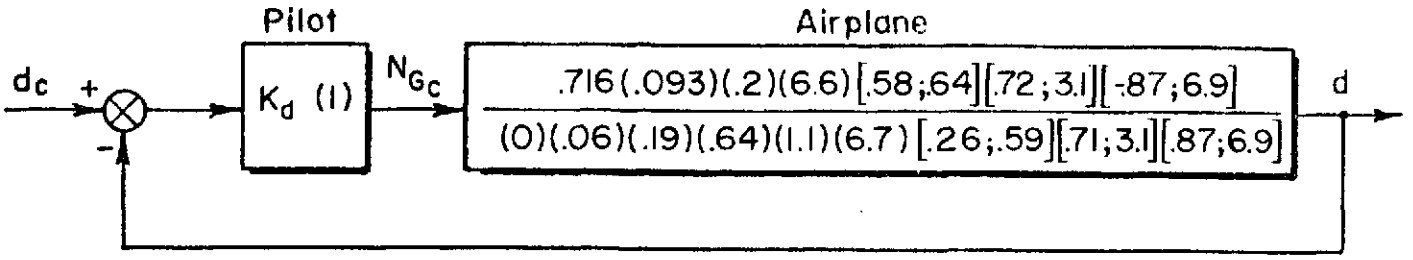

CLOSED LOOP DENOMINATOR

$\Delta = (.11)(.21)(1.1)(6.6)[.97;.35][.12;.61][.71;3.1][.86,7]$

STEP RESPONSE

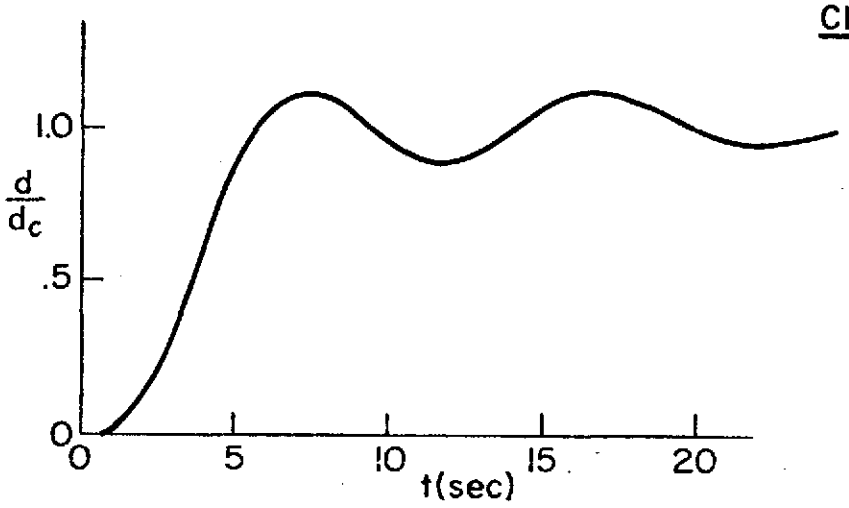

CLOSURE

Crossover .3 rad/sec
Gain .224% rpm/ft
Phase Margin 67deg
ω_{180} = .69 rad/sec
$Y_{pu} = -2.62 \frac{(-1)}{(0)}$ deg/kt
ω_{cu} = .5

ROOT LOCUS

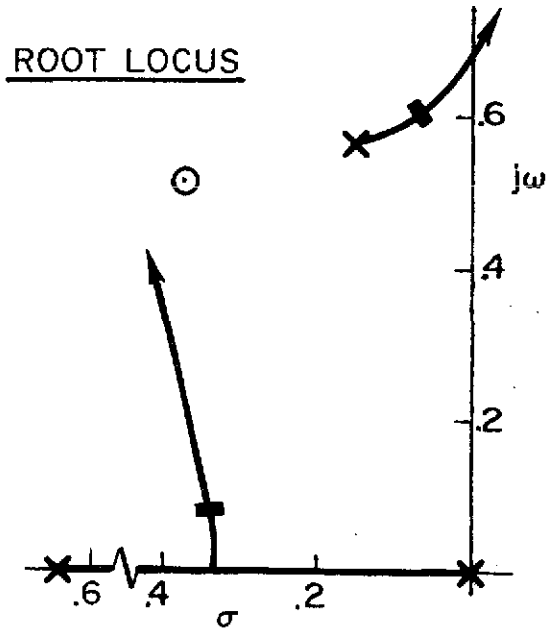

BODE

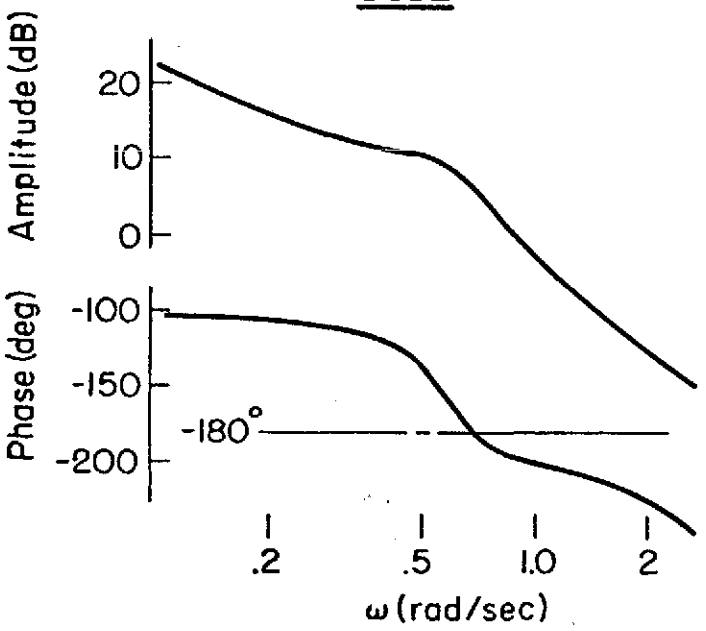

Figure B-27. Glide Slope Loop Closure, Transparency Out, 55 kt

4. Glide Slope Control in the Presence of Closed Loop Angle of Attack Control

The following analysis shows the effect of the pilot tracking angle of attack* in place of airspeed. Only two cases are shown, but these demonstrate the problems involved in tracking angle of attack.

Closure of the angle of attack loop for 65 kt is shown in Fig. B-28. The essential characteristic of this loop is that the angle of attack zeros are lightly damped. Thus as the pilot tracks α tighter the flight path mode becomes lightly damped and a PIO situation develops. In order to suppress the oscillatory characteristic, lag compensation is added by the pilot. In this case a lag was placed at 0.1 rad/sec. As the Bode plot in Fig. B-28 shows, the tight control of α, even with the lag compensation, is not good. The pilot would have to reduce his α crossover to something less than 0.3 rad/sec and this would not contribute much to the glide slope loop also being closed at about 0.3.

However, given an α loop closed as shown in Fig. B-28, the resulting glide slope loop is shown in Fig. B-29. The root locus shows us that any closure of the glide slope loop reduces the already low damping and a flight path PIO situation is unavoidable.

Reduction in approach speed is no different as shown in Figs. B-30 and B-31. Tight tracking of α again leads to a PIO situation, and if the α loop is closed loosely enough to avoid the oscillation then the bandwidth is insufficient to do any good in tracking the glide slope. However a low α crossover could be effective in keeping it within generally safe bounds.

---

* True angle of attack is used in this analysis. However, indicated angle of attack as mechanized in this simulation has the same numerator characteristics. For example: $N^{\alpha}_{\delta_e u} = -2.6$ [0.25, 0.34] while $N^{\alpha}_{\delta_e} = -1.4$ [0.24, 0.32] and $N^{\theta\,\alpha}_{\delta_e N_G u} = 1.3(0.18)$ while $N^{\theta\,\alpha}_{\delta_e N_G} = 0.7(0.18)$. Thus the essential difference is only a scale factor.

BLOCK DIAGRAM

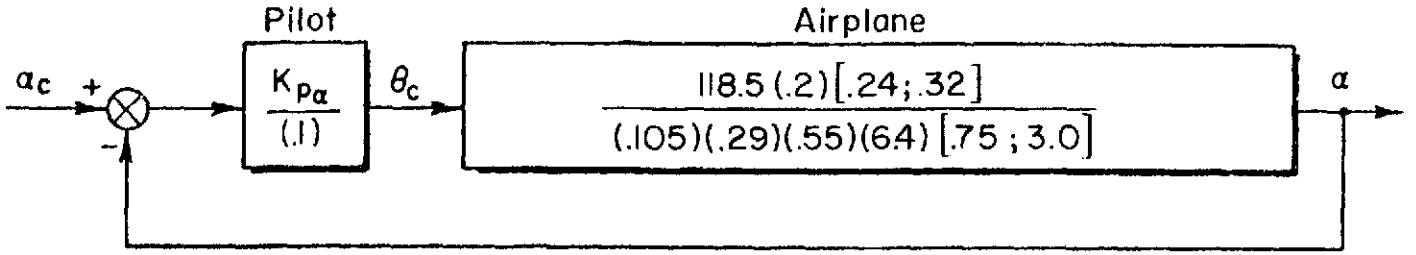

CLOSED LOOP DENOMINATOR

$$\Delta' = (.2)(6.6)[.24;.27][.25;1.6][.8;3.9]$$

STEP RESPONSE

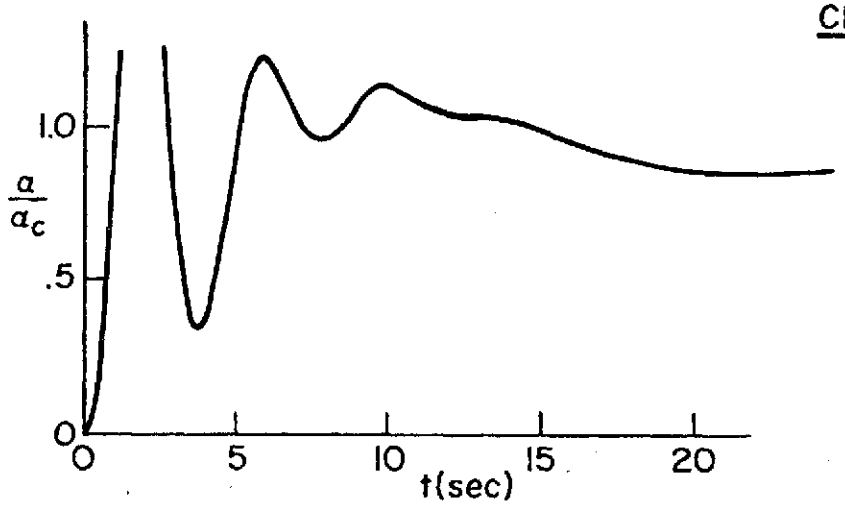

CLOSURE

Crossover 1.0 rad/sec
Gain 1.45 deg/deg
Phase Margin 63 deg
ω_{180} = 1.85 rad/sec

ROOT LOCUS

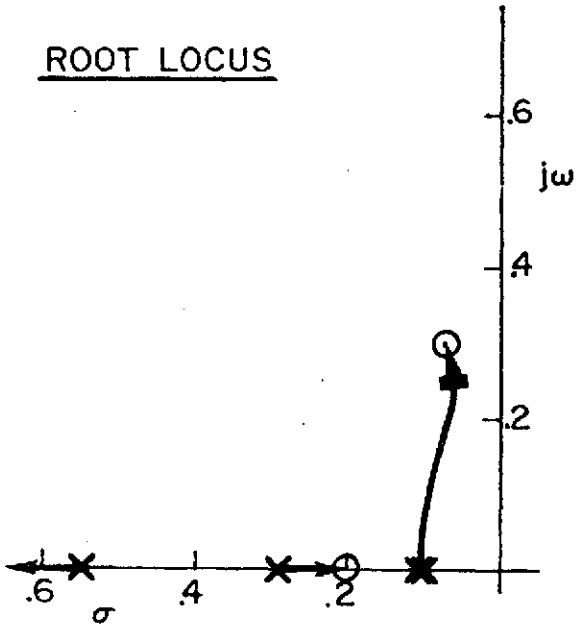

BODE

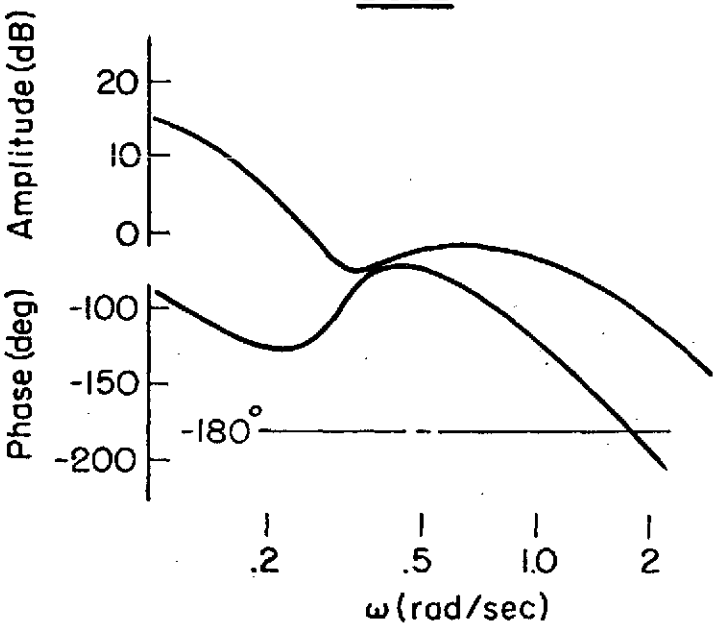

Figure B-28. Angle of Attack Loop Closure, Transparency In, 65 kt

BLOCK DIAGRAM

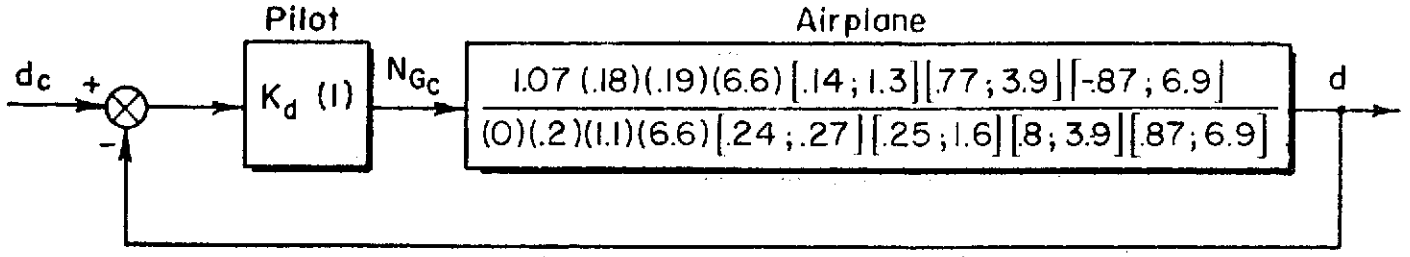

CLOSED LOOP DENOMINATOR

$$\Delta' = (.06)(.2)(1.1)(6.6)[.07; .32][.25; 1.6][.8; 3.9][.87; 7]$$

STEP RESPONSE

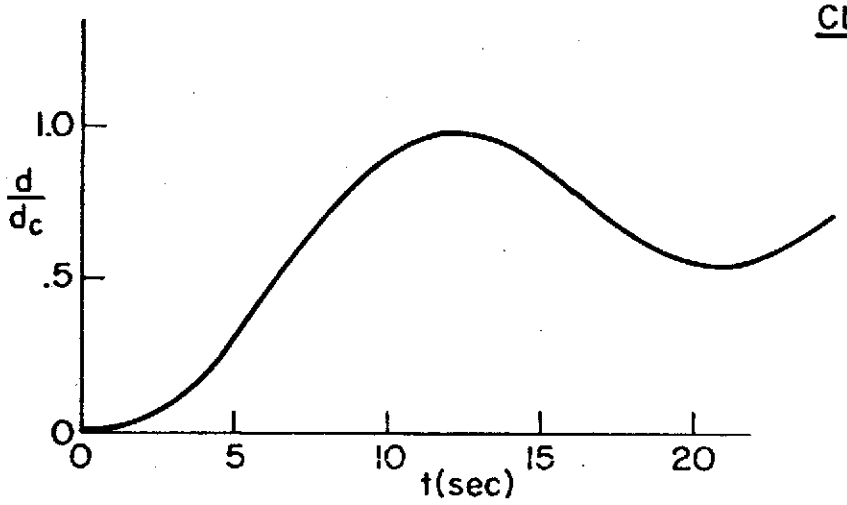

CLOSURE

Crossover .3 rad/sec

Gain -25.4 dB = .054 % rpm/ft

Phase Margin 24 deg

ω_{180} = .37 rad/sec

ROOT LOCUS

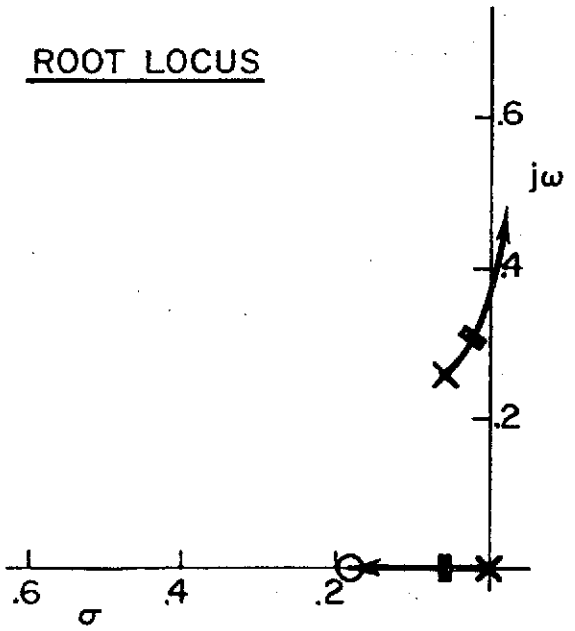

BODE

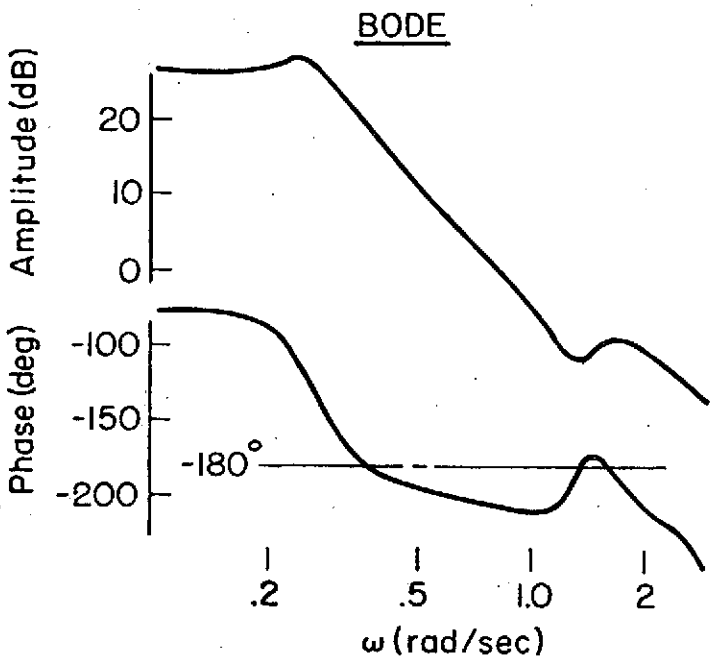

Figure B-29. Glide Slope Loop Closure, Angle of Attack Loop Closed, Transparency In, 65 kt

BLOCK DIAGRAM

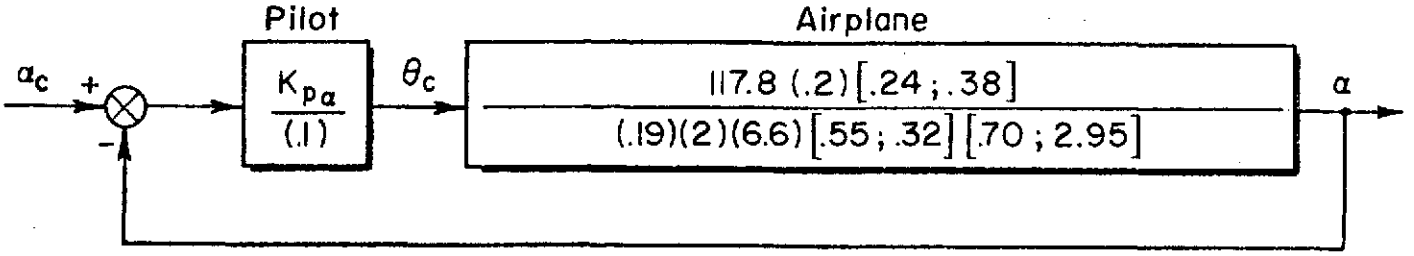

CLOSED LOOP DENOMINATOR

$\Delta' = (.20)(6.7)[.19 ; .36][.24 ; 1.40][.78 ; 3.62]$

STEP RESPONSE

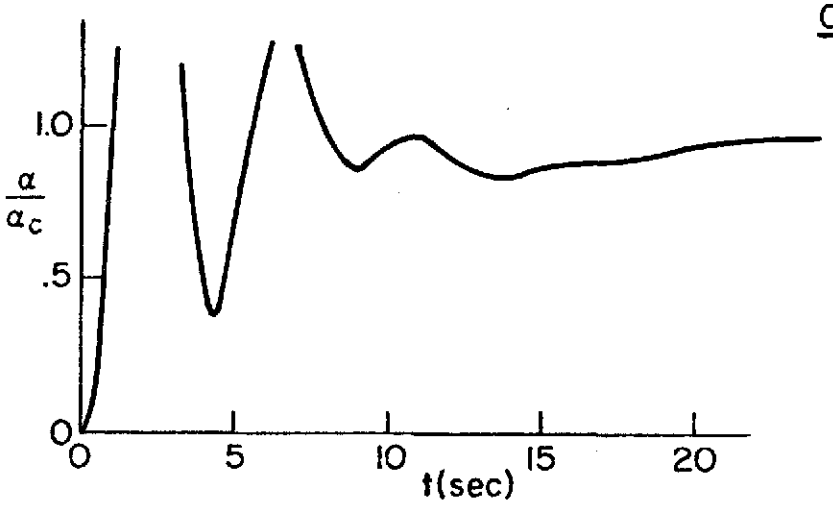

CLOSURE

Crossover 1.0 rad/sec
Gain 1.225 deg/deg
Phase Margin 41 deg
ω_{180} = 1.6 rad/sec

ROOT LOCUS

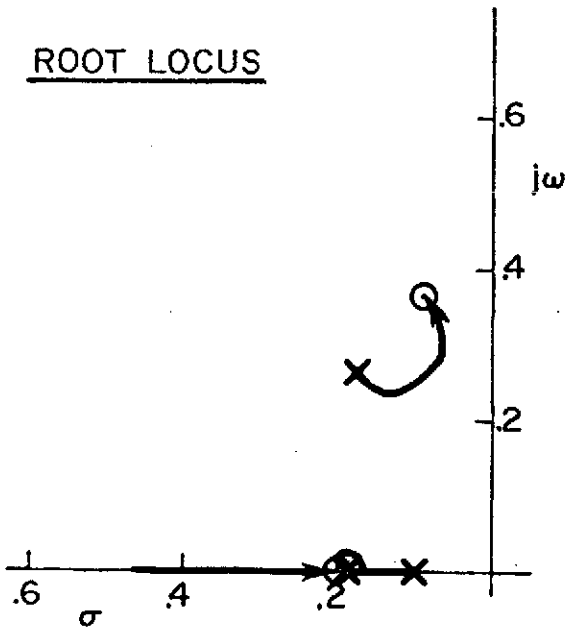

BODE

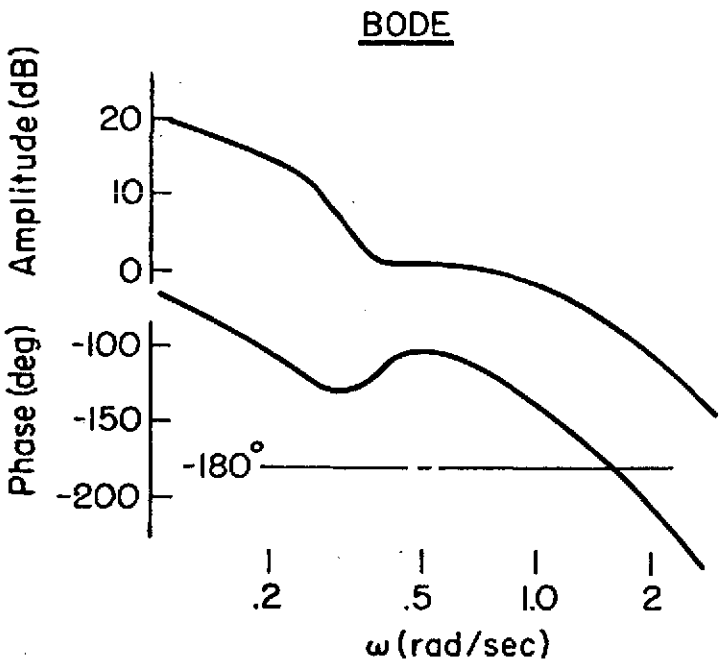

Figure B-30. Angle of Attack Loop Closure, Transparency In, 55 kt

BLOCK DIAGRAM

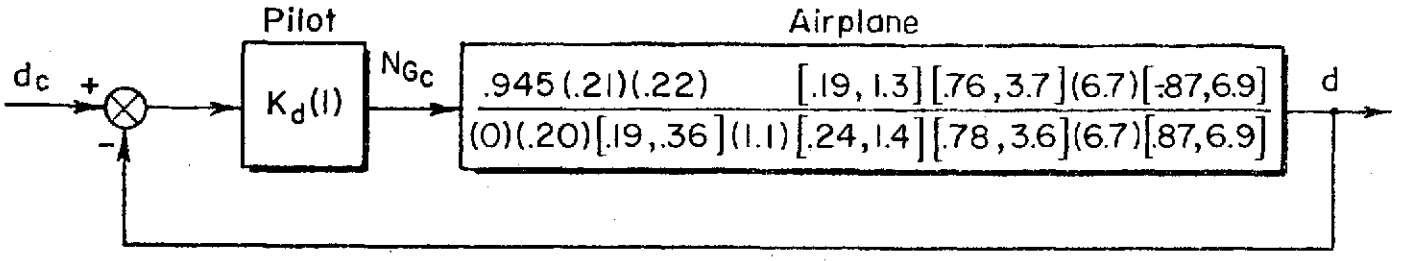

CLOSED LOOP DENOMINATOR

$\Delta' = (.06)(.20)[.07,.40](1.1)[.24,1.4][.78,3.6](6.7)[.86,6.9]$

STEP RESPONSE

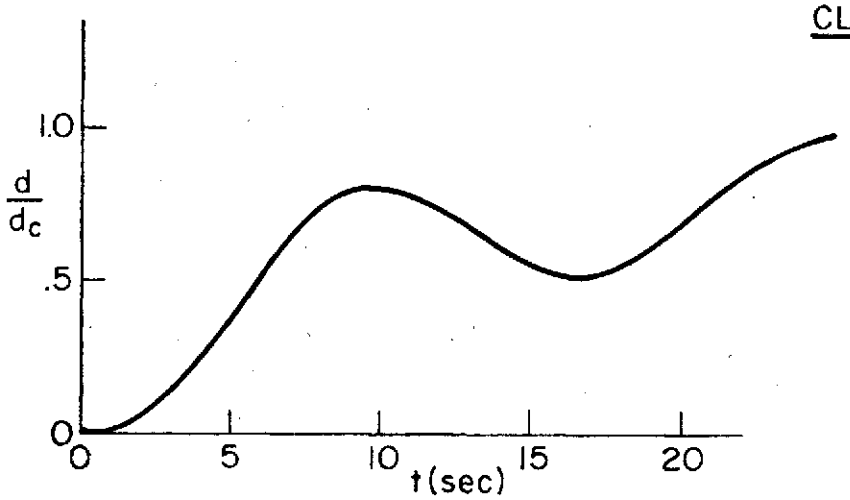

CLOSURE

Crossover .3 rad/sec
Gain -24.5 dB = .059% rpm/ft
Phase Margin 78 deg
Period of Oscillation 15.5 sec
Settling Time 37.5 sec
ω_{180} = 0.48 rad/sec

ROOT LOCUS

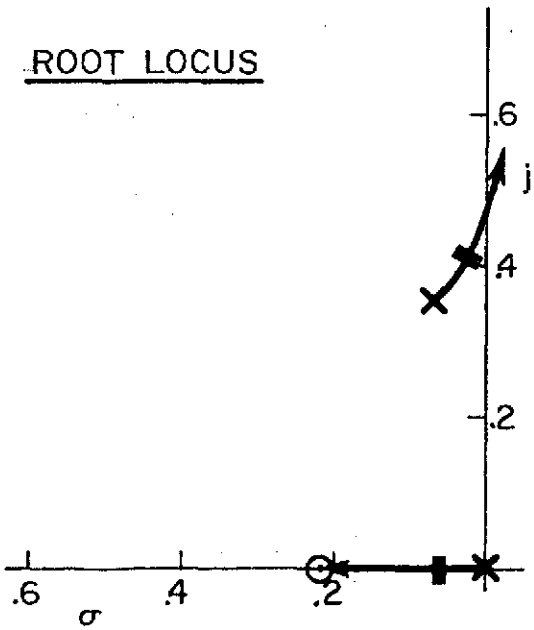

BODE

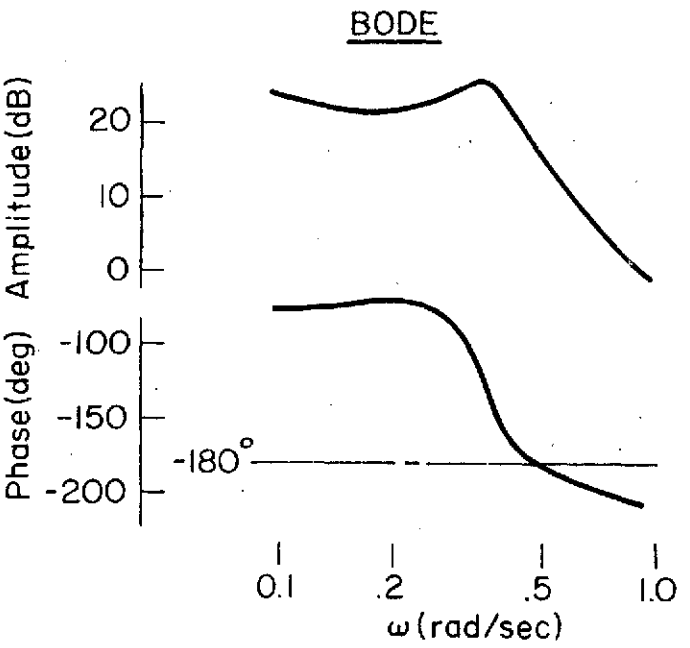

Figure B-31. Glide Slope Loop Closure, Angle of Attack Loop Closed, Transparency In, 55 kt

The fundamental dynamic relationship which sets up the potential PIO is the fact that $N^{\alpha}_{\delta_e}$ roots are always close to the phugoid mode. (To a first order approximation they are equal). Thus the flight path mode with $\alpha \longrightarrow \theta_c$ returns to the lightly damped phugoid. Figure B-32 gives a generic description of tight α control while trying to track glide slope.

5. Summary of Pilot/Vehicle Analyses

The foregoing analyses were done in considerable detail for the sake of completeness. The following will combine these results and emphasize the important features.

The glide slope control characteristics, given the various inner loop structures, can be summarized by the simplified transfer functions shown in Table B-1. The high frequency gain includes the lumping of all high frequency (> 1 rad/sec) roots. Further, this gain is in terms of throttle movement (inches) thereby reducing confusion due to non-linear controller and thrust characteristics.

A general indication of the bandwidth is provided by the damping of the denominator roots in Table B-1. For example at 65 kt and transparency in, the transfer function corresponding to no airspeed regulation is essentially a first order lag at 0.55 (the pole--zero combination at 0.29 and 0.24 effectively cancel). On the other hand, the case of closed-loop angle of attack has a lightly damped pair of oscillatory roots and a low frequency zero. Simple sketches (Fig. B-33) of the respective root locus plots reveal the relative problems in tracking glide slope.

A further overall comparison of the previous pilot/vehicle analyses is given in Fig. B-34. Here the gain and bandwidth characteristics are summarized. These terms were used in the STOL flight path control analysis reported in Ref. 4. Approximate levels are shown for minimum gain and bandwidth (0.1 g/in and 0.35 rad/sec). This simulated aircraft is marginal on both counts and especially at the lower approach speeds. Note how pilot technique can affect the gain and bandwidth. In general the bandwidth plot correlates to the oscillatory tendency exhibited in the individual closed loop analyses. The exception is in the 55 kt angle of

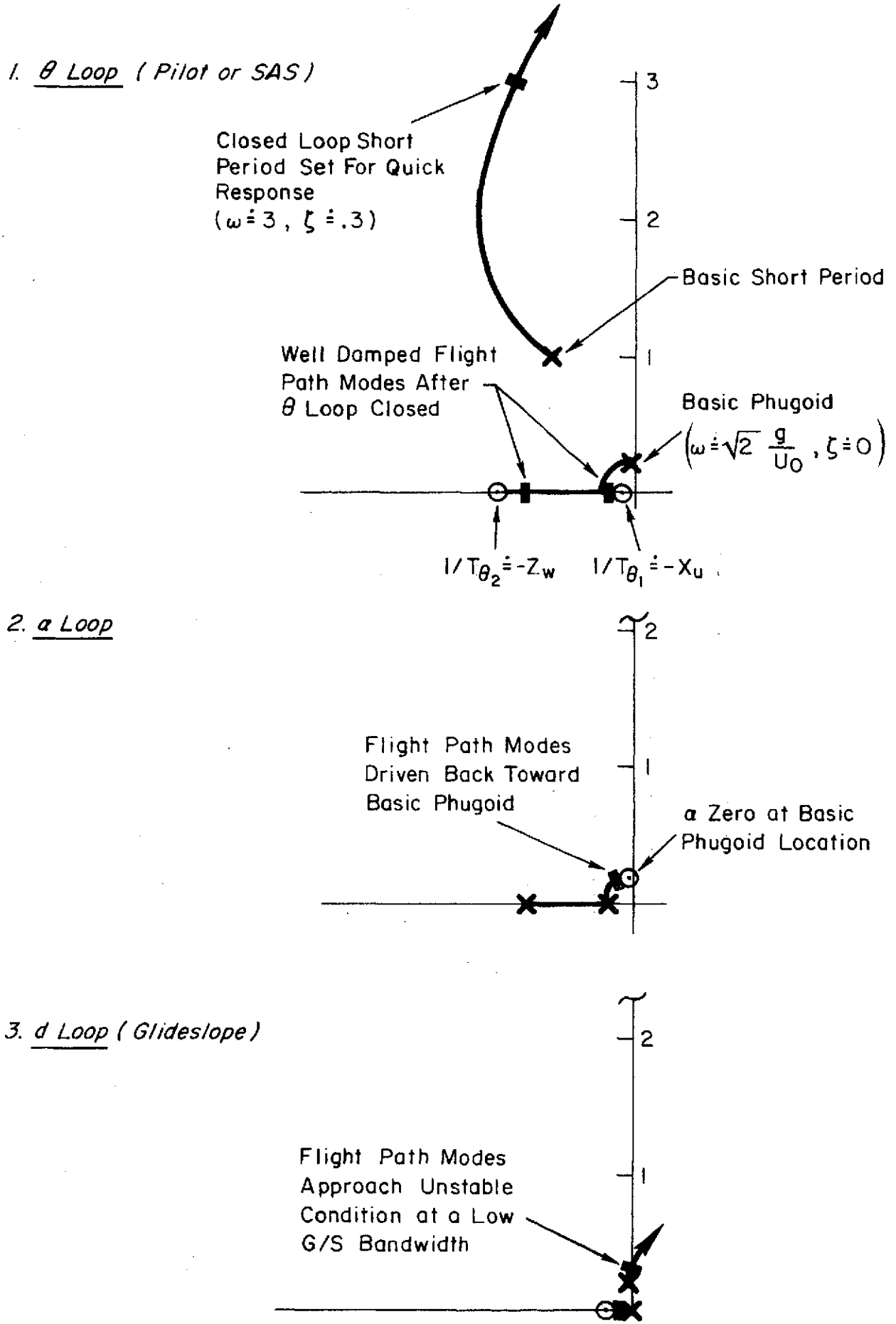

Figure B-32. Generic Description of Glide Slope Control While Tracking α Tightly

TABLE B-1

GLIDE SLOPE TRANSFER FUNCTION SUMMARY

[$\dot{d}/\delta_T$ ($\frac{ft/sec}{in}$) for $\omega < 1$ rad/sec, engine lag excluded]

	T = 12°			T = 0	
	65kt	60kt	55kt	60kt	55kt
No airspeed regulation	$\frac{4.1(0.24)}{(0.29)(0.55)}$	$\frac{3.6(0.24)}{[0.89,0.36]}$	$\frac{3.3(0.26)}{[0.55,0.32]}$	$\frac{2.2(0.23)}{[0.69,0.35]}$	$\frac{2.8(0.13)}{[0.48,0.33]}$
Ideal $N_G \longrightarrow \theta$ Crossfeed	$\frac{5.1(0.69)}{(0.55)(0.72)}$	$\frac{4.4(0.17)}{[0.89,0.36]}$	$\frac{3.1[0.62,0.35]}{(0.35)[0.55,0.32]}$	$\frac{2.2}{(0.70)}$	$\frac{2.4}{(0.40)}$
Simplified $N_G \longrightarrow \theta$ Crossfeed	$\frac{5.1(0.69)}{(0.55)(0.72)}$	$\frac{3.7(0.25)}{[0.89,0.36]}$	$\frac{2.7(0.40)}{[0.55,0.32]}$	$\frac{1.8(0.28)}{[0.69,0.35]}$	$\frac{2.3(0.36)}{[0.48,0.33]}$
Closed Loop Airspeed Control	$\frac{4.0[0.35,0.82]}{(0.76)[0.37,0.69]}$	$\frac{3.6[0.43,0.77]}{(0.74)[0.33,0.65]}$	$\frac{3.1[0.52,0.75]}{(0.55)[0.33,0.62]}$	$\frac{2.4[0.53,0.70]}{(0.83)[0.24,0.60]}$	$\frac{2.7[0.58,0.64]}{(0.64)[0.26,0.59]}$
Closed Loop Angle of Attack Control	$\frac{2.5(0.18)}{[0.24,0.27]}$		$\frac{2.8(0.22)}{[0.19,0.36]}$		

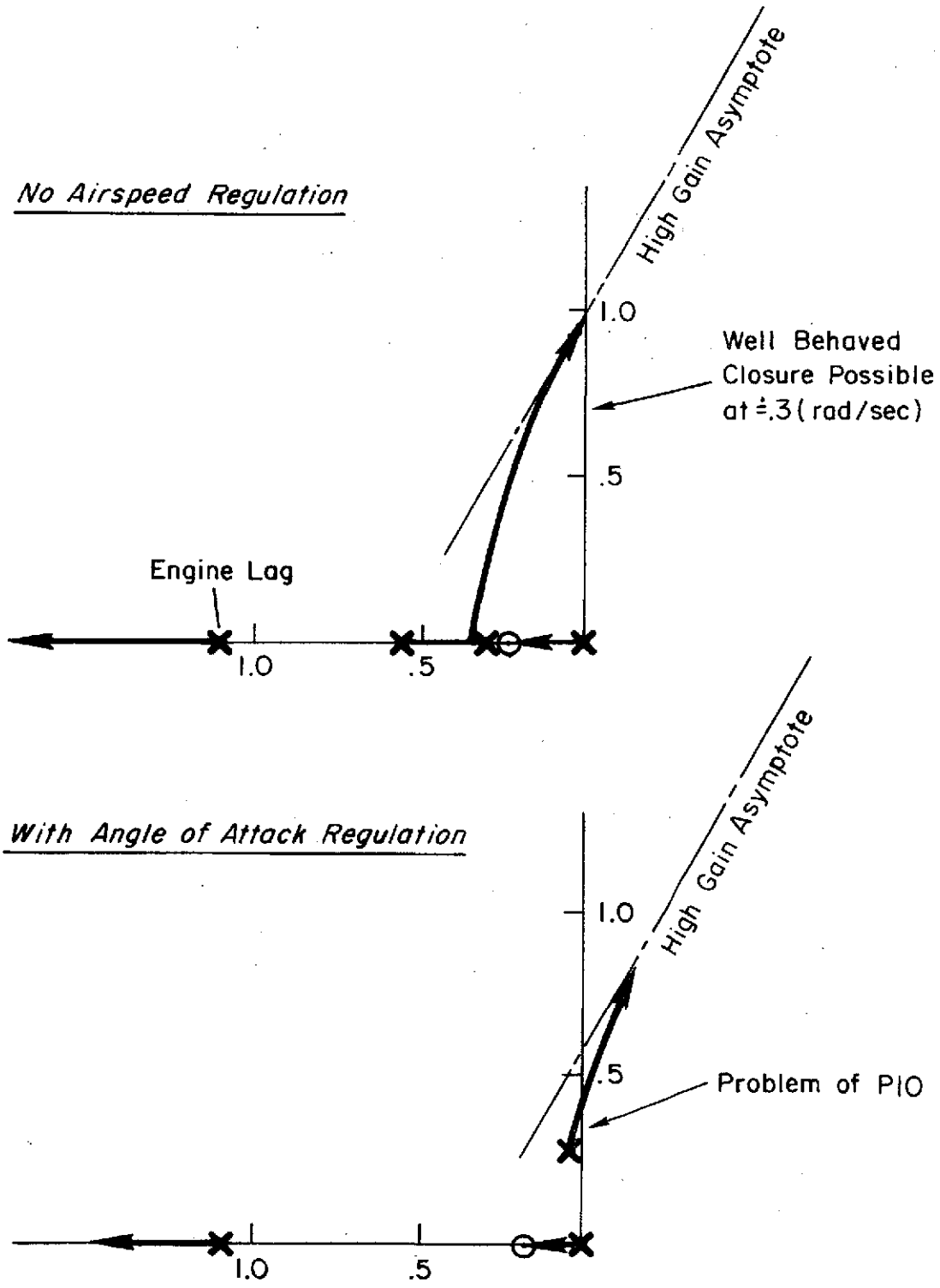

Figure B-33. Sample Comparison of Simplified Transfer Functions From Table B-1

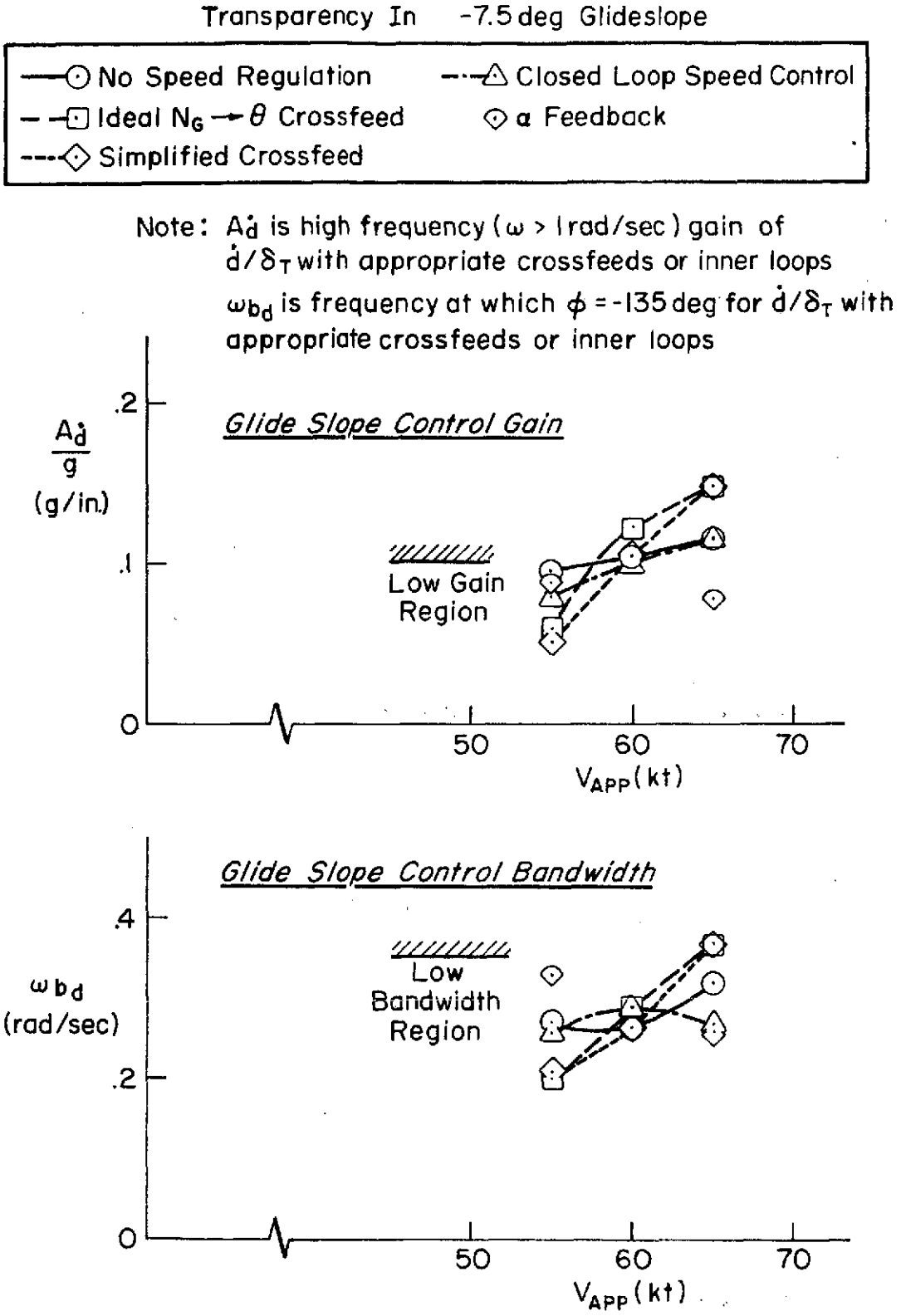

Figure B-34. Glide Slope Tracking Gain and Bandwidth Variation With Piloting Technique

attack case where a relatively high ω_{b_d} is shown yet the closed loop analysis would indicate problems.

A final pilot/vehicle analysis summary is provided in the following list of key points:

- Approach speed sensitive parameters have the most significant effect on glide slope tracking
- Degradation of glide slope tracking is characterized by a phugoid-like oscillatory tendency
- The pilot can compensate for reduced approach speed by increasing his glide slope lead or airspeed regulation
- As approach speed is decreased both glide slope bandwidth and gain worsen but both are affected by piloting technique
- Tight tracking of angle of attack in lieu of airspeed results in a PIO tendency
- The pilot is capable of generating sufficient lead to control the glide slope over the 60 to 65 kt range but the lead required at lower speeds indicates high workload
- Transparency by itself has a slight positive effect on the glide slope control problem
- The $N_G \longrightarrow \theta$ crossfeed to constrain airspeed becomes very difficult at the lower approach speeds
- A simplified (pure gain) crossfeed is of little benefit at the lower approach speeds
- The primary aerodynamic factor in limiting glide slope bandwidth as approach speed is reduced is lower heave damping (Z_w)
- Aerodynamic factors tending to set the BR 941 S apart from conventional aircraft are
  - -- Low heave damping (Z_w) coupled with high velocity damping (X_u)
  - -- Nearly vertical thrust component

- Transparency has the effect of
  - -- Increasing induced drag $\left(\frac{\partial C_D}{\partial C_L}\right)$ by about 10%
  - -- Decreasing lift by about 5% (at constant α, T_c')
  - -- Decreasing lift/drag ratio by 35% (at constant α, T_c')
  - -- This results in higher power setting and lower angle of attack.

APPENDIX C

FLARE AND TOUCHDOWN ANALYSIS

In order to examine the flare and touchdown characteristics of the airplane model used in these tests, a computer program was developed to solve for the flare trajectory for a given flare maneuver. This was used to look at general trends due to variation in approach speed, configuration, ground effect, and flare technique. Some of the results from this computer program are presented and related to performance in both the simulator and flight test. Landing data from an FAA/NASA flight test of the BR 941S in France during July 1972 are included.

1. Nature of the Flare Maneuver

For this particular airplane, possibly due to the significant nose down approach attitude (about -10 deg), the flare consisted of rotating the nose smoothly to a near level attitude. This is shown in both flight test records (Fig. C-1) and simulator records (Fig. C-2). In both sets of figures there is a fairly consistent relationship between the attitude and altitude. In most cases the flare rotation begins between 30 and 40 ft above the surface and ends in a slightly nose up attitude. Unfortunately the flight test θ vs h figures are incomplete for the time just prior to touchdown due to an apparent angle of attack effect on the static port. However, the conditions at flare initiation and at touchdown are reasonably certain. Based on these flare maneuvers the following nominal flare maneuver was used in the computer solutions:

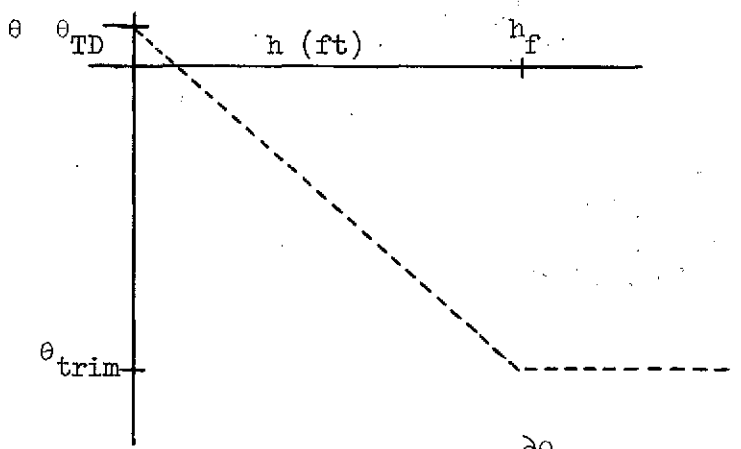

At a given altitude above the ground a constant $\frac{\partial\theta}{\partial h}$ begins and lasts until touchdown.

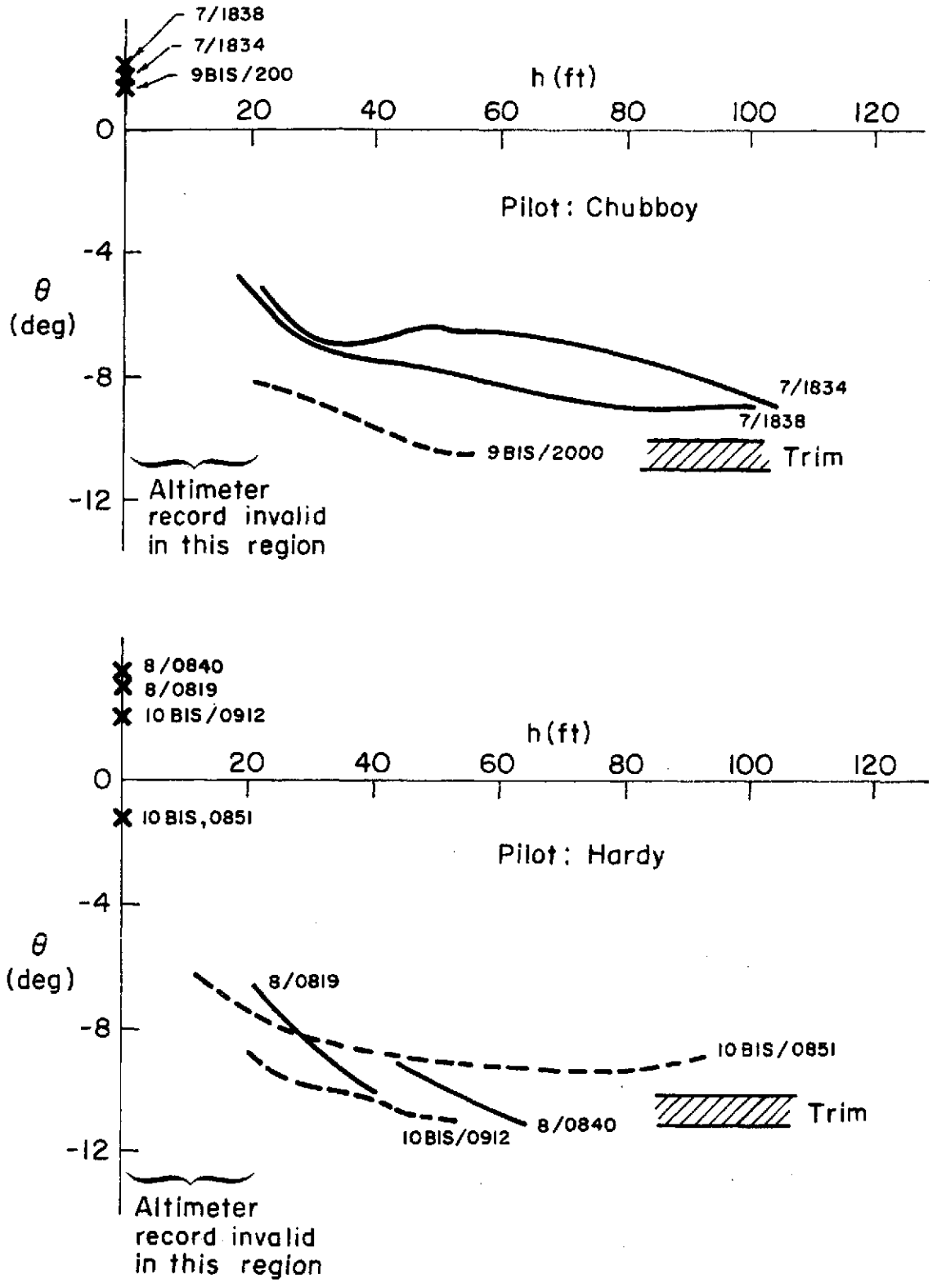

Figure C-1. Flare Maneuver (Flight Test)

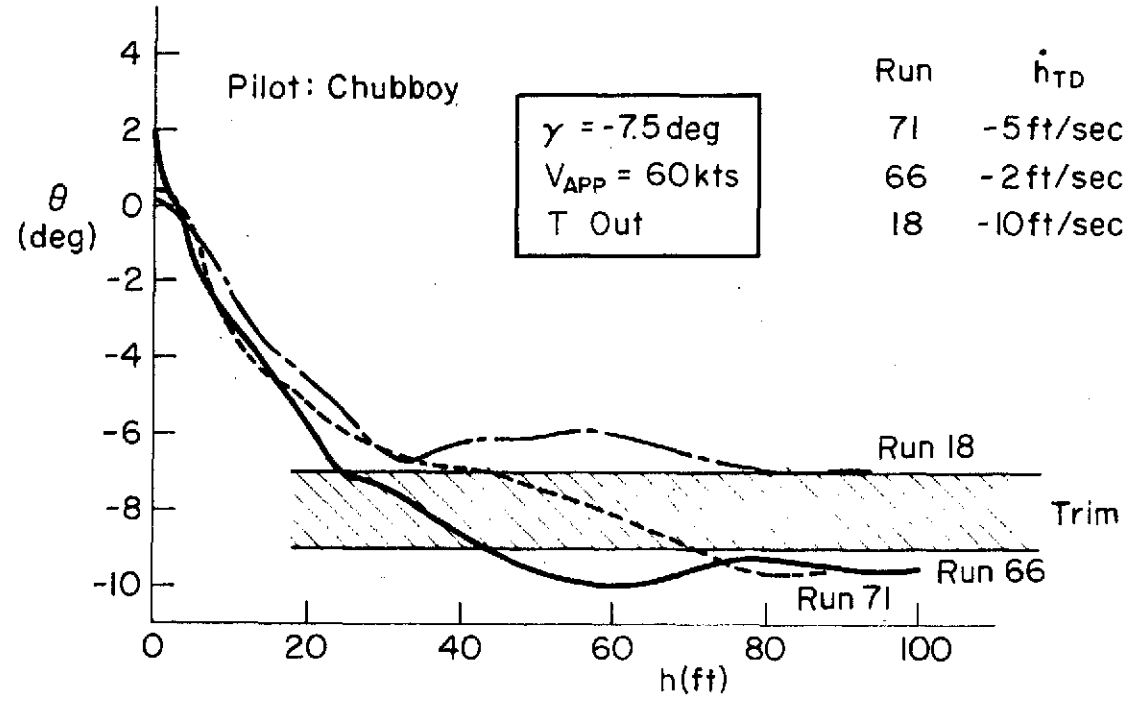

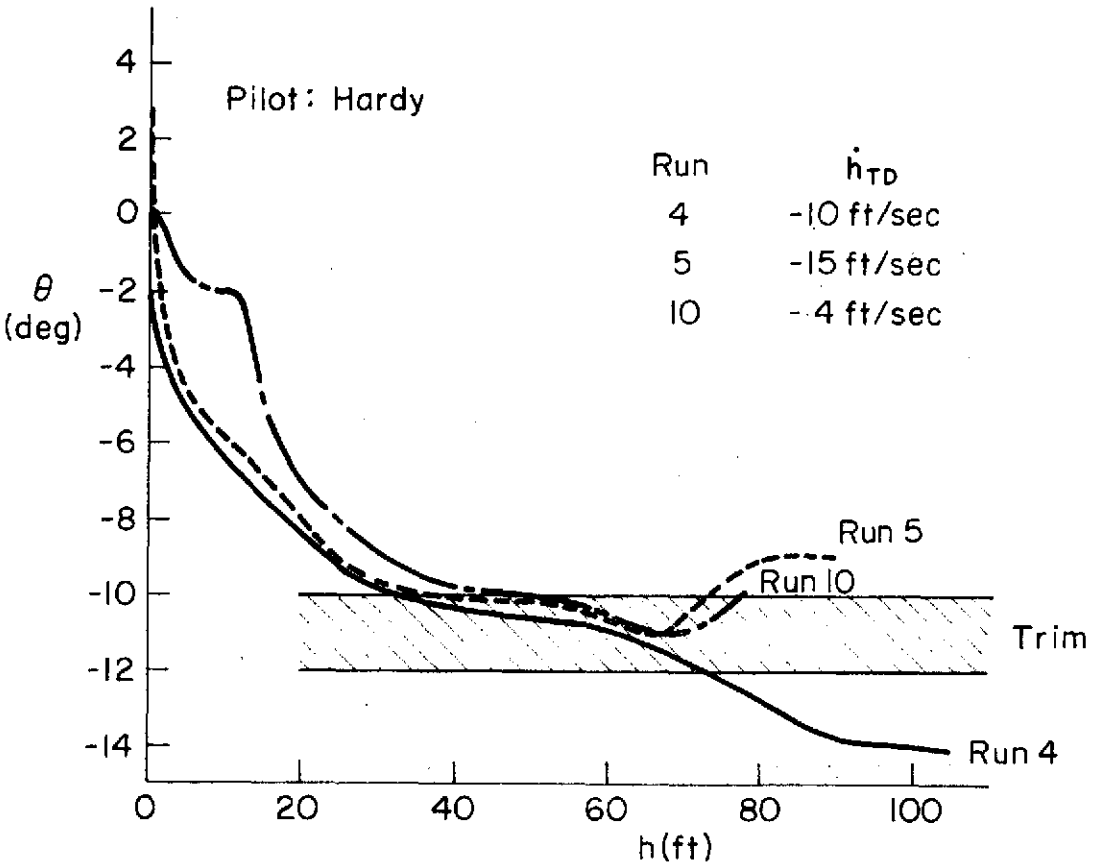

a. Transparency Out, 60 kt

Figure C-2. Flare Maneuver (Simulator)

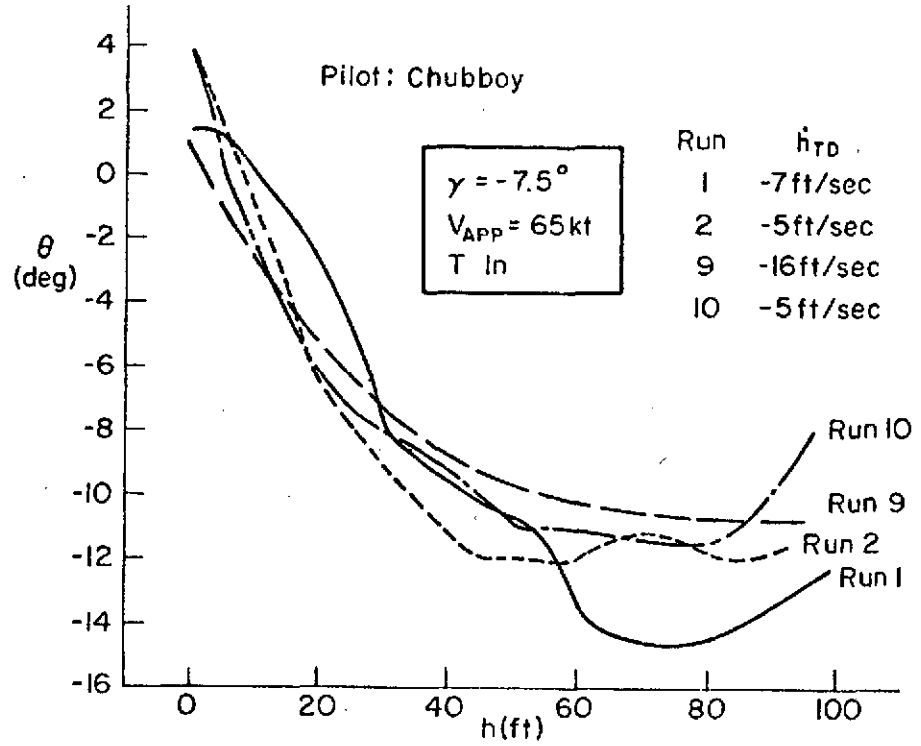

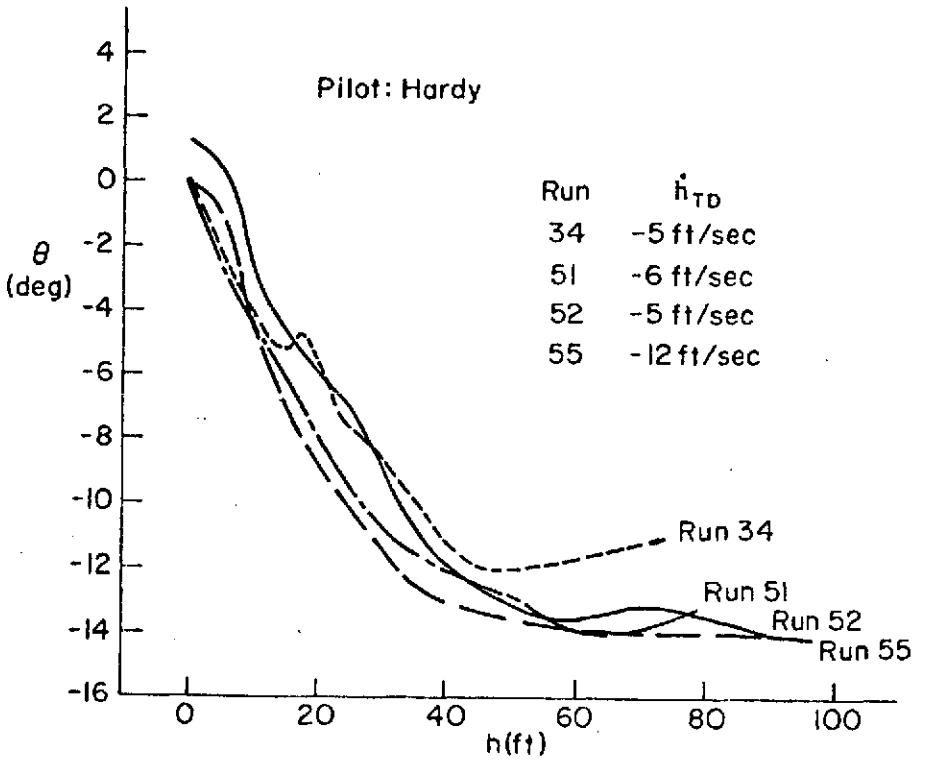

b. Transparency In, 65 kt

Figure C-2. (Concluded)

2. Flare Parameter Variation

Using the flare maneuver described above a computer solution of touchdown conditions was generated for 65 kt and 55 kt, transparency in. The nominal conditions used were h_f = 35 ft and $\Delta\theta$ = 8 deg. These correspond closely to what was observed in the April/May 1973 tests where θ_{trim} was set at -5 deg for all cases. In addition, the nominal conditions included no throttle change. The flare parameter variations included:

- Flare attitude, $\Delta\theta$
- Flare altitude, h_f
- Addition of power during flare, ΔN_G
- Altitude at which power was added.

The absolute values of $\dot{h}_{TD}$ and x_{TD} computed are not as important as the general trends shown.

Fig. C-3 shows the computed time history of the nominal flare at 65 kt, transparency in. Fig. C-4 shows the relative $\dot{h}_{TD}$ and x_{TD} as the flare maneuver is varied. The following features are revealed in these plots:

- At 65 kt reasonable landings can be made without adding power; at 55 kt a power addition is necessary.
- There is a flare attitude which gives a minimum $\dot{h}_{TD}$.
- The touchdown conditions for optimum flare attitude is reasonably close to those of the nominal flare in both cases.
- As with flare attitude there is an optimum flare altitude and the same comments apply.
- Over a reasonable range of flare attitudes and altitudes the touchdown conditions do not vary significantly for a particular configuration.
- The addition of power adds significantly more potential for breaking sink rate.

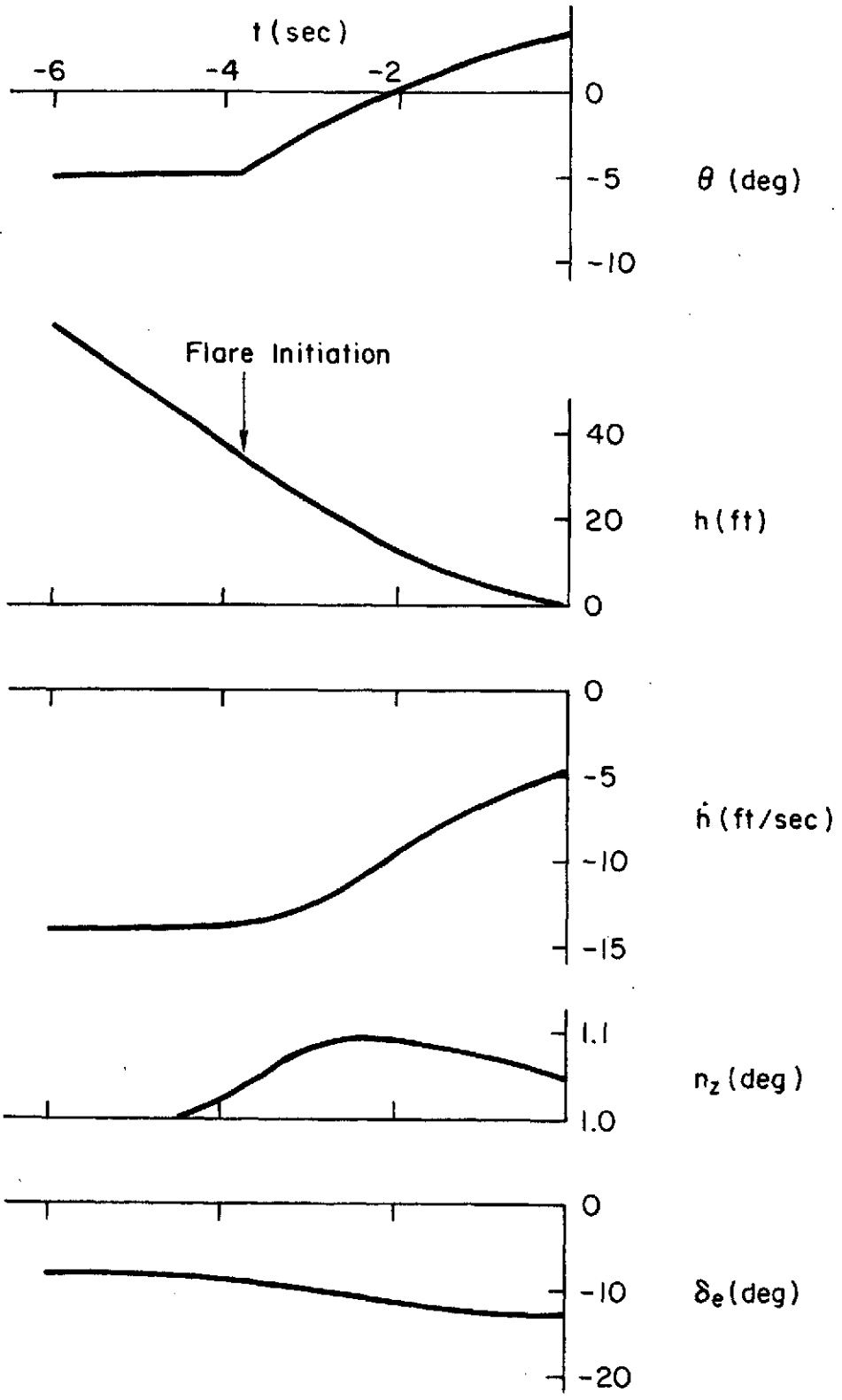

Figure C-3. Time History of Nominal Flare at 6 kt; T In

65 kt
T In
γ = -7.5 deg
Power = 92.5 % N_G
Ground Effect In

Nominal Condition
$\Delta\theta$ = 8 deg
h_f = 35 ft
No Throttle Change

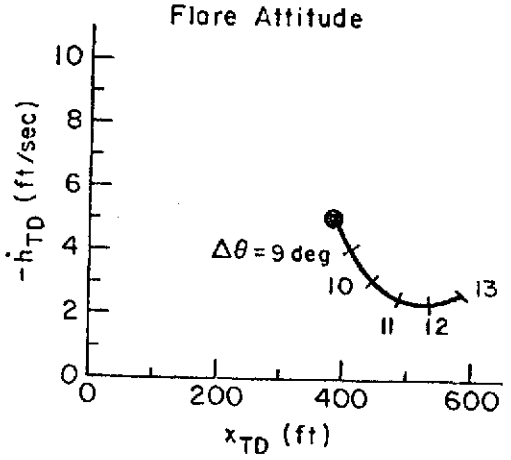

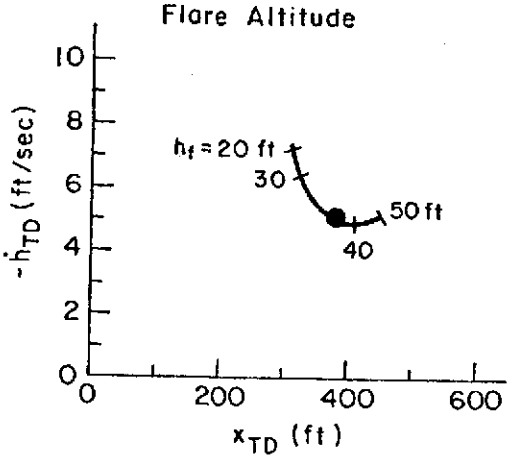

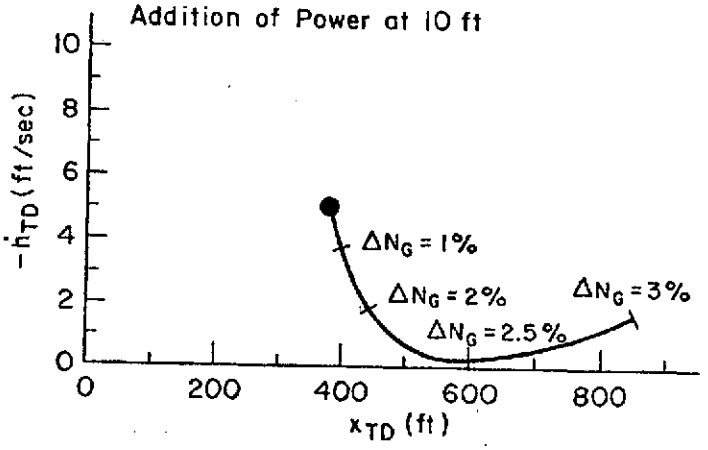

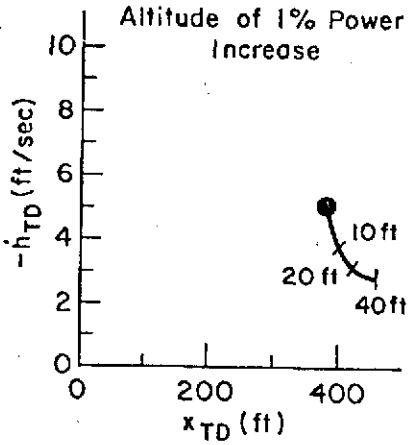

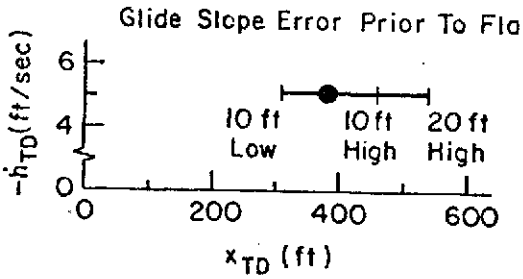

a. 65 kt

Figure C-4. Effect of Flare Controls

55 kt
T In
γ = -7.5 deg
Power = 94.7 % N_G
Ground Effect In

Nominal Condition
$\Delta\theta$ = 8 deg
h_f = 35 ft
No Throttle Change

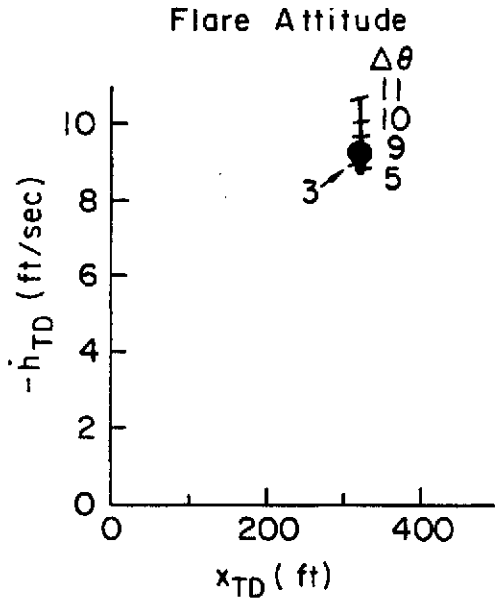

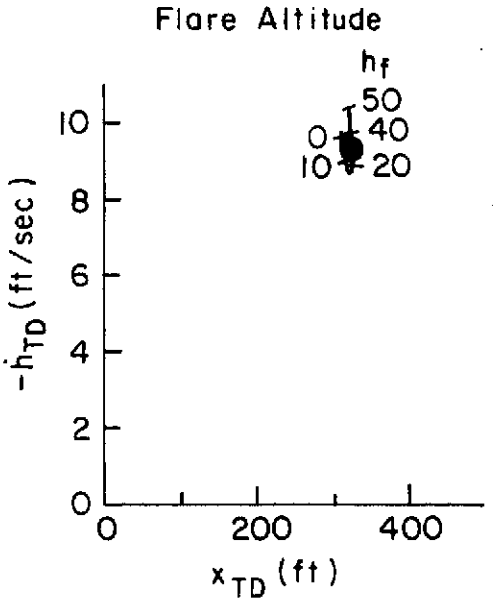

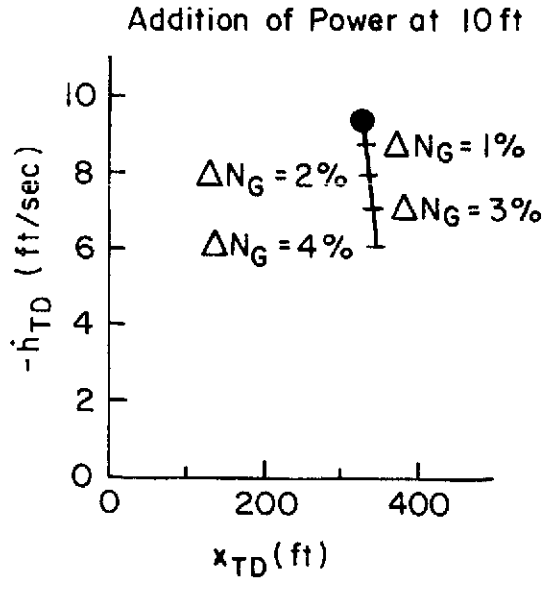

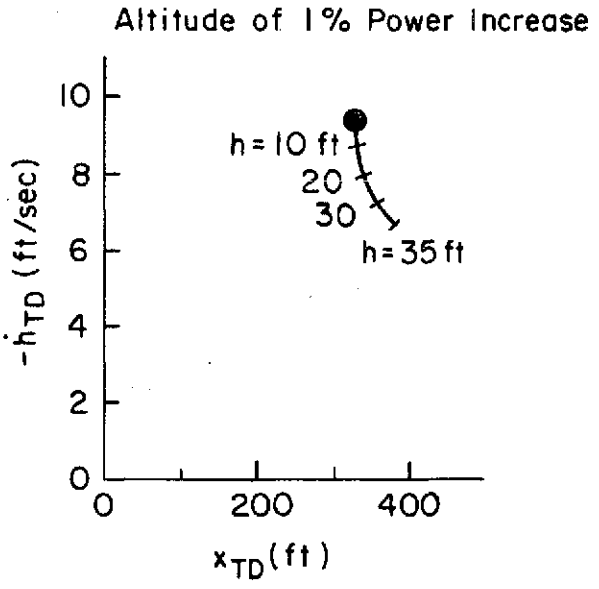

b. 55 kt

Figure C-4. (Concluded)

- The tradeoff of $\dot{h}_{TD}$ for x_{TD} is about the same for attitude versus power at either approach speed.
- To a point, the higher the altitude that power is added the softer the touchdown.

Fig. C-4 combined with Fig. C-5 shows the following general trends as a function of approach speed and transparency:

- The nominal touchdown is significantly softer at the higher approach speeds.
- A potential tradeoff of increased x_{TD} for decreased $\dot{h}_{TD}$ is more apparent at the higher approach speeds.
- Transparency in provides lower touchdown sink rates at the same approach speed.

3. Flare Response Relative to Static Performance

The flare capability for a particular flight condition can be related to where it is situated in terms of a γ versus V or $\dot{h}$ versus V performance curve. Fig. C-6 shows an example for the three approach speed conditions with transparency in. The trim conditions for the three cases are depicted by the circles at 55, 60, and 65 kt. The constant attitude and constant power contours are also given. The heavy lines headed by an arrow show the flare trajectory for an optimum flare at constant power. Each of these trajectories end at the locus of touchdown conditions, $\dot{h}_{TD}$ and V_{TD}.

Fig. C-6 shows that as the approach speed is decreased the resulting sink rate arrestment potential approaches a smaller value. This also, naturally, is strongly related to the margin above V_{min} for a particular approach condition. Fig. C-7 was constructed using this relationship, which is shown graphically in Fig. C-6. Fig. C-7 shows sink rate arrestment potential versus a normalized V_{min} margin for three BR 941S configurations at a variety of speeds on a 7.5 deg glide slope. The resulting points show a fairly strong correlation. This then suggests a way of defining a minimum flare speed provided some minimum sink rate arrestment potential can be defined.

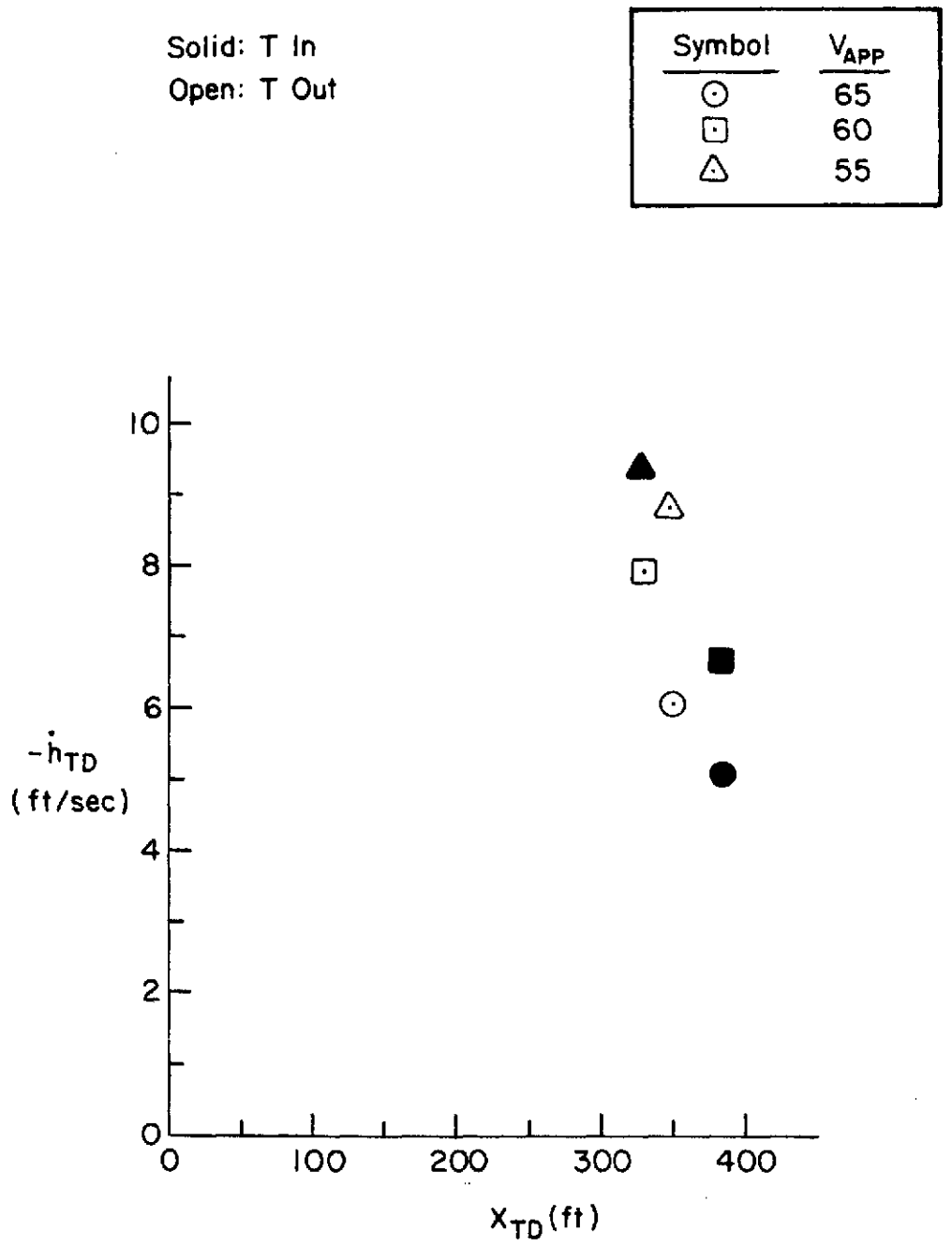

Figure C-5. Effect of Transparency (Nominal Flare)

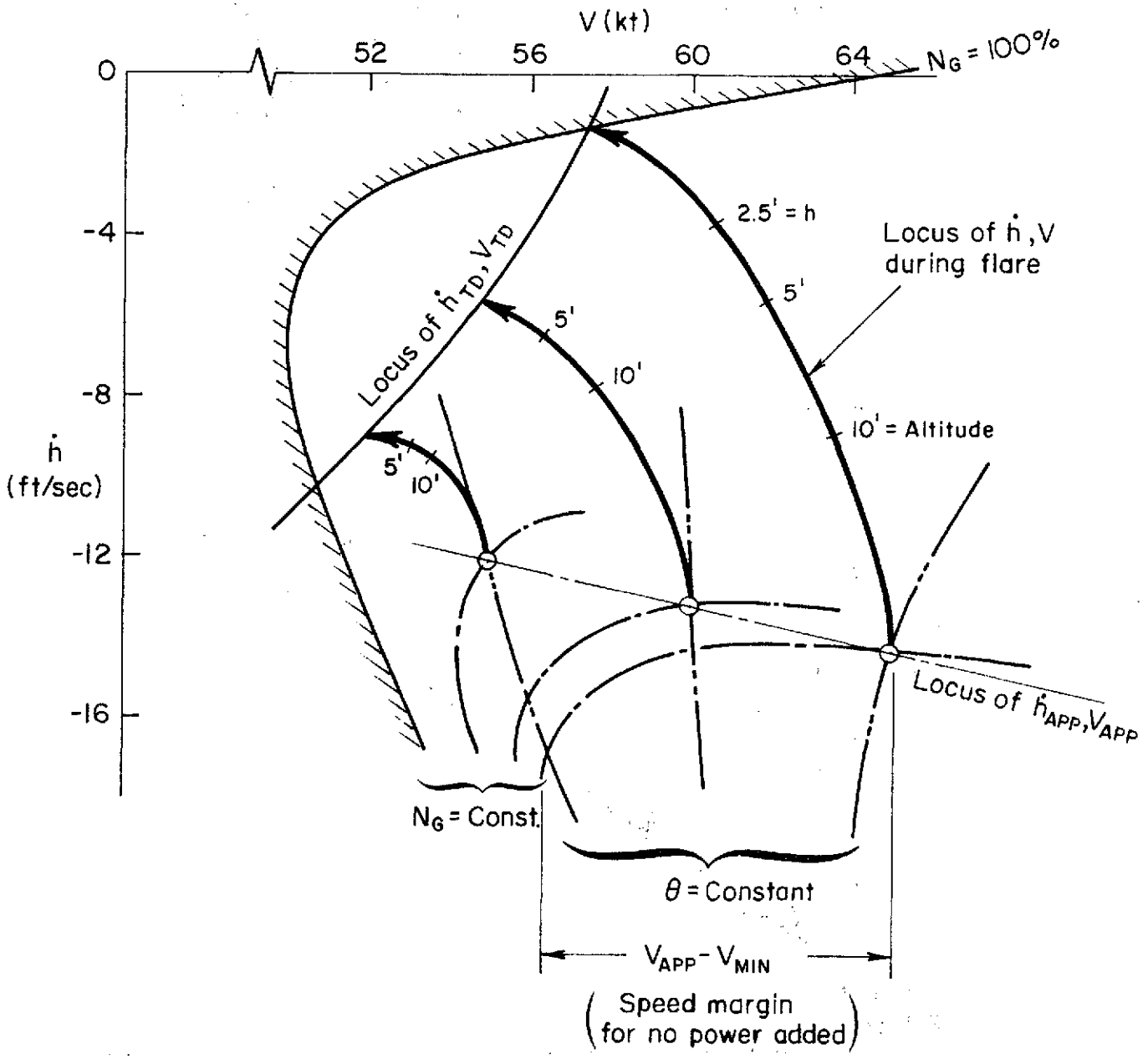

Figure C-6. Flare Trajectories in ḣ-V Plane (Optimum $\dot{h}_{TD}$ with Δ0 Only)

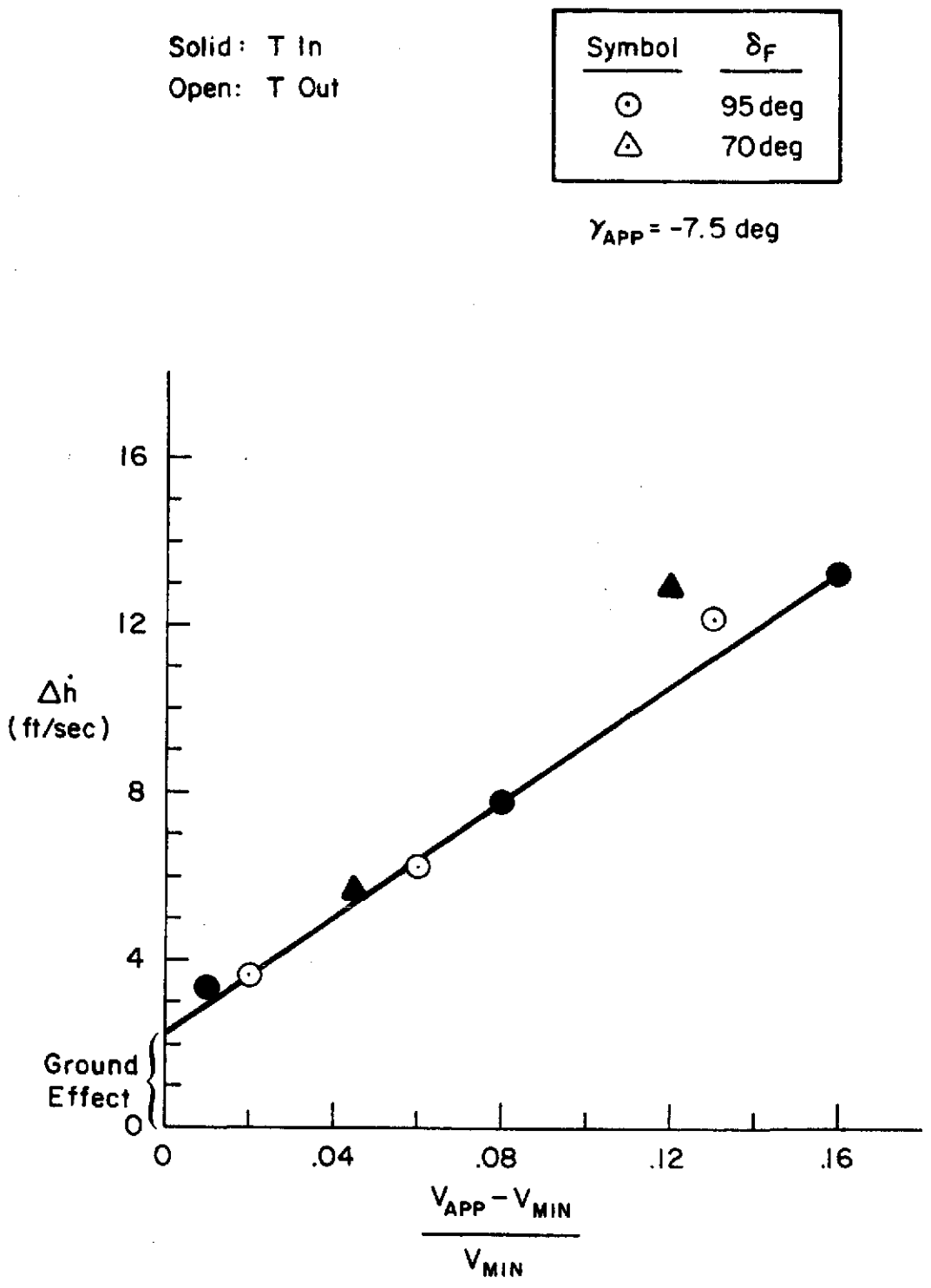

Figure C-7. Sink Rate Arrestment Potential

4. Flight Test Flare/Touchdown Data

The flight test records from the July 1972 FAA/NASA BR 941S flights were analyzed for comparison with the simulator results. The estimated touchdown conditions for each landing are given in Table C-1.

TABLE C-1

TABULATION OF FLIGHT TEST TOUCHDOWN CONDITIONS

(FAA/NASA BR 941S Flights of July 1972)

FLIGHT	TIME	PILOT	CONFIGURATION	WEIGHT	GLIDE SLOPE	V_{APP}	V_{TD}	θ_{TD}	$\dot{h}_{TD}$	REMARKS
5	1812	Chubboy	95/5	41.4K	-7.5	65	60	-2.	-3.0	Airspeed ± 1 kt
	1819		95/5	41.4K	-7.5	66	52	-1.	-2.3	
	1823		75/5	41.4K	-7.5	70	53	-2.	-3.0	
	1835		95/5	41.4K	-7.5	64	49	-2.	-3.4	
5 BIS	1938	Kennedy	70/5	41.4K	-7.5	64	50	-.9	-2.5	
	1945		95/5	41.4K	-7.5	71	58	-1.8	-2.7	
	1955		95/5	38.0K	-7.5	64	52	-1.5	-3.1	
6	0816	Hardy	95/5	42.3K	-7.5	70	57	-1.9	-3.1	Early flare
	0821		----	-----	-7.5	--	--	----	----	
	0829		95/5	42.3K	-7.5	75	61	-2.3	-2.4	
	0835		95/5	41.4K	-7.5	60	46	-2	-3.4	Early flare
	0843		95/5	41.4K	-7.5	65	43	-2.5	-3.2	Airspeed ± 1 kt
6 BIS	0949	Gough	95/5	39.6K	-7.5	70	55	-1.2	-3.5	
	0952		----	39.6K	-7.5	--	--	-1.2	----	
	1000		----	39.6K	-7.5	--	--	-1.2	----	
	1006		95/5	39.6K	-7.5	66	47	-2.5	-3.5	
	1015		95/5	39.6K	-7.5	71	67	-3.	-3.9	
7	1753	Chubboy	85/5	42.8K	-6.0	--	45	-.1	-2.5	
	1810		95/5	42.8K	-7.5	--	45	+1.1	-1.	
	1816		95/5	42.8K	-7.5	--	44	+.2	-1.	
	1834		95/5	41.8K	-7.5	--	44	+3.	-4.8	Gradual flare
	1838		95/5	41.1K	-7.5	--	46	+2.6	-5.	
7 BIS	1917	Kennedy	95/5	40.0K	-7.5?	62	52	+2.1	-6.6	
	1925		95/5	40.0K	-7.5?	60	48	+1.8	-6.2?	Glide slope trim not stable
	1946		95/5	38.7K	-7.5?	60	46	+2.6	-3.	

TABLE C-1

TABULATION OF FLIGHT TEST TOUCHDOWN CONDITIONS (Concluded)

(FAA/NASA BR 941S Flights of July 1972)

FLIGHT	TIME	PILOT	CONFIGURATION	WEIGHT	GLIDE SLOPE	V_{APP}	V_{TD}	θ_{TD}	$\dot{h}_{TD}$	REMARKS
8	0748	Hardy	95/5	43.1K	-7.5	68	48	+2.5	-3.5	
	0801		95/5	42.7K	-7.5	65	48	+.4	-4.4	
	0819		95/5	42. K	-7.5	62	53	+3.	-6.1	
	0840		95/5	40.3K	-7.5	57	54	+3.5	-6.5	
8 BIS	0945	Gough	95/5	39.2K	-6.0	61	51	-.3	-9.	Glide slope, airspeed not stable
	0955		95/5	38.8K	-7.5	64	49	-.7	-7.7	
	1003		95/5	38.2K	-7.5	60	45	+2.8	-6.0	
	1018		95/5	37.3K	-7.5	60	47	-1.	-1.2	θ not stable
	1030		95/5	37.1K	-7.5	58	47	-1.	-3.5	
9 BIS	2000	Chubboy	95/12	37.1K	-7.5	58	41	+1.8	-5.	
	2012		95/12	36.9K	-7.5	55	35	----	-3.5	
10 BIS	0851	Hardy	95/12	36.9K	-9.5	62	46	-1.	-4.3	
	0912		95/12	36.9K	-7.5	57	50	+1.	-5.9	
	0918		95/12	40.1K	-7.5	70	54	+.5	-3.5	Glide slope, airspeed, θ not stable
	0925		95/12	39.6K	-9.5	58	45	-1.	-3.2	
	0902		-----	-----	-7.5	56	--	---	----	
11	0740	Hardy	95/5	44.7K	-7.5	63	54	0.	-4.0(?)	Airspeed $\pm$ 2 kt
	0807		95/5	44.7K	-7.5	62	53	+.8	-4.5	
	0814		70/12	44.7K	-7.5	58	55	-2.	-3.0(?)	
11 BIS	0833	Gough	70/5	42.7K	-7.5	82	57	-.4	-5.6	Airspeed $\pm$ 2 kt
	0842		95/5	42.7K	-7.5	69	54	-1.8	-4.7(?)	
	0856		70/12	42.7K	-7.5	75	60	-1.2	-3.	Airspeed not stable, $\pm$ 5 kt

APPENDIX D

PILOT COMMENTS

The pilot comments which were made during the simulation experiments were paraphrased and compiled in tabular form. Table D-1 gives the pilot comments from the October/November 1972 tests and Table D-2 gives those from April/May 1973. The latter also includes pilot ratings for ILS tracking and flare.

TABLE D-1

PILOT COMMENTS
(October/November 1972)

PILOT	DATE	γ_{APP}	TRANSPARENCY	α DISPLAY	V_{APP}	TASK	COMMENTS
Chubboy	10-25	7.5	IN	OUT	65	FAM	1. Workload medium to high (instrument scan) 2. Glide slope tracking seemed good
	10-26	7.5	IN	OUT	65	TR	1. Moderate workload due to almost constant longitudinal control and to lesser degree lateral control 2. X-wind landing difficult because of vague cues; flare height judgment is also a factor
	10-27	7.5	IN	OUT	65	TEST	1. Except for large wind shear, 65 kt seemed too fast 2. X-wind landing performance improved by decrabbing at higher altitude
	10-27	7.5	IN	OUT	60	TEST	1. Difficulty in maintaining glide path and airspeed 2. Seemed harder than at 55 kt
	10-27	7.5	IN	OUT	55	TEST	1. Flight path control was good if avoid power chop 2. Thrust margin minimal especially if low and slow 3. Thrust lags seemed more evident 4. Acceptable minimum approach speed/thrust margin but no lower
	11-15	7.5	OUT	IN	60	TR	1. Down correction weak 2. Comfortable in shear, easy to over control 3. Glide slope tracking with transparency is definitely more positive 4. Flare using mild aft stick, then power reduction
	11-16	7.5	OUT	IN	60	TEST	1. In strong head wind, α sensitivity requires extraordinary attention to θ, airspeed got down to 50-51 kt 2. α obviously superior to airspeed on go-around 3. Cannot maintain both α and airspeed when changing power; I correct α and let airspeed vary
	11-16	7.5	OUT	IN	55	TEST	1. Airspeed - power response rapid; airspeed - θ slow; γ power sluggish; causes pilot anxiety at best 2. In high shear conditions, lowering nose to flare is almost intolerable
	11-17	7.5	OUT	IN	50	TEST	1. Much better glide path control than at 55 2. Lowering nose to correct for shear is unreasonable and suicidal 3. Noticeable degradation in θ and lateral control
	11-15	9.5	OUT	A/S OUT α IN	60	TEST	1. Glide path control no problem under normal conditions but for large corrections there is an obvious need for additional flight information, such as airspeed 2. Poor instrument layout
	11-15	9.5	OUT	OUT	60	TEST	1. α better for go-around (don't need climb speed) but stabilization much easier with airspeed 2. Shear seemed easier to detect
	11-17			IN		TAKEOFF	1. Directional control in x-wind excellent, quite like the real thing 2. Airspeed alone was satisfactory but airspeed and α was obviously better especially for 65-70 kt climb speed 3. With OEI at 67 kt, α is a powerful indication of the real situation 4. With a stick shaker at 14 deg α, I don't consider 67 kt a threat

TABLE D-1 Continued

PILOT	DATE	γ_{APP}	TRANSPARENCY	α DISPLAY	V_{APP}	TASK	COMMENTS
Hardy	10-31	7.5	IN	OUT	65	TR	1. Flight path control and landing maneuver adequate 2. Workload fairly high 3. Redifon - hard to pick out steady state much less rates. Makes shear control very hard
	11-2	7.5	IN	OUT	65	TEST	1. Performance very adequate IFR, VFR: shears and visual scene combine to make it inadequate 2. Speed not adequate for shears within limitations of visual scene 3. Flare: start rotation at 30 ft, adjust power if airspeed is off 4. With present speeds and shears, certification is marginal at best
	11-7	7.5	IN	OUT	60	TEST	1. Similar to 65 kt
	11-7	7.5	IN	OUT	55	TEST	1. Significantly harder to maintain airspeed 2. Altitude control with power seems slightly more sluggish, tend to run out of power 3. Flare much harder, must all be done with power 4. Not enough margin for normal operation, not enough for emergency situations with shears
	11-8	7.5	IN	IN	60	TR	1. α lagged pitch significantly (time constant = 2.0 sec) 2. Scan pattern is poor 3. α easier than airspeed for go-around
	11-9	7.5	IN	IN	65	TR	1. Fairly high workload, POR = 4.5 2. Margins seen adequate, first comfortable VFR, could be I'm learning how to cope with shears
	11-16	7.5	OUT	OUT	60	TEST	1. Flight path control quite easy except when high, it seems hard to comfortably come down
	11-16	7.5	OUT	OUT	55	TEST	1. Hard to stabilize at 55 kt, wanted to end up about 58 2. Flight path control is fairly easy at 55-60 kt, easier than 60-65 3. If airspeed drops to 52 kt there is dangerous tendency for flight path to diverge downward 4. Marginal for shears 5. Use power to flare
	11-15	9.5	IN	OUT	60	TEST	1. Airspeed easier to maintain than α, better scan pattern may contribute 2. Hard to correct downward 3. Lots of trouble with flare but can't detect much difference between α and airspeed
	11-15	9.5	IN	IN	60	TEST	1. Glide slope and α requires a high workload, POR = 6 2. Not much α margin for go-around 3. Flare performance unacceptable for emergency operation, POR $\geq$ 6.5
	11-10	9.5	IN	IN	65	TR	1. Fairly high workload about same as 7.5 deg approach 2. Having some problems with glide slope tracking at breakout 3. Flare from 9.5 deg is harder, had a tendency to flare high
	11-17			IN		TAKEOFF	1. OEI climb at 67 kt was impossible, marginal at 70, POR = 6 2. V_R = 65, V_2 = 74 case is pretty easy to fly, POR = 3.5

TABLE D-1 Continued

PILOT	DATE	γ_{APP}	TRANSPARENCY	α DISPLAY	V_{APP}	TASK	COMMENTS
Gough	11-22	7.5	IN	OUT	65	FAM	1. Used θ for flight path and power for airspeed some but had problems when airspeed low. Found myself switching 2. Seemed low on power during flare
	11-20	7.5	IN	OUT	55	TEST	1. Flight path control very difficult, used power to control 2. Just barely enough margin for shear. Very easy to use excessive power
	11-7	7.5	IN	IN	65	FAM	1. Countered shear with power ok 2. Power to control flight path
	11-8	7.5	IN	IN	60	TR	1. Over-controlling all axes, unable to judge sink rate before touchdown
	11-9	7.5	IN	IN	60	TEST	1. Ok except for countering shear, margin for shear may be ok with improved technique 2. Acceptable workload 3. Airspeed was primary, just keep α in acceptable limits, α very useful in go-around
	11-10	7.5	OUT	OUT	60	TR	1. Flight path control difficult, required large power changes, much more use of IVSI
	11-10	7.5	OUT	OUT	60	TEST	1. Same as above 2. Countered shear ok
	11-14	7.5	OUT	IN	50	TEST	1. Very poor speed to use in shear
	11-17	9.5	IN	IN	65	TEST	1. Continually reverted to θ for airspeed, checked α for safe zone. Too little time between breakout and 'impact' 2. α on go-around tended to make me level off instead of climb, indicated α too high for θ, power, and airspeed

TABLE D-1 Continued

PILOT	DATE	γ_{APP}	TRANSPARENCY	α DISPLAY	V_{APP}	TASK	COMMENTS
Kennedy	10-25	-7.5	IN	OUT	65	FAM	1. Excessive workload in tracking; lateral stability low 2. V_{min} recognition difficult due to instrument location 3. Recovery like classic power-on stall 4. Flare difficult because of visual scene and lack of training
	10-26	-7.5	IN	OUT	65	FAM	1. Configuration changes difficult 2. Stability and control primary factor in workload 3. Control technique: h ⟶ δ_T, θ constant; u, θ ⟶ δ_e
	10-26	-7.5	IN	OUT	65	TEST	1. Approach speed adequate 2. Would not certify due to controllability problems
	10-27	-7.5	IN	OUT	60	TEST	1. Approach speed adequate, getting easier with practice 2. High concentration for line-up, conversion, and glide slope capture 3. Inadequate power margin during flare for larger shears (i.e., du/dh = 15 kt per 100 ft) 4. Controllability inadequate - would not certify
	10-31	-7.5	IN	OUT	60	TEST (repeat)	1. Still on learning curve 2. Aircraft too power limited (marginal control for shears) 3. Redifon scene not adequate for flare
	10-26	-7.5	IN	OUT	55	TEST	1. Excessive concentration required for line-up, conversion, etc. 2. Good control IFR poor VFR 3. Speed margin inadequate for flare but adequate for glide slope control 4. Control power margin to low for shears 5. Wouldn't certify - inadequate margin above V_{min} - unsafe
	11-3	-7.5	IN	IN	60	TR	1. Tracking glide slope more difficult with α 2. Instrument scan bad 3. Go-around more difficult, α lags excessive 4. Tendency to regulate α at expense of attitude and speed 5. Changes in control techniques required, h ⟶ δ_T α, θ ⟶ δ_e
	11-3	-7.5	IN	IN	60	TR	1. More difficult to track glide slope than without α; due to divided attention and scan 2. Go-around maneuver seemed more difficult, α lags behind nose attitude (i.e. T_α = 2 sec) forces pilot to keep nose low too long 3. Tendency to regulate α at expense of attitude and speed during first few runs 4. Except for small α change it is necessary to adjust both attitude and power to hold α 5. α helps flare, workload excessive
	11-4	-7.5	IN	IN	60	TR	1. Same as above

TABLE D-1 Continued

PILOT	DATE	γ_{APP}	TRANSPARENCY	α DISPLAY	V_{APP}	TASK	COMMENTS
Kennedy (continued)							
	11-6	-7.5	IN	IN	65	TEST	1. High workload because you need to adjust both attitude and power as opposed to speed, stable conditions previously tested 2. Go-around, α not too useful because of lags; tends to make pilot hold to low too long, airspeed/attitude easier 3. Noted speed variation when flying α; no longer attempts to maintain constant attitude (i.e., fly glide slope with power and adjust nose attitude to achieve correct α)
	11-7	-7.5	IN	IN	55	TEST	1. Most difficult speed, very little fly-up capability 2. Heavy work load due to h ⟶ δ_T, α, θ ⟶ δ_e technique 3. Cannot integrate both α and speed cues - often missmatch in corrective action required 4. Aircraft has no margin for shear control 5. Recognized shear (one case) reversed control technique used successfully
	11-7	-7.5	OUT	IN	60	FAM and V_{min}	1. Easy task - no limiting factors 2. Workload quite acceptable with no winds 3. Good glide slope control 4. V_{min} hard to recognize, recovery easy, and conventional (i.e., push over add power), need warning 5. Roll control power weak at V_{min} 6. Excessive sink rate (>3500) results in loss of pitch control
	11-7	-7.5	OUT	IN	55	TEST	1. Did not use α except as cross check on glide slope, did at flare 2. α poor; instrument for this speed too heavily damped 3. Technique for go-around u, θ ⟶ δ_e no α, accepted α excursions 4. Heavy workload - excessively high 5. Aircraft less responsive to power changes, up or down, control power lower up or down 6. Flare problem; difficult to know how to use power
	11-8	-7.5	OUT	IN	50	TEST	1. Very difficult flight conditions, not safe 2. Difficult to use α, because slight power change radically changed α 3. α too sluggish for go-around 4. Often exceeded stick shaker speed (α = 20.7 deg) 5. Line up ok; conversion to glide slope difficult, slight miscalculation as power results in α increased beyond 20.7 deg 6. Technique for glide slope control difficult; power doesn't result in positive glide slope correction unless nose is lowered. Final technique, set power and track glide slope 7. Using opposite standard technique, nose down - up, nose up - down 8. Speed decreased with increasing power
	11-9	-7.5	OUT	OUT	60	TEST	1. Conversion difficult, glide slope more difficult with transparency out 2. Speed margin inadequate 3. Control technique h ⟶ δ_T, u, θ ⟶ δ_e
	11-9	-7.5	OUT	OUT	50	TEST	1. Conversion very difficult

TABLE D-1 Concluded

PILOT	DATE	γ_{APP}	TRANSPARENCY	α DISPLAY	V_{APP}	TASK	COMMENTS
Carrodus	11-8	7.5	IN	IN	65	FAM	1. Flight path control reasonably accurate using power but response slow 2. Controlled glide slope with pitch, never looked at α 3. Highest longitudinal workload was pitch control, little or no stability 4. Pronounced adverse yaw, low side force gives little acceleration or slip ball cues
	11-10	7.5	IN	OUT	55	TR	1. IFR glide slope holding was no problem, power changes were kept small and errors corrected slowly 2. VFR rate of descent control was extremely rough, large power changes at late stages
	11-10	7.5	IN	OUT	60	TR	1. No obvious difference from 55 kt case 2. Task became easier than 55 kt case but think it was largely due to learning process
	11-20	7.5	IN	OUT	65	TEST	1. Glide path control appeared more accurate than before, very small power corrections IFR 2. Glide path control was frequently oscillatory VFR caused largely by heave to power lags 3. Apparently greater difficulty than last flight at 60 kt
	11-22	7.5	IN	IN	55	TEST	1. Glide path errors required larger than expected power changes 2. Thrust margin unacceptable for shears 3. No particular problems with landings except with shears, power not used to flare 4. Go-arounds: To avoid V_{min} accelerated then climbed, unacceptable in real life 5. Little difference in difficulty or workload between this and previous case at 65 kt

TABLE D-2

PILOT COMMENTS
(April/May 1973)

PILOT	DATE	TRANSPARENCY	α DISPLAY	V_{APP}	PILOT RATINGS* CALM AIR	TURBULENCE	WIND SHEARS	COMMENTS
Hardy	5-2-73	IN	OUT	65	3, 3	5 1/2, 5 1/2	6 1/2, 5 1/2	1. Workload high tracking glide slope, pitch must be trimmed constantly while tracking glide slope, perhaps due to pitch SAS, using $\theta \longrightarrow V$, $\delta_t \longrightarrow \dot{h}$ 2. Some difficulty arresting $\dot{h}$, break initial $\dot{h}$ with θ and then feel for runway, using power as secondary control. Visual scene doesn't give good $\dot{h}$ cues.
	5-3-73	IN	OUT	60	3, 3 1/2	5 1/2, 6	6 1/2, 6	1. Glide slope tracking same as for 65 kt power 2. Flare requires percent or two of power increase to keep θ_{Flare} reasonable
	5-4-73	IN	OUT	55	7	---	---	1. Impossible to get downward correction in $\dot{h}$ without getting on bottom side of γ - V curve.
	5-4-73	OUT	OUT	65	3 1/2, 3 1/2	6, 6	--	1. IIS tracking virtually the same as 65 kt, transparency in, except power response is more sluggish 2. Flare just about like 60 kt, transparency in, have to add a bit of power
	5-7-73	OUT	OUT	60	3 1/2, 3 1/2	6 1/2, 6	6 1/2, 6	1. Many problems with glide slope tracking--(a) power response insensitive, (b) feels like $\dot{h}$ response almost unstable, very hard to control, get a few knots slow and vehicle goes on bottom side of γ - V curve, (c) 3 1/2 rating for calm air glide slope tracking is subject to question. Vehicle very close to bottom side of γ - V curve, could be degraded to 6 1/2 2. Flare is about the same as 60 kt, transparency in
	5-9-73	OUT	IN	60	3 1/2, 3 1/2	6, 6	6 1/2, 6	1. Using α display gives pilot more confidence and would probably operate aircraft slightly slower than with only airspeed indicator 2. Main difference between this and 60 kt, transparency out, is that bottom side operation is avoided. 3. Had trouble with α donuts--tended to close too tight a loop around them
	5-9-73	IN	IN	55	5	6-6 1/2, 6 1/2	---	1. Reducing engine lag from 1.4 to 0.5 sec had no effect on ILS tracking. Helped flare 1/2 rating point (ratings in pilot ratings column are for nominal engine lag = 1.4 sec)
Gough	4-30-73	IN	OUT	65	3	5	4 1/2†	1. In calm air difficult to stabilize heading--end up bracketing heading. With turbulence, began to accept small localizer errors to reduce overcontrolling 2. IIS tracking very difficult close to window. If you break out then VFR task very easy 3. Pilot technique is to rely on IVSI, if no α display--try to maintain constant $\dot{h}$, but very hard to recover from high on glide slope 4. VFR portion and flare fairly easy. Hardest task is power reduction to get correct 'squat' with turbulence--no worries about undershooting runway. 5. In X-wind favor crabbing until flare--then stuff in rudder and drop wing--will accept reasonable displacement from runway center line.

* First rating is IIS tracking; second is flare.

† No distinction made between ILS tracking and flare.

TABLE D-2 Concluded

PILOT	DATE	TRANSPARENCY	α DISPLAY	V_{APP}	PILOT RATINGS CALM AIR	PILOT RATINGS TURBULENCE	PILOT RATINGS WIND SHEARS	COMMENTS
Gough (cont.)	5-1-73	IN	OUT	60	3 1/2	5 1/2	6 1/2	1. Localizer tracking similar to 65 kt 2. Glide slope tracking very difficult, θ ⟶ V, δ_{TH} ⟶ G/S. Very unresponsive--takes gross power changes. Used IVSI as primary performance reference 3. Turbulence makes ILS tracking workload higher than is liked 4. Flare feels precarious. Technique is to correct ḣ with power, but this can result in too much power to continue landing. Result is you end up jockeying quite a bit 5. Hitting stops consistently with aileron, occasionally with rudder just prior to flare
	5-1-73	IN	OUT	55	4 1/2	6 1/2	7	1. ILS tracking very difficult--response sluggish--correcting for high glide slope error most difficult--stick shaker on 10% of time--very hard to stabilize on speed, tend to get fast 2. Glide slope tracking requires so much effort that localizer tracking becomes more difficult 3. Pilot technique for IIS tracking is to trade altitude for speed, power for glide slope 4. Technique for flare takes a delicate mix of increasing θ and power--then cut power at contact to prevent bounce 5. Wind shears made it very difficult to control ḣ prior to flare 6. X-wind technique same as 65 kt, but felt like I was very close to rudder control limits
	5-2-73	OUT	OUT	65	3	5 1/2	7	1. Localizer tracking hardest task in calm air, but not objectionable 2. Flare very satisfactory--used slight power reduction to squat
	5-3-73	OUT	OUT	65	3	5 1/2	7	1. Glide slope tracking hardest task, gross power changes required--spent much time at flight idle 2. Flare was delicate--seemed to have too much power prior to flare and had to reduce it prior to landing--resulted in long landings 3. IVSI becoming more and more of a primary instrument, using it and localizer error at about 250' to decide on go-around or not 4. Using attitude change to fly glide slope with power follow up
	5-2-73	OUT	OUT	60	4	7 1/2	9	1. Glide slope very hard to track, especially for large errors. Combined θ and δ_{TH} for glide slope, seemed less able to separate technique. Then couldn't hold aim airspeed on glide slope without excessive power corrections. Turbulence made it very difficult to track ILS close to window 2. Localizer seemed difficult to track, probably due to preoccupation with glide slope 3. During flare, had to adjust ḣ carefully with power, often difficult to do with acceptable precision
	5-3-73	OUT	IN	60	2 1/2	6	6	1. ILS tracking very hard, takes too long to correct error 2. Basically ignore α donuts, still using IVSI as primary instrument 3. Flare in calm air is nice, in turbulence or shears have to play with power and attitude too much
	5-4-73	IN	IN	55	5	8-8 1/2	---	1. Localizer tracking difficult--aircraft is rolling and yawing a lot...more than previously 2. Glide slope tracking is very difficult--never did track, always passing through. Turbulence aggravated ILS tracking 3. Flare made by adding power at same rate pitch was added, turbulence aggravated flare by leaving you with too much power to land 4. The aircraft doesn't want to seem to fly well in this situation

VOL. II

☆ U. S. GOVERNMENT PRINTING OFFICE 1975 689—190/4116